essd-2019-183, Global Carbon Budget 2019, responses to review comments

Dear editor, you'll find below a point-by-point response to all comments.
In addition, in the revised manuscript, we updated (as we always do) the 2019 projections of emissions and atmospheric CO2, using the latest available data to date. We also included one additional land model (CLM5.0) and one additional ocean model (NEMO-PISCES (IPSL)) who both had technical issues for some of their simulations at the time of the initial submission. These two additional models do not change the result in any significant manner (no more than 0.1GtC/yr difference in land or ocean estimates between initial submission and current submission). Finally, we made some minor editorial corrections as requested by the authors team.

We also attach to this document the marked-up manuscript version.

Editors comments

Lines 207, 208 and 237, 238 and 1468: Andrew et al Cement Budget latest version should have reached publication status in ESSD. Change to 'in press' or full as-published reference? Certainly by proof stage?

Done, updated to Andrew et al., (2019), full reference being :
Andrew, R. M.: Global CO2 emissions from cement production, 1928-2018, Earth Syst. Sci. Data, doi:10.5194/essd-2019-152, 2019.

Line 1189, parentheses wrong? I think you want "(range of 1.8 to 3.7%) published in Le Quéré et al. (2018b) based on national emissions"? Proofreaders will not catch this so you need to ensure you have punctuated it correctly for your intent.

Done, changed to: "…(range of 1.8 to 3.7%) published in Le Quéré et al. (2018b)"

Order of appendices will sort itself. The suggestion by one reviewer to move conclusion section ahead of data availability section and then to finish the narrative with that data availability section seems useful. Many ESSD products follow that sequence.

Done, we moved the conclusion (now section 5), before the data availability (now section 6)

All reviewers worry about the text in lines 1287-1291. I tend to agree. I see two issues. First, the emerging confusion between this careful carbon source/sink accounting, which you / we properly label as a 'global carbon budget' while - as one reviewer confirms - the much-less careful (one might even say 'casual' or 'incautious'?) public and press use the term 'carbon budget' to refer to remaining carbon emissions. The research community follows your terminology: what you refer to as "permissible emissions for a given climate stabilization target" in line 97 and as the ""remaining carbon budget"" at lines 1288-1289. The carbon community will need to deal with this growing confusion. You tread carefully here, appreciated, but you may need to deal even more explicitly with 'remaining carbon' in the future. Second, and more closely related to the text at 1287-1291, as I read it you have introduced confusion

rather than clarity: you urge caution at using cumulative emissions for any purpose but then you seem to encourage remaining carbon estimates by a (relatively) straightforward extrapolation from present day values into the future? You have several options here: a) delete these two sentences; b) keep only the first sentence, perhaps appended to the previous paragraph; or c) revise these sentences to convey a clearer message?

Done, we clarified in the introduction what is meant here by the global carbon budget and suggest to adopt remaining carbon emissions for the "budget" consistent with a future climate target. The paragraph now reads as follow:
"The global carbon budget presented here refers to the mean, variations, and trends in the perturbation of CO_2 in the environment, referenced to the beginning of the Industrial Era (defined here as 1750). This paper describes the components of the global carbon cycle over the historical period with a stronger focus on the recent period (since 1958, onset of atmospheric CO_2 measurements), the last decade (2009-2018) and the current year (2019). We quantify the input of CO_2 to the atmosphere by emissions from human activities, the growth rate of atmospheric CO_2 concentration, and the resulting changes in the storage of carbon in the land and ocean reservoirs in response to increasing atmospheric CO_2 levels, climate change and variability, and other anthropogenic and natural changes (Fig. 2). An understanding of this perturbation budget over time and the underlying variability and trends of the natural carbon cycle is necessary to understand the response of natural sinks to changes in climate, CO_2 and land-use change drivers, and the permissible emissions for a given climate stabilization target. Note that this paper does not estimate the remaining future carbon emissions consistent with a given climate target (often referred to as the remaining carbon budget (Millar et al., 2017; Rogelj et al., 2016, 2019)."

We also rewrote section 3.5 as suggested by the editor and reviewers, removing the last sentence that added to the confusion. The paragraph now reads as:
"Given the large and persistent uncertainties in historical cumulative emissions, we suggest extreme caution is needed if using this estimate to determine the remaining cumulative CO_2 emissions consistent with an ambition to stay below a given temperature limit (Millar et al., 2017; Rogelj et al., 2016, 2019)."

Lines 1405, 1406. In prior versions: "a growing understanding of and improved capacity to anticipate the evolution of the carbon cycle in the future". In this version: "a better understanding of the causes of climate change, and an improved capacity to anticipate the evolution of the carbon cycle in the future". The new phrase introduces a new hesitancy? You really do not intend such apparent confusion? (Indeed, why then do we have GGP and annual GCB?). I think you mean "better quantification of" or "better accounting of" in place of 'better understanding'?

Done, we rephrased the sentence as follow " Second, over the last decade we have seen unprecedented changes in the human and biophysical environments (e.g. changes in the growth of fossil fuel emissions, Earth's temperatures, and strength of the carbon sinks), which call for frequent assessments of the state of the planet, a better quantification of the causes of changes in the contemporary global carbon cycle, and an improved capacity to anticipate its evolution in the future. "

Reviewer 1

1) There is an increasingly problematic terminology confusion that has arisen as a result of the phrase "carbon budget" being used for two completely different concepts -- i.e. the current use (current sources and sinks of CO2) and the "emissions budget" use (where "carbon budget" refers to the total or remaining allowable cumulative emissions for a given climate target). A nice solution to this problem would be to adopt here the phrase "global carbon cycle budget" here rather than "global carbon budget" -- this would serve to differentiate more clearly from the "remaining carbon budget" which is increasingly widely used as a term but is not at all the same thing as what is reported in the current paper.

Done, we clarified in the introduction what is meant here by the global carbon budget and suggest to adopt remaining carbon emissions for the "budget" consistent with a future climate target. We also clarified this in section 3.5, also removing the last sentence that added to the confusion. See new text in the above response to the editor

*2) Along the same lines, it would be very helpful to clearly distinguish between what "carbon budget" means in this paper and the allowable emissions use of "carbon budget" elsewhere in the literature. I had a colleague recently refer to Corine Le Quere as *the* world expert on calculating remaining carbon budgets ... which does of course speak highly of her reputation, but is also not really accurate since this would be the other kind of carbon budget. So it would help to provide this distinction at the outset of the paper (which would be easier if you would consider adopting "global carbon cycle budget" ...)*

Done, see response to editor's comment.

3) On lines 158-159 the authors refer to 1850 as the base year for historical simulations in CMIP6, and 1870 as the base year for cumulative emissions in AR5 based on the availability of global temperature data. It would be nice to update this: the upcoming IPCC report will use 1850-1900 as a consistent base year for both model simulations and historical temperature data, so it would make sense to align the estimate of historical cumulative emissions in Table 8 with this new standard base period -- i.e. either use the mid-point (1875, rather than 1870), or subtract the mean annual emissions for 1850-1900 from the sum since 1850 so as to calculate the total relative to this base period.

Thanks for this. We simplified the discussion on cumulative emissions in the text and in Table 8, keeping the full industrial period (1750-2018) for completeness, but then estimating cumulative budgets from 1850 as this is the reference year for historical simulations in IPCC (CMIP5 and CMIP6 historical period). We do not use 1870 as a starting year anymore. We understand the reviewer suggestion that one could now use 1875 (mid-point of the 1850-1900 period), but we prefer to defer such decision until the IPCC AR6 is published. The relevant text in the introduction now reads:
"Finally it provides cumulative emissions from fossil fuels and land-use change since the year 1750, the pre-industrial period; and since the year 1850, the reference year for historical simulations in IPCC (AR6)."
We also updated Table 8, Figure 3 and figure 9 (both now starting in 1850).

4) I am not sure about the statement on lines 1287-1291 regarding the recommendation to calculate the remaining carbon budget as an anomaly from present-day. I understand where this is coming from, but I would argue that the uncertainty in historical cumulative emissions is also relevant to the uncertainty in the remaining budget, and discarding this does tend to artificially deflate the uncertainty in the remaining budget estimate.

Agreed, we removed the last sentence that was suggesting to calculate the remaining carbon budget as an anomaly from present-day. See response to the editor above.

Reviewer 2

L 61. I would suggest to move line 61-l 65 closer to the end of the abstract, after line 72. That makes the reading a bit more logical. To be honest, I am not quite sure of the added value of the projections. They are somewhat relevant, but maybe a bit out of place in the paper and would benefit from a separate paper explain more about the details and problems involved.

Rejected, we prefer to keep the flow in the abstract as it is. Describing the 2019 projections right after the 2018 carbon budget estimates.

L 107. Insert "fully" before accounted

Done

L449. Suggest that only in H&N peat burning and drainage are added. When reading line 456 one notices that this is also the case for BLUE. I would suggest to phrase this not as a discrepancy but as a similarity, so: "In both H& Blue…."

Agreed. Changes made accordingly. The new text now reads as follow:
"For both H&N2017 and BLUE, we add carbon emissions from peat burning based on the Global Fire Emission Database (GFED4s; van der Werf et al., 2017), and peat drainage, based on estimates by Hooijer et al. (2010) to the output of their bookkeeping model for the countries of Indonesia and Malaysia. Peat burning and emissions from the organic layers of drained peat soils, which are not captured by bookkeeping methods directly, need to be included to represent the substantially larger emissions and interannual variability due to synergies of land-use and climate variability in Southeast Asia, in particular during El-Niño events."

L 458. delete "also"

Done

l 742. In my understanding el-Nino is an atmosphere-ocean interaction, with a dominant variability of the order of a few years, rather than less than one year. I may be wrong but I do not quite understand this.

Reviewer is right. Misleading sentence has been removed.

L 935. I know you have a lot of figures, but I would prefer B4 to be in the main text, as it shows the history of the paper, and importantly the progress in calculating the budget.

Rejected, we always had this figure as supplementary information. It is instructive as it shows continuity across the annual global carbon budget assessment but it does not provide any new information that we feel relevant for the main reader.

L977. It is a pity that one of the reasons why one would prefer to use a DGVM (not so much for calculating land use change effects), for estimating the response of the sink to climate and CO2, does not clarify this issue. Is there not a clever way to separate these two effects? If not currently existing, what would be the way forward?

We revised the sentence to clarify that for the last decade the discrepancy is largely coming from the ELUC estimate, the DGVM being 33% larger than the bookkeeping models. The revised text reads as follow:
"Over the last decade, the land use emission estimate from the DGVMs is significantly larger than the bookkeeping estimate, mainly explaining why the DGVMs total atmosphere-to-land flux estimate is lower than the other estimates."

L993. While honest, it is disturbing that DGVMs cannot do well in terms of NEE and some of the other carbon variables. Last year I made a remark on lack of progress in inversions. In this case I would also like to see a stronger statement on their failings and maybe their way forward. The fact that they exist is in itself no good reason to use them.

It is unclear to us how much of this is a "failing". Reproducing NEE is not straightforward. NEE is benchmarked against the MPI-Jena fluxcom dataset and also the fluxnet site level data. The site data contributes more to the overall score, site data metrics have a 0.7 weighting and the Fluxcom data a 0.3 weighting. On the DGVM side, NEE is simply diagnosed from the balance between GPP and ecosystem respiration (Ra+Rh). We are well aware that such comparison has intrinsic limitations. Site level flux data are controlled by the local meteorology, as opposed to the DGVMs driven by global climate forcing (CRU-JRA). Also fluxnet site level data and hence fluxcom global dataset do not account for land use, fires or disturbances, while the DGVMs do in the simulations benchmarked here. Even if not explicitly accounted in GPP-Ra-Rh, it is implicitly included as GPP, Ra and Rh are affected by land use change, fires or disturbances that have occurred previously (a legacy effect).
Also, as discussed in the manuscript (section 2.5), the benchmarking is not used to select models. The 3 criteria used for models inclusion in the budget as described in section 2.5.2 are only based global NBP SLAND and ELUC estimates, not on the iLAMB benchmarking of individual variables. Currently, we would not feel confident using criteria arising from the benchmarking itself as there isn't yet any consensus on which observations and which associated metrics to be used to weight/select models in order to get the best estimate of the land carbon sink or the land use emissions.

L979-l1001. It would be nice if the uncertainties mentioned here would be made comparable, for instance by giving bias and RSME for all three of them in similar units.

This is unfortunately impossible. RMSE is given in the units of the variable benchmarked. The benchmark for the ocean models uses pco2 estimates (in microatm). For the DGVMs models several variables with different units are benchmarked (gC/m2, gC/m2/yr, mm/yr, m2/m2, etc) . Inversions are benchmarked against atmospheric CO2 (in ppm).

L1023. factor>factors

Done

L1143. There is increasing literature on the impact of land management, not just forest management. I would expand this statement by either adding a sentence on other land management or just delete the word forest.

Done, new text reads as:
"They could either reflect a bias in the inversions or missing processes or biases in the process models, such as the lack of adequate parameterizations for land management for the DGVMs."

L1147. Not sure the standard reply of getting more observations will help here. We have gotten a lot more in recent years. Maybe there still is a lack of understanding that needs to be clarified.

We clarified in the text how observations combined with process understanding could help. New text reads as:
"Resolving the differences in the Northern Hemisphere land sink will require the consideration and inclusion of larger volumes of semi-continuous observations of concentrations, fluxes as well as auxiliary variables collected from (tall) towers close to the surface CO_2 exchange. Moreover, effective use of such information would demand a more process-based approach to land-surface exchange of CO_2 than currently employed in inverse models. Such process-based approach would represent constraints on carbon exchange derived from local observations and biogeochemical relations on multiple time-scales, which in turn would be constrained by the regional-to-continental scale mass-balance of atmospheric CO_2. Some of these near-surface data are now becoming available, but not used in the current inverse models sometimes due to the short records, and sometimes because the coarse transport models cannot adequately represent these time series."

L 1287-1291. I understand the caution the authors find appropriate, but lines 1289-1291 are now incomprehensible. It is also the question why this cannot be used in this way? It would be nice to see the current results being so strong that they could be used!

Done, sentence has been removed, see response to editor.

Another suggestion is to move the conclusions forward to after the discussion and end the paper with data availability. This would make the paper more readable for the majority of the authors who do not wish to dive into the data sources.

Done, see response to editor.

One final remark. It would help in reviewing the paper, if changes compared to last year are highlighted. That helps concentrating reviewers of a 130-page paper.

Sorry for not doing this this time, we'll do it next year.

Reviewer 3

1) Who will read this paper? As it stands, it is primarily a reference for scientists who are interested in the details of where the datasets come from and how they were compiled and synthesised into the global numbers presented here. As such it is quite comprehensive and complete, and thus adequate for a data paper in ESSD. However, the global carbon budget is also of relevance for stakeholders as the authors of this paper allude to. For this readership the paper is way too complicated and detailed. Non-specialists and non-carbon cycle scientists will get the impression that understanding the global carbon balance is a very complex undertaking. Even the key information of the whole paper (except for Figure 2), Tables 5 and 6 are now very complicated - compare this e.g. with the global carbon budget table in the first assessment report of IPCC (1992, p. 13). The numbers given there are almost the same as those in the present Table 6 for the decade 1980-89 (within their or the present uncertainties). And at that time no sophisticated process models were used to establish the global budget. Thus the concept of the global carbon cycle must be fundamentally quite simple. I think a terse kind of "policymaker summary" summarising the key messages/numbers would make very much sense. And much of the present detailed analysis/synthesis/model intercomparison and model evaluation material could go into an appendix as reference and documentation.

This paper is a living document intending to give an annual update of the full global carbon cycle, including all anthropogenic emissions the change in atmospheric CO_2 and the partitioning between land and ocean carbon sinks at global and regional level, going to national level for fossil fuel emissions. This effort is significantly more comprehensive than the IPCC 1992 assessment. By the way, it is unclear to us what the reviewers refers to with IPCC 92, p13 as this page presents the some results (including CO_2 emissions) following the six according to the 6 IPCC 1992 greenhouse gas scenarios, not comparable to our current assessment of contemporary and historical global carbon budget. That being said we are aware that policymakers are not very likely to read the whole of the ESSD paper, our main target is the scientific community. The global carbon project always provides companion papers focusing more on some specific, more policy relevant aspects of the carbon cycle. Also, in addition to the companion papers, the publication of the ESSD paper always comes along a large amount of material, such as the global carbon budget slides, a list of key messages, and press releases aimed at a larger audience, including policymakers. This communication and dissemination strategy has been proven being extremely successful in the past.

2) In-line with the comment above, I believe the present methodology is way too much based on comprehensive models. Observational constraints for the budget or individual terms are only used as (coarse) evaluation of the complex process-based models. There are several non-model based approaches (e.g. isotopes, oxygen, bottom-up inventories, flux estimates etc.) which could provide independent constraints on the global budget. And it would also better highlight the value of observational data. The present model evaluation does this to some extent, but is not readily visible. Also, complex model results are often for the non-specialists, especially for the skeptics (!), (a) suspicious, (b) can not be reproduced and (c) provide no insight. In climate science we have a whole hierarchy from complex high-end climate models over EMICS to

conceptual simple models, which all are useful in their domain and which complement each other. Why not here? Ultimately the global carbon budget consists of just 4 independent time series that need to be explained and understood. I think it would make the message of the paper here much more strong - also to the non-specialist.

The global carbon budget is based on all available sources of evidences. This includes modelling of the land and ocean carbon sinks, but also includes atmospheric observations of CO2, atmospheric observations of O2/N2 ratio and oceanic measurements of pCO2. O2/N2 data are used to constrain the model results, providing a unique constrain on the global partitioning between the global land and global ocean sinks on decadal average. The pCO2 data are used to provide additional constrains on the ocean CO2 sink, using neural network models to upscale the pCO2 data and provide global ocean coverage of CO2 fluxes. In addition, atmospheric inversions that make use of the entire atmospheric CO2 observation network are also used in the global carbon budget to further evaluate the land/ocean partitioning and the regional distribution of the sinks (northern hemisphere, tropics, southern hemisphere). As for the complexity of the models used, we are using state-of-the-art models for the estimation of the land and ocean carbon sinks as well as for the estimation of the emissions from land-use changes. We are not aware of any simple models (such as an EMIC for the carbon cycle) that would provide similar estimates with the same level of understanding of the key driving processes. One could envisage a simple box model of the carbon cycle that generate global mean land and ocean sinks, but such model would very likely not be able to inform on regional aspects as presented here, nor it would be able to inform on annual changes that are largely driven by climate variability such as ENSO. Finally, we also note that IPCC assessment are adopting the same methodology as ours, AR4, AR5 and probably AR6 using the global carbon budget annual estimates and the decadal results presented here for their periodic assessments.

p. 5 l 57: write "fossil emissions"

Done

p. 5 l 59: The canonical factor converting ppm to GtC is 2.124. If so, 2.4 ppm/yr = 5.1 GtC/yr. Where does the small (0.01ppm) uncertainty for the decadal CO2 increase come from?

Thanks for spotting this. The reviewer is right. CO2 growth rate for 2018 was 2.42 ppm which equals to 5.1 GtC. This has been corrected in the manuscript. The assessment of uncertainty on the decadal CO2 growth rate is explained in the main text, section 2.3.1: "At this time, we estimate the uncertainty of the decadal averaged growth rate after 1980 at 0.02 GtC yr-1 based on the calibration and the annual growth rate uncertainty, but stretched over a 10-year interval."

p.6 l 90: Indicate the year of the beginning of the industrial era

Done, sentence now reads:
"The global carbon budget presented here refers to the mean, variations, and trends in the perturbation of CO_2 in the environment, referenced to the beginning of the Industrial Era (defined here as 1750)"

p. 7 l 115: Where does the factor 1 ppm = 2.124 GtC come from?

As written in that sentence, this conversion factor is described in Table 1, with references given (Ballantyne et al. (2012). We added the reference in the main text for clarity.

p. 21 l 533: Why are only positive E_LUC model output retained? Does this mean that the entire data of a model with E_LUC<0 during the 1990s is discarded? Or are negative values set to zero? This procedure is not described clearly.

We clarified that sentence as follow:
"As a criterion for inclusion in this carbon budget, we only retain models that simulate outputs with a positive ELUC, i.e. a positive flux to the atmosphere, during the 1990s, as assessed in the IPCC AR4 (Denman et al., 2007) and AR5 (Ciais et al., 2013)."

p. 22 l 583 and Table 1: AR5 used as conversion factor 2.12 PgC/ppm, compiled in Prather et al., 2012.

Indeed AR5 used 2.12, but, for several years, we have been using 2.124 which is more accurate, as described in Ballantyne et al 2012.

p. l 943: The grow rates in %/yr are not shown in Figure 5.

Indeed. reference to Fig 5 has been removed from that sentence.

p. 37 l 1009: This sentence could be challenged: Formally, the models were selected to fall within some consensus interval in 1990s, the models are driven by atmospheric CO2 and clearly, development was not "blind" to the global carbon budget constraint.

The reviewer is only partially correct. We check if models are consistent with the atmospheric constraint (primarily from O2/N2 budget) for the 1990s, and we didn't have to exclude any model results, all models passed this test. That being said, as the reviewer pointed out, there is potentially some level of model parameters tuning done by the modelling group over time in order for their model to "fit in" get the "desired" results (similarly to climate models getting the historical trends). This is extremely difficult (if not impossible) to assess. However, as mentioned in the text, the budget constraint is only applied for the 1990s, while the overall near-zero mean and trend in the budget imbalance we report is robust over every decade of the full 60 years record (1959-2018), as shown in Table 6. The budget imbalance is under 0.5GtC/yr for every decade, despite significant variability in the decadal CO2 growth rate and airborne fraction (ranging from 0.39 to 0.51 on decadal average).

p 39 l 1081: Why is much of the material in section 3.2.3 not already included in section 3.1? Section 3.2 focuses on the last decade, while the key Figure in section 3.2.3 (fig 4) shows the entire classical budget broken into the three latitude bands. I understand that most of the observational constraints are available more for the recent decade(s), but much of the arguments put forward here relate to the time frame since the 1980's (e.g. the discussion of the land budgets of the northern extratropics vs the tropics). I'd move section 3.2.3 up into section 3.1.

We are aware that Figure 8 shows indeed the regional carbon budget since 1960s (with inversions data from 1980s only). However, the text is focusing on the last decade (2009-2018 period). hence we feel it is more appropriate to keep that sub-section where it currently is, that is under section 3.2 Global carbon budget for the last decade (2009 – 2018).

p 46 l 1287: This last paragraph is difficult to understand for the un-initated, since it moves beyond pure carbon cycle science. I'd restrict to say here (in a carbon cycle data paper) that there are remaining uncertainties in the cumulative budgets. Everything related to scenarios, remaining carbon budget, and the time frames for which it is to be calculated is nor really the topic of this paper.

Done, see previous response to the editor.

p 93, Table 3: Am astonished: up to the budget in 2016 the terrestrial sink was estimated as a residual; the DGVM models were used as a corroboration. "

Indeed, this was the case until 2016. Now DGVMs are used to provide an independent estimate of the land sink. Thank you for noting the improvement in our methodology.

Global Carbon Budget 2019

Pierre Friedlingstein[1,2], Matthew W. Jones[3], Michael O'Sullivan[1], Robbie M. Andrew[4], Judith Hauck[5], Glen P. Peters[4], Wouter Peters[6,7], Julia Pongratz[8,9], Stephen Sitch[10], Corinne Le Quéré[3], Dorothee C. E. Bakker[3], Josep G. Canadell[11], Philippe Ciais[12], Rob Jackson[13], Peter Anthoni[14], Leticia Barbero[15,16], Ana Bastos[8], Vladislav Bastrikov[12], Meike Becker[17,18], Laurent Bopp[2], Erik Buitenhuis[3], Naveen Chandra[19], Frédéric Chevallier[12], Louise P. Chini[20], Kim I. Currie[21], Richard A. Feely[22], Marion Gehlen[12], Dennis Gilfillan[23], Thanos Gkritzalis[24], Daniel S. Goll[25], Nicolas Gruber[26], Sören Gutekunst[27], Ian Harris[28], Vanessa Haverd[11], Richard A. Houghton[29], George Hurtt[20], Tatiana Ilyina[9], Atul K. Jain[30], Emilie Joetzjer[31], Jed O. Kaplan[32], Etsushi Kato[33], Kees Klein Goldewijk[34,35], Jan Ivar Korsbakken[4], Peter Landschützer[9], Siv K. Lauvset[36,18], Nathalie Lefèvre[37], Andrew Lenton[38,39], Sebastian Lienert[40], Danica Lombardozzi[41], Gregg Marland[23], Patrick C. McGuire[42], Joe R. Melton[43], Nicolas Metzl[37], David R. Munro[44], Julia E. M. S. Nabel[9], Shin-Ichiro Nakaoka[45], Craig Neill[38], Abdirahman M. Omar[36,18], Tsuneo Ono[46], Anna Peregon[12,47], Denis Pierrot[15,16], Benjamin Poulter[48], Gregor Rehder[49], Laure Resplandy[50], Eddy Robertson[51], Christian Rödenbeck[52], Roland Séférian[53], Jörg Schwinger[36,18], Naomi Smith[6,54], Pieter P. Tans[55], Hanqin Tian[56], Bronte Tilbrook[38,57], Francesco N Tubiello[58], Guido R. van der Werf[59], Andrew J. Wiltshire[51], Sönke Zaehle[52]

[1] College of Engineering, Mathematics and Physical Sciences, University of Exeter, Exeter EX4 4QF, UK

[2] Laboratoire de Météorologie Dynamique, Institut Pierre-Simon Laplace, CNRS-ENS-UPMC-X, Département de Géosciences, Ecole Normale Supérieure, 24 rue Lhomond, 75005 Paris, Franc

[3] Tyndall Centre for Climate Change Research, School of Environmental Sciences, University of East Anglia, Norwich Research Park, Norwich NR4 7TJ, UK

[4] CICERO Center for International Climate Research, Oslo 0349, Norway

[5] Alfred Wegener Institute Helmholtz Centre for Polar and Marine Research, Postfach 120161, 27515 Bremerhaven, Germany

[6] Wageningen University, Environmental Sciences Group, P.O. Box 47, 6700AA, Wageningen, The Netherlands

[7] University of Groningen, Centre for Isotope Research, Groningen, The Netherlands

[8] Ludwig-Maximilans-Universität Munich, Luisenstr. 37, 80333 München, Germany

[9] Max Planck Institute for Meteorology, Hamburg, Germany

[10] College of Life and Environmental Sciences, University of Exeter, Exeter EX4 4RJ, UK

[11] CSIRO Oceans and Atmosphere, GPO Box 1700, Canberra, ACT 2601, Australia

[12] Laboratoire des Sciences du Climat et de l'Environnement, Institut Pierre-Simon Laplace, CEA-CNRS-UVSQ, CE Orme des Merisiers, 91191 Gif sur Yvette Cedex, France

[13] Department of Earth System Science, Woods Institute for the Environment, and Precourt Institute for Energy, Stanford University, Stanford, CA 94305–2210, United States of America

[14] Karlsruhe Institute of Technology, Institute of Meteorology and Climate, Research/Atmospheric Environmental Research, 82467 Garmisch-Partenkirchen, Germany

[15] Cooperative Institute for Marine and Atmospheric Studies, Rosenstiel School for Marine and Atmospheric Science, University of Miami, Miami, FL 33149, USA

[16] National Oceanic & Atmospheric Administration/Atlantic Oceanographic & Meteorological Laboratory (NOAA/AOML), Miami, FL 33149, USA

[17] Geophysical Institute, University of Bergen, Bergen, Norway

[18] Bjerknes Centre for Climate Research, Allégaten 70, 5007 Bergen, Norway

[19] Earth Surface System Research Center (ESS), Japan Agency for Marine-Earth Science and Technology (JAMSTEC), Yokohama, 236-0001, Japan

[20] Department of Geographical Sciences, University of Maryland, College Park, Maryland 20742, USA

[21] NIWA / UoO Research Centre for Oceanography, PO Box 56, Dunedin 9054, New Zealand

[22] Pacific Marine Environmental Laboratory, National Oceanic and Atmospheric Administration, 7600 Sand Point Way NE, Seattle, WA 98115-6349, USA

[23] Research Institute for Environment, Energy, and Economics, Appalachian State University, Boone, North Carolina, USA

[24] Flanders Marine Institute (VLIZ), InnovOceanSite, Wandelaarkaai 7, 8400 Ostend, Belgium

[25] Lehrstuhl für Physische Geographie mit Schwerpunkt Klimaforschung, Universität Augsburg, Augsburg, Germany

[26] Environmental Physics Group, ETH Zürich, Institute of Biogeochemistry and Pollutant Dynamics and Center for Climate Systems Modeling (C2SM)

[27] GEOMAR Helmholtz Centre for Ocean Research Kiel, Düsternbrooker Weg 20, 24105 Kiel, Germany

[28] NCAS-Climate, Climatic Research Unit, School of Environmental Sciences, University of East Anglia, Norwich Research Park, Norwich, NR4 7TJ, UK

[29] Woods Hole Research Center (WHRC), Falmouth, MA 02540, USA

[30] Department of Atmospheric Sciences, University of Illinois, Urbana, IL 61821, USA

[31] Centre National de Recherche Meteorologique, Unite mixte de recherche 3589 Météo-France/CNRS, 42 Avenue Gaspard Coriolis, 31100 Toulouse, France

[32] Department of Earth Sciences, University of Hong Kong, Pokfulam Road, Hong Kong

[33] Institute of Applied Energy (IAE), Minato-ku, Tokyo 105-0003, Japan

[34] PBL Netherlands Environmental Assessment Agency, Bezuidenhoutseweg 30, P.O. Box 30314, 2500 GH, The Hague, the Netherlands

[35] Faculty of Geosciences, Department IMEW, Copernicus Institute of Sustainable Development, Heidelberglaan 2, P.O. Box 80115, 3508 TC, Utrecht, Netherlands

[36] NORCE Norwegian Research Centre, NORCE Climate, Jahnebakken 70, 5008 Bergen, Norway

[37] LOCEAN/IPSL laboratory, Sorbonne Université, CNRS/IRD/MNHN, Paris, France

[38] CSIRO Oceans and Atmosphere, Hobart, TAS, Australia

[39] Institute for Marine and Antarctic Studies, University of Tasmania, Hobart, Tasmania

[40] Climate and Environmental Physics, Physics Institute and Oeschger Centre for Climate Change Research, University of Bern, Bern, Switzerland

[41] National Center for Atmospheric Research, Climate and Global Dynamics, Terrestrial Sciences Section, Boulder, CO 80305, USA

[42] Department of Meteorology, Department of Geography & Environmental Science, National Centre for Atmospheric Science, University of Reading, Reading, UK,

[43] Climate Research Division, Environment and Climate Change Canada, Victoria, BC, Canada

[44] Cooperative Institute for Research in Environmental Sciences, University of Colorado, Boulder, CO, USA

[45] Center for Global Environmental Research, National Institute for Environmental Studies (NIES), 16-2 Onogawa, Tsukuba, Ibaraki, 305-8506, Japan

[46] Japan Fisheries Research and Education Agency, 2-12-4 Fukuura, Kanazawa-Ku, Yokohama 236-8648, Japan

[47] Institute of Soil Science and Agrochemistry, Siberian Branch Russian Academy of Sciences (SB RAS), Pr. Akademika Lavrentyeva, 8/2, 630090, Novosibirsk, Russia

[48] NASA Goddard Space Flight Center, Biospheric Sciences Laboratory, Greenbelt, Maryland 20771, USA

[49] Leibniz Institute for Baltic Sea Research Warnemuende (IOW), Seestrasse 15; 18119 Rostock, Germany

[50] Princeton University, Department of Geosciences and Princeton Environmental Institute, Princeton, NJ, USA

[51] Met Office Hadley Centre, FitzRoy Road, Exeter EX1 3PB, UK

[52] Max Planck Institute for Biogeochemistry, P.O. Box 600164, Hans-Knöll-Str. 10, 07745 Jena, Germany

[53] CNRM (Météo-France/CNRS)-UMR 3589

[54] ICOS Carbon Portal, Lund University, Lund, Sweden

[55] National Oceanic & Atmospheric Administration, Earth System Research Laboratory (NOAA/ESRL), Boulder, CO 80305, USA

[56] International Center for Climate and Global Change Research, School of Forestry and Wildlife Sciences, Auburn University, 602 Ducan Drive, Auburn, AL 36849, USA

[57] Australian Antarctic Partnership Program, University of Tasmania, Hobart, Australia

[58] Statistics Division, Food and Agriculture Organization of the United Nations, Via Terme di Caracalla, Rome 00153, Italy

[59] Faculty of Science, Vrije Universiteit, Amsterdam, The Netherlands

Correspondence: Pierre Friedlingstein (p.friedlingstein@exeter.ac.uk)

Abstract

Accurate assessment of anthropogenic carbon dioxide (CO_2) emissions and their redistribution among the atmosphere, ocean, and terrestrial biosphere – the 'global carbon budget' – is important to better understand the global carbon cycle, support the development of climate policies, and project future climate change. Here we describe data sets and methodology to quantify the five major components of the global carbon budget and their uncertainties. Fossil CO_2 emissions (E_{FF}) are based on energy statistics and cement production data, while emissions from land-use change (E_{LUC}), mainly deforestation, are based on land-use and land-use change data and bookkeeping models. Atmospheric CO_2 concentration is measured directly and its growth rate (G_{ATM}) is computed from the annual changes in concentration. The ocean CO_2 sink (S_{OCEAN}) and terrestrial CO_2 sink (S_{LAND}) are estimated with global process models constrained by observations. The resulting carbon budget imbalance (B_{IM}), the difference between the estimated total emissions and the estimated changes in the atmosphere, ocean, and terrestrial biosphere, is a measure of imperfect data and understanding of the contemporary carbon cycle. All uncertainties are reported as ±1σ. For the last decade available (2009-2018), E_{FF} was 9.5 ± 0.5 GtC yr^{-1}, E_{LUC} 1.5 ± 0.7 GtC yr^{-1}, G_{ATM} 4.9 ± 0.02 GtC yr^{-1} (2.3 ± 0.01 ppm yr^{-1}), S_{OCEAN} 2.5 ± 0.6 GtC yr^{-1}, and S_{LAND} 3.2 ± 0.6 GtC yr^{-1}, with a budget imbalance B_{IM} of 0.4 GtC yr^{-1} indicating overestimated emissions and/or underestimated sinks. For year 2018 alone, the growth in E_{FF} was about 2.1% and fossil emissions increased to 10.0 ± 0.5 GtC yr^{-1}, reaching 10 GtC yr^{-1} for the first time in history, E_{LUC} was 1.5 ± 0.7 GtC yr^{-1}, for a total anthropogenic CO_2 emissions of 11.5± 0.9 GtC yr^{-1} (42.5 ± 3.3 $GtCO_2$). Also for 2018, G_{ATM} was 5.1 ± 0.2 GtC yr^{-1} (2.4 ± 0.1 ppm yr^{-1}), S_{OCEAN} was 2.6 ± 0.6 GtC yr^{-1} and S_{LAND} was 3.5 ± 0.7 GtC yr^{-1}, with a B_{IM} of 0.3 GtC. The global atmospheric CO_2 concentration reached 407.38 ± 0.1 ppm averaged over 2018. For 2019, preliminary data for the first 6-10 months indicate a reduced growth in E_{FF} of +0.5% (range of −0.3% to 1.4%) based on national emissions projections for China, USA, the EU and India, and projections of Gross Domestic Product corrected for recent changes in the carbon intensity of the economy for the rest of the world. Overall, The mean and trend in the five components of the global carbon budget are consistently estimated over the period 1959-2018, but discrepancies of up to 1 GtC yr^{-1} persist for the representation of semi-decadal variability in CO_2

fluxes. A detailed comparison among individual estimates and the introduction of a broad range of observations shows: (1) no consensus in the mean and trend in land-use change emissions over the last decade, (2) a persistent low agreement between the different methods on the magnitude of the land CO_2 flux in the northern extra-tropics, and (3) an apparent underestimation of the CO_2 variability by ocean models outside the tropics. This living data update documents changes in the methods and data sets used in this new global carbon budget and the progress in understanding of the global carbon cycle compared with previous publications of this data set (Le Quéré et al., 2018b, 2018a, 2016, 2015b, 2015a, 2014, 2013). The data generated by this work are available at https://doi.org/10.18160/gcp-2019 (Friedlingstein et al., 2019).

1   Introduction

The concentration of carbon dioxide (CO_2) in the atmosphere has increased from approximately 277 parts per million (ppm) in 1750 (Joos and Spahni, 2008), the beginning of the Industrial Era, to 407.38 ± 0.1 ppm in 2018 (Dlugokencky and Tans, 2019); Fig. 1). The atmospheric CO_2 increase above pre-industrial levels was, initially, primarily caused by the release of carbon to the atmosphere from deforestation and other land-use change activities (Ciais et al., 2013)(Ciais et al., 2013). While emissions from fossil fuels started before the Industrial Era, they only became the dominant source of anthropogenic emissions to the atmosphere from around 1950 and their relative share has continued to increase until present. Anthropogenic emissions occur on top of an active natural carbon cycle that circulates carbon between the reservoirs of the atmosphere, ocean, and terrestrial biosphere on time scales from sub-daily to millennia, while exchanges with geologic reservoirs occur at longer timescales (Archer et al., 2009).

The global carbon budget presented here refers to the mean, variations, and trends in the perturbation of CO_2 in the environment, referenced to the beginning of the Industrial Era (defined here as 1750). This paper describes the components of the global carbon cycle over the historical period with a stronger focus on the recent period (since 1958, onset of atmospheric CO_2 measurements), the last decade (2009-2018) and the current year (2019). We quantify the input of CO_2 to the atmosphere by emissions from human activities, the growth rate of atmospheric CO_2 concentration, and the resulting changes in the storage of carbon in the land and ocean reservoirs in response to increasing atmospheric CO_2 levels, climate change and variability, and other anthropogenic and natural changes (Fig. 2). An understanding of this

perturbation budget over time and the underlying variability and trends of the natural carbon cycle is necessary to understand the response of natural sinks to changes in climate, CO_2 and land-use change drivers, and the permissible emissions for a given climate stabilization target. Note that this paper does not estimate the remaining future carbon emissions consistent with a given climate target (often referred to as the remaining carbon budget (Millar et al., 2017; Rogelj et al., 2016, 2019).

The components of the CO_2 budget that are reported annually in this paper include separate estimates for the CO_2 emissions from (1) fossil fuel combustion and oxidation from all energy and industrial processes and cement production (E_{FF}; GtC yr^{-1}) and (2) the emissions resulting from deliberate human activities on land, including those leading to land-use change (E_{LUC}; GtC yr^{-1}); and their partitioning among (3) the growth rate of atmospheric CO_2 concentration (G_{ATM}; GtC yr^{-1}), and the uptake of CO_2 (the 'CO_2 sinks') in (4) the ocean (S_{OCEAN}; GtC yr^{-1}) and (5) on land (S_{LAND}; GtC yr^{-1}). The CO_2 sinks as defined here conceptually include the response of the land (including inland waters and estuaries) and ocean (including coasts and territorial sea) to elevated CO_2 and changes in climate, rivers, and other environmental conditions, although in practice not all processes are fully accounted for (see Section 2.7). The global emissions and their partitioning among the atmosphere, ocean and land are in reality in balance, however due to imperfect spatial and/or temporal data coverage, errors in each estimate, and smaller terms not included in our budget estimate (discussed in Section 2.7), their sum does not necessarily add up to zero. We estimate a budget imbalance (B_{IM}), which is a measure of the mismatch between the estimated emissions and the estimated changes in the atmosphere, land and ocean, with the full global carbon budget as follows:

$$E_{FF} + E_{LUC} = G_{ATM} + S_{OCEAN} + S_{LAND} + B_{IM} \hspace{4cm} (1)$$

G_{ATM} is usually reported in ppm yr^{-1}, which we convert to units of carbon mass per year, GtC yr^{-1}, using 1 ppm = 2.124 GtC (Ballantyne et al., 2012; Table 1). We also include a quantification of E_{FF} by country, computed with both territorial and consumption-based accounting (see SectionSect. 2), and discuss missing terms from sources other than the combustion of fossil fuels (see SectionSect. 2.7).

The CO_2 budget has been assessed by the Intergovernmental Panel on Climate Change (IPCC) in all assessment reports (Prentice et al., 2001; Schimel et al., 1995; Watson et al., 1990; Denman et al., 2007; Ciais et al., 2013)Ballantyne et al., 2012(Prentice et al., 2001; Schimel et al., 1995;

Watson et al., 1990; Denman et al., 2007; Ciais et al., 2013), and by others (e.g. Ballantyne et al., 2012). The IPCC methodology has been revised and used by the Global Carbon Project (GCP, www.globalcarbonproject.org, last access: 27 September 2019), which has coordinated this cooperative community effort for the annual publication of global carbon budgets for the year 2005 Raupach et al., 2007(Raupach et al., 2007; including fossil emissions only), year 2006 (Canadell et al., 2007), year 2007 (published online; GCP, 2007), year 2008 (Le Quéré et al., 2009), year (Friedlingstein et al., 2010)2010 (Peters et al., 2012b), year (Peters et al., 2012b)2012 (Le Quéré et al., 2013; Peters et al., 2013), year (Le Quéré et al., 2013; Peters et al., 2013)2013 (Le Quéré et al., 2014), year 2014 (Le Quéré et al., 2015a; Friedlingstein et al., 2014), year 2015 (Jackson et al., 2016; Le Quéré et al., 2015b), year (Le Quéré et al., 2014)(Le Quéré et al., 2015a; Friedlingstein et al., 2014)(Jackson et al., 2016; Le Quéré et al., 2015b)(Le Quéré et al., 2016)2016 (Le Quéré et al., 2016), year 2017 (Le Quéré et al., 2018a; Peters et al., 2017) and most recently year 2018 (Le Quéré et al., 2018b; Jackson et al., 2018). Each of these papers updated previous estimates with the latest available information for the entire time series.

We adopt a range of ±1 standard deviation (σ) to report the uncertainties in our estimates, representing a likelihood of 68% that the true value will be within the provided range if the errors have a Gaussian distribution and no bias is assumed. This choice reflects the difficulty of characterising the uncertainty in the CO_2 fluxes between the atmosphere and the ocean and land reservoirs individually, particularly on an annual basis, as well as the difficulty of updating the CO_2 emissions from land-use change. A likelihood of 68% provides an indication of our current capability to quantify each term and its uncertainty given the available information. For comparison, the Fifth Assessment Report of the IPCC (AR5) generally reported a likelihood of 90% for large data sets whose uncertainty is well characterised, or for long time intervals less affected by year-to-year variability. Our 68% uncertainty value is near the 66% which the IPCC characterises as 'likely' for values falling into the ±1σ interval. The uncertainties reported here combine statistical analysis of the underlying data and expert judgement of the likelihood of results lying outside this range. The limitations of current information are discussed in the paper and have been examined in detail elsewhere (Ballantyne et al., 2015; Zscheischler et al., 2017). We also use a qualitative assessment of confidence level to characterise the annual estimates from each term based on the type, amount, quality and consistency of the evidence as defined by the IPCC (Stocker et al., 2013).

Deleted:).

Deleted: (

Deleted: ;

Deleted: (Canadell et al., 2007),

Deleted: GCP, 2007),

Deleted: (Le Quéré et al., 2009), year 2009 (Friedlingstein et al., 2010),

Deleted: 2009

Deleted: ,

Deleted: 2010

Deleted: ,

Deleted: 2012

Deleted: ,

Deleted: 2013

Deleted: , year 2014

Deleted: , year 2015

Deleted: , year 2016

Deleted: ,

Deleted: (Le Quéré et al., 2018a; Peters et al., 2017)

Deleted: (Le Quéré et al., 2018b; Jackson et al., 2018).

Deleted: (Ballantyne et al., 2015; Zscheischler et al., 2017).

Deleted: (Stocker et al., 2013).

All quantities are presented in units of gigatonnes of carbon (GtC, 10^{15} gC), which is the same as petagrams of carbon (PgC; Table 1). Units of gigatonnes of CO_2 (or billion tonnes of CO_2) used in policy are equal to 3.664 multiplied by the value in units of GtC.

This paper provides a detailed description of the data sets and methodology used to compute the global carbon budget estimates for the industrial period, from 1750 to 2018, and in more detail for the period since 1959. It also provides decadal averages starting in 1960 including the last decade (2009-2018), results for the year 2018, and a projection for year 2019. Finally it provides cumulative emissions from fossil fuels and land-use change since the year 1750, the pre-industrial period; and since the year 1850, the reference year for historical simulations in IPCC (AR6(Stocker et al., 2013)). This paper is updated every year using the format of 'living data' to keep a record of budget versions and the changes in new data, revision of data, and changes in methodology that lead to changes in estimates of the carbon budget. Additional materials associated with the release of each new version will be posted at the Global Carbon Project (GCP) website (http://www.globalcarbonproject.org/carbonbudget, last access: 27 September 2019), with fossil fuel emissions also available through the Global Carbon Atlas (http://www.globalcarbonatlas.org, last access: 4 December 2019). With this approach, we aim to provide the highest transparency and traceability in the reporting of CO_2, the key driver of climate change.

2 Methods

Multiple organizations and research groups around the world generated the original measurements and data used to complete the global carbon budget. The effort presented here is thus mainly one of synthesis, where results from individual groups are collated, analysed and evaluated for consistency. We facilitate access to original data with the understanding that primary data sets will be referenced in future work (see Table 2 for how to cite the data sets). Descriptions of the measurements, models, and methodologies follow below and detailed descriptions of each component are provided elsewhere.

This is the 14th version of the global carbon budget and the eighth revised version in the format of a living data update in Earth System Science Data. It builds on the latest published global carbon budget of (Le Quéré et al., 2018b). The main changes are: (1) the inclusion of data to year 2018 (inclusive) and a projection for the global carbon budget for year 2019; (2) further developments to the metrics that evaluate components of the individual models used to

estimate S_{OCEAN} and S_{LAND} using observations, as an effort to document, encourage and support model improvements through time; (3) a projection of the 'rest of world' emissions by fuel type; (4) changed method for projecting current-year global atmospheric CO_2 concentration increment; and (5) global emissions are calculated as the sum of countries' emissions and bunker fuels rather than taken directly from Carbon Dioxide Information Analysis Center (CDIAC). The main methodological differences between recent annual carbon budgets (2015-2018) are summarised in Table 3 and changes since 2005 are provided in Table A7.

2.1 Fossil CO_2 emissions (E_{FF})

2.1.1 Emissions estimates

The estimates of global and national fossil CO_2 emissions (E_{FF}) include the combustion of fossil fuels through a wide range of activities (e.g. transport, heating and cooling, industry, fossil industry own use & natural gas flaring), the production of cement, and other process emissions (e.g. the production of chemicals & fertilizers). The estimates of E_{FF} rely primarily on energy consumption data, specifically data on hydrocarbon fuels, collated and archived by several organisations (Andres et al., 2012). We use four main data sets for historical emissions (1750-2018):

1. Global and national emission estimates for coal, oil, natural gas as well as peat fuel extraction from CDIAC for the time period 1750-2016 (Gilfillan et al., 2019), as it is the only data set that extends back to 1750 by country.

2. Official UNFCCC national inventory reports annually for 1990-2017 for the 42 Annex I countries in the UNFCCC (UNFCCC, 2019). We assess these to be the most accurate estimates because they are compiled by experts within countries that have access to the most detailed data, and they are periodically reviewed.

3. The BP Statistical Review of World Energy (BP, 2019), as these are the most up-to-date estimates of national energy statistics.

4. Global and national cement emissions updated from (Andrew, 2018) following (Andrew, in review)Andrew (2019) to include the latest estimates of cement production and clinker ratios.

In the following section we provide more details for each data set and describe the additional modifications that are required to make the data set consistent and usable.

CDIAC: The CDIAC estimates have been updated annually to the year 2016, derived primarily from energy statistics published by the United Nations (UN, 2018). Fuel masses and volumes are converted to fuel energy content using country-level coefficients provided by the UN, and then converted to CO_2 emissions using conversion factors that take into account the relationship between carbon content and energy (heat) content of the different fuel types (coal, oil, natural gas, natural gas flaring) and the combustion efficiency (Marland and Rotty, 1984).

UNFCCC: Estimates from the UNFCCC national inventory reports follow the IPCC guidelines (IPCC, 2006), but have a slightly larger system boundary than CDIAC by including emissions coming from carbonates other than in cement manufacture. We reallocate the detailed UNFCCC estimates to the CDIAC definitions of coal, oil, natural gas, cement, and other to allow more consistent comparisons over time and between countries.

Specific country updates: China and Saudi Arabia: The most recent version of CDIAC introduces what appear to be spurious interannual variations for these two countries (IEA, 2018), therefore we use data from the 2018 global carbon budget (Le Quéré et al., 2018b). Norway: CDIAC's method of apparent consumption results in large errors for Norway, and we therefore overwrite emissions before 1990 with estimates based on official Norwegian statistics.

BP: For the most recent period when the UNFCCC and CDIAC estimates are not available, we generate preliminary estimates using energy consumption data from the BP Statistical Review of World Energy (Andres et al., 2014; BP, 2019; Myhre et al., 2009). We apply the BP growth rates by fuel type (coal, oil, natural gas) to estimate 2018 emissions based on 2017 estimates (UNFCCC Annex I countries), and to estimate 2017-2018 emissions based on 2016 estimates (remaining countries). BP's data set explicitly covers about 70 countries (96% of global energy emissions), and for the remaining countries we use growth rates from the sub-region the country belongs to. For the most recent years, natural gas flaring is assumed constant from the most recent available year of data (2017 for Annex I countries, 2016 for the remainder).

Cement: Estimates of emissions from cement production are taken directly from (Andrew, in review)Andrew (2019). Additional calcination and carbonation processes are not included explicitly here, except in national inventories provided by Annex I countries, but are discussed in Section 2.7.2.

Deleted: (UN, 2018).

Deleted: (Marland and Rotty, 1984).

Deleted: (IPCC, 2006),

Deleted: (IEA, 2018),

Deleted: (Le Quéré et al., 2018b).

Deleted: (Andres et al., 2014; BP, 2019; Myhre et al., 2009).

Deleted: .

Country mappings: The published CDIAC data set includes 257 countries and regions. This list includes countries that no longer exist, such as the USSR and Yugoslavia. We reduce the list to 214 countries by reallocating emissions to currently defined territories, using mass-preserving aggregation or disaggregation. Examples of aggregation include merging East and West Germany to the currently defined Germany. Examples of disaggregation include reallocating the emissions from former USSR to the resulting independent countries. For disaggregation, we use the emission shares when the current territories first appeared (e.g. USSR in 1992), and thus historical estimates of disaggregated countries should be treated with extreme care. In the case of the USSR, we were able to disaggregate 1990 and 1991 using data from the IEA. In addition, we aggregate some overseas territories (e.g. Réunion, Guadeloupe) into their governing nations (e.g. France) to align with UNFCCC reporting.

Global total: The global estimate is the sum of the individual countries' emissions and international aviation and marine bunkers. This is different to last year, where we used the independent global total estimated by CDIAC (combined with cement from Andrew (2018)). The CDIAC global total differs to the sum of the countries and bunkers since 1) the sum of imports in all countries is not equal to the sum of exports because of reporting inconsistencies, 2) changes in stocks, and 3) the share of non-oxidised carbon (e.g. as solvents, lubricants, feedstocks, etc.) at the global level is assumed to be fixed at the 1970's average while it varies in the country level data based on energy data (Andres et al., 2012). From the 2019 edition CDIAC now includes changes in stocks in the global total (pers. comm., Dennis Gilfillan), removing one contribution to this discrepancy. The discrepancy has grown over time from around zero in 1990 to over 500 $MtCO_2$ in recent years, consistent with the growth in non-oxidised carbon (IEA, 2018). To remove this discrepancy we now calculate the global total as the sum of the countries and international bunkers.

2.1.2 Uncertainty assessment for E_{FF}

We estimate the uncertainty of the global fossil CO_2 emissions at ±5% (scaled down from the published ±10 % at ±2σ to the use of ±1σ bounds reported here; Andres et al., 2012). This is consistent with a more detailed analysis of uncertainty of ±8.4% at ±2σ (Andres et al., 2014) and at the high-end of the range of ±5-10% at ±2σ reported by (Ballantyne et al., 2015). This includes an assessment of uncertainties in the amounts of fuel consumed, the carbon and heat contents of fuels, and the combustion efficiency. While we consider a fixed uncertainty of ±5%

for all years, the uncertainty as a percentage of the emissions is growing with time because of the larger share of global emissions from emerging economies and developing countries (Marland et al., 2009). Generally, emissions from mature economies with good statistical processes have an uncertainty of only a few per cent (Marland, 2008), while emissions from developing countries such as China have uncertainties of around ±10% (for ±1σ; Gregg et al., 2008). Uncertainties of emissions are likely to be mainly systematic errors related to underlying biases of energy statistics and to the accounting method used by each country.

We assign a medium confidence to the results presented here because they are based on indirect estimates of emissions using energy data (Durant et al., 2011). There is only limited and indirect evidence for emissions, although there is high agreement among the available estimates within the given uncertainty (Andres et al., 2012, 2014), and emission estimates are consistent with a range of other observations (Ciais et al., 2013)(Ciais et al., 2013), even though their regional and national partitioning is more uncertain (Francey et al., 2013).

2.1.3 Emissions embodied in goods and services

CDIAC, UNFCCC, and BP national emission statistics 'include greenhouse gas emissions and removals taking place within national territory and offshore areas over which the country has jurisdiction' (Rypdal et al., 2006) and are called territorial emission inventories. Consumption-based emission inventories allocate emissions to products that are consumed within a country, and are conceptually calculated as the territorial emissions minus the 'embodied' territorial emissions to produce exported products plus the emissions in other countries to produce imported products (Consumption = Territorial – Exports + Imports). Consumption-based emission attribution results (e.g. Davis and Caldeira, 2010) provide additional information to territorial-based emissions that can be used to understand emission drivers (Hertwich and Peters, 2009) and quantify emission transfers by the trade of products between countries (Peters et al., 2011b). The consumption-based emissions have the same global total, but reflect the trade-driven movement of emissions across the Earth's surface in response to human activities.

We estimate consumption-based emissions from 1990-2016 by enumerating the global supply chain using a global model of the economic relationships between economic sectors within and between every country (Andrew and Peters, 2013; Peters et al., 2011a). Our analysis is based on the economic and trade data from the Global Trade and Analysis Project (GTAP; Narayanan

Deleted: (Marland et al., 2009).

Deleted: (Marland, 2008),

Deleted: Gregg et al., 2008).

Deleted: (Durant et al., 2011).

Deleted: (Andres et al., 2012, 2014),

Deleted: ,

Deleted: (Francey et al., 2013).

Deleted: (Rypdal et al., 2006),

Deleted: Davis and Caldeira, 2010)

Deleted: (Hertwich and Peters, 2009)

Deleted: (Peters et al., 2011b).

Deleted: (Andrew and Peters, 2013; Peters et al., 2011a).

et al., 2015), and we make detailed estimates for the years 1997 (GTAP version 5), 2001 (GTAP6), and 2004, 2007, and 2011 (GTAP9.2), covering 57 sectors and 141 countries and regions. The detailed results are then extended into an annual time-series from 1990 to the latest year of the Gross Domestic Product (GDP) data (2016 in this budget), using GDP data by expenditure in current exchange rate of US dollars (USD; from the UN National Accounts main Aggregrates database; UN, 2017) and time series of trade data from GTAP (based on the methodology in (Peters et al., 2011b). We estimate the sector-level CO_2 emissions using the GTAP data and methodology, include flaring and cement emissions from CDIAC, and then scale the national totals (excluding bunker fuels) to match the emission estimates from the carbon budget. We do not provide a separate uncertainty estimate for the consumption-based emissions, but based on model comparisons and sensitivity analysis, they are unlikely to be significantly different than for the territorial emission estimates (Peters et al., 2012a).

2.1.4 Growth rate in emissions

We report the annual growth rate in emissions for adjacent years (in percent per year) by calculating the difference between the two years and then normalising to the emissions in the first year: $(E_{FF}(t_{0+1})-E_{FF}(t_0))/E_{FF}(t_0) \times 100\%$. We apply a leap-year adjustment where relevant to ensure valid interpretations of annual growth rates. This affects the growth rate by about 0.3% yr^{-1} (1/365) and causes growth rates to go up approximately 0.3% if the first year is a leap year and down 0.3% if the second year is a leap year.

The relative growth rate of E_{FF} over time periods of greater than one year can be rewritten using its logarithm equivalent as follows:

$$\frac{1}{E_{FF}}\frac{dE_{FF}}{dt} = \frac{d(lnE_{FF})}{dt} \qquad (2)$$

Here we calculate relative growth rates in emissions for multi-year periods (e.g. a decade) by fitting a linear trend to $ln(E_{FF})$ in Eq. (2), reported in percent per year.

2.1.5 Emissions projections

To gain insight on emission trends for 2019, we provide an assessment of global fossil CO_2 emissions, E_{FF}, by combining individual assessments of emissions for China, USA, the EU, and India (the four countries/regions with the largest emissions), and the rest of the world.

Formatted Table

Our 2019 estimate for China uses: (1) the sum of monthly domestic production of raw coal, crude oil, natural gas and cement from the National Bureau of Statistics (NBS, 2019d)(NBS, 2019c), (2) monthly and net imports (General Administration of Customs of the People's Republic of China, 2019a, 2019b)of coal, coke, crude oil, refined petroleum products and natural gas from the General Administration of Customs of the People's Republic of China (2019a); and (3) annual energy consumption data by fuel type and annual production data for cement (NBS, 2019d) from the NBS, using final data for 2000-2017 (NBS, 2019c) and preliminary data for 2018 (NBS, 2019b). We estimate the full-year growth rate for 2019 using a Bayesian regression for the ratio between the annual energy consumption data (3 above) from 2014 through 2018 and monthly production plus net imports (NBS, 2015, 2019b)(NBS, 2019c)Jackson et al. (2018)through September of each year (1+2 above). The uncertainty range uses the standard deviations of the resulting posteriors. Sources of uncertainty and deviations between the monthly and annual growth rates include lack of monthly data on stock changes and energy density, variance in the trend during the last three months of the year, and partially unexplained discrepancies between supply-side and consumption data even in the final annual data. Note that in recent years, the absolute value of the annual growth rate for coal energy consumption, and hence total CO_2 emissions, has been consistently lower (closer to zero) than the growth suggested by the monthly, tonnage-based production and import data, and this is reflected in the projection. This pattern is only partially explained by stock changes and changes in energy content(NBS, 2015, 2019b). It is therefore not possible to be certain that it will continue in the current year, but it is made plausible by a separate statement by the National Bureau of Statistics on energy consumption growth in the first half of 2019, which suggests no significant growth in energy consumption from coal (NBS, 2019a)for January-June (NBS, 2019a). Results and uncertainties are discussed further in Section 3.4.1.

For the USA, we use the forecast of the U.S. Energy Information Administration (EIA) for emissions from fossil fuels (EIA, 2019). This is based on an energy forecasting model which is updated monthly (last update with data through September 2019), and takes into account heating-degree days, household expenditures by fuel type, energy markets, policies, and other effects. We combine this with our estimate of emissions from cement production using the monthly U.S. cement data from USGS for January-July 2019, assuming changes in cement production over the first part of the year apply throughout the year. While the EIA's forecasts for current full-year emissions have on average been revised downwards, only ten such

Formatted ... [1]
Formatted ... [2]
Formatted ... [3]
Formatted ... [4]
Deleted: for coal, oil
Formatted ... [5]
Deleted: natural gas and
Formatted ... [6]
Deleted: of
Formatted ... [7]
Formatted ... [8]
Formatted ... [9]
Deleted: statistics for January through August of 2019; and (2) ... [10]
Formatted ... [11]
Deleted: and
Formatted ... [12]
Deleted: and full-year statistics for consumption using final data ... [13]
Deleted: and preliminary data for 2018
Deleted: . See also
Deleted: for further discussions on methods.
Formatted ... [14]
Deleted: is based on the
Formatted ... [15]
Deleted: of
Formatted ... [16]
Deleted: difference between the January–August
Formatted ... [17]
Deleted: full-year
Formatted ... [18]
Deleted: from historical data, as well as typical variance
Deleted: preliminary full-year data used for 2018 and typical
Formatted ... [19]
Formatted ... [20]
Deleted: the
Formatted ... [21]
Deleted: of coal for the period of 2013–2017
Deleted: . The resulting estimate for the growth in coal ... [22]
Formatted ... [23]
Deleted: concerning growth in total
Formatted ... [24]
Deleted: and reductions in the share of
Formatted ... [25]
Deleted: in total energy consumption
Deleted: . Based on this and similar gaps between supply-side and ... [26]
Deleted: Sect.
Formatted ... [27]
Deleted: (EIA, 2019).
Deleted: to
Deleted: May

forecasts are available, so we conservatively use the full range of adjustments following revision, and additionally assume symmetrical uncertainty to give ±2.3% around the central forecast.

For India, we use (1) monthly coal production and sales data from the (Ministry of Mines, 2019), Coal India Limited (CIL, 2019) and Singareni Collieries Company Limited (SCCL, 2019), combined with import data from the Ministry of Commerce and Industry (MCI, 2019) and power station stocks data from the Central Electricity Authority (CEA, 2019)(CEA, 2019a); (2) monthly oil production and consumption data from the Ministry of Petroleum and Natural Gas (PPAC, 2019b); (3) monthly natural gas production and import data from the Ministry of Petroleum and Natural Gas (PPAC, 2019a); and (4) monthly cement production data from the Office of the Economic Advisor (OEA, 2019). All data were available for January to September or October 2019. We use Holt-Winters exponential smoothing with multiplicative seasonality (Chatfield, 1978) on each of these four emissions series to project to the end of India's current financial year (March 2020). This iterative method produces estimates of both trend and seasonality at the end of the observation period that are a function of all prior observations, weighted most strongly to more recent data, while maintaining some smoothing effect. The main source of uncertainty in the projection of India's emissions is the assumption of continued trends and typical seasonality.

For the EU, we use (1) monthly coal supply data from Eurostat for the first 6-9 months of 2019 (Eurostat, 2019) cross-checked with more recent data on coal-generated electricity from ENTSO-E for January through October 2019 (ENTSO-E, 2019); (2) monthly oil and gas demand data for January through August from the Joint Organisations Data Initiative (JODI, 2019); and (3) cement production is assumed stable. For oil and natural gas emissions we apply the Holt-Winters method separately to each country and energy carrier to project to the end of the current year, while for coal — which is much less strongly seasonal because of strong weather variations – we assume the remaining months of the year are the same as the previous year in each country.

For the rest of the world, we use the close relationship between the growth in GDP and the growth in emissions (Raupach et al., 2007) to project emissions for the current year. This is based on a simplified Kaya Identity, whereby E_{FF} (GtC yr^{-1}) is decomposed by the product of GDP (USD yr^{-1}) and the fossil fuel carbon intensity of the economy (I_{FF}; GtC USD^{-1}) as follows:

$$E_{FF} = GDP \times I_{FF}$$

Taking a time derivative of Equation (3) and rearranging gives:

$$\frac{1}{E_{FF}}\frac{dE_{FF}}{dt} = \frac{1}{GDP}\frac{dGDP}{dt} + \frac{1}{I_{FF}}\frac{dI_{FF}}{dt}$$

where the left-hand term is the relative growth rate of E_{FF}, and the right-hand terms are the relative growth rates of GDP and I_{FF}, respectively, which can simply be added linearly to give the overall growth rate.

As preliminary estimates of annual change in GDP are made well before the end of a calendar year, making assumptions on the growth rate of I_{FF} allows us to make projections of the annual change in CO_2 emissions well before the end of a calendar year. The I_{FF} is based on GDP in constant PPP (purchasing power parity) from the International Energy Agency (IEA) up to 2016 (IEA/OECD, 2018), and extended using the International Monetary Fund (IMF) growth rates through 2018 (IMF, 2019)(IMF, 2019a).. Interannual variability in I_{FF} is the largest source of uncertainty in the GDP-based emissions projections. We thus use the standard deviation of the annual I_{FF} for the period 2009-2018 as a measure of uncertainty, reflecting a ±1σ as in the rest of the carbon budget. In this year's budget, we have extended the rest-of-the-world method to fuel type to get separate projections for coal, oil, natural gas, cement, flaring, and other components. This allows, for the first time, consistent projections of global emissions by both countries and by fuel type.

The 2019 projection for the world is made of the sum of the projections for China, USA, EU, India, and the rest of the world, where the sum is consistent if done by fuel type (coal, oil, natural gas) or based on total emissions. The uncertainty is added in quadrature among the five regions. The uncertainty here reflects the best of our expert opinion.

2.2 CO_2 emissions from land-use, land-use change and forestry (E_{LUC})

The net CO_2 flux from land-use, land-use change and forestry (E_{LUC}, called land-use change emissions in the rest of the text) include CO_2 fluxes from deforestation, afforestation, logging and forest degradation (including harvest activity), shifting cultivation (cycle of cutting forest for agriculture, then abandoning), and regrowth of forests following wood harvest or abandonment of agriculture. Only some land management activities are included in our land-use change emissions estimates (Table A1). Some of these activities lead to emissions of CO_2 to

the atmosphere, while others lead to CO_2 sinks. E_{LUC} is the net sum of emissions and removals due to all anthropogenic activities considered. Our annual estimate for 1959-2018 is provided as the average of results from two bookkeeping models (Section 2.2.1): the estimate published by (Houghton and Nassikas, 2017; hereafter H&N2017) updated to 2018, and an estimate using the Bookkeeping of Land Use Emissions model (Hansis et al., 2015; hereafter BLUE). Both data sets are then extrapolated to provide a projection for 2019 (Section 2.2.4). In addition, we use results from Dynamic Global Vegetation Models (DGVMs; see Section 2.2.2 and Table 4), to help quantify the uncertainty in E_{LUC} (Section 2.2.3), and thus better characterise our understanding.

2.2.1 Bookkeeping models

Land-use change CO_2 emissions and uptake fluxes are calculated by two bookkeeping models. Both are based on the original bookkeeping approach of Houghton (2003) that keeps track of the carbon stored in vegetation and soils before and after a land-use change (transitions between various natural vegetation types, croplands and pastures). Literature-based response curves describe decay of vegetation and soil carbon, including transfer to product pools of different lifetimes, as well as carbon uptake due to regrowth. In addition, the bookkeeping models represent long-term degradation of primary forest as lowered standing vegetation and soil carbon stocks in secondary forests, and also include forest management practices such as wood harvests.

The bookkeeping models do not include land ecosystems' transient response to changes in climate, atmospheric CO_2 and other environmental factors, and the carbon densities are based on contemporary data reflecting stable environmental conditions at that time. Since carbon densities remain fixed over time in bookkeeping models, the additional sink capacity that ecosystems provide in response to CO_2-fertilization and some other environmental changes is not captured by these models (Pongratz et al., 2014; see Section 2.7.4).

The H&N2017 and BLUE models differ in (1) computational units (country-level vs spatially explicit treatment of land-use change), (2) processes represented (see Table A1), and (3) carbon densities assigned to vegetation and soil of each vegetation type. A notable change of H&N2017 over the original approach by Houghton (2003) used in earlier budget estimates is that no shifting cultivation or other back- and forth-transitions at a level below country are included. Only a decline in forest area in a country as indicated by the Forest Resource Assessment of the FAO that exceeds the expansion of agricultural area as indicated by FAO is

assumed to represent a concurrent expansion and abandonment of cropland. In contrast, the BLUE model includes sub-grid-scale transitions at the grid level between all vegetation types as indicated by the harmonized land-use change data (LUH2) data set (https://doi.org/10.22033/ESGF/input4MIPs.1127; Hurtt et al., 2011; Hurtt et al., in prep.). Furthermore, H&N2017 assume conversion of natural grasslands to pasture, while BLUE allocates pasture proportionally on all natural vegetation that exist in a grid-cell. This is one reason for generally higher emissions in BLUE. For both H&N2017 and BLUE, we add carbon emissions from peat burning based on the Global Fire Emission Database (GFED4s; van der Werf et al., 2017), and peat drainage, based on estimates by Hooijer et al. (2010) to the output of their bookkeeping model for the countries of Indonesia and Malaysia. Peat burning and emissions from the organic layers of drained peat soils, which are not captured by bookkeeping methods directly, need to be included to represent the substantially larger emissions and interannual variability due to synergies of land-use and climate variability in Southeast Asia, in particular during El-Niño events.

The two bookkeeping estimates used in this study differ with respect to the land-use change data used to drive the models. H&N2017 base their estimates directly on the Forest Resource Assessment of the FAO which provides statistics on forest-area change and management at intervals of five years currently updated until 2015 (FAO, 2015). The data is based on country reporting to FAO, and may include remote-sensing information in more recent assessments. Changes in land-use other than forests are based on annual, national changes in cropland and pasture areas reported by FAO (FAOSTAT, 2015)(FAOSTAT, 2015). H&N2017 was extended here for 2016 to 2018 by adding the annual change in total tropical emissions to the H&N2017 estimate for 2015, including estimates of peat drainage and peat burning as described above as well as emissions from tropical deforestation and degradation fires from GFED4.1s (van der Werf et al., 2017). On the other hand, BLUE uses the harmonised land-use change data LUH2 covering the entire 850-2018 period (https://doi.org/10.22033/ESGF/input4MIPs.1127; Hurtt et al., 2011; Hurtt et al., in prep.; see Section 2.2.2), which describes land-use change, also based on the FAO data as well as the HYDE dataset (Goldewijk et al., 2017a, 2017b), but downscaled at a quarter-degree spatial resolution, considering sub-grid-scale transitions between primary forest, secondary forest, cropland, pasture and rangeland. The LUH2 data provides a distinction between rangelands and pasture, based on inputs from HYDE. To constrain the models' interpretation on whether rangeland implies the original natural vegetation to be transformed

to grassland or not (e.g., browsing on shrubland), a forest mask was provided with LUH2; forest is assumed to be transformed, while all other natural vegetation remains. This is implemented in BLUE.

Hooijer et al. (2010)(van der Werf et al., 2017)For E_{LUC} from 1850 onwards we average the estimates from BLUE and H&N2017. For the cumulative numbers starting 1750 an average of four earlier publications is added (30 ± 20 PgC 1750-1850, rounded to nearest 5; Le Quéré et al., 2016)

2.2.2 Dynamic Global Vegetation Models (DGVMs)

Land-use change CO_2 emissions have also been estimated using an ensemble of 15 DGVM simulations. The DGVMs account for deforestation and regrowth, the most important components of E_{LUC}, but they do not represent all processes resulting directly from human activities on land (Table A1). All DGVMs represent processes of vegetation growth and mortality, as well as decomposition of dead organic matter associated with natural cycles, and include the vegetation and soil carbon response to increasing atmospheric CO_2 concentration and to climate variability and change. Some models explicitly simulate the coupling of carbon and nitrogen cycles and account for atmospheric N deposition and N fertilisers (Table A1). The DGVMs are independent from the other budget terms except for their use of atmospheric CO_2 concentration to calculate the fertilization effect of CO_2 on plant photosynthesis.

Many DGVMs used the HYDE land-use change data set (Goldewijk et al., 2017a, 2017b), which provides annual (1700-2018), half-degree, fractional data on cropland and pasture. The data are based on the available annual FAO statistics of change in agricultural land area available until 2015. Last year's HYDE version used FAO statistics until 2012, which are now supplemented using the annual change anomalies from FAO data for years 2013-2015 relative to year 2012. HYDE forcing was also corrected for Brazil for years 1951-2012. After the year 2015 HYDE extrapolates cropland, pasture, and urban land-use data until the year 2018. Some models also use the LUH2 data set, an update of the more comprehensive harmonised land-use data set (Hurtt et al., 2011) that further includes fractional data on primary and secondary forest vegetation, as well as all underlying transitions between land-use states (1700-2019) (https://doi.org/10.22033/ESGF/input4MIPs.1127; Hurtt et al., 2011; Hurtt et al., in prep.; Table A1). This new data set is of quarter degree fractional areas of land-use states and all transitions between those states, including a new wood harvest reconstruction, new representation of

shifting cultivation, crop rotations, management information including irrigation and fertilizer application. The land-use states include five different crop types in addition to the pasture-rangeland split discussed before. Wood harvest patterns are constrained with Landsat-based tree cover loss data (Hansen et al. 2013). Updates of LUH2 over last year's version are using the most recent HYDE/FAO release (covering the time period up to including 2015), which also corrects an error in the version used for the 2018 budget in Brazil.

DGVMs implement land-use change differently (e.g. an increased cropland fraction in a grid cell can either be at the expense of grassland or shrubs, or forest, the latter resulting in deforestation; land cover fractions of the non-agricultural land differ between models). Similarly, model-specific assumptions are applied to convert deforested biomass or deforested area, and other forest product pools into carbon, and different choices are made regarding the allocation of rangelands as natural vegetation or pastures.

The DGVM model runs were forced by either the merged monthly CRU and 6 hourly JRA-55 data set or by the monthly CRU data set, both providing observation-based temperature, precipitation, and incoming surface radiation on a 0.5°x0.5° grid and updated to 2018 (Harris et al., 2014). The combination of CRU monthly data with 6 hourly forcing from JRA-55 (Kobayashi et al., 2015) is performed with methodology used in previous years (Viovy, 2016) adapted to the specifics of the JRA-55 data. The forcing data also include global atmospheric CO_2, which changes over time (Dlugokencky and Tans, 2019), and gridded, time dependent N deposition and N fertilisers (as used in some models; Table A1).

Two sets of simulations were performed with the DGVMs. Both applied historical changes in climate, atmospheric CO_2 concentration, and N inputs. The two sets of simulations differ, however, with respect to land-use: one set applies historical changes in land-use, the other a time-invariant pre-industrial land cover distribution and pre-industrial wood harvest rates. By difference of the two simulations, the dynamic evolution of vegetation biomass and soil carbon pools in response to land-use change can be quantified in each model (E_{LUC}). Using the difference between these two DGVM simulations to diagnose E_{LUC} means the DGVMs account for the loss of additional sink capacity (around 0.4 ± 0.3 GtC yr-1; see Section 2.7.4), while the bookkeeping models do not.

As a criterion for inclusion in this carbon budget, we only retain models that simulate a positive E_{LUC} during the 1990s, as assessed in the IPCC AR4 (Denman et al., 2007) and AR5 (Ciais et al.,

2013). All DGVMs met this criteria, although one model was not included in the E_{LUC} estimate from DGVMs as it exhibited a spurious response to the transient land cover change forcing after its initial spin-up.

2.2.3 Uncertainty assessment for E_{LUC}

Differences between the bookkeeping models and DGVM models originate from three main sources: the different methodologies; the underlying land-use/land cover data set, and the different processes represented (Table A1). We examine the results from the DGVM models and of the bookkeeping method, and use the resulting variations as a way to characterise the uncertainty in E_{LUC}.

The E_{LUC} estimate from the DGVMs multi-model mean is consistent with the average of the emissions from the bookkeeping models (Table 5). However there are large differences among individual DGVMs (standard deviation at around 0.5 GtC yr^{-1}; Table 5), between the two bookkeeping models (average difference of 0.7 GtC yr^{-1}), and between the current estimate of H&N2017 and its previous model version (Houghton et al., 2012). The uncertainty in E_{LUC} of ±0.7 GtC yr^{-1} reflects our best value judgment that there is at least 68% chance (±1σ) that the true land-use change emission lies within the given range, for the range of processes considered here. Prior to the year 1959, the uncertainty in E_{LUC} was taken from the standard deviation of the DGVMs. We assign low confidence to the annual estimates of E_{LUC} because of the inconsistencies among estimates and of the difficulties to quantify some of the processes in DGVMs.

2.2.4 Emissions projections

We project the 2019 land-use emissions for both H&N2017 and BLUE, starting from their estimates for 2018 and adding observed changes in emissions from peat drainage (update on (Hooijer et al., 2010) as well as emissions from peat fires, tropical deforestation and degradation as estimated using active fire data (MCD14ML; Giglio et al., 2016). Those latter scale almost linearly with GFED over large areas (van der Werf et al., 2017) and thus allows for tracking fire emissions in deforestation and tropical peat zones in near-real time. During most years, emissions during January-September cover most of the fire season in the Amazon and Southeast Asia, where a large part of the global deforestation takes place. While the degree to which the fires in 2019 in the Amazon are related to land-use change requires more scrutiny,

initial analyses based on fire radiative power (FRP) of the fires detected indicate that many fires were associated with deforestation (http://www.globalfiredata.org/forecast.html, accessed September 23, 2019). Most fires burning in Indonesia were on peatlands, which also represent a net source of CO_2.

2.3 Growth rate in atmospheric CO_2 concentration (G_{ATM})

2.3.1 Global growth rate in atmospheric CO_2 concentration

The rate of growth of the atmospheric CO_2 concentration is provided by the US National Oceanic and Atmospheric Administration Earth System Research Laboratory (NOAA/ESRL; Dlugokencky and Tans, 2019), which is updated from Ballantyne et al. (2012). For the 1959-1979 period, the global growth rate is based on measurements of atmospheric CO_2 concentration averaged from the Mauna Loa and South Pole stations, as observed by the CO_2 Program at Scripps Institution of Oceanography (Keeling et al., 1976). For the 1980-2018 time period, the global growth rate is based on the average of multiple stations selected from the marine boundary layer sites with well-mixed background air (Ballantyne et al., 2012), after fitting each station with a smoothed curve as a function of time, and averaging by latitude band (Masarie and Tans, 1995). The annual growth rate is estimated by Dlugokencky and Tans (2019) from atmospheric CO_2 concentration by taking the average of the most recent December-January months corrected for the average seasonal cycle and subtracting this same average one year earlier. The growth rate in units of ppm yr^{-1} is converted to units of GtC yr^{-1} by multiplying by a factor of 2.124 GtC per ppm (Ballantyne et al., 2012).

The uncertainty around the atmospheric growth rate is due to three main factors. First, the long-term reproducibility of reference gas standards (around 0.03 ppm for 1σ from the 1980s; Dlugokencky and Tans, 2019). Second, small unexplained systematic analytical errors that may have a duration of several months to two years come and go. They have been simulated by randomizing both the duration and the magnitude (determined from the existing evidence) in a Monte Carlo procedure. Third, the network composition of the marine boundary layer with some sites coming or going, gaps in the time series at each site, etc (Dlugokencky and Tans, 2019). The latter uncertainty was estimated by NOAA/ESRL with a Monte Carlo method by constructing 100 "alternative" networks (Masarie and Tans, 1995; NOAA/ESRL, 2019). The second and third uncertainties, summed in quadrature, add up to 0.085 ppm on average (Dlugokencky and Tans, 2019). Fourth, the uncertainty associated with using the average CO_2

concentration from a surface network to approximate the true atmospheric average CO_2 concentration (mass-weighted, in 3 dimensions) as needed to assess the total atmospheric CO_2 burden. In reality, CO_2 variations measured at the stations will not exactly track changes in total atmospheric burden, with offsets in magnitude and phasing due to vertical and horizontal mixing. This effect must be very small on decadal and longer time scales, when the atmosphere can be considered well mixed. Preliminary estimates suggest this effect would increase the annual uncertainty, but a full analysis is not yet available. We therefore maintain an uncertainty around the annual growth rate based on the multiple stations data set ranges between 0.11 and 0.72 GtC yr^{-1}, with a mean of 0.61 GtC yr^{-1} for 1959-1979 and 0.17 GtC yr^{-1} for 1980-2018, when a larger set of stations were available as provided by Dlugokencky and Tans (2019), but recognise further exploration of this uncertainty is required. At this time, we estimate the uncertainty of the decadal averaged growth rate after 1980 at 0.02 GtC yr^{-1} based on the calibration and the annual growth rate uncertainty, but stretched over a 10-year interval. For years prior to 1980, we estimate the decadal averaged uncertainty to be 0.07 GtC yr^{-1} based on a factor proportional to the annual uncertainty prior and after 1980 (0.02 * [0.61/0.17] GtC yr^{-1}).

We assign a high confidence to the annual estimates of G_{ATM} because they are based on direct measurements from multiple and consistent instruments and stations distributed around the world (Ballantyne et al., 2012).

In order to estimate the total carbon accumulated in the atmosphere since 1750 or 1850, we use an atmospheric CO_2 concentration of 277 ± 3 ppm or 286 ± 3 ppm, respectively, based on a cubic spline fit to ice core data (Joos and Spahni, 2008). The uncertainty of ±3 ppm (converted to ±1σ) is taken directly from the IPCC's assessment (Ciais et al., 2013)(Ciais et al., 2013). Typical uncertainties in the growth rate in atmospheric CO_2 concentration from ice core data are equivalent to ±0.1-0.15 GtC yr^{-1} as evaluated from the Law Dome data (Etheridge et al., 1996) for individual 20-year intervals over the period from 1850 to 1960 (Bruno and Joos, 1997).

2.3.2 Atmospheric growth rate projection

We provide an assessment of G_{ATM} for 2019 based on the monthly calculated global atmospheric CO_2 concentration (GLO) through July (Dlugokencky and Tans, 2019), (Dlugokencky and Tans, 2019) and bias-adjusted Holt–Winters exponential smoothing with additive seasonality (Chatfield, 1978) to project to January 2020. The assessment method used this year

differs from the forecast method used last year (Le Quéré et al., 2018b), which was based on the observed concentrations at Mauna Loa (MLO) only, using the historical relationship between the MLO and GLO series. Additional analysis suggests that the first half of the year shows more interannual variability than the second half of the year, so that the exact projection method applied to the second half of the year has a relatively smaller impact on the projection of the full year. Uncertainty is estimated from past variability using the standard deviation of the last 5 years' monthly growth rates.

2.4 Ocean CO_2 sink

Estimates of the global ocean CO_2 sink S_{OCEAN} are from an ensemble of global ocean biogeochemistry models (GOBMs, Table A2) that meet observational constraints over the 1990s (see below). We use observation-based estimates of S_{OCEAN} to provide a qualitative assessment of confidence in the reported results, and two diagnostic ocean models to estimate S_{OCEAN} over the industrial era (see below).

2.4.1 Observation-based estimates

We use the observational constraints assessed by IPCC of a mean ocean CO_2 sink of 2.2 ± 0.4 GtC yr^{-1} for the 1990s (Denman et al., 2007) to verify that the GOBMs provide a realistic assessment of S_{OCEAN}. This is based on indirect observations with seven different methodologies and their uncertainties, using the methods that are deemed most reliable for the assessment of this quantity (Denman et al., 2007). The IPCC confirmed this assessment in 2013 (Ciais et al., 2013)(Ciais et al., 2013). The observational-based estimates use the ocean/land CO_2 sink partitioning from observed atmospheric O_2/N_2 concentration trends (Manning and Keeling, 2006; updated in Keeling and Manning, 2014), an oceanic inversion method constrained by ocean biogeochemistry data (Mikaloff Fletcher et al., 2006), and a method based on penetration time scale for chlorofluorocarbons (McNeil et al., 2003). The IPCC estimate of 2.2 GtC yr^{-1} for the 1990s is consistent with a range of methods (Wanninkhof et al., 2013).

We also use three estimates of the ocean CO_2 sink and its variability based on interpolations of measurements of surface ocean fugacity of CO_2 (pCO$_2$ corrected for the non-ideal behaviour of the gas; Pfeil et al., 2013). We refer to these as pCO$_2$-based flux estimates. The measurements are from the Surface Ocean CO_2 Atlas version 2019, which is an update of version 3 (Bakker et al., 2016) and contains quality-controlled data to 2018 (see data attribution Table A4). The

SOCAT v2019 data were mapped using a data-driven diagnostic method (Rödenbeck et al., 2013; referred to here as Jena-MLS), a combined self-organising map and feed-forward neural network (Landschützer et al., 2014; MPI-SOMFFN), and an artificial neural network model (Denvil-Sommer et al., 2019; Copernicus Marine Environment Monitoring Service (CMEMS)). The global pCO_2-based flux estimates were adjusted to remove the pre-industrial ocean source of CO_2 to the atmosphere of 0.78 GtC yr^{-1} from river input to the ocean (Resplandy et al., 2018), per our definition of S_{OCEAN}. Several other ocean sink products based on observations are also available but they continue to show large unresolved discrepancies with observed variability. Here we used, as in our previous annual budgets, the two pCO_2-based flux products that had the best fit to observations for their representation of tropical and global variability (Rödenbeck et al., 2015), plus CMEMS which has a similarly good fit with observations. The CO_2 flux from each pCO_2-based product is scaled by the ratio of the total ocean area covered by the respective product to the total ocean area (361.9e6 km^2) from ETOPO1 (Amante and Eakins, 2009; Eakins and Sharman, 2010). In products where the covered area varies with time (MPI-SOMFFN, CMEMS) we use the maximum area coverage. The data-products cover 88% (MPI-SOMFFN, CMEMS) to 101% of the observed total ocean area, so two products are effectively corrected upwards by a factor of 1.126.

We further use results from two diagnostic ocean models of Khatiwala et al. (2013) and DeVries (2014) to estimate the anthropogenic carbon accumulated in the ocean prior to 1959. The two approaches assume constant ocean circulation and biological fluxes, with S_{OCEAN} estimated as a response in the change in atmospheric CO_2 concentration calibrated to observations. The uncertainty in cumulative uptake of ±20 GtC (converted to ±1σ) is taken directly from the IPCC's review of the literature (Rhein et al., 2013), or about ±30% for the annual values (Khatiwala et al., 2009).

2.4.2 Global Ocean Biogeochemistry Models (GOBMs)

The ocean CO_2 sink for 1959-2018 is estimated using nine GOBMs (Table A2). The GOBMs represent the physical, chemical and biological processes that influence the surface ocean concentration of CO_2 and thus the air-sea CO_2 flux. The GOBMs are forced by meteorological reanalysis and atmospheric CO_2 concentration data available for the entire time period. They mostly differ in the source of the atmospheric forcing data (meteorological reanalysis), spin up strategies, and in their horizontal and vertical resolutions (Table A2). GOBMs do not include the

Deleted: (Rödenbeck et al., 2013;

Deleted: (Landschützer et al., 2014;

Deleted: (Denvil-Sommer et al., 2019;

Deleted: (Resplandy et al., 2018),

Deleted: (Rödenbeck et al., 2015),

Deleted: (Amante and Eakins, 2009; Eakins and Sharman, 2010).

Deleted: results

Deleted: Khatiwala et al. (2013) and DeVries (2014)

Deleted: (Rhein et al., 2013),

Deleted: (Khatiwala et al., 2009).

Deleted: eight

effects of anthropogenic changes in nutrient supply, which could lead to an increase of the ocean sink of up to about 0.3 GtC yr^{-1} over the industrial period (Duce et al., 2008). They also do not include the perturbation associated with changes in riverine organic carbon (see Section 2.7.3).

The annual mean air-sea CO_2 flux from the GOBMs is corrected for any model bias or drift by subtracting the time-dependent model bias. The time-dependent model bias is calculated as a linear fit to the annual CO_2 flux from a control simulation with no climate variability and change and constant pre-industrial CO_2 concentration. The absolute biases per model in the 1990s vary between 0.005 GtC yr^{-1} and 0.362 GtC yr^{-1}, with some models having positive and some having negative biases. The bias-correction reduces the model mean ocean carbon sink by 0.06 GtC yr^{-1} in the 1990s. The CO_2 flux from each model is scaled by the ratio of the total ocean area covered by the respective GOBM to the total ocean area (361.9e6 km^2) from ETOPO1 (Amante and Eakins, 2009; Eakins and Sharman, 2010). The ocean models cover 97% to 101% of the total ocean area, so the effect of this correction is small. All models fell within the observational constraint for the 1990s before and after applying the corrections.

2.4.3   GOBM evaluation and uncertainty assessment for S_{OCEAN}

The mean ocean CO_2 sink for all GOBMs falls within 90% confidence of the observed range, or 1.6 to 2.8 GtC yr^{-1} for the 1990s. Here we have adjusted the confidence interval to the IPCC confidence interval of 90% to avoid rejecting models that may be outliers but are still plausible.

The GOBMs and flux products have been further evaluated using air-sea CO_2 flux (fCO$_2$) from the SOCAT v2019 database (Bakker et al., 2016, updated). We focused this evaluation on the root mean squared error (RMSE) between observed fCO$_2$ and modelled pCO$_2$ and on a measure of the amplitude of the interannual variability of the flux (Rödenbeck et al., 2015). The amplitude of the S_{OCEAN} interannual variability (A-IAV)) is calculated as the temporal standard deviation of a 12-months running mean over the CO_2 flux time-series (Rödenbeck et al., 2015).

The RMSE is only calculated for open ocean (water depth > 400 m) grid points on a 1 degree x 1 degree x monthly grid where actual observations exist. These metrics are chosen because RMSE is the most direct measure of data-model mismatch and the A-IAV is a direct measure of the variability of S_{OCEAN} on interannual timescales. We apply these metrics globally and by latitude bands (Fig. B1). Results are shown in Fig. B1 and discussed in Section 3.1.3.

The uncertainty around the mean ocean sink of anthropogenic CO_2 was quantified by Denman et al. (2007) for the 1990s (see Section 2.4.1). To quantify the uncertainty around annual values, we examine the standard deviation of the GOBM ensemble, which averages 0.3 GtC yr^{-1} during 1959-2018. We estimate that the uncertainty in the annual ocean CO_2 sink is about ± 0.5 GtC yr^{-1} from the combined uncertainty of the mean flux based on observations of ± 0.4 GtC yr^{-1} (Denman et al., 2007) and the standard deviation across GOBMs of up to ± 0.4 GtC yr^{-1}, reflecting both the uncertainty in the mean sink from observations during the 1990's (Denman et al., 2007, Section 2.4.1) and in the interannual variability as assessed by GOBMs.

We examine the consistency between the variability of the model-based and the pCO_2-based flux products to assess confidence in S_{OCEAN}. The interannual variability of the ocean fluxes (quantified as the standard deviation) of the three pCO_2-based flux products for 1985-2018 (where they overlap) is ± 0.37 GtC yr^{-1} (Jena-MLS), ± 0.46 GtC yr^{-1} (MPI-SOMFFN) and ± 0.51 GtC yr^{-1} (CMEMS). The inter-annual variability in the mean of the pCO_2-based flux estimates is ± 0.41 GtC yr-1 for the 1985-2018 period, compared to ±0.31 GtC yr^{-1} for the GOBM ensemble. The standard deviation includes a component of trend and decadal variability in addition to interannual variability, and their relative influence differs across estimates. Individual estimates (both GOBM and flux products) generally produce a higher ocean CO_2 sink during strong El Niño events. The annual pCO_2-based flux products correlate with the ocean CO_2 sink estimated here with a correlation of r = 0.75 (0.55 to 0.79 for individual GOBMs), r = 0.86 (0.70 to 0.87) and 0.93 (0.83 to 0.93) for the pCO_2-based flux products of Jena-MLS, MPI-SOMFFN and CMEMS, respectively (simple linear regression). The average of the GOBM estimates and of the data-based estimates have a mutual correlation of 0.91. The agreement between the models and the flux products reflects some consistency in their representation of underlying variability since there is little overlap in their methodology or use of observations. We assess a medium confidence level to the annual ocean CO_2 sink and its uncertainty because it is based on multiple lines of evidence, and the results are consistent in that the interannual variability in the GOBMs and data-based estimates are all generally small compared to the variability in the growth rate of atmospheric CO_2 concentration.

Deleted: Denman et al. (2007)
Deleted: Sect.
Deleted: (Denman et al., 2007)
Deleted: (Denman et al., 2007;
Deleted: 77
Deleted: 63
Formatted: Font color: Black
Deleted: 87
Deleted: 78
Formatted: Font color: Black
Formatted: Font color: Black
Deleted: 85
Deleted: 92
Deleted: The use of annual data for the correlation may reduce the strength of the relationship because the dominant source of variability associated with El Niño events is less than one year.

2.5 Terrestrial CO$_2$ sink

2.5.1 DGVM simulations

The terrestrial land sink (S$_{LAND}$) is thought to be due to the combined effects of fertilisation by rising atmospheric CO$_2$ and N inputs on plant growth, as well as the effects of climate change such as the lengthening of the growing season in northern temperate and boreal areas. S$_{LAND}$ does not include land sinks directly resulting from land-use and land-use change (e.g. regrowth of vegetation) as these are part of the land-use flux (E$_{LUC}$), although system boundaries make it difficult to attribute exactly CO$_2$ fluxes on land between S$_{LAND}$ and E$_{LUC}$ (Erb et al., 2013).

S$_{LAND}$ is estimated from the multi-model mean of 16 DGVMs (Table 4). As described in section 2.2.2, DGVM simulations include all climate variability and CO$_2$ effects over land, with some DGVMs also including the effect of N inputs. The DGVMs do not include the export of carbon to aquatic systems or its historical perturbation, which is discussed in section 2.7.3.

2.5.2 DGVM evaluation and uncertainty assessment for S$_{LAND}$

We apply three criteria for minimum DGVM realism by including only those DGVMs with (1) steady state after spin up, (2) net land fluxes (S$_{LAND}$ – E$_{LUC}$) that is an atmosphere-to-land carbon flux over the 1990s ranging between -0.3 and 2.3 GtC yr^{-1}, within 90% confidence of constraints by global atmospheric and oceanic observations (Keeling and Manning, 2014; Wanninkhof et al., 2013), and (3) global E$_{LUC}$ that is a carbon source to the atmosphere over the 1990s, as mentioned in section 2.2.2. All 16 DGVMs meet these three criteria.

In addition, the DGVM results are also evaluated using the International Land Model Benchmarking system (ILAMB; Collier et al., 2018). This evaluation is provided here to document, encourage and support model improvements through time. ILAMB variables cover key processes that are relevant for the quantification of S$_{LAND}$ and resulting aggregated outcomes. The selected variables are vegetation biomass, gross primary productivity, leaf area index, net ecosystem exchange, ecosystem respiration, evapotranspiration, soil carbon, and runoff (see Fig. B2 for the results and for the list of observed databases). Results are shown in Fig. B2 and discussed in Section 3.1.3.

For the uncertainty for S$_{LAND}$, we use the standard deviation of the annual CO$_2$ sink across the DGVMs, averaging to about ± 0.6 GtC yr^{-1} for the period 1959 to 2018. We attach a medium confidence level to the annual land CO$_2$ sink and its uncertainty because the estimates from the

residual budget and averaged DGVMs match well within their respective uncertainties (Table 5).

2.6 The atmospheric perspective

The world-wide network of atmospheric measurements can be used with atmospheric inversion methods to constrain the location of the combined total surface CO_2 fluxes from all sources, including fossil and land-use change emissions and land and ocean CO_2 fluxes. The inversions assume E_{FF} to be well known, and they solve for the spatial and temporal distribution of land and ocean fluxes from the residual gradients of CO_2 between stations that are not explained by fossil fuel emissions.

Three atmospheric inversions (Table A3) used atmospheric CO_2 data to the end of 2018 (including preliminary values in some cases) to infer the spatio-temporal distribution of the CO_2 flux exchanged between the atmosphere and the land or oceans. We focus here on the largest and most consistent sources of information, namely the total land and ocean CO_2 flux and their partitioning among the mid-high latitude region of the Northern Hemisphere (30°N-90°N), the tropics (30°S-30°N) and the mid-high latitude region of the Southern Hemisphere (30°S-90°S). We also break down those estimates for the land and ocean regions separately, to further scrutinise the constraints from atmospheric observations. We use these estimates to comment on the consistency across various data streams and process-based estimates.

2.6.1 Atmospheric inversions

The three inversion systems used in this release are the CarbonTracker Europe (CTE; Van Der Laan-Luijkx et al., 2017), the Jena CarboScope (Rödenbeck, 2005, with updates from Rödenbeck et al., 2018) and the Copernicus Atmosphere Monitoring Service (CAMS; Chevallier et al., 2005). See Table A3 for version numbers. The inversions are based on Bayesian inversion principles with prior information on fluxes and their uncertainty that interpret the same, for the most part, observed time series (or subsets thereof), but use different methodologies (Table A3). These differences mainly concern the selection of atmospheric CO_2 data, the used prior fluxes, spatial breakdown (i.e. grid size), assumed correlation structures, and mathematical approach. The details of these approaches are documented extensively in the references provided above. Each system uses a different transport model, which was demonstrated to be a driving factor behind differences in atmospheric-based flux estimates, and specifically their distribution across latitudinal bands (e.g., Gaubert et al., 2018).

The inversions use atmospheric CO_2 observations from various flask and in situ networks, as detailed in Table A3. They prescribe global fossil fuel emissions, which is already scaled to the present estimate of E_{FF} for CAMS, while CTE and CarboScope used slightly different E_{FF} values (<0.39 GtC yr^{-1}) based on alternative emissions compilations. Since this is known to result in different total CO_2 uptake in atmospheric inversions (Peylin et al., 2013; Gaubert et al., 2018), we adjusted the land sink of each inversion estimate (where most of the fossil fuel emissions occur) by its fossil fuel difference to the CAMS model. These differences amount to up to 0.5 GtC for certain years in the region NH and are thus an important consideration in an inverse flux comparison.

The land/ocean CO_2 fluxes from atmospheric inversions contain anthropogenic perturbation and natural pre-industrial CO_2 fluxes. Natural pre-industrial fluxes are primarily land CO_2 sinks and ocean CO_2 sources corresponding to carbon taken up on land, transported by rivers from land to ocean, and outgassed by the ocean. These pre-industrial land CO_2 sinks are thus compensated over the globe by ocean CO_2 sources corresponding to the outgassing of riverine carbon inputs to the ocean. We apply the distribution of land-to-ocean C fluxes from rivers in three latitude bands using estimates from Resplandy et al. (2018), which are constrained by ocean heat transport to a total land-to-ocean carbon transfer of 0.78 GtC yr^{-1}. The latitude distribution of river-induced ocean CO_2 sources (North: 0.20 GtC yr^{-1}, Tropics: 0.19 GtC yr^{-1}, South: 0.38 GtC yr^{-1}) are derived from a simulation of the IPSL GOBM using as an input the river flux constrained by heat transport of Resplandy et al. (2018). To facilitate the comparison, we adjusted the inversions estimates of the land and ocean fluxes per latitude band with these numbers based on these results to produce historical perturbation CO_2 fluxes from inversions.

The atmospheric inversions are also evaluated using vertical profiles of atmospheric CO_2 concentrations (Fig. B3). More than 30 aircraft programs over the globe, either regular programs or repeated surveys over at least 9 months, have been used in order to draw a robust picture of the model performance (with space-time data coverage irregular and denser in the 0-45°N latitude band). The three models are compared to the independent aircraft CO_2 measurements between 2 and 7 km above sea level between 2001 and 2017. Results are shown in Fig. B3 and discussed in Section 3.1.3.

2.7 Processes not included in the global carbon budget

The contribution of anthropogenic CO and CH_4 to the global carbon budget is not fully accounted for in Eq. (1) and is described in Section 2.7.1. The contributions of other carbonates to CO_2 emissions is described in Section 2.7.2. The contribution of anthropogenic changes in river fluxes is conceptually included in Eq. (1) in S_{OCEAN} and in S_{LAND}, but it is not represented in the process models used to quantify these fluxes. This effect is discussed in Section 2.7.3 . Similarly, the loss of additional sink capacity from reduced forest cover is missing in the combination of approaches used here to estimate both land fluxes (E_{LUC} and S_{LAND}) and its potential effect is discussed and quantified in Section 2.7.4.

2.7.1 Contribution of anthropogenic CO and CH_4 to the global carbon budget

Equation (1) includes only partly the net input of CO_2 to the atmosphere from the chemical oxidation of reactive carbon-containing gases from sources other than the combustion of fossil fuels, such as: (1) cement process emissions, since these do not come from combustion of fossil fuels, (2) the oxidation of fossil fuels, (3) the assumption of immediate oxidation of vented methane in oil production. It omits however any other anthropogenic carbon-containing gases that are eventually oxidised in the atmosphere, such as anthropogenic emissions of CO and CH_4. An attempt is made in this section to estimate their magnitude, and identify the sources of uncertainty. Anthropogenic CO emissions are from incomplete fossil fuel and biofuel burning and deforestation fires. The main anthropogenic emissions of fossil CH_4 that matter for the global carbon budget are the fugitive emissions of coal, oil and gas upstream sectors (see below). These emissions of CO and CH_4 contribute a net addition of fossil carbon to the atmosphere.

In our estimate of E_{FF} we assumed (Section 2.1.1) that all the fuel burned is emitted as CO_2, thus CO anthropogenic emissions associated with incomplete combustion and their atmospheric oxidation into CO_2 within a few months are already counted implicitly in E_{FF} and should not be counted twice (same for E_{LUC} and anthropogenic CO emissions by deforestation fires). Anthropogenic emissions of fossil CH_4 are not included in E_{FF}, because these fugitive emissions are not included in the fuel inventories. Yet they contribute to the annual CO_2 growth rate after CH_4 gets oxidized into CO_2. Anthropogenic emissions of fossil CH_4 represent 15% of total CH_4 emissions (Kirschke et al., 2013), that is 0.072 GtC yr^{-1} for the past decade. Assuming steady state, these emissions are all converted to CO_2 by OH oxidation, and thus explain 0.06 GtC yr^{-1}

of the global CO_2 growth rate in the past decade, or 0.07-0.1 GtC yr^{-1} using the higher CH_4 emissions reported recently (Schwietzke et al., 2016).

Other anthropogenic changes in the sources of CO and CH_4 from wildfires, vegetation biomass, wetlands, ruminants or permafrost changes are similarly assumed to have a small effect on the CO_2 growth rate. The CH_4 and CO emissions and sinks are published and analysed separately in the Global Methane Budget and Global Carbon Monoxide Budget publications, which follow a similar approach to that presented here (Saunois et al., 2016; Zheng et al., 2019).

2.7.2 Contribution of other carbonates to CO_2 emissions

The contribution of fossil carbonates other than cement production is not systematically included in estimates of E_{FF}, except at the national level where they are accounted in the UNFCCC national inventories. The missing processes include CO_2 emissions associated with the calcination of lime and limestone outside cement production, and the reabsorption of CO_2 by the rocks and concrete from carbonation through their lifetime (Xi et al., 2016). Carbonates are used in various industries, including in iron and steel manufacture and in agriculture. They are found naturally in some coals. Carbonation from cement life-cycle, including demolition and crushing, was estimated by one study to be around 0.25 GtC yr^{-1} for year 2013 (Xi et al., 2016). Carbonation emissions from cement life-cycle would offset calcination emissions from lime and limestone production. The balance of these two processes is not clear.

2.7.3 Anthropogenic carbon fluxes in the land-to-ocean aquatic continuum

The approach used to determine the global carbon budget refers to the mean, variations, and trends in the perturbation of CO_2 in the atmosphere, referenced to the pre-industrial era. Carbon is continuously displaced from the land to the ocean through the land-ocean aquatic continuum (LOAC) comprising freshwaters, estuaries and coastal areas (Bauer et al., 2013; Regnier et al., 2013). A significant fraction of this lateral carbon flux is entirely 'natural' and is thus a steady state component of the pre-industrial carbon cycle. We account for this pre-industrial flux where appropriate in our study. However, changes in environmental conditions and land-use change have caused an increase in the lateral transport of carbon into the LOAC – a perturbation that is relevant for the global carbon budget presented here.

The results of the analysis of Regnier et al. (2013) can be summarized in two points of relevance for the anthropogenic CO_2 budget. First, the anthropogenic perturbation has increased the

Deleted: (Schwietzke et al., 2016).

Deleted: (Saunois et al., 2016; Zheng et al., 2019).

Deleted: (Xi et al., 2016).

Deleted: (Xi et al., 2016).

Deleted: (Bauer et al., 2013; Regnier et al., 2013).

Deleted: Regnier et al. (2013)

organic carbon export from terrestrial ecosystems to the hydrosphere by as much as 1.0 ± 0.5 GtC yr^{-1} since pre-industrial, mainly owing to enhanced carbon export from soils. Second, this exported anthropogenic carbon is partly respired through the LOAC, partly sequestered in sediments along the LOAC and to a lesser extent, transferred to the open ocean where it may accumulate. The increase in storage of land-derived organic carbon in the LOAC and open ocean combined is estimated by Regnier et al. (2013) at 0.65 ± 0.35GtC yr^{-1}. We do not attempt to incorporate the changes in LOAC in our study.

The inclusion of freshwater fluxes of anthropogenic CO_2 affects the estimates of, and partitioning between, S_{LAND} and S_{OCEAN} in Eq. (1), but does not affect the other terms. This effect is not included in the GOBMs and DGVMs used in our global carbon budget analysis presented here.

2.7.4 Loss of additional sink capacity

Historical land-cover change was dominated by transitions from vegetation types that can provide a large carbon sink per area unit (typically, forests) to others less efficient in removing CO_2 from the atmosphere (typically, croplands). The resultant decrease in land sink, called the 'loss of sink capacity', is calculated as the difference between the actual land sink under changing land-cover and the counter-factual land sink under pre-industrial land-cover. An efficient protocol has yet to be designed to estimate the magnitude of the loss of additional sink capacity in DGVMs. Here, we provide a quantitative estimate of this term to be used in the discussion. Our estimate uses the compact Earth system model OSCAR whose land carbon cycle component is designed to emulate the behaviour of DGMVs (Gasser et al., 2017). We use OSCAR v2.2.1 (an update of v2.2 with minor changes) in a probabilistic setup identical to the one of (Arneth et al., 2017) but with a Monte Carlo ensemble of 2000 simulations. For each, we calculate separately S_{LAND} and the loss of additional sink capacity. We then constrain the ensemble by weighting each member to obtain a distribution of cumulative S_{LAND} over 1850-2005 close to the DGVMs used here. From this ensemble, we estimate a loss of additional sink capacity of 0.4 ± 0.3 GtC yr^{-1} on average over 2005-2014, and of about 20 ± 15 GtC when accumulated between 1850 and 2018 (using a linear extrapolation of the trend to estimate the last few years).

3   Results

3.1   Global carbon budget mean and variability for 1959 – 2018

The global carbon budget averaged over the last half-century is shown in Fig. 3. For this time period, 82% of the total emissions (E_{FF} + E_{LUC}) were caused by fossil CO_2 emissions, and 18% by land-use change. The total emissions were partitioned among the atmosphere (45%), ocean (24%) and land (29%), with an unattributed budget imbalance (2%). All components except land-use change emissions have significantly grown since 1959, with important interannual variability in the growth rate in atmospheric CO_2 concentration and in the land CO_2 sink (Fig. 4), and some decadal variability in all terms (Table 6). Differences with previous budget releases is documented in Fig. B4.

3.1.1 CO_2 emissions

Global fossil CO_2 emissions have increased every decade from an average of 3.0 ± 0.2 GtC yr^{-1} in the 1960s to an average of 9.5 ± 0.5 GtC yr^{-1} during 2009-2018 (Table 6, Fig. 2 and Fig. 5). The growth rate in these emissions decreased between the 1960s and the 1990s, from 4.4% yr^{-1} in the 1960s (1960-1969), 2.8% yr^{-1} in the 1970s (1970-1979), 1.9% yr^{-1} in the 1980s (1980-1989), to 0.9% yr^{-1} in the 1990s (1990-1999). After this period, the growth rate began increasing again in the 2000s at an average growth rate of 3.0% yr^{-1}, decreasing to 1.3% yr^{-1} for the last decade (2009-2018).

In contrast, CO_2 emissions from land-use, land-use change and forestry have remained relatively constant, at around 1.3 ± 0.7 GtC yr^{-1} over the past half-century (Table 6) but with large spread across estimates (Table 5, Fig. 6). These emissions are also relatively constant in the DGVM ensemble of models, except during the last decade when they increase to 2.0 ± 0.5 GtC yr^{-1}. However, there is no agreement on this recent increase between the two bookkeeping models, each suggesting an opposite trend (Fig. 6).

3.1.2   Partitioning among the atmosphere, ocean and land

The growth rate in atmospheric CO_2 level increased from 1.8 ± 0.07 GtC yr^{-1} in the 1960s to 4.9 ± 0.02 GtC yr^{-1} during 2009-2018 with important decadal variations (Table 6 and Fig. 2). Both ocean and land CO_2 sinks have increased roughly in line with the atmospheric increase, but with significant decadal variability on land (Table 6 and Fig. 6), and possibly in the ocean (Fig. 7). The ocean CO_2 sink increased from 1.0 ± 0.6 GtC yr^{-1} in the 1960s to 2.5 ± 0.6 GtC yr^{-1} during 2009-

2018, with interannual variations of the order of a few tenths of GtC yr^{-1} generally showing an increased ocean sink during large El Niño events (i.e. 1997-1998) (Fig. Rödenbeck et al., 2014)7; Rödenbeck et al., 2014). There is coherence among the GOBMs and pCO$_2$-based flux products regarding the mean, and the patterns of temporal variability, however, the ocean models underestimate the magnitude of decadal variability (Section 2.4.3 and Fig. 7; DeVries et al., 2019).

The terrestrial CO$_2$ sink increased from 1.3 ± 0.4 GtC yr^{-1} in the 1960s to 3.2 ± 0.7 GtC yr^{-1} during 2009-2018, with important interannual variations of up to 2 GtC yr^{-1} generally showing a decreased land sink during El Niño events (Fig. 6), responsible for the corresponding enhanced growth rate in atmospheric CO$_2$ concentration. The larger land CO$_2$ sink during 2009-2018 compared to the 1960s is reproduced by all the DGVMs in response to the combined atmospheric CO$_2$ increase and the changes in climate, and consistent with constraints from the other budget terms (Table 5).

The total atmosphere-to-land fluxes ($S_{LAND} - E_{LUC}$), calculated here as the difference between S_{LAND} from the DGVMs and E_{LUC} from the bookkeeping models, increased from a 0.2 ±0.8 GtC yr^{-1} source in the 1960s to a 1.7 ± 0.9 GtC yr^{-1} sink during 2009-2018 (Table 5). Estimates of total atmosphere-to-land fluxes ($S_{LAND} - E_{LUC}$) from the DGVMs alone are consistent with our estimate and also with the global carbon budget constraint (E_{FF}-G_{ATM}-S_{OCEAN}, Table 5), except during 2009-2018, where the DGVM ensemble estimates a total atmosphere-to-land flux of 1.0 ± 0.8 GtC yr^{-1}, likely below both our estimate of 1.7 ± 0.9 GtC yr^{-1} and the carbon budget constraint of 2.1 ± 0.7 GtC yr^{-1} but still within the range of the inversions (1.1-2.2 GtC yr^{-1}) (Table 5). Over the last decade, the land use emission estimate from the DGVMs is significantly larger than the bookkeeping estimate, mainly explaining why the DGVMs total atmosphere-to-land flux estimate is lower than the other estimates.

3.1.3 Model evaluation

The evaluation of the ocean estimates (Fig. B1) shows a RMSE of 15 to 17 μatm for the three pCO$_2$-based flux products over the globe, relative to the pCO$_2$ observations from the SOCAT v2019 database for the period 1985-2018. The GOBM RMSEs are a factor of two to three larger and range between 29 to 49 μatm. The RMSEs are generally larger at high latitudes compared to the tropics, for both the flux products and the GOBMs. The three flux products have similar RMSEs of around 12 to 14 μatm in the tropics, around 17 to 18 μatm in the north, and 17 to 24

μatm in the south. Note that the flux products are based on the SOCAT v2019 database, hence these are no independent data set for the evaluation of the flux products. The GOBM RMSEs are more spread across regions, ranging from 21 to 34 μatm in the tropics, 32 to 48 μatm in the North, and 31 to 77 μatm in the South. The higher RMSEs occur in regions with stronger climate variability, such as the northern and southern high latitudes (poleward of the subtropical gyres).

The evaluation of the DGVMs (Fig. B2) shows generally high skill scores across models for runoff, and to a lesser extent for vegetation biomass, GPP, and ecosystem respiration (Fig. B2, left panel). Skill score was lowest for leaf area index and net ecosystem exchange, with a widest disparity among models for soil carbon. Further analysis of the results will be provided separately, focusing on the strengths and weaknesses in the DGVM ensemble and its validity for use in the global carbon budget.

The evaluation of the atmospheric inversions (Fig. B3) shows long-term mean biases in the free troposphere better than 0.4 ppm in absolute values for each product. These biases show some dependency on latitude and are different for each inverse model, which may reveal biases in the surface fluxes (e.g., Houweling et al., 2015). Such model- and campaign-specific performance will be analysed separately.

3.1.4 Budget imbalance

The carbon budget imbalance (B_{IM}; Eq. 1) quantifies the mismatch between the estimated total emissions and the estimated changes in the atmosphere, land and ocean reservoirs. The mean budget imbalance from 1959 to 2018 is small (average of 0.17 GtC yr^{-1}) and shows no trend over the full time series. The process models (GOBMs and DGVMs) have been selected to match observational constraints in the 1990s but no further constraints have been applied to their representation of trend and variability. Therefore, the near-zero mean and trend in the budget imbalance is an indirect evidence of a coherent community understanding of the emissions and their partitioning on those time scales (Fig. 4). However, the budget imbalance shows substantial variability of the order of ± 1 GtC yr^{-1}, particularly over semi-decadal time scales, although most of the variability is within the uncertainty of the estimates. The positive carbon imbalance during the 1960s, early 1990s, and in the last decade, suggest that either the emissions were overestimated or the sinks were underestimated during these periods. The reverse is true for the 1970s and around 1995-2000 (Fig. 4).

We cannot attribute the cause of the variability in the budget imbalance with our analysis, only to note that the budget imbalance is unlikely to be explained by errors or biases in the emissions alone because of its large semi-decadal variability component, a variability that is untypical of emissions and has not changed in the past 50 years in spite of a near tripling in emissions (Fig. 4). Errors in S_{LAND} and S_{OCEAN} are more likely to be the main cause for the budget imbalance. For example, underestimation of the S_{LAND} by DGVMs has been reported following the eruption of Mount Pinatubo in 1991 possibly due to missing responses to changes in diffuse radiation (Mercado et al., 2009) or other yet unknown factors, and DGVMs are suspected to overestimate the land sink in response to the wet decade of the 1970s (Sitch et al., 2008). Decadal and semi-decadal variability in the ocean sink has also been reported recently (DeVries et al., 2019, 2017; Landschützer et al., 2015), with the pCO_2-based ocean flux products and a decadal ocean inverse model suggesting a smaller than expected ocean CO_2 sink in the 1990s and a larger than expected sink in the 2000s (Fig. 7; DeVries et al., 2019). The decadal variability is possibly caused by changes in ocean circulation (DeVries et al., 2017) not captured in coarse resolution GOBMs used here (Dufour et al., 2013), or by internal variability, which is not captured by single realizations of coarse resolution model simulations (Li and Ilyina, 2018). The decadal variability is thought to be largest in regions with strong seasonal and interannual climate variability, i.e. the high latitude ocean regions (poleward of the subtropical gyres) and the equatorial Pacific (Li and Ilyina, 2018; McKinley et al., 2016). Some of these errors could be driven by errors in the climatic forcing data, particularly precipitation (for S_{LAND}) and wind (for S_{OCEAN}) rather than in the models.

3.2 Global carbon budget for the last decade (2009 – 2018)

The global carbon budget averaged over the last decade (2009-2018) is shown in Fig. 2 and Fig. 9. For this time period, 86% of the total emissions ($E_{FF} + E_{LUC}$) were from fossil CO_2 emissions (E_{FF}), and 14% from land-use change (E_{LUC}). The total emissions were partitioned among the atmosphere (44%), ocean (23%) and land (29%), with a unattributed budget imbalance (4%).

3.2.1 CO_2 emissions

Global fossil CO_2 emissions grew at a rate of 1.3% yr^{-1} for the last decade (2009-2018). China's emissions increased by +2.2% yr^{-1} on average (increasing by +0.063 GtC yr^{-1} during the 10-year period) dominating the global trend, followed by India's emissions increase by +5.1% yr^{-1} (increasing by +0.025 GtC yr^{-1}), while emissions decreased in EU28 by –1.4% yr^{-1} (decreasing by

Deleted: (Mercado et al., 2009)

Deleted: factor

Deleted: (Sitch et al., 2008).

Deleted: (DeVries et al., 2019, 2017; Landschützer et al., 2015),

Deleted: DeVries et al., 2019).

Deleted: (DeVries et al., 2017)

Deleted: (Dufour et al., 2013),

Deleted: (Li and Ilyina, 2018)

Deleted: (Li and Ilyina, 2018; McKinley et al., 2016).

Deleted: remaining

−0.010 GtC yr^{-1}), and in the USA by −0.5% yr^{-1} (decreasing by −0.002 GtC yr^{-1}). (Le Quéré et al., 2019) In the past decade, fossil CO_2 emissions decreased significantly (at the 95% level) in 19 growing economies: Belgium, Croatia, Czech Republic, Denmark, Finland, France, Italy, Latvia, Luxembourg, Republic of Macedonia, Malta, the Netherlands, Romania, Slovenia, Sweden, Switzerland, United Kingdom, USA and Uzbekistan. The drivers of recent decarbonisation are examined in Le Quéré et al. (2019).

In contrast, there is no clear trend in CO_2 emissions from land-use change over the last decade (Fig. 6), though the data are very uncertain, with only one of the two bookkeeping estimates showing a positive trend over the last decade. Larger emissions are expected increasingly over time for DGVM-based estimates as they include the loss of additional sink capacity, while the bookkeeping estimates do not. The LUH2 data set also features large dynamics in land-use in particular in the tropics in recent years, causing higher emissions in DGVMs and BLUE than in H&N.

3.2.2 Partitioning among the atmosphere, ocean and land

The growth rate in atmospheric CO_2 concentration increased during 2009-2018, in contrast to more constant levels in the previous decade and reflecting a similar decrease in the land sink compared to an increase in the previous decade, albeit with large interannual variability (Fig. 4). During the same period, the ocean CO_2 sink appears to have intensified, an effect which is particularly apparent in the pCO_2-based flux products (Fig. 7) and a decadal ocean inverse model (DeVries et al., 2019). The GOBMs show the same patterns of decadal variability as the mean of the pCO_2-based flux products, but of weaker magnitude (Fig. 7). The pCO_2-based flux products and the ocean inverse model highlight different regions as the main origin of this decadal variability, with the pCO_2-based flux products placing more of the weakening trend in the Southern Ocean and the ocean inverse model suggesting that more of the weakening trend occurred in the North Atlantic and North Pacific (DeVries et al., 2019). Both approaches show also decadal trends in the low-latitude oceans (DeVries et al., 2019).

The budget imbalance (Table 6) and the residual sink from global budget (Table 5) include an error term due to the inconsistency that arises from using E_{LUC} from bookkeeping models, and S_{LAND} from DGVMs. This error term includes the fundamental differences between bookkeeping models and DGVMs, most notably the loss of additional sink capacity. Other differences include: an incomplete accounting of LUC practices and processes in DGVMs, while they are all

accounted for in bookkeeping models by using observed carbon densities, and bookkeeping error of keeping present-day carbon densities fixed in the past. That the budget imbalance shows no clear trend towards larger values over time is an indication that the loss of additional sink capacity plays a minor role compared to other errors in S_{LAND} or S_{OCEAN} (discussed in Section 3.1.4).

3.2.3 Regional distribution

Fig. 8 shows the partitioning of the total atmosphere-to-surface fluxes excluding fossil CO_2 emissions ($S_{LAND} + S_{OCEAN} - E_{LUC}$) according to the multi-model average of the process models in the ocean and on land (GOBMs and DGVMs), and to the atmospheric inversions. Fig. 8 provides information on the regional distribution of those fluxes by latitude bands. The global mean total atmosphere-to-surface CO_2 fluxes from process models for 2009-2018 is 3.5 ± 0.9 GtC yr^{-1}. This is below but still within the uncertainty range of a global mean atmosphere-to-surface flux of 4.6 ± 0.5 GtC yr^{-1} inferred from the carbon budget ($E_{FF} - G_{ATM}$ in Equation 1; Table 6). The total atmosphere-to-surface CO_2 fluxes from the three inversions are very similar, ranging from 4.6 to 4.9 GtC yr^{-1}, consistent with the carbon budget as expected from the constraints on the inversions and the adjustments to the same E_{FF} distribution (See Section 2.6).

In the south (south of 30°S), the atmospheric inversions suggest an atmosphere-to-surface flux for 2009-2018 around 1.7-2.0 GtC yr^{-1}, slightly above the process models' estimate of 1.4 ± 0.3 GtC yr^{-1} (Fig. 8). The higher flux in the pCO$_2$-based flux products than in the ocean models might be explained by a known lack of surface ocean pCO$_2$ observations in winter, when CO_2 outgassing occurs south of the Polar Front (Gray et al., 2018).

The interannual variability in the south is low because of the dominance of ocean area with low variability compared to land areas. The split between land ($S_{LAND}-E_{LUC}$) and ocean (S_{OCEAN}) shows a small contribution to variability in the south coming from the land, with no consistency between the DGVMs and the inversions or among inversions. This is expected due to the difficulty of separating exactly the land and oceanic fluxes when viewed from atmospheric observations alone. The oceanic variability in the south is estimated to be significant in the three pCO$_2$-based flux products, with decadal variability of 0.18 to 0.22 GtC yr^{-1} (Fig. B1). The GOBMs show slightly lower interannual variability (0.11 to 0.18 GtC yr^{-1}, Fig. B1).

In the tropics (30°S-30°N), both the atmospheric inversions and process models suggest the total carbon balance in this region is close to neutral on average over the past decade. The three inversion models suggest an atmosphere-to-surface flux between –0.5 and +0.3 GtC yr^{-1} for the 2009-2018 period, which is within the range of the process models' estimates of 0.1 ± 0.4 GtC yr^{-1} The agreement between inversions and models is significantly better for the last decade than for any previous decade, although the reasons for this better agreement are still unclear. Both the process models and the inversions consistently allocate more year-to-year variability of CO_2 fluxes to the tropics compared to the north (north of 30°N; Fig. 8). The split between the land and ocean indicates the land is the origin of most of the tropical variability, consistently among models (both for the land and for the ocean) and inversions. The oceanic variability in the tropics is similar among the three ocean flux products (A-IAV 0.12 to 0.14 GtC yr^{-1}) and the models, although the model spread is larger (A-IAV 0.08 to 0.19 GtC yr^{-1}, Section 3.1.3, Fig. B1). While the inversions indicate that atmosphere-to-land CO_2 fluxes are more variable than atmosphere-to-ocean CO_2 fluxes in the tropics, the correspondence between the inversions and the ocean flux products or GOBMs is much poorer, partly caused by a substantial tropical ocean carbon sink produced by one of the three inversions.

In the north (north of 30°N), models, inversions and pCO_2-based flux products consistently suggest that most of the variability stems from the land (Fig. 8). Inversions, GOBMs and pCO_2-based flux products agree on the mean of S_{OCEAN}, but with a higher variability in the pCO_2-based flux products (A-IAV: 0.12 to 0.13 GtC yr^{-1}) than in the models (A-IAV: 0.03 to 0.08 GtC yr^{-1}, Fig. B1). Atmospheric inversions and process models show less agreement on the magnitude of the atmosphere-to-land flux, with the ensemble mean of the process models suggesting a total Northern Hemisphere sink for 2009-2018 of 2.1 ± 0.5 GtC yr^{-1}, below the estimates from the inversions ranging from 2.5 to 3.4 GtC yr^{-1} (Fig. 8). The discrepancy in the north-tropics distribution of CO_2 fluxes between the inversions and models arises from the differences in mean fluxes over the northern land. This discrepancy is also evidenced over the previous decade and highlights not only persistent issues with the quantification of the drivers of the net land CO_2 flux (Arneth et al., 2017; Huntzinger et al., 2017) but also the distribution of atmosphere-to-land fluxes between the tropics and higher latitudes that is particularly marked in previous decades, as highlighted previously (Baccini et al., 2017; Schimel et al., 2015; Stephens et al., 2007).

Differences between inversions may be related for example to differences in their interhemispheric transport, and other inversion settings (Table A3). Separate analysis has shown that the influence of the chosen prior land and ocean fluxes is minor compared to other aspects of each inversion, while fossil fuel inputs were adjusted to match that of E_{FF} used in this analysis (see Section 2.6), therefore removing differences due to fossil emissions prior. Differences between inversions and the ensemble of process models in the north cannot be simply explained. They could either reflect a bias in the inversions or missing processes or biases in the process models, such as the lack of adequate parameterizations for land management for the DGVMs. The estimated contribution of the north and its uncertainty from process models is sensitive both to the ensemble of process models used and to the specifics of each inversion.

Resolving the differences in the Northern Hemisphere land sink will require the consideration and inclusion of larger volumes of semi-continuous observations of concentrations, fluxes as well as auxiliary variables collected from (tall) towers close to the surface CO_2 exchange. Moreover, effective use of such information would demand a more process-based approach to land-surface exchange of CO_2 than currently employed in inverse models. Such process-based approach would represent constraints on carbon exchange derived from local observations and biogeochemical relations on multiple time-scales, which in turn would be constrained by the regional-to-continental scale mass-balance of atmospheric CO_2. Some of these near-surface data are now becoming available, but not used in the current inverse models sometimes due to the short records, and sometimes because the coarse transport models cannot adequately represent these time series. Improvements in model resolution and atmospheric transport realism together with expansion of the observational record (also in the data sparse Boreal Eurasian area) will help anchor the mid-latitude fluxes per continent. In addition, new metrics could potentially differentiate between the more- and less realistic realisations of the Northern Hemisphere land sink shown in Fig. 8.

3.2.4 Budget imbalance

The budget imbalance was +0.4 GtC yr^{-1} on average over 2009-2018. Although the uncertainties are large in each term, the sustained imbalance over this last decade suggests an overestimation of the emissions and/or an underestimation of the sinks. An origin in the land and/or ocean sink may be more likely, given the large variability of the land sink and the

suspected underestimation of decadal variability in the ocean sink. An underestimate of S_{LAND} would also reconcile model results with inversions estimates for fluxes in the total land during the past decade (Fig. 8; Table 5). An underestimation of S_{OCEAN} is also possible given slightly higher estimates for S_{OCEAN} from ocean interior carbon observations over the period 1994 to 2007 (2.6 ± 0.3 GtC yr^{-1}; Gruber et al., 2019) compared to the estimate from GOBMs of 2.1 ± 0.5 GtC yr^{-1} over the same period, although uncertainties overlap. However, we cannot exclude that the budget imbalance over the last decade could partly be due to an overestimation of CO_2 emissions, in particular from land-use change, given their large uncertainty, as has been suggested elsewhere (Piao et al., 2018). More integrated use of observations in the Global Carbon Budget, either on their own or for further constraining model results, should help resolve some of the budget imbalance (Peters et al., 2017; Section 4).

3.3 Global carbon budget for year 2018

3.3.1 CO_2 emissions

Preliminary estimates of global fossil CO_2 emissions are for growth of 2.1% between 2017 and 2018 to reach 10.0 ± 0.5 GtC in 2018 (Fig. 5), distributed among coal (40%), oil (34%), natural gas (20%), cement (4%) and others (1.3%). Compared to the previous year, emissions from coal increased by 1.4%, while emissions from oil, natural gas, and cement increased by 1.2%, 5.4%, and 2.1%, respectively. All growth rates presented are adjusted for the leap year, unless stated otherwise.

In 2018, the largest absolute contributions to global CO_2 emissions were from China (28%), the USA (15%), the EU (28-member states; 9%), and India (7%). These four regions account for 59% of global CO_2 emissions, while the rest of the world contributed 41% which includes aviation and marine bunker fuels (3.4% of the total). Growth rates for these countries from 2017 to 2018 were +2.3% (China), 2.8% (USA), −2.1% (EU28), and 8.0% (India), with +1.8% for the rest of the world. The per-capita CO_2 emissions in 2018 were 1.3 tC person^{-1} yr^{-1} for the globe, and were 4.5 (USA), 1.9 (China), 1.8 (EU28) and 0.5 (India) tC person^{-1} yr^{-1} for the four highest emitting countries (Fig. 5).

The growth in emissions of 2.1% in 2018 is within the range of the projected growth of 2.7% (range of 1.8 to 3.7%) published in (Le Quéré et al., 2018b)Le Quéré et al. (2018b) based on national emissions projections for China, the USA, and India and projections of gross domestic product corrected for I_{FF} trends for the rest of the world. The growth in emissions in 2018 for

China, the USA, EU28, India, and the rest of the world were all within their previously projected range (Table 7).

In 2016 (the last year available), the largest absolute contributions to global CO_2 emissions from a consumption perspective were China (25%), USA (16%), the EU (12%), and India (6%). The difference between territorial and consumption emissions (the net emission transfer via international trade) has generally increased from 1990 to around 2005 and remained relatively stable afterwards until the last year available (2016; Fig. 5).

The global CO_2 emissions from land-use change are estimated as 1.5 ± 0.7 GtC in 2018, close to the previous decade but with low confidence in the annual change. This brings the total CO_2 emissions from fossil plus land-use change ($E_{FF}+E_{LUC}$) to 11.5 ± 0.9 GtC (42.5 ± 3.3 $GtCO_2$).

3.3.2 Partitioning among the atmosphere, ocean and land

The growth rate in atmospheric CO_2 concentration was 5.1 ± 0.2 GtC in 2018 (2.42 ± 0.08 ppm; Fig. Dlugokencky and Tans, 2019)4; Dlugokencky and Tans, 2019). This is near the 2009-2018 average of 4.9 ± 0.02 GtC yr^{-1}.

The estimated ocean CO_2 sink was 2.6 ± 0.6 GtC in 2018. The multi-model mean agrees with the mean of the pCO_2-based flux products on an average increase of 0.11 GtC in 2018. Six models and two flux products show an increase of SOCEAN (up to +0.38 GtC), while three models and one flux product show no change or a decrease of SOCEAN (down to -0.15 GtC) (Fig. 7).

The terrestrial CO_2 sink from the DGVM model ensemble was 3.5 ± 0.7 GtC in 2018, slightly above the decadal average (Fig. 4) and consistent with constraints from the rest of the budget (Table 5). The budget imbalance was +0.3 GtC in 2018, consistent with its average over the last decade (Table 6). This imbalance is indicative only, given the large uncertainties in the estimation of the B_{IM}.

3.4 Global carbon budget projection for year 2019

3.4.1 CO_2 emissions

Based on the available data as of 5 November 2019 (see Section 2.1.5), fossil CO_2 emissions (E_{FF}) for 2019 are projected to increase by +0.5% (range of -0.3% to +1.4%; Table 7). Our method contains several assumptions that could influence the estimate beyond the given range, and as

such, it has an indicative value only. Within the given assumptions, global emissions would be 10.0 ± 0.5 GtC (36.7 ± 1.8 GtCO$_2$) in 2019.

For China, the expected change is for an increase in emissions of +2.6% (range of +0.7% to +4.4%) in 2019 compared to 2018. This is based on estimated growth in coal (+0.8%; the main fuel source in China), oil (+6.9%), natural gas (+9.1%) consumption, and cement production (+6.3%). The uncertainty range considers the variations in the difference between preliminary January–September data and final full-year data, lack of monthly data on stock changes, variances in the discrepancies between supply-side and demand data, the uncertainty in the preliminary data used for the 2018 base, and uncertainty in the evolution of the average energy density of each of the fossil fuels.

For the USA, the EIA emissions projection for 2019 combined with cement data from USGS gives a decrease of −2.4% (range of −5.0 to +0.0 %) compared to 2018. This is based on separate projections for coal −12.8%, oil −0.8%, natural gas +3.2%, and cement +0.7%.

For the European Union, our projection for 2019 is for a decrease of −1.7% (range of −3.4% to +0.1%) over 2018. This is based on separate projections for coal of −10.0%, oil of +0.5%, natural gas of +3.0%, and stable cement emissions. Uncertainty is largest in coal, where two alternative methods give divergent estimates.

For India, our projection for 2019 is for an increase of +1.8% (range of -0.7% to +3.7%) over 2018. This is based on separate projections for coal (+2.0%), oil (+1.5%), natural gas (+2.5%) and cement (+0.0%). The wide uncertainty range reflects an anomalous year: the 2019 monsoon year produced above average rainfall, particularly in September, with 52% higher rainfall than the long-term average (IMD, 2019). This heavier rainfall led both to flooded coal mines (Varadhan, 2019) and high hydropower generation (CEA, 2019b). In addition, the Indian economy has slowed rapidly during the year (IMF, 2019b). Furthermore, our forecast for India covers its financial year, April 2019 to March 2020, reflecting the underlying emissions data, adding to uncertainty.

For the rest of the world, the expected growth for 2019 is +0.5% (range of −0.8% to +1.8%). This is computed using the GDP projection for the world excluding China, USA, EU, and India, of 1.9% made by the IMF (IMF, 2019)(IMF, 2019a) and a decrease in I$_{FF}$ of −1.4% yr^{-1} which is the average from 2009-2018. The uncertainty range is based on the standard deviation of the interannual variability in I$_{FF}$ during 2009-2018 of ±0.8% yr^{-1} and our estimate of uncertainty in

the IMF's GDP forecast of ±0.5%. The methodology allows independent projections for coal, oil, natural gas, cement, and other components, which add to the total emissions in the rest of the world. The 2019 growth rates for coal were +0.1% (range −2.9% to +3.2%), oil +0.1% (range −0.9% to +1.2%), natural gas +1.4% (range −0.7% to +3.4%), and cement +1.3% (range −1.2% to +3.9%).

Each of our regional projections contains separate projections for coal, oil, natural gas, cement, and other smaller components. This allows us, for the first time, to supplement our global fossil CO_2 emission projection of +0.5% (range of -0.4% to +1.4%) with separate global projections of the CO_2 emissions from coal -1.1% (range −2.3% to +0.2%), oil +0.9% (range 0.1% to +1.7%), natural gas +2.5% (range +1.2% to +3.9%), and cement +3.7% (range +0.4% to +7.3%).

Preliminary estimate of fire emissions in deforestation zones indicate that emissions from land-use change (E_{LUC}) for 2019 were above the 2009-2018 average, amounting to 427 TgC by October 31st, and are expected to remain at this level for the remainder of the year. We therefore expect E_{LUC} emissions of around 1.7 GtC in 2019, for a total anthropogenic CO_2 emissions of 11.7 ± 0.9 GtC (42.9 ± 3.2 $GtCO_2$) in 2019.

3.4.2 Partitioning among the atmosphere, ocean and land

The 2019 growth in atmospheric CO_2 concentration (G_{ATM}) is projected to be 4.6 ± 0.9 GtC (2.2 ± 0.4 ppm) based on GLO observations until the end of July 2019, bringing the atmospheric CO_2 concentration to an expected level of 410 ppm averaged over the year. Combining projected E_{FF}, E_{LUC} and G_{ATM} suggests a combined land and ocean sink (S_{LAND} + S_{OCEAN}) of about 7.1 GtC for 2019. Although each term has large uncertainty, the oceanic sink S_{OCEAN} has generally low interannual variability and is likely to remain close to its 2018 value of around 2.6 GtC, leaving a rough estimated land sink S_{LAND} (including any budget imbalance) of around 4.5 GtC, substantially above the 2018 estimate.

3.5 Cumulative sources and sinks

Cumulative historical sources and sinks are estimated as in Eq. (1) with semi-independent estimates for each term and a global carbon budget imbalance. Cumulative fossil CO_2 emissions for 1850-2018 were 440 ± 20 GtC for E_{FF} and 205 ± 60 GtC for E_{LUC} (Table 8; Fig. 9), for a total of 645 ± 65 GtC. The cumulative emissions from E_{LUC} are particularly uncertain, with large spread among individual estimates of 150 GtC (H&N) and 260 GtC (BLUE) for the two bookkeeping

models and a similar wide estimate of 185 ± 60 GtC for the DGVMs. These estimates are consistent with indirect constraints from vegetation biomass observations (Li et al., 2017)(Li et al., 2017), but given the large spread a best estimate is difficult to ascertain.

Emissions during the period 1850-2018 were partitioned among the atmosphere (255 ± 5 GtC; 40%), ocean (160 ± 20 GtC; 25%), and the land (195 ± 40 GtC; 31%). This cumulative land sink is broadly equal to the cumulative land-use emissions, making the global land near neutral over the 1850-2018 period. The use of nearly independent estimates for the individual terms shows a cumulative budget imbalance of 30 GtC (4%) during 1850-2018 (Fig. 2), which, if correct, suggests emissions are too high by the same proportion or the land or ocean sinks are underestimated. The bulk of the imbalance could originate from the estimation of large E_{LUC} between the mid 1920s and the mid 1960s which is unmatched by a growth in atmospheric CO_2 concentration as recorded in ice cores (Fig. 3). The known loss of additional sink capacity of about 20 ± 15 GtC due to reduced forest cover has not been accounted in our method and would further exacerbate the budget imbalance (Section 2.7.4).

Cumulative emissions through to year 2019 increase to 655 ± 65 GtC (2340 ± 240 GtCO$_2$), with about 70% contribution from E_{FF} and about 30% contribution from E_{LUC}. Cumulative emissions and their partitioning for different periods are provided in Table 8.

Given the large and persistent uncertainties in historical cumulative emissions, we suggest extreme caution is needed if using this estimate to determine the remaining cumulative CO_2 emissions consistent with an ambition to stay below a given temperature limit (Rogelj et al., 2016)(Millar et al., 2017; Rogelj et al., 2019)(Millar et al., 2017; Rogelj et al., 2016, 2019).

4   Discussion

Each year when the global carbon budget is published, each flux component is updated for all previous years to consider corrections that are the result of further scrutiny and verification of the underlying data in the primary input data sets. Annual estimates may improve with improvements in data quality and timeliness (e.g. to eliminate the need for extrapolation of forcing data such as land-use). Of the various terms in the global budget, only the fossil CO_2 emissions and the growth rate in atmospheric CO_2 concentration are based primarily on empirical inputs supporting annual estimates in this carbon budget. Although it is an imperfect measure, the carbon budget imbalance provides a strong indication of the limitations in

observations, in understanding or full representation of processes in models, and/or in the integration of the carbon budget components.

The persistent unexplained variability in the carbon budget imbalance limits our ability to verify reported emissions (Peters et al., 2017) and suggests we do not yet have a complete understanding of the underlying carbon cycle processes. Resolving most of this unexplained variability should be possible through different and complementary approaches. First, as intended with our annual updates, the imbalance as an error term is reduced by improvements of individual components of the global carbon budget that follow from improving the underlying data and statistics and by improving the models through the resolution of some of the key uncertainties detailed in Table 9. Second, additional clues to the origin and processes responsible for the current imbalance could be obtained through a closer scrutiny of carbon variability in light of other Earth system data (e.g. heat balance, water balance), and the use of a wider range of biogeochemical observations to better understand the land-ocean partitioning of the carbon imbalance (e.g. oxygen, carbon isotopes). Finally, additional information could also be obtained through higher resolution and process knowledge at the regional level, and through the introduction of inferred fluxes such as those based on satellite CO_2 retrievals. The limit of the resolution of the carbon budget imbalance is yet unclear, but most certainly not yet reached given the possibilities for improvements that lie ahead.

The assessment of the GOBMs used for S_{OCEAN} with flux products based on observations highlights substantial discrepancy at mid and high latitudes. Given the good data coverage of pCO_2 observations in the Northern Hemisphere (Bakker et al., 2016) this discrepancy points at an underestimation of variability in the GOBMs globally and consequently, the variability in S_{OCEAN} appears to be underestimated. The size of the underestimation of the amplitude of interannual variability (order of 0.1 GtC yr^{-1}, A-IAV, see Fig. B1) could account for some of the budget imbalance, but not all. Increasing model resolution or using model ensembles (Li and Ilyina, 2018) have been suggested as ways to increase model variability (Section 3.1.4).

The assessment of the net land-atmosphere exchange derived from land sink and net land-use change flux with atmospheric inversions also shows substantial discrepancy, particularly for the estimate of the total land flux over the northern extra-tropics in the past decade. This discrepancy highlights the difficulty to quantify complex processes (CO_2 fertilisation, nitrogen deposition, N fertilisers, climate change and variability, land management, etc.) that collectively

determine the net land CO_2 flux. Resolving the differences in the Northern Hemisphere land sink will require the consideration and inclusion of larger volumes of observations (Section 3.2.3).

Estimates of E_{LUC} suffer from a range of intertwined issues, including the poor quality of historical land-cover and land-use change maps, the rudimentary representation of management processes in most models, and the confusion in methodologies and boundary conditions used across methods (e.g. Arneth et al., 2017; Pongratz et al., 2014), and Section 2.7.4 on the loss of sink capacity). Uncertainties in current and historical carbon stocks in soils and vegetation also add uncertainty in the LUC flux estimates. Unless a major effort to resolve these issues is made, little progress is expected in the resolution of E_{LUC}. This is particularly concerning given the growing importance of E_{LUC} for climate mitigation strategies, and the large issues in the quantification of the cumulative emissions over the historical period that arise from large uncertainties in E_{LUC}.

As introduced last year, we provide metrics for the evaluation of the ocean and land models and atmospheric inversions. These metrics expand the use of observations in the global carbon budget, helping 1) to support improvements in the ocean and land carbon models that produce the sink estimates, and 2) to constrain the representation of key underlying processes in the models and to allocate the regional partitioning of the CO_2 fluxes. This is an initial step towards the introduction of a broader range of observations that we hope will support continued improvements in the annual estimates of the global carbon budget.

We assessed before (Peters et al., 2017) that a sustained decrease of −1% in global emissions could be detected at the 66% likelihood level after a decade only. Similarly, a change in behaviour of the land and/or ocean carbon sink would take as long to detect, and much longer if it emerges more slowly. Reducing the carbon imbalance, regionalising the carbon budget, and integrating multiple variables are powerful ways to shorten the detection limit and ensure the research community can rapidly identify growing issues of concern in the evolution of the global carbon cycle under the current rapid and unprecedented changing environmental conditions.

5 Conclusions

The estimation of global CO_2 emissions and sinks is a major effort by the carbon cycle research community that requires a careful compilation and synthesis of measurements, statistical estimates and model results. The delivery of an annual carbon budget serves two purposes. First, there is a large demand for up-to-date information on the state of the anthropogenic perturbation of the climate system and its underpinning causes. A broad stakeholder community relies on the data sets associated with the annual carbon budget including scientists, policy makers, businesses, journalists, and non-governmental organizations engaged in adapting to and mitigating human-driven climate change. Second, over the last decade we have seen unprecedented changes in the human and biophysical environments (e.g. changes in the growth of fossil fuel emissions, Earth's temperatures, and strength of the carbon sinks), which call for frequent assessments of the state of the planet, a better quantification of the causes of changes in the contemporary global carbon cycle, and an improved capacity to anticipate its evolution in the future. Building this scientific understanding to meet the extraordinary climate mitigation challenge requires frequent, robust, transparent and traceable data sets and methods that can be scrutinized and replicated. This paper via 'living data' helps to keep track of new budget updates.

6 Data availability

The data presented here are made available in the belief that their wide dissemination will lead to greater understanding and new scientific insights of how the carbon cycle works, how humans are altering it, and how we can mitigate the resulting human-driven climate change. The free availability of these data does not constitute permission for publication of the data. For research projects, if the data are essential to the work, or if an important result or conclusion depends on the data, co-authorship may need to be considered for the relevant data providers. Full contact details and information on how to cite the data shown here are given at the top of each page in the accompanying database and summarised in Table 2.

The accompanying database includes two Excel files organised in the following spreadsheets:

File Global_Carbon_Budget_2019v1.0.xlsx includes the following:

1. Summary

2. The global carbon budget (1959-2018);

3. Global CO_2 emissions from fossil fuels and cement production by fuel type, and the per-capita emissions (1959-2018);

4. CO_2 emissions from land-use change from the individual methods and models (1959-2018);

5. Ocean CO_2 sink from the individual ocean models and pCO_2-based products (1959-2018);

6. Terrestrial CO_2 sink from the DGVMs (1959-2018);

7. Additional information on the historical global carbon budget prior to 1959 (1750-2018).

File National_Carbon_Emissions_2019v1.0.xlsx includes the following:

1. Summary

2. Territorial country CO_2 emissions from fossil CO_2 emissions (1959-2018) from CDIAC with UNFCCC data overwritten where available, extended to 2018 using BP data;

3. Consumption country CO_2 emissions from fossil CO_2 emissions and emissions transfer from the international trade of goods and services (1990-2016) using CDIAC/UNFCCC data (worksheet 3 above) as reference;

4. Emissions transfers (Consumption minus territorial emissions; 1990-2016);

5. Country definitions;

6. Details of disaggregated countries;

7. Details of aggregated countries.

Both spreadsheets are published by the Integrated Carbon Observation System (ICOS) Carbon Portal and are available at https://doi.org/10.18160/gcp-2019 (Friedlingstein et al., 2019). National emissions data are also available from the Global Carbon Atlas (http://www.globalcarbonatlas.org/, last access: 4 December 2019).

Author contributions. PF, MWJ, MOS, CLQ, RMA, JH, GPP, WP, JP, SS, DCEB, JGC, PC and RBJ designed the study, conducted the analysis, and wrote the paper. RMA, GPP and JIK produced the emissions and their uncertainties, 2019 emission projections, and analysed the emissions data. DG and GM provided emission data. PPT provided key atmospheric CO_2 data. WP, PC, FC,

Moved up [1]: <#>Conclusions¶
<#>The estimation of global CO_2 emissions and sinks is a major effort by the carbon cycle research community that requires a careful compilation and synthesis of measurements, statistical estimates and model results. The delivery of an annual carbon budget serves two purposes. First, there is a large demand for up-to-date information on the state of the anthropogenic perturbation of the climate system and its underpinning causes. A broad stakeholder community relies on the data sets associated with the annual carbon budget including scientists, policy makers, businesses, journalists, and non-governmental organizations engaged in adapting to and mitigating human-driven climate change. Second, over the last decade we have seen unprecedented changes in the human and biophysical environments (e.g. changes in the growth of fossil fuel emissions, Earth's temperatures, and strength of the carbon sinks), which call for frequent assessments of the state of the planet, a better

Moved up [2]: <#> Building this scientific understanding to meet the extraordinary climate mitigation challenge requires frequent, robust, transparent and traceable data sets and methods that can be scrutinized and replicated. This paper via 'living data' helps to keep track of new budget updates.¶

CR, NN and NS provided an updated atmospheric inversion, developed the protocol and produced the evaluation. JP, AB and RAH provided updated bookkeeping land-use change emissions. LPC, GH, KKG, FNT, and GRvdW provided forcing data for land-use change. PA, VB, DSG, VH, AKJ, EJ, EK, SL, DL, PCM, JRM, JEMSN, BP, HT, APW, AJW and SZ provided an update of a DGVM. IH and JOK provided forcing data for the DGVMs. ER provided the evaluation of the DGVMs. JH, LBo, EB, NG, TI, AL, JS and RS provided an update of a GOBM. MG, PL and CR provided an update of an ocean flux product. LBa, MB, KIC, RAF, TG, SG, NL, NM, DRM, SIN, CN, AMO, TO, DP, GR and BT provided ocean pCO_2 measurements for the year 2018, with synthesis by DCEB and SKL. LR provided an updated river flux estimate. AP contributed to setting up the GCB dataset at globalcarbonatlas.org. PF, MWJ and MOS revised all figures, tables, text and/or numbers to ensure the update is clear from the 2018 edition and in phase with the globalcarbonatlas.org.

Competing interests. The authors declare that they have no conflict of interest.

Acknowledgements. We thank all people and institutions who provided the data used in this carbon budget; Vivek Arora, Jinfeng Chang, Eunkyoung Choi, Julie Deshayes, Christian Ethé, M. Fortier, Tristan Quaife, Shijie Shu, Anthony Walker and Ulrich Weber for their involvement in the development, use and analysis of the models and data-products used here. We thank Ed Dlugokencky for providing atmospheric CO_2 measurements; Benjamin Pfeil, and Steve Jones of the Bjerknes Climate Data Centre and the ICOS Ocean Thematic Centre of the EU Integrated Carbon Observation System (ICOS) at the University of Bergen, as well as Karl Smith and Kevin O'Brien of NOAA's Pacific Marine Environmental Laboratory , who helped with SOCAT data management; and Alice Benoit-Cattin-Breton; Sólveig Ólafsdóttir, Frank Millero and Geun-Ha

Park, who contributed to the provision of ocean pCO_2 observations (see Table A4). This is NOAA-PMEL contribution number 4847. We thank the institutions and funding agencies responsible for the collection and quality control of the data in SOCAT, and the International Ocean Carbon Coordination Project (IOCCP) for its support. We thank FAO and its member countries for the collection and free dissemination of data relevant to this work. We thank data providers to ObsPack GLOBALVIEWplus v4.2 and NRT v4.40 for atmospheric CO_2 observations. We thank Trang Chau who produced the CMEMS pCO_2-based ocean flux data and designed the system together with MG, Anna Denvil-Sommer, and FC. We thank the individuals and institutions that provided the databases used for the model evaluations introduced here, and Nigel Hawtin for producing Figure 2 and Figure 9. We thank Fortunat Joos, Samar Khatiwala and Timothy DeVries for providing historical data. We thank all people and institutions who provided the data used in this carbon budget and the Global Carbon Project members for their input throughout the development of this update. Finally, we thank all funders who have supported the individual and joint contributions to this work (see Table A5), as well as the reviewers of this manuscript and previous versions, and the many researchers who have provided feedback.

References

Amante, C. and Eakins, B. W.: ETOPO1 1 Arc-Minute Global Relief Model: Procedures, Data
Sources and Analysis. NOAA Technical Memorandum NESDIS NGDC-24. National
Geophysical Data Center, NOAA. doi:10.7289/V5C8276M, 2009.

Andres, R. J., Boden, T. A., Bréon, F. M., Ciais, P., Davis, S., Erickson, D., Gregg, J. S., Jacobson, A.,
Marland, G., Miller, J., Oda, T., Olivier, J. G. J., Raupach, M. R., Rayner, P. and Treanton, K.:
A synthesis of carbon dioxide emissions from fossil-fuel combustion, Biogeosciences,
doi:10.5194/bg-9-1845-2012, 2012.

Andres, R. J., Boden, T. A. and Higdon, D.: A new evaluation of the uncertainty associated with
CDIAC estimates of fossil fuel carbon dioxide emission, Tellus Ser. B-Chemical Phys.
Meteorol., 66, 23616, doi:ARTN 2361610.3402/tellusb.v66.23616, 2014.

Andrew, R. M.: Global CO2 emissions from cement production, 1928-2017, Earth Syst. Sci. Data,
10(4), 2213–2239, doi:10.5194/essd-10-2213-2018, 2018.

Andrew, R. M.: Global CO2 emissions from cement production, 1928–2018, Earth Syst. Sci. Data
Discuss., doi:10.5194/essd-2019-152, n.d.

Andrew, R. M. and Peters, G. P.: A Multi-Region Input-Output Table Based on the Global Trade
Analysis Project Database (Gtap-Mrio), Econ. Syst. Res., 25(1), 99–121,
doi:10.1080/09535314.2012.761953, 2013.

Archer, D., Eby, M., Brovkin, V., Ridgwell, A., Cao, L., Mikolajewicz, U., Caldeira, K., Matsumoto,
K., Munhoven, G., Montenegro, A. and Tokos, K.: Atmospheric Lifetime of Fossil Fuel
Carbon Dioxide, Annu. Rev. Earth Planet. Sci., 37, 117–134,
doi:10.1146/annurev.earth.031208.100206, 2009.

Arneth, A., Sitch, S., Pongratz, J., Stocker, B. D., Ciais, P., Poulter, B., Bayer, A. D., Bondeau, A.,
Calle, L., Chini, L. P., Gasser, T., Fader, M., Friedlingstein, P., Kato, E., Li, W., Lindeskog, M.,

Nabel, J. E. M. S., Pugh, T. A. M., Robertson, E., Viovy, N., Yue, C. and Zaehle, S.: Historical carbon dioxide emissions caused by land-use changes are possibly larger than assumed, Nat. Geosci., 10(2), 79–84, doi:10.1038/ngeo2882, 2017.

Arora, V. K., Boer, G. J., Christian, J. R., Curry, C. L., Denman, K. L., Zahariev, K., Flato, G. M., Scinocca, J. F., Merryfield, W. J. and Lee, W. G.: The Effect of Terrestrial Photosynthesis Down Regulation on the Twentieth-Century Carbon Budget Simulated with the CCCma Earth System Model, J. Clim., 22(22), 6066–6088, doi:10.1175/2009jcli3037.1, 2009.

Avitabile, V., Herold, M., Heuvelink, G. B. M., Lewis, S. L., Phillips, O. L., Asner, G. P., Armston, J., Ashton, P. S., Banin, L., Bayol, N., Berry, N. J., Boeckx, P., de Jong, B. H. J., DeVries, B., Girardin, C. A. J., Kearsley, E., Lindsell, J. A., Lopez-Gonzalez, G., Lucas, R., Malhi, Y., Morel, A., Mitchard, E. T. A., Nagy, L., Qie, L., Quinones, M. J., Ryan, C. M., Ferry, S. J. W., Sunderland, T., Laurin, G. V., Gatti, R. C., Valentini, R., Verbeeck, H., Wijaya, A. and Willcock, S.: An integrated pan-tropical biomass map using multiple reference datasets, Glob. Chang. Biol., 22(4), 1406–1420, doi:10.1111/gcb.13139, 2016.

Baccini, A., Walker, W., Carvalho, L., Farina, M., Sulla-Menashe, D. and Houghton, R. A.: Tropical forests are a net carbon source based on aboveground measurements of gain and loss, Science (80-.)., 358(6360), 230–234, doi:10.1126/science.aam5962, 2017.

Bakker, D. C. E., Pfeil, B., Landa, C. S., Metzl, N., O'Brien, K. M., Olsen, A., Smith, K., Cosca, C., Harasawa, S., Jones, S. D., Nakaoka, S., Nojiri, Y., Schuster, U., Steinhoff, T., Sweeney, C., Takahashi, T., Tilbrook, B., Wada, C., Wanninkhof, R., Alin, S. R., Balestrini, C. F., Barbero, L., Bates, N. R., Bianchi, A. A., Bonou, F., Boutin, J., Bozec, Y., Burger, E. F., Cai, W. J., Castle, R. D., Chen, L. Q., Chierici, M., Currie, K., Evans, W., Featherstone, C., Feely, R. A., Fransson, A., Goyet, C., Greenwood, N., Gregor, L., Hankin, S., Hardman-Mountford, N. J., Harlay, J., Hauck, J., Hoppema, M., Humphreys, M. P., Hunt, C., Huss, B., Ibanhez, J. S. P.,

Johannessen, T., Keeling, R., Kitidis, V., Kortzinger, A., Kozyr, A., Krasakopoulou, E., Kuwata, A., Landschutzer, P., Lauvset, S. K., Lefevre, N., Lo Monaco, C., Manke, A., Mathis, J. T., Merlivat, L., Millero, F. J., Monteiro, P. M. S., Munro, D. R., Murata, A., Newberger, T., Omar, A. M., Ono, T., Paterson, K., Pearce, D., Pierrot, D., Robbins, L. L., Saito, S., Salisbury, J., Schlitzer, R., Schneider, B., Schweitzer, R., Sieger, R., Skjelvan, I., Sullivan, K. F., Sutherland, S. C., Sutton, A. J., Tadokoro, K., Telszewski, M., Tuma, M., van Heuven, S. M. A. C., Vandemark, D., Ward, B., Watson, A. J. and Xu, S. Q.: A multi-decade record of high-quality fCO(2) data in version 3 of the Surface Ocean CO2 Atlas (SOCAT), Earth Syst. Sci. Data, 8(2), 383–413, doi:10.5194/essd-8-383-2016, 2016.

Ballantyne, A. P., Alden, C. B., Miller, J. B., Tans, P. P. and White, J. W. C.: Increase in observed net carbon dioxide uptake by land and oceans during the past 50 years, Nature, 488(7409), 70–72, doi:10.1038/nature11299, 2012.

Ballantyne, A. P., Andres, R., Houghton, R., Stocker, B. D., Wanninkhof, R., Anderegg, W., Cooper, L. A., DeGrandpre, M., Tans, P. P., Miller, J. B., Alden, C. and White, J. W. C.: Audit of the global carbon budget: Estimate errors and their impact on uptake uncertainty, Biogeosciences, 12(8), 2565–2584, doi:10.5194/bg-12-2565-2015, 2015.

Bauer, J. E., Cai, W.-J., Raymond, P. a, Bianchi, T. S., Hopkinson, C. S. and Regnier, P. a G.: The changing carbon cycle of the coastal ocean, Nature, 504(7478), 61–70, doi:10.1038/nature12857, 2013.

Berthet, S., Séférian, R., Bricaud, C., Chevallier, M., Voldoire, A. and Ethé, C.: Evaluation of an Online Grid-Coarsening Algorithm in a Global Eddy-Admitting Ocean Biogeochemical Model, J. Adv. Model. Earth Syst., 11(6), 1759–1783, doi:10.1029/2019MS001644, 2019.

Best, M. J., Pryor, M., Clark, D. B., Rooney, G. G., Essery, R. . L. H., Ménard, C. B., Edwards, J. M., Hendry, M. A., Porson, A., Gedney, N., Mercado, L. M., Sitch, S., Blyth, E., Boucher, O., Cox,

P. M., Grimmond, C. S. B. and Harding, R. J.: The Joint UK Land Environment Simulator (JULES), model description – Part 1: Energy and water fluxes, Geosci. Model Dev., 4(3), 677–699, doi:10.5194/gmd-4-677-2011, 2011.

BP: BP Statistical Review of World Energy June 2019, available at: https://www.bp.com/en/global/corporate/energy-economics/statistical-review-of-world-energy.html, last access: June 2019., 2019.

Bruno, M. and Joos, F.: Terrestrial carbon storage during the past 200 years: A Monte Carlo Analysis of CO_2 data from ice core and atmospheric measurements, Global Biogeochem. Cycles, 11(1), 111–124, doi:10.1029/96GB03611, 1997.

Buitenhuis, E. T., Hashioka, T. and Quéré, C. Le: Combined constraints on global ocean primary production using observations and models, Global Biogeochem. Cycles, 27(3), 847–858, doi:10.1002/gbc.20074, 2013.

Canadell, J. G., Le Quere, C., Raupach, M. R., Field, C. B., Buitenhuis, E. T., Ciais, P., Conway, T. J., Gillett, N. P., Houghton, R. A. and Marland, G.: Contributions to accelerating atmospheric CO_2 growth from economic activity, carbon intensity, and efficiency of natural sinks, Proc. Natl. Acad. Sci., 104(47), 18866–18870, doi:10.1073/pnas.0702737104, 2007.

Carbontracker Team: Compilation of near real time atmospheric carbon dioxide data provided by NOAA and EC; obspack_co2_1_NRT_v4.4.2_2019-06-10; NOAA Earth System Research Laboratory, Global Monitoring Division. doi:10.25925/20190610., 2019.

CEA: Central Electricity Authority (CEA): Daily Coal – Archive. Central Electricity Authority, available at: http://www.cea.nic.in/dailyarchive.html, last access: 18 September 2019., 2019.

CGADIP: Cooperative Global Atmospheric Data Integration Project: Multi-laboratory compilation of atmospheric carbon dioxide data for the period 1957-2017;

obspack_co2_1_GLOBALVIEWplus_v4.2.2_2019-06-05, Earth System Research Laboratory,

Global Monitoring Division., 2019.

Chatfield, C.: The Holt-Winters Forecasting Procedure, Appl. Stat., 27(3), 264–279,

doi:10.2307/2347162, 1978.

Chevallier, F., Fisher, M., Peylin, P., Serrar, S., Bousquet, P., Bréon, F.-M., Chédin, A. and Ciais,

P.: Inferring CO_2 sources and sinks from satellite observations: Method and application to

TOVS data, J. Geophys. Res., 110(D24), D24309, doi:10.1029/2005JD006390, 2005.

Ciais, P., Sabine, C., Govindasamy, B., Bopp, L., Brovkin, V., Canadell, J., Chhabra, A., DeFries, R.,

Galloway, J., Heimann, M., Jones, C., Le Quéré, C., Myneni, R., Piao, S. and Thornton, P.:

Chapter 6: Carbon and Other Biogeochemical Cycles, in Climate Change 2013 The Physical

Science Basis, edited by T. Stocker, D. Qin, and G.-K. Platner, Cambridge University Press,

Cambridge., 2013.

CIL: Coal India Limited: Production and Offtake Performance of CIL and Subsidiary Companies,

available at: https://www.coalindia.in/en-us/performance/physical.aspx, last access: 3

September 2019., 2019.

Clark, D. B., Mercado, L. M., Sitch, S., Jones, C. D., Gedney, N., Best, M. J., Pryor, M., Rooney, G.

G., Essery, R. L. H., Blyth, E., Boucher, O., Harding, R. J., Huntingford, C. and Cox, P. M.: The

Joint UK Land Environment Simulator (JULES), model description – Part 2: Carbon fluxes

and vegetation dynamics, Geosci. Model Dev., 4(3), 701–722, doi:10.5194/gmd-4-701-

2011, 2011.

Collier, N., Hoffman, F. M., Lawrence, D. M., Keppel-Aleks, G., Koven, C. D., Riley, W. J., Mu, M.

Q. and Randerson, J. T.: The International Land Model Benchmarking (ILAMB) System:

Design, Theory, and Implementation, J. Adv. Model. Earth Syst., 10(11), 2731–2754,

doi:10.1029/2018ms001354, 2018.

Cox, P. M., Pearson, D., Booth, B. B., Friedlingstein, P., Huntingford, C., Jones, C. D. and Luke, C. M.: Sensitivity of tropical carbon to climate change constrained by carbon dioxide variability, Nature, 494(7437), 341–344, doi:10.1038/nature11882, 2013.

Dai, A. and Trenberth, K. E.: Estimates of Freshwater Discharge from Continents: Latitudinal and Seasonal Variations, J. Hydrometeorol., 3(6), 660–687, doi:10.1175/1525-7541(2002)003<0660:EOFDFC>2.0.CO;2, 2002.

Davis, S. J. and Caldeira, K.: Consumption-based accounting of CO2 emissions, Proc. Natl. Acad. Sci., 107(12), 5687–5692, doi:10.1073/pnas.0906974107, 2010.

Decharme, B., Delire, C., Minvielle, M., Colin, J., Vergnes, J., Alias, A., Saint-Martin, D., Séférian, R., Sénési, S. and Voldoire, A.: Recent Changes in the ISBA-CTRIP Land Surface System for Use in the CNRM-CM6 Climate Model and in Global Off-Line Hydrological Applications, J. Adv. Model. Earth Syst., 11(5), 1207–1252, doi:10.1029/2018MS001545, 2019.

Denman, K. L., Brasseur, G., Chidthaisong, A., Ciais, P., Cox, P. M., Dickinson, R. E., Hauglustaine, D., Heinze, C., Holland, E., Jacob, D., Lohmann, U., Ramachandran, S., Leite da Silva Dias, P., Wofsy, S. C. and Zhang, X.: Couplings Between Changes in the Climate System and Biogeochemistry, in Climate Change 2007: The Physical Science Basis. Contribution of Working Group I to the Fourth Assessment Report of the Intergovernmental Panel on Climate Change, edited by S. Solomon, Qin D., Manning M., Marquis M., Averyt K., Tignor M. M. B., H. L. Miller, and Chen Z. L., pp. 499–587, Cambridge University Press, Cambridge, UK and New York, USA., 2007.

Denvil-Sommer, A., Gehlen, M., Vrac, M. and Mejia, C.: LSCE-FFNN-v1: LSCE-FFNN-v1: a two-step neural network model for the reconstruction of surface ocean pCO2 over the global ocean, Geosci. Model Dev., 12(5), 2091–2105, doi:10.5194/gmd-12-2091-2019, 2019.

DeVries, T.: The oceanic anthropogenic CO2 sink: Storage, air-sea fluxes, and transports over

the industrial era, Global Biogeochem. Cycles, 28(7), 631–647, doi:10.1002/2013gb004739, 2014.

DeVries, T., Holzer, M. and Primeau, F.: Recent increase in oceanic carbon uptake driven by weaker upper-ocean overturning, Nature, 542(7640), 215–218, doi:10.1038/nature21068, 2017.

DeVries, T., Le Quéré, C., Andrews, O., Berthet, S., Hauck, J., Ilyina, T., Landschützer, P., Lenton, A., Lima, I. D., Nowicki, M., Schwinger, J. and Séférian, R.: Decadal trends in the ocean carbon sink, Proc. Natl. Acad. Sci., doi:10.1073/pnas.1900371116, 2019.

Dlugokencky, E. and Tans, P.: Trends in atmospheric carbon dioxide, National Oceanic & Atmospheric Administration, Earth System Research Laboratory (NOAA/ESRL), available at: http://www.esrl.noaa.gov/gmd/ccgg/trends/global.html, last access: 27 September 2019., 2019.

Doney, S. C., Lima, I., Feely, R. A., Glover, D. M., Lindsay, K., Mahowald, N., Moore, J. K. and Wanninkhof, R.: Mechanisms governing interannual variability in upper-ocean inorganic carbon system and air-sea CO_2 fluxes: Physical climate and atmospheric dust, Deep. Res. Part Ii-Topical Stud. Oceanogr., 56(8–10), 640–655, doi:10.1016/j.dsr2.2008.12.006, 2009.

Duce, R. A., LaRoche, J., Altieri, K., Arrigo, K. R., Baker, A. R., Capone, D. G., Cornell, S., Dentener, F., Galloway, J., Ganeshram, R. S., Geider, R. J., Jickells, T., Kuypers, M. M., Langlois, R., Liss, P. S., Liu, S. M., Middelburg, J. J., Moore, C. M., Nickovic, S., Oschlies, A., Pedersen, T., Prospero, J., Schlitzer, R., Seitzinger, S., Sorensen, L. L., Uematsu, M., Ulloa, O., Voss, M., Ward, B. and Zamora, L.: Impacts of Atmospheric Anthropogenic Nitrogen on the Open Ocean, Science (80-.)., 320(5878), 893–897, doi:10.1126/science.1150369, 2008.

Dufour, C. O., Le Sommer, J., Gehlen, M., Orr, J. C., Molines, J. M., Simeon, J. and Barnier, B.: Eddy compensation and controls of the enhanced sea-to-air CO_2 flux during positive

phases of the Southern Annular Mode, Global Biogeochem. Cycles, 27(3), 950–961, doi:10.1002/gbc.20090, 2013.

Durant, A. J., Le Quéré, C., Hope, C. and Friend, A. D.: Economic value of improved quantification in global sources and sinks of carbon dioxide, Philos Trans A Math Phys Eng Sci, 369(1943), 1967–1979, doi:10.1098/rsta.2011.0002, 2011.

Eakins, B. W. and Sharman, G. F.: Volumes of the World's Oceans from ETOPO1; NOAA National Geophysical Data Center, available at: http://www.ngdc.noaa.gov/mgg/global/etopo1_ocean_volumes.html, last accessed: 27 September 2019., 2010.

EIA: U.S. Energy Information Administration, Short-Term Energy Outlook, available at: http://www.eia.gov/forecasts/steo/outlook.cfm, last access: 27 September 2019., 2019.

ENTSO-E: The European Network of Transmission System Operators Electricity Transparency Platform, available at: https://transparency.entsoe.eu/, last access: 24 September 2019., 2019.

Erb, K. H., Kastner, T., Luyssaert, S., Houghton, R. A., Kuemmerle, T., Olofsson, P. and Haberl, H.: COMMENTARY: Bias in the attribution of forest carbon sinks, Nat. Clim. Chang., 3(10), 854–856, doi:10.1038/nclimate2004, 2013.

Etheridge, D. M., Steele, L. P., Langenfelds, R. L., Francey, R. J., Barnola, J. M. and Morgan, V. I.: Natural and anthropogenic changes in atmospheric CO2 over the last 1000 years from air in Antarctic ice and firn, J. Geophys. Res., 101(D2), 4115–4128, doi:Doi 10.1029/95jd03410, 1996.

Eurostat: Supply and transformation of solid fuels - monthly data (nrg_101m), available at: https://ec.europa.eu/eurostat/data/database, last access: 23 September 2019., 2019.

FAO: Food and Agriculture Organization of the United Nations: Global Forest Resources

Assessment 2015, available at: http://www.fao.org/forest-resources-assessment/past-assessments/fra-2015/en/, last access: 27 September 2019, Rome, Italy., 2015.

FAOSTAT: Food and Agriculture Organization Statistics Division, available at: http://faostat.fao.org/, last access: 27 September 2019., 2015.

Francey, R. J., Trudinger, C. M., van der Schoot, M., Law, R. M., Krummel, P. B., Langenfelds, R. L., Steele, L. P., Allison, C. E., Stavert, A. R., Andres, R. J. and Rödenbeck, C.: Reply to "Anthropogenic CO_2 emissions," Nat. Clim. Chang., 3(7), 604, doi:10.1038/nclimate1925, 2013.

Friedlingstein, P., Houghton, R. A., Marland, G., Hackler, J., Boden, T. A., Conway, T. J., Canadell, J. G., Raupach, M. R., Ciais, P. and Le Quéré, C.: Update on CO_2 emissions, Nat. Geosci., 3(12), 811–812, doi:10.1038/ngeo1022, 2010.

Friedlingstein, P., Andrew, R. M., Rogelj, J., Peters, G. P., Canadell, J. G., Knutti, R., Luderer, G., Raupach, M. R., Schaeffer, M., van Vuuren, D. P. and Le Quere, C.: Persistent growth of CO_2 emissions and implications for reaching climate targets, Nat. Geosci., 7(10), 709–715, doi:10.1038/Ngeo2248, 2014.

Friedlingstein, P., Jones, M. W., O'Sullivan, M., Andrew, R. M., Hauck, J., Peters, G. P., Peters, W., Pongratz, J., Sitch, S., Quéré, C. Le, Bakker, D. C. E., Canadell, J. G., Ciais, P., Jackson, R., Anthoni, P., Barbero, L., Bastos, A., Bastrikov, V., Becker, M., Bopp, L., Buitenhuis, E., Chandra, N., Chevallier, F., Chini, L. P., Currie, K. I., Feely, R. A., Gehlen, M., Gilfillan, D., Gkritzalis, T., Goll, D. S., Gruber, N., Gutekunst, S., Harris, I., Haverd, V., Houghton, R. A., Hurtt, G., Ilyina, T., Jain, A. K., Joetzjer, E., Kaplan, J. O., Kato, E., Goldewijk, K. K., Korsbakken, J. I., Landschützer, P., Lauvset, S. K., Lefèvre, N., Lenton, A., Lienert, S., Lombardozzi, D., Marland, G., McGuire, P. C., Melton, J. R., Metzl, N., Munro, D. R., Nabel, J. E. M. S., Nakaoka, S.-I., Neill, C., Omar, A. M., Ono, T., Peregon, A., Pierrot, D., Poulter, B.,

Rehder, G., Resplandy, L., Robertson, E., Rödenbeck, C., Séférian, R., Schwinger, J., Smith, N., Tans, P. P., Tian, H., Tilbrook, B., Tubiello, F. N., van der Werf, G. R., Wiltshire, A. J. and Zaehle, S.: Supplemental data of the Global Carbon Budget 2019, available at: https://doi.org/10.18160/gcp-2019, ICOS-ERIC Carbon Portal, last accessed: 2 October 2019, 2019.

Gasser, T., Ciais, P., Boucher, O., Quilcaille, Y., Tortora, M., Bopp, L. and Hauglustaine, D.: The compact Earth system model OSCAR v2.2: description and first results, Geosci. Model Dev., 10(1), 271–319, doi:10.5194/gmd-10-271-2017, 2017.

Gaubert, B., Stephens, B. B., Basu, S., Chevallier, F., Deng, F., Kort, E. A., Patra, P. K., Peters, W., Rödenbeck, C., Saeki, T., Schimel, D., Van der Laan-Luijkx, I., Wofsy, S. and Yin, Y.: Global atmospheric CO₂ inverse models converging on neutral tropical land exchange but diverging on fossil fuel and atmospheric growth rate, Biogeosciences Discuss., 2018, 1–25, doi:10.5194/bg-2018-384, 2018.

GCP: The Global Carbon Budget 2007, available at: http://www.globalcarbonproject.org/carbonbudget/archive.htm, last access: 7 November 2016., 2007.

General Administration of Customs of the People's Republic of China: Table of value and quantity of major export articles, August 2019 (2019年8月出口主要商品量值表), available at: http://www.customs.gov.cn/customs/302249/302274/302277/302276/2604030/index.html. Last access 23 September 2019., 2019a.

General Administration of Customs of the People's Republic of China: Table of value and quantity of major import articles, August 2019 (2019年8月进口主要商品量值表),

available at:

http://www.customs.gov.cn/customs/302249/302274/302277/302276/2604033/index.ht

ml. Last access 23 September 2019., 2019b.

Giglio, L., Schroeder, W. and Justice, C. O.: The collection 6 MODIS active fire detection

algorithm and fire products, Remote Sens. Environ., 178, 31–41,

doi:10.1016/j.rse.2016.02.054, 2016.

Gilfillan, D., Marland, G., Boden, T. and Andres, R.: Global, Regional, and National Fossil-Fuel

CO2 Emissions, available at: https://energy.appstate.edu/CDIAC, last access: 27 September

2019, 2019.

Gitz, V. and Ciais, P.: Amplifying effects of land-use change on future atmospheric CO 2 levels,

Global Biogeochem. Cycles, 17(1), 1024, doi:10.1029/2002GB001963, 2003.

Goldewijk, K. K., Beusen, A., Doelman, J. and Stehfest, E.: Anthropogenic land use estimates for

the Holocene - HYDE 3.2, Earth Syst. Sci. Data, 9(2), 927–953, doi:10.5194/essd-9-927-

2017, 2017a.

Goldewijk, K. K., Dekker, S. C. and van Zanden, J. L.: Per-capita estimations of long-term

historical land use and the consequences for global change research, J. Land Use Sci.,

12(5), 313–337, doi:10.1080/1747423x.2017.1354938, 2017b.

Goll, D. S., Winkler, A. J., Raddatz, T., Dong, N., Colin Prentice, I., Ciais, P. and Brovkin, V.:

Carbon-nitrogen interactions in idealized simulations with JSBACH (version 3.10), Geosci.

Model Dev., 10(5), 2009–2030, doi:10.5194/gmd-10-2009-2017, 2017.

Goll, D. S., Joetzjer, E., Huang, M. and Ciais, P.: Low Phosphorus Availability Decreases

Susceptibility of Tropical Primary Productivity to Droughts, Geophys. Res. Lett., 45(16),

8231–8240, doi:10.1029/2018GL077736, 2018.

Gray, A. R., Johnson, K. S., Bushinsky, S. M., Riser, S. C., Russell, J. L., Talley, L. D., Wanninkhof,

R., Williams, N. L. and Sarmiento, J. L.: Autonomous Biogeochemical Floats Detect

Significant Carbon Dioxide Outgassing in the High-Latitude Southern Ocean, Geophys. Res.

Lett., 45(17), 9049–9057, doi:10.1029/2018GL078013, 2018.

Gregg, J. S., Andres, R. J. and Marland, G.: China: Emissions pattern of the world leader in CO2

emissions from fossil fuel consumption and cement production, Geophys. Res. Lett., 35(8),

L08806, doi:Artn L0880610.1029/2007gl032887, 2008.

Gruber, N., Clement, D., Carter, B. R., Feely, R. A., van Heuven, S., Hoppema, M., Ishii, M., Key,

R. M., Kozyr, A., Lauvset, S. K., Lo Monaco, C., Mathis, J. T., Murata, A., Olsen, A., Perez, F.

F., Sabine, C. L., Tanhua, T. and Wanninkhof, R.: The oceanic sink for anthropogenic CO 2

from 1994 to 2007, Science (80-.)., 363(6432), 1193–1199, doi:10.1126/science.aau5153,

2019.

Hansis, E., Davis, S. J. and Pongratz, J.: Relevance of methodological choices for accounting of

land use change carbon fluxes, Global Biogeochem. Cycles, 29(8), 1230–1246,

doi:10.1002/2014GB004997, 2015.

Harris, I., Jones, P. D., Osborn, T. J. and Lister, D. H.: Updated high-resolution grids of monthly

climatic observations - the CRU TS3.10 Dataset, Int. J. Climatol., 34(3), 623–642,

doi:10.1002/joc.3711, 2014.

Haverd, V., Smith, B., Nieradzik, L., Briggs, P. R., Woodgate, W., Trudinger, C. M., Canadell, J. G.

and Cuntz, M.: A new version of the CABLE land surface model (Subversion revision r4601)

incorporating land use and land cover change, woody vegetation demography, and a novel

optimisation-based approach to plant coordination of photosynthesis, Geosci. Model Dev.,

11(7), 2995–3026, doi:10.5194/gmd-11-2995-2018, 2018.

Hertwich, E. G. and Peters, G. P.: Carbon footprint of nations: a global, trade-linked analysis,

Env. Sci Technol, 43(16), 6414–6420, doi:10.1021/es803496a, 2009.

Hooijer, A., Page, S., Canadell, J. G., Silvius, M., Kwadijk, J., Wosten, H. and Jauhiainen, J.: Current and future CO_2 emissions from drained peatlands in Southeast Asia, Biogeosciences, 7(5), 1505–1514, doi:10.5194/bg-7-1505-2010, 2010.

Houghton, R. A.: Revised estimates of the annual net flux of carbon to the atmosphere from changes in land use and land management 1850-2000, Tellus Ser. B-Chemical Phys. Meteorol., 55(2), 378–390, doi:DOI 10.1034/j.1600-0889.2003.01450.x, 2003.

Houghton, R. A. and Nassikas, A. A.: Global and regional fluxes of carbon from land use and land cover change 1850-2015, Global Biogeochem. Cycles, 31(3), 456–472, doi:10.1002/2016gb005546, 2017.

Houghton, R. A., House, J. I., Pongratz, J., Van Der Werf, G. R., Defries, R. S., Hansen, M. C., Le Quéré, C. and Ramankutty, N.: Carbon emissions from land use and land-cover change, Biogeosciences, 9(12), 5125–5142, doi:10.5194/bg-9-5125-2012, 2012.

Houweling, S., Baker, D., Basu, S., Boesch, H., Butz, A., Chevallier, F., Deng, F., Dlugokencky, E. J., Feng, L., Ganshin, A., Hasekamp, O., Jones, D., Maksyutov, S., Marshall, J., Oda, T., O'Dell, C. W., Oshchepkov, S., Palmer, P. I., Peylin, P., Poussi, Z., Reum, F., Takagi, H., Yoshida, Y. and Zhuravlev, R.: An intercomparison of inverse models for estimating sources and sinks of CO_2 using GOSAT measurements, J. Geophys. Res., 120(10), 5253–5266, doi:10.1002/2014jd022962, 2015.

Hugelius, G., Bockheim, J. G., Camill, P., Elberling, B., Grosse, G., Harden, J. W., Johnson, K., Jorgenson, T., Koven, C. D., Kuhry, P., Michaelson, G., Mishra, U., Palmtag, J., Ping, C. L., O'Donnell, J., Schirrmeister, L., Schuur, E. A. G., Sheng, Y., Smith, L. C., Strauss, J. and Yu, Z.: A new data set for estimating organic carbon storage to 3m depth in soils of the northern circumpolar permafrost region, Earth Syst. Sci. Data, 5(2), 393–402, doi:10.5194/essd-5-393-2013, 2013.

Huntzinger, D. N., Michalak, A. M., Schwalm, C., Ciais, P., King, A. W., Fang, Y., Schaefer, K., Wei, Y., Cook, R. B., Fisher, J. B., Hayes, D., Huang, M., Ito, A., Jain, A. K., Lei, H., Lu, C., Maignan, F., Mao, J., Parazoo, N., Peng, S., Poulter, B., Ricciuto, D., Shi, X., Tian, H., Wang, W., Zeng, N. and Zhao, F.: Uncertainty in the response of terrestrial carbon sink to environmental drivers undermines carbon-climate feedback predictions, Sci. Rep., 7(1), 4765, doi:10.1038/s41598-017-03818-2, 2017.

Hurtt, G., Chini, L., Sahajpal, R., Frolking, S., Calvin, K., Fujimori, S., Klein Goldewijk, K., Hasegawa, T., Havlik, P. and Heinemann, A.: Harmonization of global land-use change and management for the period 850–2100, Geosci. Model Dev., n.d.

Hurtt, G. C., Chini, L. P., Frolking, S., Betts, R. A., Feddema, J., Fischer, G., Fisk, J. P., Hibbard, K., Houghton, R. A., Janetos, A., Jones, C. D., Kindermann, G., Kinoshita, T., Goldewijk, K. K., Riahi, K., Shevliakova, E., Smith, S., Stehfest, E., Thomson, A., Thornton, P., van Vuuren, D. P. and Wang, Y. P.: Harmonization of land-use scenarios for the period 1500-2100: 600 years of global gridded annual land-use transitions, wood harvest, and resulting secondary lands, Clim. Change, 109(1–2), 117–161, doi:10.1007/s10584-011-0153-2, 2011.

IEA/OECD: International Energy Agency/Organisation for Economic Cooperation and Development: CO_2 emissions from fuel combustion, available at: https://webstore.iea.org/co2-emissions-from-fuel-combustion-2018-highlights, Paris., 2018.

IEA: World Energy Statistics (2018 Edition), available at: www.iea.org, 2018.

IMF: IMF: World Economic Outlook Update, July 2019: Still Sluggish Global Growth, available at: http://www.imf.org, last access: July 2019., 2019.

IPCC: 2006 IPCC Guidelines for National Greenhouse Gas Inventories, Prepared by the National Greenhouse Gas Inventories Programme, edited by S. Eggleston, L. Buendia, K. Miwa, T.

Ngara, and K. Tanabe, Intergovernmental Panel on Climate Change, Institute for Global Environmental Strategies, Japan., 2006.

Ito, A. and Inatomi, M.: Use of a process-based model for assessing the methane budgets of global terrestrial ecosystems and evaluation of uncertainty, Biogeosciences, 9(2), 759–773, doi:10.5194/bg-9-759-2012, 2012.

Jackson, R. B., Canadell, J. G., Le Quéré, C., Andrew, R. M., Korsbakken, J. I., Peters, G. P. and Nakicenovic, N.: Reaching peak emissions, Nat. Clim. Chang., 6(1), 7–10, doi:10.1038/nclimate2892, 2016.

Jackson, R. B., Le Quéré, C., Andrew, R. M., Canadell, J. G., Korsbakken, J. I., Liu, Z., Peters, G. P. and Zheng, B.: Global energy growth is outpacing decarbonization, Environ. Res. Lett., 13(12), 120401, doi:10.1088/1748-9326/aaf303, 2018.

Jacobson, A. R., Mikaloff Fletcher, S. E., Gruber, N., Sarmiento, J. L. and Gloor, M.: A joint atmosphere-ocean inversion for surface fluxes of carbon dioxide: 2. Regional results, Global Biogeochem. Cycles, 21(1), doi:10.1029/2006GB002703, 2007.

JODI: Joint Organisations Data Initiative, available at: https://www.jodidata.org, last access: 20 September 2019., 2019.

Joetzjer, E., Delire, C., Douville, H., Ciais, P., Decharme, B., Carrer, D., Verbeeck, H., De Weirdt, M. and Bonal, D.: Improving the ISBA$_{CC}$ land surface model simulation of water and carbon fluxes and stocks over the Amazon forest, Geosci. Model Dev., 8(6), 1709–1727, doi:10.5194/gmd-8-1709-2015, 2015.

Joos, F. and Spahni, R.: Rates of change in natural and anthropogenic radiative forcing over the past 20,000 years, Proc. Natl. Acad. Sci., doi:10.1073/pnas.0707386105, 2008.

Jung, M., Reichstein, M., Ciais, P., Seneviratne, S. I., Sheffield, J., Goulden, M. L., Bonan, G., Cescatti, A., Chen, J., de Jeu, R., Dolman, A. J., Eugster, W., Gerten, D., Gianelle, D., Gobron,

N., Heinke, J., Kimball, J., Law, B. E., Montagnani, L., Mu, Q., Mueller, B., Oleson, K., Papale, D., Richardson, A. D., Roupsard, O., Running, S., Tomelleri, E., Viovy, N., Weber, U., Williams, C., Wood, E., Zaehle, S. and Zhang, K.: Recent decline in the global land evapotranspiration trend due to limited moisture supply, Nature, 467(7318), 951–954, doi:10.1038/nature09396, 2010.

Kato, E., Kinoshita, T., Ito, A., Kawamiya, M. and Yamagata, Y.: Evaluation of spatially explicit emission scenario of land-use change and biomass burning using a process-based biogeochemical model, J. Land Use Sci., 8(1), 104–122, doi:10.1080/1747423x.2011.628705, 2013.

De Kauwe, M. G., Disney, M. I., Quaife, T., Lewis, P. and Williams, M.: An assessment of the MODIS collection 5 leaf area index product for a region of mixed coniferous forest, Remote Sens. Environ., 115(2), 767–780, doi:10.1016/j.rse.2010.11.004, 2011.

Keeling, C. D., Bacastow, R. B., Bainbridge, A. E., Ekdahl, C. A., Guenther, P. R., Waterman, L. S. and Chin, J. F. S.: Atmospheric Carbon-Dioxide Variations at Mauna-Loa Observatory, Hawaii, Tellus, 28(6), 538–551, doi:10.1111/j.2153-3490.1976.tb00701.x, 1976.

Keeling, R. F. and Manning, A. C.: Studies of Recent Changes in Atmospheric O2 Content, in Treatise on Geochemistry, vol. 5, edited by H. D. Holland and K. K. Turekian, pp. 385–404, Elsevier, Oxford., 2014.

Khatiwala, S., Primeau, F. and Hall, T.: Reconstruction of the history of anthropogenic CO2 concentrations in the ocean, Nature, 462(7271), 346-U110, doi:10.1038/nature08526, 2009.

Khatiwala, S., Tanhua, T., Fletcher, S. M., Gerber, M., Doney, S. C., Graven, H. D., Gruber, N., McKinley, G. A., Murata, A., Rios, A. F. and Sabine, C. L.: Global ocean storage of anthropogenic carbon, Biogeosciences, 10(4), 2169–2191, doi:10.5194/bg-10-2169-2013,

2013.

Kirschke, S., Bousquet, P., Ciais, P., Saunois, M., Canadell, J. G., Dlugokencky, E. J., Bergamaschi,
P., Bergmann, D., Blake, D. R., Bruhwiler, L., Cameron-Smith, P., Castaldi, S., Chevallier, F.,
Feng, L., Fraser, A., Heimann, M., Hodson, E. L., Houweling, S., Josse, B., Fraser, P. J.,
Krummel, P. B., Lamarque, J. F., Langenfelds, R. L., Le Quere, C., Naik, V., O'Doherty, S.,
Palmer, P. I., Pison, I., Plummer, D., Poulter, B., Prinn, R. G., Rigby, M., Ringeval, B., Santini,
M., Schmidt, M., Shindell, D. T., Simpson, I. J., Spahni, R., Steele, L. P., Strode, S. A., Sudo,
K., Szopa, S., van der Werf, G. R., Voulgarakis, A., van Weele, M., Weiss, R. F., Williams, J. E.
and Zeng, G.: Three decades of global methane sources and sinks, Nat. Geosci., 6(10), 813–
823, doi:10.1038/Ngeo1955, 2013.

Kobayashi, S., Ota, Y., Harada, Y., Ebita, A., Moriya, M., Onoda, H., Onogi, K., Kamahori, H.,
Kobayashi, C., Endo, H., Miyaoka, K. and Takahashi, K.: The JRA-55 Reanalysis: General
Specifications and Basic Characteristics, J. Meteorol. Soc. Japan, 93(1), 5–48,
doi:10.2151/jmsj.2015-001, 2015.

Korsbakken, J. I., Peters, G. P. and Andrew, R. M.: Uncertainties around reductions in China's
coal use and CO 2 emissions, Nat. Clim. Chang., 6(7), 687–690, doi:10.1038/nclimate2963,
2016.

Krinner, G., Viovy, N., de Noblet-Ducoudré, N., Ogée, J., Polcher, J., Friedlingstein, P., Ciais, P.,
Sitch, S. and Prentice, I. C.: A dynamic global vegetation model for studies of the coupled
atmosphere-biosphere system, Global Biogeochem. Cycles, 19(1), 1–33,
doi:10.1029/2003GB002199, 2005.

Van Der Laan-Luijkx, I. T., Van Der Velde, I. R., Van Der Veen, E., Tsuruta, A., Stanislawska, K.,
Babenhauserheide, A., Fang Zhang, H., Liu, Y., He, W., Chen, H., Masarie, K. A., Krol, M. C.
and Peters, W.: The CarbonTracker Data Assimilation Shell (CTDAS) v1.0: Implementation

and global carbon balance 2001-2015, Geosci. Model Dev., 10(7), 2785–2800, doi:10.5194/gmd-10-2785-2017, 2017.

Landschützer, P., Gruber, N., Bakker, D. C. E. and Schuster, U.: Recent variability of the global ocean carbon sink, Global Biogeochem. Cycles, 28(9), 927–949, doi:10.1002/2014GB004853, 2014.

Landschützer, P., Gruber, N., Haumann, F. A., Rödenbeck, C., Bakker, D. C. E., van Heuven, S., Hoppema, M., Metzl, N., Sweeney, C., Takahashi, T., Tilbrook, B. and Wanninkhof, R.: The reinvigoration of the Southern Ocean carbon sink, Science (80-.)., 349(6253), 1221–1224, doi:10.1126/science.aab2620, 2015.

Landschützer, P., Gruber, N. and Bakker, D. C. E.: Decadal variations and trends of the global ocean carbon sink, Global Biogeochem. Cycles, 30(10), 1396–1417, doi:10.1002/2015gb005359, 2016.

Landschützer, P., Gruber, N., Bakker, D. C. E., Stemmler, I. and Six, K. D.: Strengthening seasonal marine CO2 variations due to increasing atmospheric CO2, Nat. Clim. Chang., 8(2), 146–150, doi:10.1038/s41558-017-0057-x, 2018.

Lasslop, G., Reichstein, M., Papale, D., Richardson, A. D., Arneth, A., Barr, A., Stoy, P. and Wohlfahrt, G.: Separation of net ecosystem exchange into assimilation and respiration using a light response curve approach: critical issues and global evaluation, Glob. Chang. Biol., 16(1), 187–208, doi:10.1111/j.1365-2486.2009.02041.x, 2010.

Li, H. and Ilyina, T.: Current and Future Decadal Trends in the Oceanic Carbon Uptake Are Dominated by Internal Variability, Geophys. Res. Lett., 45(2), 916–925, doi:10.1002/2017gl075370, 2018.

Li, W., Ciais, P., Peng, S., Yue, C., Wang, Y., Thurner, M., Saatchi, S. S., Arneth, A., Avitabile, V., Carvalhais, N., Harper, A. B., Kato, E., Koven, C., Liu, Y. Y., Nabel, J. E. M. S., Pan, Y.,

Pongratz, J., Poulter, B., Pugh, T. A. M., Santoro, M., Sitch, S., Stocker, B. D., Viovy, N.,
Wiltshire, A., Yousefpour, R. and Zaehle, S.: Land-use and land-cover change carbon
emissions between 1901 and 2012 constrained by biomass observations, Biogeosciences,
14(22), doi:10.5194/bg-14-5053-2017, 2017.

Lienert, S. and Joos, F.: A Bayesian ensemble data assimilation to constrain model parameters
and land-use carbon emissions, Biogeosciences, 15(9), 2909–2930, doi:10.5194/bg-15-
2909-2018, 2018.

Liu, Z., Guan, D., Wei, W., Davis, S. J., Ciais, P., Bai, J., Peng, S., Zhang, Q., Hubacek, K., Marland,
G., Andres, R. J., Crawford-Brown, D., Lin, J., Zhao, H., Hong, C., Boden, T. A., Feng, K.,
Peters, G. P., Xi, F., Liu, J., Li, Y., Zhao, Y., Zeng, N. and He, K.: Reduced carbon emission
estimates from fossil fuel combustion and cement production in China, Nature,
doi:10.1038/nature14677, 2015.

Manning, A. C. and Keeling, R. F.: Global oceanic and land biotic carbon sinks from the scripps
atmospheric oxygen flask sampling network, Tellus, Ser. B Chem. Phys. Meteorol., 58(2),
95–116, doi:10.1111/j.1600-0889.2006.00175.x, 2006.

Marland, G.: Uncertainties in Accounting for CO 2 From Fossil Fuels, J. Ind. Ecol., 12(2), 136–
139, doi:10.1111/j.1530-9290.2008.00014.x, 2008.

Marland, G. and Rotty, R. M.: Carbon-Dioxide Emissions from Fossil-Fuels - a Procedure for
Estimation and Results for 1950-1982, Tellus Ser. B-Chemical Phys. Meteorol., 36(4), 232–
261, doi:DOI 10.1111/j.1600-0889.1984.tb00245.x, 1984.

Marland, G., Hamal, K. and Jonas, M.: How Uncertain Are Estimates of CO2 Emissions?, J. Ind.
Ecol., 13(1), 4–7, doi:10.1111/j.1530-9290.2009.00108.x, 2009.

Masarie, K. A. and Tans, P. P.: Extension and Integration of Atmospheric Carbon-Dioxide Data
into a Globally Consistent Measurement Record, J. Geophys. Res., 100(D6), 11593–11610,

doi:Doi 10.1029/95jd00859, 1995.

Mauritsen, T., Bader, J., Becker, T., Behrens, J., Bittner, M., Brokopf, R., Brovkin, V., Claussen,
M., Crueger, T., Esch, M., Fast, I., Fiedler, S., Fläschner, D., Gayler, V., Giorgetta, M., Goll, D.
S., Haak, H., Hagemann, S., Hedemann, C., Hohenegger, C., Ilyina, T., Jahns, T., Jimenéz-de-
la-Cuesta, D., Jungclaus, J., Kleinen, T., Kloster, S., Kracher, D., Kinne, S., Kleberg, D.,
Lasslop, G., Kornblueh, L., Marotzke, J., Matei, D., Meraner, K., Mikolajewicz, U., Modali,
K., Möbis, B., Müller, W. A., Nabel, J. E. M. S., Nam, C. C. W., Notz, D., Nyawira, S., Paulsen,
H., Peters, K., Pincus, R., Pohlmann, H., Pongratz, J., Popp, M., Raddatz, T. J., Rast, S.,
Redler, R., Reick, C. H., Rohrschneider, T., Schemann, V., Schmidt, H., Schnur, R.,
Schulzweida, U., Six, K. D., Stein, L., Stemmler, I., Stevens, B., Storch, J., Tian, F., Voigt, A.,
Vrese, P., Wieners, K., Wilkenskjeld, S., Winkler, A. and Roeckner, E.: Developments in the
MPI-M Earth System Model version 1.2 (MPI-ESM1.2) and Its Response to Increasing CO 2,
J. Adv. Model. Earth Syst., 11(4), 998–1038, doi:10.1029/2018MS001400, 2019.

MCI: Ministry of Commerce and Industry: Foreign Trade Data Dissemination Portal, available at:
http://121.241.212.146, last access: 16 September 2019., 2019.

McKinley, G. A., Pilcher, D. J., Fay, A. R., Lindsay, K., Long, M. C. and Lovenduski, N. S.:
Timescales for detection of trends in the ocean carbon sink, Nature, 530(7591), 469–472,
doi:10.1038/nature16958, 2016.

McNeil, B. I., Matear, R. J., Key, R. M., Bullister, J. L. and Sarmiento, J. L.: Anthropogenic CO2
uptake by the ocean based on the global chlorofluorocarbon data set, Science (80-.).,
299(5604), 235–239, doi:10.1126/science.1077429, 2003.

Meiyappan, P., Jain, A. K. and House, J. I.: Increased influence of nitrogen limitation on CO2
emissions from future land use and land use change, Global Biogeochem. Cycles, 29(9),
1524–1548, doi:10.1002/2015gb005086, 2015.

Melton, J. R. and Arora, V. K.: Competition between plant functional types in the Canadian Terrestrial Ecosystem Model (CTEM) v. 2.0, Geosci. Model Dev., 9(1), 323–361, doi:10.5194/gmd-9-323-2016, 2016.

Mercado, L. M., Bellouin, N., Sitch, S., Boucher, O., Huntingford, C., Wild, M. and Cox, P. M.: Impact of changes in diffuse radiation on the global land carbon sink, Nature, 458(7241), 1014–1017, doi:10.1038/nature07949, 2009.

Mikaloff Fletcher, S. E., Gruber, N., Jacobson, A. R., Doney, S. C., Dutkiewicz, S., Gerber, M., Follows, M., Joos, F., Lindsay, K., Menemenlis, D., Mouchet, A., Müller, S. A. and Sarmiento, J. L.: Inverse estimates of anthropogenic CO 2 uptake, transport, and storage by the ocean, Global Biogeochem. Cycles, 20(2), GB2002, doi:10.1029/2005GB002530, 2006.

Millar, R. J., Fuglestvedt, J. S., Friedlingstein, P., Rogelj, J., Grubb, M. J., Matthews, H. D., Skeie, R. B., Forster, P. M., Frame, D. J. and Allen, M. R.: Emission budgets and pathways consistent with limiting warming to 1.5 °C, Nat. Geosci., 10(10), 741–747, doi:10.1038/ngeo3031, 2017.

Ministry of Mines: Ministry of Mines: Mineral Production, available at: http://ibm.nic.in/index.php?c=pages&m=index&id=497, last access: 18 September 2019., 2019.

Van Minnen, J. G., Klein Goldewijk, K., Stehfest, E., Eickhout, B., van Drecht, G. and Leemans, R.: The importance of three centuries of land-use change for the global and regional terrestrial carbon cycle, Clim. Change, 97(1–2), 123–144, doi:10.1007/s10584-009-9596-0, 2009.

Myhre, G., Alterskjær, K. and Lowe, D.: A fast method for updating global fossil fuel carbon dioxide emissions, Environ. Res. Lett., 4(3), 034012, doi:10.1088/1748-9326/4/3/034012, 2009.

Myneni, R. B., Ramakrishna, R., Nemani, R. and Running, S. W.: Estimation of global leaf area index and absorbed par using radiative transfer models, IEEE Trans. Geosci. Remote Sens., 35(6), 1380–1393, doi:10.1109/36.649788, 1997.

Narayanan, B., Aguiar, A. and McDougall, R.: Global Trade, Assistance, and Production: The GTAP 9 Data Base, Cent. Glob. Trade Anal. Purdue Univ., 2015(September) [online] Available from: https://www.gtap.agecon.purdue.edu/databases/v9/default.asp, 2015.

NBS: National Bureau of Statistics, 2015. China Energy Statistical Yearbook 2014. China Statistics Press, Beijing. ISBN 978-7-5037-7499-7., 2015.

NBS: Energy supply growth is speeding up, and the share of clean energy is continuously increasing. The department director interprets the half-yearly report. http://www.stats.gov.cn/tjsj/sjjd/201907/t20190717_1676924.html. Last access 23 September 2019., National Bureau of Statistics., 2019a.

NBS: National Bureau of Statistics, 2019. China Energy Statistical Yearbook 2018. China Statistics Press, Beijing. ISBN 978-7-5037-8788-1., 2019b.

NBS: National Bureau of Statistics, 2019. Statistical Communiqué of the People's Republic of China on the 2018 National Economic and Social Development, available at: http://www.stats.gov.cn/english/PressRelease/201902/t20190228_1651335.html. Last access: 23 S., 2019c.

NBS: Value-added by industrial enterprises above the reporting limit grew 4.4% in August 2019 (2019年8月份规模以上工业增加值增长4.4%). Available at

http://www.stats.gov.cn/tjsj/zxfb/201909/t20190916_1697619.html. Last access: 23 September 2019., National Bureau of Statistics., 2019d.

NOAA/ESRL: NOAA Greenhouse Gas Marine Boundary Layer Reference, available at: https://www.esrl.noaa.gov/gmd/ccgg/mbl/mbl.html, last access: 27 September 2019.,

2019.

OEA: Index of Eight Core Industries, available at: http://eaindustry.nic.in/home.asp, last access: 17 September 2019., 2019.

Paulsen, H., Ilyina, T., Six, K. D. and Stemmler, I.: Incorporating a prognostic representation of marine nitrogen fixers into the global ocean biogeochemical model HAMOCC, J. Adv. Model. Earth Syst., 9(1), 438–464, doi:10.1002/2016MS000737, 2017.

Peters, G. P., Andrew, R. and Lennox, J.: Constructing an environmentally-extended multi-regional input-output table using the GTAP database, Econ. Syst. Res., 23(2), 131–152, doi:10.1080/09535314.2011.563234, 2011a.

Peters, G. P., Minx, J. C., Weber, C. L. and Edenhofer, O.: Growth in emission transfers via international trade from 1990 to 2008, Proc. Natl. Acad. Sci., 108(21), 8903–8908, doi:10.1073/pnas.1006388108, 2011b.

Peters, G. P., Davis, S. J. and Andrew, R.: A synthesis of carbon in international trade, Biogeosciences, 9(8), 3247–3276, doi:10.5194/bg-9-3247-2012, 2012a.

Peters, G. P., Marland, G., Le Quéré, C., Boden, T., Canadell, J. G. and Raupach, M. R.: Rapid growth in CO_2 emissions after the 2008–2009 global financial crisis, Nat. Clim. Chang., 2(1), 2–4, doi:10.1038/nclimate1332, 2012b.

Peters, G. P., Andrew, R. M., Boden, T., Canadell, J. G., Ciais, P., Le Quéré, C., Marland, G., Raupach, M. R. and Wilson, C.: The challenge to keep global warming below 2 °C, Nat. Clim. Chang., 3(1), 4–6, doi:10.1038/nclimate1783, 2013.

Peters, G. P., Le Quéré, C., Andrew, R. M., Canadell, J. G., Friedlingstein, P., Ilyina, T., Jackson, R. B., Joos, F., Korsbakken, J. I., McKinley, G. A., Sitch, S. and Tans, P.: Towards real-time verification of CO_2 emissions, Nat. Clim. Chang., 7(12), 848–850, doi:10.1038/s41558-017-0013-9, 2017.

Peylin, P., Law, R. M., Gurney, K. R., Chevallier, F., Jacobson, A. R., Maki, T., Niwa, Y., Patra, P. K., Peters, W., Rayner, P. J., Rödenbeck, C., van der Laan-Luijkx, I. T. and Zhang, X.: Global atmospheric carbon budget: results from an ensemble of atmospheric CO2 inversions, Biogeosciences, 10(10), 6699–6720, doi:10.5194/bg-10-6699-2013, 2013.

Pfeil, B., Olsen, A., Bakker, D. C. E., Hankin, S., Koyuk, H., Kozyr, A., Malczyk, J., Manke, A., Metzl, N., Sabine, C. L., Akl, J., Alin, S. R., Bates, N., Bellerby, R. G. J., Borges, A., Boutin, J., Brown, P. J., Cai, W. J., Chavez, F. P., Chen, A., Cosca, C., Fassbender, A. J., Feely, R. A., Gonzalez-Davila, M., Goyet, C., Hales, B., Hardman-Mountford, N., Heinze, C., Hood, M., Hoppema, M., Hunt, C. W., Hydes, D., Ishii, M., Johannessen, T., Jones, S. D., Key, R. M., Kortzinger, A., Landschutzer, P., Lauvset, S. K., Lefevre, N., Lenton, A., Lourantou, A., Merlivat, L., Midorikawa, T., Mintrop, L., Miyazaki, C., Murata, A., Nakadate, A., Nakano, Y., Nakaoka, S., Nojiri, Y., Omar, A. M., Padin, X. A., Park, G. H., Paterson, K., Perez, F. F., Pierrot, D., Poisson, A., Rios, A. F., Santana-Casiano, J. M., Salisbury, J., Sarma, V. V. S. S., Schlitzer, R., Schneider, B., Schuster, U., Sieger, R., Skjelvan, I., Steinhoff, T., Suzuki, T., Takahashi, T., Tedesco, K., Telszewski, M., Thomas, H., Tilbrook, B., Tjiputra, J., Vandemark, D., Veness, T., Wanninkhof, R., Watson, A. J., Weiss, R., Wong, C. S. and Yoshikawa-Inoue, H.: A uniform, quality controlled Surface Ocean CO2 Atlas (SOCAT), Earth Syst. Sci. Data, 5(1), 125–143, doi:10.5194/essd-5-125-2013, 2013.

Piao, S., Huang, M., Liu, Z., Wang, X. H., Ciais, P., Canadell, J. G., Wang, K., Bastos, A., Friedlingstein, P., Houghton, R. A., Le Quere, C., Liu, Y. W., Myneni, R. B., Peng, S. S., Pongratz, J., Sitch, S., Yan, T., Wang, Y. L., Zhu, Z. C., Wu, D. H. and Wang, T.: Lower land-use emissions responsible for increased net land carbon sink during the slow warming period, Nat. Geosci., 11(10), 739-+, doi:10.1038/s41561-018-0204-7, 2018.

Pongratz, J., Reick, C. H., Raddatz, T. and Claussen, M.: Effects of anthropogenic land cover

change on the carbon cycle of the last millennium, Global Biogeochem. Cycles, doi:10.1029/2009GB003488, 2009.

Pongratz, J., Reick, C. H., Houghton, R. A. and House, J. I.: Terminology as a key uncertainty in net land use and land cover change carbon flux estimates, Earth Syst. Dyn., 5(1), 177–195, doi:10.5194/esd-5-177-2014, 2014.

Poulter, B., Frank, D. C., Hodson, E. L. and Zimmermann, N. E.: Impacts of land cover and climate data selection on understanding terrestrial carbon dynamics and the CO_2 airborne fraction, Biogeosciences, 8(8), 2027–2036, doi:10.5194/bg-8-2027-2011, 2011.

PPAC: Natural Gas. Petroleum Planning and Analysis Cell, Ministry of Petroleum and Natural Gas, available at: http://eaindustry.nic.in/home.asp, last access: 26 September 2019., 2019a.

PPAC: Petroleum. Petroleum Planning and Analysis Cell, Ministry of Petroleum and Natural Gas, available at: http://eaindustry.nic.in/home.asp, last access: 12 September 2019., 2019b.

Prentice, I. C., Farquhar, G. D., Fasham, M. J. R., Goulden, M. L., Heimann, M., Jaramillo, V. J., Kheshgi, H. S., Le Quéré, C., Scholes, R. J., Wallace, D. W. R. and Press, C. U.: The Carbon Cycle and Atmospheric Carbon Dioxide, in Climate Change 2001: The Scientific Basis. Contribution of Working Group I to the Third Assessment Report of the Intergovernmental Panel on Climate Change, edited by J. T. Houghton, Y. Ding, D. J. Griggs, M. Noguer, P. J. van der Linden, X. Dai, K. Maskell, and C. A. Johnson, pp. 183–237, Cambridge University Press, Cambridge, United Kingdom and New York, NY, USA., 2001.

Price, J. T. and Warren, R.: Review of the Potential of "Blue Carbon" Activities to Reduce Emissions; available at http://avoid-net-uk.cc.ic.ac.uk/wp-content/uploads/delightful-downloads/2016/03/Literature-review-of-the-potential-of-blue-carbon-activities-to-reduce-emissions-AVOID2-W., 2016.

Le Quéré, C., Raupach, M. R., Canadell, J. G., Marland, G., Bopp, L., Ciais, P., Conway, T. J.,
Doney, S. C., Feely, R. A., Foster, P., Friedlingstein, P., Gurney, K., Houghton, R. A., House, J.
I., Huntingford, C., Levy, P. E., Lomas, M. R., Majkut, J., Metzl, N., Ometto, J. P., Peters, G.
P., Prentice, I. C., Randerson, J. T., Running, S. W., Sarmiento, J. L., Schuster, U., Sitch, S.,
Takahashi, T., Viovy, N., Van Der Werf, G. R. and Woodward, F. I.: Trends in the sources
and sinks of carbon dioxide, Nat. Geosci., 2(12), 831–836, doi:10.1038/ngeo689, 2009.

Le Quéré, C., Andres, R. J., Boden, T., Conway, T., Houghton, R. A., House, J. I., Marland, G.,
Peters, G. P., van der Werf, G. R., Ahlström, A., Andrew, R. M., Bopp, L., Canadell, J. G.,
Ciais, P., Doney, S. C., Enright, C., Friedlingstein, P., Huntingford, C., Jain, A. K., Jourdain, C.,
Kato, E., Keeling, R. F., Klein Goldewijk, K., Levis, S., Levy, P., Lomas, M., Poulter, B.,
Raupach, M. R., Schwinger, J., Sitch, S., Stocker, B. D., Viovy, N., Zaehle, S. and Zeng, N.:
The global carbon budget 1959–2011, Earth Syst. Sci. Data, 5(1), 165–185,
doi:10.5194/essd-5-165-2013, 2013.

Le Quéré, C., Peters, G. P., Andres, R. J., Andrew, R. M., Boden, T. a., Ciais, P., Friedlingstein, P.,
Houghton, R. a., Marland, G., Moriarty, R., Sitch, S., Tans, P., Arneth, A., Arvanitis, A.,
Bakker, D. C. E., Bopp, L., Canadell, J. G., Chini, L. P., Doney, S. C., Harper, A., Harris, I.,
House, J. I., Jain, a. K., Jones, S. D., Kato, E., Keeling, R. F., Klein Goldewijk, K., Körtzinger,
A., Koven, C., Lefèvre, N., Maignan, F., Omar, A., Ono, T., Park, G.-H., Pfeil, B., Poulter, B.,
Raupach, M. R., Regnier, P., Rödenbeck, C., Saito, S., Schwinger, J., Segschneider, J.,
Stocker, B. D., Takahashi, T., Tilbrook, B., van Heuven, S., Viovy, N., Wanninkhof, R.,
Wiltshire, A. and Zaehle, S.: Global carbon budget 2013, Earth Syst. Sci. Data, 6(1), 235–
263, doi:10.5194/essd-6-235-2014, 2014.

Le Quéré, C., Moriarty, R., Andrew, R. M., Peters, G. P., Ciais, P., Friedlingstein, P., Jones, S. D.,
Sitch, S., Tans, P., Arneth, A., Boden, T. A., Bopp, L., Bozec, Y., Canadell, J. G., Chini, L. P.,

Chevallier, F., Cosca, C. E., Harris, I., Hoppema, M., Houghton, R. A., House, J. I., Jain, A. K., Johannessen, T., Kato, E., Keeling, R. F., Kitidis, V., Klein Goldewijk, K., Koven, C., Landa, C. S., Landschützer, P., Lenton, A., Lima, I. D., Marland, G., Mathis, J. T., Metzl, N., Nojiri, Y., Olsen, A., Ono, T., Peng, S., Peters, W., Pfeil, B., Poulter, B., Raupach, M. R., Regnier, P., Rödenbeck, C., Saito, S., Salisbury, J. E., Schuster, U., Schwinger, J., Séférian, R., Segschneider, J., Steinhoff, T., Stocker, B. D., Sutton, A. J., Takahashi, T., Tilbrook, B., van der Werf, G. R., Viovy, N., Wang, Y.-P., Wanninkhof, R., Wiltshire, A. and Zeng, N.: Global carbon budget 2014, Earth Syst. Sci. Data, 7(1), 47–85, doi:10.5194/essd-7-47-2015, 2015a.

Le Quéré, C., Moriarty, R., Andrew, R. M., Canadell, J. G., Sitch, S., Korsbakken, J. I., Friedlingstein, P., Peters, G. P., Andres, R. J., Boden, T. A., Houghton, R. A., House, J. I., Keeling, R. F., Tans, P., Arneth, A., Bakker, D. C. E., Barbero, L., Bopp, L., Chang, J., Chevallier, F., Chini, L. P., Ciais, P., Fader, M., Feely, R. A., Gkritzalis, T., Harris, I., Hauck, J., Ilyina, T., Jain, A. K., Kato, E., Kitidis, V., Klein Goldewijk, K., Koven, C., Landschützer, P., Lauvset, S. K., Lefèvre, N., Lenton, A., Lima, I. D., Metzl, N., Millero, F., Munro, D. R., Murata, A., S. Nabel, J. E. M., Nakaoka, S., Nojiri, Y., O'Brien, K., Olsen, A., Ono, T., Pérez, F. F., Pfeil, B., Pierrot, D., Poulter, B., Rehder, G., Rödenbeck, C., Saito, S., Schuster, U., Schwinger, J., Séférian, R., Steinhoff, T., Stocker, B. D., Sutton, A. J., Takahashi, T., Tilbrook, B., Van Der Laan-Luijkx, I. T., Van Der Werf, G. R., Van Heuven, S., Vandemark, D., Viovy, N., Wiltshire, A., Zaehle, S. and Zeng, N.: Global Carbon Budget 2015, Earth Syst. Sci. Data, doi:10.5194/essd-7-349-2015, 2015b.

Le Quéré, C., Andrew, R. M., Canadell, J. G., Sitch, S., Ivar Korsbakken, J., Peters, G. P., Manning, A. C., Boden, T. A., Tans, P. P., Houghton, R. A., Keeling, R. F., Alin, S., Andrews, O. D., Anthoni, P., Barbero, L., Bopp, L., Chevallier, F., Chini, L. P., Ciais, P., Currie, K., Delire, C., Doney, S. C., Friedlingstein, P., Gkritzalis, T., Harris, I., Hauck, J., Haverd, V., Hoppema, M.,

Klein Goldewijk, K., Jain, A. K., Kato, E., Körtzinger, A., Landschützer, P., Lefèvre, N., Lenton, A., Lienert, S., Lombardozzi, D., Melton, J. R., Metzl, N., Millero, F., Monteiro, P. M. S., Munro, D. R., Nabel, J. E. M. S., Nakaoka, S. I., O'Brien, K., Olsen, A., Omar, A. M., Ono, T., Pierrot, D., Poulter, B., Rödenbeck, C., Salisbury, J., Schuster, U., Schwinger, J., Séférian, R., Skjelvan, I., Stocker, B. D., Sutton, A. J., Takahashi, T., Tian, H., Tilbrook, B., Van Der Laan-Luijkx, I. T., Van Der Werf, G. R., Viovy, N., Walker, A. P., Wiltshire, A. J. and Zaehle, S.: Global Carbon Budget 2016, Earth Syst. Sci. Data, doi:10.5194/essd-8-605-2016, 2016.

Le Quéré, C., Andrew, R. M., Friedlingstein, P., Sitch, S., Pongratz, J., Manning, A. C., Korsbakken, J. I., Peters, G. P., Canadell, J. G., Jackson, R. B., Boden, T. A., Tans, P. P., Andrews, O. D., Arora, V. K., Bakker, D. C. E., Barbero, L., Becker, M., Betts, R. A., Bopp, L., Chevallier, F., Chini, L. P., Ciais, P., Cosca, C. E., Cross, J., Currie, K., Gasser, T., Harris, I., Hauck, J., Haverd, V., Houghton, R. A., Hunt, C. W., Hurtt, G., Ilyina, T., Jain, A. K., Kato, E., Kautz, M., Keeling, R. F., Klein Goldewijk, K., Körtzinger, A., Landschützer, P., Lefèvre, N., Lenton, A., Lienert, S., Lima, I., Lombardozzi, D., Metzl, N., Millero, F., Monteiro, P. M. S., Munro, D. R., Nabel, J. E. M. S., Nakaoka, S., Nojiri, Y., Padin, X. A., Peregon, A., Pfeil, B., Pierrot, D., Poulter, B., Rehder, G., Reimer, J., Rödenbeck, C., Schwinger, J., Séférian, R., Skjelvan, I., Stocker, B. D., Tian, H., Tilbrook, B., Tubiello, F. N., van der Laan-Luijkx, I. T., van der Werf, G. R., van Heuven, S., Viovy, N., Vuichard, N., Walker, A. P., Watson, A. J., Wiltshire, A. J., Zaehle, S. and Zhu, D.: Global Carbon Budget 2017, Earth Syst. Sci. Data, 10(1), 405–448, doi:10.5194/essd-10-405-2018, 2018a.

Le Quéré, C., Andrew, R. M., Friedlingstein, P., Sitch, S., Hauck, J., Pongratz, J., Pickers, P. A., Korsbakken, J. I., Peters, G. P., Canadell, J. G., Arneth, A., Arora, V. K., Barbero, L., Bastos, A., Bopp, L., Chevallier, F., Chini, L. P., Ciais, P., Doney, S. C., Gkritzalis, T., Goll, D. S., Harris, I., Haverd, V., Hoffman, F. M., Hoppema, M., Houghton, R. A., Hurtt, G., Ilyina, T., Jain, A.

K., Johannessen, T., Jones, C. D., Kato, E., Keeling, R. F., Goldewijk, K. K., Landschützer, P., Lefèvre, N., Lienert, S., Liu, Z., Lombardozzi, D., Metzl, N., Munro, D. R., Nabel, J. E. M. S., Nakaoka, S., Neill, C., Olsen, A., Ono, T., Patra, P., Peregon, A., Peters, W., Peylin, P., Pfeil, B., Pierrot, D., Poulter, B., Rehder, G., Resplandy, L., Robertson, E., Rocher, M., Rödenbeck, C., Schuster, U., Schwinger, J., Séférian, R., Skjelvan, I., Steinhoff, T., Sutton, A., Tans, P. P., Tian, H., Tilbrook, B., Tubiello, F. N., van der Laan-Luijkx, I. T., van der Werf, G. R., Viovy, N., Walker, A. P., Wiltshire, A. J., Wright, R., Zaehle, S. and Zheng, B.: Global Carbon Budget 2018, Earth Syst. Sci. Data, 10(4), 2141–2194, doi:10.5194/essd-10-2141-2018, 2018b.

Le Quéré, C., Korsbakken, J. I., Wilson, C., Tosun, J., Andrew, R., Andres, R. J., Canadell, J. G., Jordan, A., Peters, G. P. and van Vuuren, D. P.: Drivers of declining CO2 emissions in 18 developed economies, Nat. Clim. Chang., 9(3), 213–217, doi:10.1038/s41558-019-0419-7, 2019.

Raupach, M. R., Marland, G., Ciais, P., Le Quere, C., Canadell, J. G., Klepper, G. and Field, C. B.: Global and regional drivers of accelerating CO2 emissions, Proc Natl Acad Sci U S A, 104(24), 10288–10293, doi:10.1073/pnas.0700609104, 2007.

Regnier, P., Friedlingstein, P., Ciais, P., Mackenzie, F. T., Gruber, N., Janssens, I. A., Laruelle, G. G., Lauerwald, R., Luyssaert, S., Andersson, A. J., Arndt, S., Arnosti, C., Borges, A. V., Dale, A. W., Gallego-Sala, A., Goddéris, Y., Goossens, N., Hartmann, J., Heinze, C., Ilyina, T., Joos, F., LaRowe, D. E., Leifeld, J., Meysman, F. J. R., Munhoven, G., Raymond, P. A., Spahni, R., Suntharalingam, P. and Thullner, M.: Anthropogenic perturbation of the carbon fluxes from land to ocean, Nat. Geosci., 6(8), 597–607, doi:10.1038/ngeo1830, 2013.

Remaud, M., Chevallier, F., Cozic, A., Lin, X. and Bousquet, P.: On the impact of recent developments of the LMDz atmospheric general circulation model on the simulation of CO2 transport, Geosci. Model Dev., 11(11), 4489–4513, doi:10.5194/gmd-11-4489-2018,

2018.

Resplandy, L., Keeling, R. F., Rödenbeck, C., Stephens, B. B., Khatiwala, S., Rodgers, K. B., Long, M. C., Bopp, L. and Tans, P. P.: Revision of global carbon fluxes based on a reassessment of oceanic and riverine carbon transport, Nat. Geosci., 11(7), 504-+, doi:10.1038/s41561-018-0151-3, 2018.

Rhein, M., Rintoul, S. R., Aoki, S., Campos, E., Chambers, D., Feely, R. A., Gulev, S., Johnson, G. C., Josey, S. A., Kostianoy, A., Mauritzen, C., Roemmich, D., Talley, L. D., Wang, F., Stocker, T., Qin, D. and Platner, G.-K.: Chapter 3: Observations: Ocean, in Climate Change 2013 The Physical Science Basis, Cambridge University Press., 2013.

Rödenbeck, C.: Estimating CO2 sources and sinks from atmospheric mixing ratio measurements using a global inversion of atmospheric transport, Technical Report 6, available at: http://www.bgc-jena.mpg.de/CarboScope/s/tech_report6.pdf, Max Planck Institute for Biogeochemistry, Jena., 2005.

Rödenbeck, C., Houweling, S., Gloor, M. and Heimann, M.: CO_2 flux history 1982–2001 inferred from atmospheric data using a global inversion of atmospheric transport, Atmos. Chem. Phys. Discuss., 3(3), 2575–2659, doi:10.5194/acpd-3-2575-2003, 2003.

Rödenbeck, C., Keeling, R. F., Bakker, D. C. E., Metzl, N., Olsen, A., Sabine, C. and Heimann, M.: Global surface-ocean $p CO_2$ and sea–air CO_2 flux variability from an observation-driven ocean mixed-layer scheme, Ocean Sci., 9(2), 193–216, doi:10.5194/os-9-193-2013, 2013.

Rödenbeck, C., Bakker, D. C. E., Metzl, N., Olsen, A., Sabine, C., Cassar, N., Reum, F., Keeling, R. F. and Heimann, M.: Interannual sea–air CO_2 flux variability from an observation-driven ocean mixed-layer scheme, Biogeosciences, 11(17), 4599–4613,

doi:10.5194/bg-11-4599-2014, 2014.

Rödenbeck, C., Bakker, D. C. E., Gruber, N., Iida, Y., Jacobson, A. R., Jones, S., Landschützer, P., Metzl, N., Nakaoka, S., Olsen, A., Park, G.-H., Peylin, P., Rodgers, K. B., Sasse, T. P., Schuster, U., Shutler, J. D., Valsala, V., Wanninkhof, R. and Zeng, J.: Data-based estimates of the ocean carbon sink variability – first results of the Surface Ocean pCO2 Mapping intercomparison (SOCOM), Biogeosciences, 12(23), 7251–7278, doi:10.5194/bg-12-7251-2015, 2015.

Rödenbeck, C., Zaehle, S., Keeling, R. and Heimann, M.: How does the terrestrial carbon exchange respond to inter-annual climatic variations? A quantification based on atmospheric CO2 data, Biogeosciences, 15(8), 2481–2498, doi:10.5194/bg-15-2481-2018, 2018.

Rogelj, J., Schaeffer, M., Friedlingstein, P., Gillett, N. P., van Vuuren, D. P., Riahi, K., Allen, M. and Knutti, R.: Differences between carbon budget estimates unravelled, Nat. Clim. Chang., 6(3), 245–252, doi:10.1038/Nclimate2868, 2016.

Rogelj, J., Forster, P. M., Kriegler, E., Smith, C. J. and Séférian, R.: Estimating and tracking the remaining carbon budget for stringent climate targets, Nature, 571(7765), 335–342, doi:10.1038/s41586-019-1368-z, 2019.

Rypdal, K., Paciomik, N., Eggleston, S., Goodwin, J., Irving, W., Penman, J. and Woodfield, M.: Chapter 1 Introduction to the 2006 Guidelines, in 2006 IPCC Guidelines for National Greenhouse Gas Inventories, edited by S. Eggleston, L. Buendia, K. Miwa, T. Ngara, and K. Tanabe, Institute for Global Environmental Strategies (IGES), Hayama, Kanagawa, Japan., 2006.

Saatchi, S. S., Harris, N. L., Brown, S., Lefsky, M., Mitchard, E. T. A., Salas, W., Zutta, B. R., Buermann, W., Lewis, S. L., Hagen, S., Petrova, S., White, L., Silman, M. and Morel, A.:

Benchmark map of forest carbon stocks in tropical regions across three continents, Proc. Natl. Acad. Sci., 108(24), 9899–9904, doi:10.1073/pnas.1019576108, 2011.

Saunois, M., Bousquet, P., Poulter, B., Peregon, A., Ciais, P., Canadell, J. G., Dlugokencky, E. J., Etiope, G., Bastviken, D., Houweling, S., Janssens-Maenhout, G., Tubiello, F. N., Castaldi, S., Jackson, R. B., Alexe, M., Arora, V. K., Beerling, D. J., Bergamaschi, P., Blake, D. R., Brailsford, G., Brovkin, V., Bruhwiler, L., Crevoisier, C., Crill, P., Covey, K., Curry, C., Frankenberg, C., Gedney, N., Höglund-Isaksson, L., Ishizawa, M., Ito, A., Joos, F., Kim, H. S., Kleinen, T., Krummel, P., Lamarque, J. F., Langenfelds, R., Locatelli, R., Machida, T., Maksyutov, S., McDonald, K. C., Marshall, J., Melton, J. R., Morino, I., Naik, V., O'Doherty, S., Parmentier, F. J. W., Patra, P. K., Peng, C., Peng, S., Peters, G. P., Pison, I., Prigent, C., Prinn, R., Ramonet, M., Riley, W. J., Saito, M., Santini, M., Schroeder, R., Simpson, I. J., Spahni, R., Steele, P., Takizawa, A., Thornton, B. F., Tian, H., Tohjima, Y., Viovy, N., Voulgarakis, A., Van Weele, M., Van Der Werf, G. R., Weiss, R., Wiedinmyer, C., Wilton, D. J., Wiltshire, A., Worthy, D., Wunch, D., Xu, X., Yoshida, Y., Zhang, B., Zhang, Z. and Zhu, Q.: The global methane budget 2000-2012, Earth Syst. Sci. Data, 8(2), 697–751, doi:10.5194/essd-8-697-2016, 2016.

SCCL: Singareni Collieries Company Limited (SCCL): Provisional Production and Dispatches Performance. Singareni Collieries Company Limited, available at: https://scclmines.com/scclnew/performance_production.asp, last access: 3 September 2019., 2019.

Schimel, D., Alves, D., Enting, I., Heimann, M., Joos, F., Raynaud, D., Wigley, T., Prater, M., Derwent, R., Ehhalt, D., Fraser, P., Sanhueza, E., Zhou, X., Jonas, P., Charlson, R., Rodhe, H., Sadasivan, S., Shine, K. P., Fouquart, Y., Ramaswamy, V., Solomon, S., Srinivasan, J., Albritton, D., Derwent, R., Isaksen, I., Lal, M., Wuebbles, D. and Press, C. U.: Radiative

Forcing of Climate Change, in Climate Change 1995 The Science of Climate Change. Contribution of Working Group I to the Second Assessment Report of the Intergovernmental Panel on Climate Change, edited by J. T. Houghton, L. G. Meira Rilho, B. A. Callander, N. Harris, A. Kattenberg, and K. Maskell, Cambridge University Press, Cambridge, United Kingdom and New York, NY, USA., 1995.

Schimel, D., Stephens, B. B. and Fisher, J. B.: Effect of increasing CO2 on the terrestrial carbon cycle, Proc Natl Acad Sci U S A, 112(2), 436–441, doi:10.1073/pnas.1407302112, 2015.

Schwietzke, S., Sherwood, O. A., Bruhwiler, L. M., Miller, J. B., Etiope, G., Dlugokencky, E. J., Michel, S. E., Arling, V. A., Vaughn, B. H., White, J. W. and Tans, P. P.: Upward revision of global fossil fuel methane emissions based on isotope database, Nature, 538(7623), 88–91, doi:10.1038/nature19797, 2016.

Schwinger, J., Goris, N., Tjiputra, J. F., Kriest, I., Bentsen, M., Bethke, I., Ilicak, M., Assmann, K. M. and Heinze, C.: Evaluation of NorESM-OC (versions 1 and 1.2), the ocean carbon-cycle stand-alone configuration of the Norwegian Earth System Model (NorESM1), Geosci. Model Dev., 9(8), 2589–2622, doi:10.5194/gmd-9-2589-2016, 2016.

Séférian, R., Delire, C., Decharme, B., Voldoire, A., Salas y Melia, D., Chevallier, M., Saint-Martin, D., Aumont, O., Calvet, J.-C., Carrer, D., Douville, H., Franchistéguy, L., Joetzjer, E. and Sénési, S.: Development and evaluation of CNRM Earth system model – CNRM-ESM1, Geosci. Model Dev., 9(4), 1423–1453, doi:10.5194/gmd-9-1423-2016, 2016.

Shevliakova, E., Pacala, S. W., Malyshev, S., Hurtt, G. C., Milly, P. C. D., Caspersen, J. P., Sentman, L. T., Fisk, J. P., Wirth, C. and Crevoisier, C.: Carbon cycling under 300 years of land use change: Importance of the secondary vegetation sink, Global Biogeochem. Cycles, 23(2), doi:10.1029/2007GB003176, 2009.

Sitch, S., Huntingford, C., Gedney, N., Levy, P. E., Lomas, M., Piao, S. L., Betts, R., Ciais, P., Cox,

P., Friedlingstein, P., Jones, C. D., Prentice, I. C. and Woodward, F. I.: Evaluation of the terrestrial carbon cycle, future plant geography and climate-carbon cycle feedbacks using five Dynamic Global Vegetation Models (DGVMs), Glob. Chang. Biol., 14(9), 2015–2039, doi:10.1111/j.1365-2486.2008.01626.x, 2008.

Smith, B., Warlind, D., Arneth, A., Hickler, T., Leadley, P., Siltberg, J. and Zaehle, S.: Implications of incorporating N cycling and N limitations on primary production in an individual-based dynamic vegetation model, Biogeosciences, 11(7), 2027–2054, doi:10.5194/bg-11-2027-2014, 2014.

Stephens, B. B., Gurney, K. R., Tans, P. P., Sweeney, C., Peters, W., Bruhwiler, L., Ciais, P., Ramonet, M., Bousquet, P., Nakazawa, T., Aoki, S., Machida, T., Inoue, G., Vinnichenko, N., Lloyd, J., Jordan, A., Heimann, M., Shibistova, O., Langenfelds, R. L., Steele, L. P., Francey, R. J. and Denning, A. S.: Weak northern and strong tropical land carbon uptake from vertical profiles of atmospheric CO2, Science (80-.)., 316(5832), 1732–1735, doi:10.1126/science.1137004, 2007.

Stocker, T., Qin, D. and Platner, G.-K.: Climate Change 2013 The Physical Science Basis, Cambridge University Press., 2013.

Swart, N. C., Fyfe, J. C., Saenko, O. A. and Eby, M.: Wind-driven changes in the ocean carbon sink, Biogeosciences, 11(21), 6107–6117, doi:10.5194/bg-11-6107-2014, 2014.

Tian, H., Xu, X., Lu, C., Liu, M., Ren, W., Chen, G., Melillo, J. and Liu, J.: Net exchanges of CO2, CH4, and N2O between China's terrestrial ecosystems and the atmosphere and their contributions to global climate warming, J. Geophys. Res., 116(G2), doi:10.1029/2010jg001393, 2011.

Tian, H., Chen, G., Lu, C., Xu, X., Hayes, D. J., Ren, W., Pan, S., Huntzinger, D. N. and Wofsy, S. C.: North American terrestrial CO2 uptake largely offset by CH4 and N2O emissions: toward a

full accounting of the greenhouse gas budget, Clim Chang., 129(3–4), 413–426, doi:10.1007/s10584-014-1072-9, 2015.

Todd-Brown, K. E. O., Randerson, J. T., Post, W. M., Hoffman, F. M., Tarnocai, C., Schuur, E. A. G. and Allison, S. D.: Causes of variation in soil carbon simulations from CMIP5 Earth system models and comparison with observations, Biogeosciences, 10(3), 1717–1736, doi:10.5194/bg-10-1717-2013, 2013.

UN: United Nations Statistics Division: National Accounts Main Aggregates Database, available at: http://unstats.un.org/unsd/snaama/Introduction.asp, last access: 2 January 2018., 2017.

UN: United Nations Statistics Division: Energy Statistics, available at: http://unstats.un.org/unsd/energy/, last access: 27 September 2019., 2018.

UNFCCC: National Inventory Submissions, available at: https://unfccc.int/process-and-meetings/transparency-and-reporting/reporting-and-review-under-the-convention/greenhouse-gas-inventories-annex-i-parties/national-inventory-submissions-2019, last access: June 20., 2019.

van der Velde, I. R., Miller, J. B., Schaefer, K., van der Werf, G. R., Krol, M. C. and Peters, W.: Terrestrial cycling of ¹³CO₂ by photosynthesis, respiration, and biomass burning in SiBCASA, Biogeosciences, 11(23), 6553–6571, doi:10.5194/bg-11-6553-2014, 2014.

Viovy, N.: CRUNCEP data set, available at: ftp://nacp.ornl.gov/synthesis/2009/frescati/temp/land_use_change/original/readme.htm, last access: June 2016., 2016.

Walker, A. P., Quaife, T., van Bodegom, P. M., De Kauwe, M. G., Keenan, T. F., Joiner, J., Lomas, M. R., MacBean, N., Xu, C. G., Yang, X. J. and Woodward, F. I.: The impact of alternative

trait-scaling hypotheses for the maximum photosynthetic carboxylation rate (V-cmax) on

global gross primary production, New Phytol., 215(4), 1370–1386, doi:10.1111/nph.14623,

2017.

Wanninkhof, R., Park, G. H., Takahashi, T., Sweeney, C., Feely, R., Nojiri, Y., Gruber, N., Doney, S.

C., McKinley, G. A., Lenton, A., Le Quere, C., Heinze, C., Schwinger, J., Graven, H. and

Khatiwala, S.: Global ocean carbon uptake: magnitude, variability and trends,

Biogeosciences, 10(3), 1983–2000, doi:10.5194/bg-10-1983-2013, 2013.

Watson, R. T., Rodhe, H., Oeschger, H., Siegenthaler, U. and Press, C. U.: Greenhouse Gases and

Aerosols, in Climate Change: The IPCC Scientific Assessment. Intergovernmental Panel on

Climate Change (IPCC), edited by J. T. Houghton, G. J. Jenkins, and J. J. Ephraums, pp. 1–40,

Cambridge University Press, Cambridge., 1990.

Wenzel, S., Cox, P. M., Eyring, V. and Friedlingstein, P.: Projected land photosynthesis

constrained by changes in the seasonal cycle of atmospheric CO2, Nature, 538(7626), 499–

501, doi:10.1038/nature19772, 2016.

van der Werf, G. R., Randerson, J. T., Giglio, L., Collatz, G. J., Mu, M., Kasibhatla, P. S., Morton,

D. C., DeFries, R. S., Jin, Y. and van Leeuwen, T. T.: Global fire emissions and the

contribution of deforestation, savanna, forest, agricultural, and peat fires (1997–2009),

Atmos. Chem. Phys., 10(23), 11707–11735, doi:10.5194/acp-10-11707-2010, 2010.

van der Werf, G. R., Randerson, J. T., Giglio, L., van Leeuwen, T. T., Chen, Y., Rogers, B. M., Mu,

M., van Marle, M. J. E., Morton, D. C., Collatz, G. J., Yokelson, R. J. and Kasibhatla, P. S.:

Global fire emissions estimates during 1997–2016, Earth Syst. Sci. Data, 9(2), 697–720,

doi:10.5194/essd-9-697-2017, 2017.

Wilkenskjeld, S., Kloster, S., Pongratz, J., Raddatz, T. and Reick, C. H.: Comparing the influence

of net and gross anthropogenic land-use and land-cover changes on the carbon cycle in the

MPI-ESM, Biogeosciences, 11(17), 4817–4828, doi:10.5194/bg-11-4817-2014, 2014.

Woodward, F. I. and Lomas, M. R.: Vegetation dynamics – simulating responses to climatic change, Biol. Rev., 79(3), 643–670, doi:10.1017/S1464793103006419, 2004.

Xi, F., Davis, S. J., Ciais, P., Crawford-Brown, D., Guan, D., Pade, C., Shi, T., Syddall, M., Lv, J., Ji, L., Bing, L., Wang, J., Wei, W., Yang, K.-H., Lagerblad, B., Galan, I., Andrade, C., Zhang, Y. and Liu, Z.: Substantial global carbon uptake by cement carbonation, Nat. Geosci., 9(12), 880–883, doi:10.1038/ngeo2840, 2016.

Yin, X. W.: Responses of leaf nitrogen concentration and specific leaf area to atmospheric CO2 enrichment: a retrospective synthesis across 62 species, Glob. Chang. Biol., 8(7), 631–642, doi:DOI 10.1046/j.1365-2486.2002.00497.x, 2002.

Zaehle, S. and Friend, A. D.: Carbon and nitrogen cycle dynamics in the O-CN land surface model: 1. Model description, site-scale evaluation, and sensitivity to parameter estimates, Global Biogeochem. Cycles, 24(1), n/a-n/a, doi:10.1029/2009GB003521, 2010.

Zaehle, S., Ciais, P., Friend, A. D. and Prieur, V.: Carbon benefits of anthropogenic reactive nitrogen offset by nitrous oxide emissions, Nat. Geosci., 4(9), 601–605, doi:10.1038/ngeo1207, 2011.

Zheng, B., Chevallier, F., Yin, Y., Ciais, P., Fortems-Cheiney, A., Deeter, M. N., Parker, R. J., Wang, Y., Worden, H. M. and Zhao, Y.: Global atmospheric carbon monoxide budget 2000–2017 inferred from multi-species atmospheric inversions, Earth Syst. Sci. Data, 11(3), 1411–1436, doi:10.5194/essd-11-1411-2019, 2019.

Zscheischler, J., Mahecha, M. D., Avitabile, V., Calle, L., Carvalhais, N., Ciais, P., Gans, F., Gruber, N., Hartmann, J., Herold, M., Ichii, K., Jung, M., Landschutzer, P., Laruelle, G. G., Lauerwald, R., Papale, D., Peylin, P., Poulter, B., Ray, D., Regnier, P., Rödenbeck, C., Roman-Cuesta, R. M., Schwalm, C., Tramontana, G., Tyukavina, A., Valentini, R., van der Werf, G., West, T. O.,

Wolf, J. E. and Reichstein, M.: Reviews and syntheses: An empirical spatiotemporal description of the global surface-atmosphere carbon fluxes: opportunities and data limitations, Biogeosciences, 14(15), 3685–3703, doi:10.5194/bg-14-3685-2017, 2017.

Adcroft, A., Anderson, W., Balaji, V., Blanton, C., Bushuk, M., Dufour, C. O., Dunne, J. P., Griffies, S. M., Hallberg, R., Harrison, M. J., Held, I. M., Jansen, M. F., John, J. G., Krasting, J. P., Langenhorst, A. R., Legg, S., Liang, Z., McHugh, C., Radhakrishnan, A., Reichl, B. G., Rosati, T., Samuels, B. L., Shao, A., Stouffer, R., Winton, M., Wittenberg, A. T., Xiang, B., Zadeh, N. and Zhang, R.: The GFDL Global Ocean and Sea Ice Model OM4.0: Model Description and Simulation Features, J. Adv. Model. Earth Syst., 2019MS001726, doi:10.1029/2019MS001726, 2019.

Alton, P. B.: Retrieval of seasonal Rubisco-limited photosynthetic capacity at global FLUXNET sites from hyperspectral satellite remote sensing: Impact on carbon modelling, Agric. For. Meteorol., 232, 74–88, doi:10.1016/j.agrformet.2016.08.001, 2017.

Amante, C. and Eakins, B. W.: ETOPO1 1 Arc-Minute Global Relief Model: Procedures, Data Sources and Analysis. NOAA Technical Memorandum NESDIS NGDC-24. National Geophysical Data Center, NOAA. doi:10.7289/V5C8276M, 2009.

Andres, R. J., Boden, T. A., Bréon, F. M., Ciais, P., Davis, S., Erickson, D., Gregg, J. S., Jacobson, A., Marland, G., Miller, J., Oda, T., Olivier, J. G. J., Raupach, M. R., Rayner, P. and Treanton, K.: A synthesis of carbon dioxide emissions from fossil-fuel combustion, Biogeosciences, doi:10.5194/bg-9-1845-2012, 2012.

Andres, R. J., Boden, T. A. and Higdon, D.: A new evaluation of the uncertainty associated with CDIAC estimates of fossil fuel carbon dioxide emission, Tellus Ser. B-Chemical Phys. Meteorol., 66, 23616, doi:ARTN 2361610.3402/tellusb.v66.23616, 2014.

Andrew, R. M.: Global CO_2 emissions from cement production, 1928-2017, Earth Syst. Sci. Data, 10(4), 2213–2239, doi:10.5194/essd-10-2213-2018, 2018.

Andrew, R. M.: Global CO_2 emissions from cement production, 1928–2018, Earth Syst. Sci. Data, doi:10.5194/essd-2019-152, 2019.

Andrew, R. M. and Peters, G. P.: A Multi-Region Input-Output Table Based on the Global Trade Analysis Project Database (Gtap-Mrio), Econ. Syst. Res., 25(1), 99–121, doi:10.1080/09535314.2012.761953, 2013.

Archer, D., Eby, M., Brovkin, V., Ridgwell, A., Cao, L., Mikolajewicz, U., Caldeira, K., Matsumoto, K., Munhoven, G., Montenegro, A. and Tokos, K.: Atmospheric Lifetime of Fossil Fuel Carbon Dioxide, Annu. Rev. Earth Planet. Sci., 37, 117–134, doi:10.1146/annurev.earth.031208.100206, 2009.

Arneth, A., Sitch, S., Pongratz, J., Stocker, B. D., Ciais, P., Poulter, B., Bayer, A. D., Bondeau, A., Calle, L., Chini, L. P., Gasser, T., Fader, M., Friedlingstein, P., Kato, E., Li, W., Lindeskog, M., Nabel, J. E. M. S., Pugh, T. A. M., Robertson, E., Viovy, N., Yue, C. and Zaehle, S.: Historical carbon dioxide emissions caused by land-use changes are possibly larger than assumed, Nat. Geosci., 10(2), 79–84, doi:10.1038/ngeo2882, 2017.

Arora, V. K., Boer, G. J., Christian, J. R., Curry, C. L., Denman, K. L., Zahariev, K., Flato, G. M., Scinocca, J. F., Merryfield, W. J. and Lee, W. G.: The Effect of Terrestrial Photosynthesis Down Regulation on the Twentieth-Century Carbon Budget Simulated with the CCCma Earth System Model, J. Clim., 22(22), 6066–6088, doi:10.1175/2009jcli3037.1, 2009.

Aumont, O., Ethé, C., Tagliabue, A., Bopp, L. and Gehlen, M.: PISCES-v2: an ocean biogeochemical model for carbon and ecosystem studies, Geosci. Model Dev., 8(8), 2465–2513, doi:10.5194/gmd-8-2465-2015, 2015.

Avitabile, V., Herold, M., Heuvelink, G. B. M., Lewis, S. L., Phillips, O. L., Asner, G. P., Armston, J.,

Ashton, P. S., Banin, L., Bayol, N., Berry, N. J., Boeckx, P., de Jong, B. H. J., DeVries, B., Girardin, C. A. J., Kearsley, E., Lindsell, J. A., Lopez-Gonzalez, G., Lucas, R., Malhi, Y., Morel, A., Mitchard, E. T. A., Nagy, L., Qie, L., Quinones, M. J., Ryan, C. M., Ferry, S. J. W., Sunderland, T., Laurin, G. V., Gatti, R. C., Valentini, R., Verbeeck, H., Wijaya, A. and Willcock, S.: An integrated pan-tropical biomass map using multiple reference datasets, Glob. Chang. Biol., 22(4), 1406–1420, doi:10.1111/gcb.13139, 2016.

Baccini, A., Walker, W., Carvalho, L., Farina, M., Sulla-Menashe, D. and Houghton, R. A.: Tropical forests are a net carbon source based on aboveground measurements of gain and loss, Science (80-.)., 358(6360), 230–234, doi:10.1126/science.aam5962, 2017.

Bakker, D. C. E., Pfeil, B., Landa, C. S., Metzl, N., O'Brien, K. M., Olsen, A., Smith, K., Cosca, C., Harasawa, S., Jones, S. D., Nakaoka, S., Nojiri, Y., Schuster, U., Steinhoff, T., Sweeney, C., Takahashi, T., Tilbrook, B., Wada, C., Wanninkhof, R., Alin, S. R., Balestrini, C. F., Barbero, L., Bates, N. R., Bianchi, A. A., Bonou, F., Boutin, J., Bozec, Y., Burger, E. F., Cai, W. J., Castle, R. D., Chen, L. Q., Chierici, M., Currie, K., Evans, W., Featherstone, C., Feely, R. A., Fransson, A., Goyet, C., Greenwood, N., Gregor, L., Hankin, S., Hardman-Mountford, N. J., Harlay, J., Hauck, J., Hoppema, M., Humphreys, M. P., Hunt, C., Huss, B., Ibanhez, J. S. P., Johannessen, T., Keeling, R., Kitidis, V., Kortzinger, A., Kozyr, A., Krasakopoulou, E., Kuwata, A., Landschutzer, P., Lauvset, S. K., Lefevre, N., Lo Monaco, C., Manke, A., Mathis, J. T., Merlivat, L., Millero, F. J., Monteiro, P. M. S., Munro, D. R., Murata, A., Newberger, T., Omar, A. M., Ono, T., Paterson, K., Pearce, D., Pierrot, D., Robbins, L. L., Saito, S., Salisbury, J., Schlitzer, R., Schneider, B., Schweitzer, R., Sieger, R., Skjelvan, I., Sullivan, K. F., Sutherland, S. C., Sutton, A. J., Tadokoro, K., Telszewski, M., Tuma, M., van Heuven, S. M. A. C., Vandemark, D., Ward, B., Watson, A. J. and Xu, S. Q.: A multi-decade record of high-quality fCO(2) data in version 3 of the Surface Ocean CO_2 Atlas (SOCAT), Earth Syst. Sci.

Data, 8(2), 383–413, doi:10.5194/essd-8-383-2016, 2016.

Ballantyne, A. P., Alden, C. B., Miller, J. B., Tans, P. P. and White, J. W. C.: Increase in observed net carbon dioxide uptake by land and oceans during the past 50 years, Nature, 488(7409), 70–72, doi:10.1038/nature11299, 2012.

Ballantyne, A. P., Andres, R., Houghton, R., Stocker, B. D., Wanninkhof, R., Anderegg, W., Cooper, L. A., DeGrandpre, M., Tans, P. P., Miller, J. B., Alden, C. and White, J. W. C.: Audit of the global carbon budget: Estimate errors and their impact on uptake uncertainty, Biogeosciences, 12(8), 2565–2584, doi:10.5194/bg-12-2565-2015, 2015.

Bauer, J. E., Cai, W.-J., Raymond, P. a, Bianchi, T. S., Hopkinson, C. S. and Regnier, P. a G.: The changing carbon cycle of the coastal ocean, Nature, 504(7478), 61–70, doi:10.1038/nature12857, 2013.

Berthet, S., Séférian, R., Bricaud, C., Chevallier, M., Voldoire, A. and Ethé, C.: Evaluation of an Online Grid-Coarsening Algorithm in a Global Eddy-Admitting Ocean Biogeochemical Model, J. Adv. Model. Earth Syst., 11(6), 1759–1783, doi:10.1029/2019MS001644, 2019.

Best, M. J., Pryor, M., Clark, D. B., Rooney, G. G., Essery, R. . L. H., Ménard, C. B., Edwards, J. M., Hendry, M. A., Porson, A., Gedney, N., Mercado, L. M., Sitch, S., Blyth, E., Boucher, O., Cox, P. M., Grimmond, C. S. B. and Harding, R. J.: The Joint UK Land Environment Simulator (JULES), model description – Part 1: Energy and water fluxes, Geosci. Model Dev., 4(3), 677–699, doi:10.5194/gmd-4-677-2011, 2011.

BP: BP Statistical Review of World Energy June 2019, available at: https://www.bp.com/en/global/corporate/energy-economics/statistical-review-of-world-energy.html, last access: June 2019., 2019.

Bruno, M. and Joos, F.: Terrestrial carbon storage during the past 200 years: A Monte Carlo Analysis of CO 2 data from ice core and atmospheric measurements, Global Biogeochem.

Cycles, 11(1), 111–124, doi:10.1029/96GB03611, 1997.

Buitenhuis, E. T., Hashioka, T. and Le Quéré, C.: Combined constraints on global ocean primary production using observations and models, Global Biogeochem. Cycles, 27(3), 847–858, doi:10.1002/gbc.20074, 2013.

Canadell, J. G., Le Quéré, C., Raupach, M. R., Field, C. B., Buitenhuis, E. T., Ciais, P., Conway, T. J., Gillett, N. P., Houghton, R. A. and Marland, G.: Contributions to accelerating atmospheric CO_2 growth from economic activity, carbon intensity, and efficiency of natural sinks, Proc. Natl. Acad. Sci., 104(47), 18866–18870, doi:10.1073/pnas.0702737104, 2007.

Carbontracker Team: Compilation of near real time atmospheric carbon dioxide data provided by NOAA and EC; obspack_co2_1_NRT_v4.4.2_2019-06-10; NOAA Earth System Research Laboratory, Global Monitoring Division. doi:10.25925/20190610., 2019.

CEA: Central Electricity Authority (CEA): Daily Coal – Archive. Central Electricity Authority, available at: http://www.cea.nic.in/dailyarchive.html, last access: 3 November 2019., 2019a.

CEA: Generation Overview Report September 2019: Summary All India. Available at http://cea.nic.in/reports/monthly/generation/2019/September/actual/actual.html. Last accessed 6 November 2019., 2019b.

CGADIP: Cooperative Global Atmospheric Data Integration Project: Multi-laboratory compilation of atmospheric carbon dioxide data for the period 1957-2017; obspack_co2_1_GLOBALVIEWplus_v4.2.2_2019-06-05, Earth System Research Laboratory, Global Monitoring Division., 2019.

Chatfield, C.: The Holt-Winters Forecasting Procedure, Appl. Stat., 27(3), 264–279, doi:10.2307/2347162, 1978.

Chevallier, F., Fisher, M., Peylin, P., Serrar, S., Bousquet, P., Bréon, F.-M., Chédin, A. and Ciais,

P.: Inferring CO 2 sources and sinks from satellite observations: Method and application to TOVS data, J. Geophys. Res., 110(D24), D24309, doi:10.1029/2005JD006390, 2005.

Ciais, P., Sabine, C., Govindasamy, B., Bopp, L., Brovkin, V., Canadell, J., Chhabra, A., DeFries, R., Galloway, J., Heimann, M., Jones, C., Le Quéré, C., Myneni, R., Piao, S. and Thornton, P.: Chapter 6: Carbon and Other Biogeochemical Cycles, in Climate Change 2013 The Physical Science Basis, edited by T. Stocker, D. Qin, and G.-K. Platner, Cambridge University Press, Cambridge., 2013.

CIL: Coal India Limited: Production and Offtake Performance of CIL and Subsidiary Companies, available at: https://www.coalindia.in/en-us/performance/physical.aspx, last access: 1 November 2019., 2019.

Clark, D. B., Mercado, L. M., Sitch, S., Jones, C. D., Gedney, N., Best, M. J., Pryor, M., Rooney, G. G., Essery, R. L. H., Blyth, E., Boucher, O., Harding, R. J., Huntingford, C. and Cox, P. M.: The Joint UK Land Environment Simulator (JULES), model description – Part 2: Carbon fluxes and vegetation dynamics, Geosci. Model Dev., 4(3), 701–722, doi:10.5194/gmd-4-701-2011, 2011.

Collier, N., Hoffman, F. M., Lawrence, D. M., Keppel-Aleks, G., Koven, C. D., Riley, W. J., Mu, M. Q. and Randerson, J. T.: The International Land Model Benchmarking (ILAMB) System: Design, Theory, and Implementation, J. Adv. Model. Earth Syst., 10(11), 2731–2754, doi:10.1029/2018ms001354, 2018.

Cox, P. M., Pearson, D., Booth, B. B., Friedlingstein, P., Huntingford, C., Jones, C. D. and Luke, C. M.: Sensitivity of tropical carbon to climate change constrained by carbon dioxide variability, Nature, 494(7437), 341–344, doi:10.1038/nature11882, 2013.

Dai, A. and Trenberth, K. E.: Estimates of Freshwater Discharge from Continents: Latitudinal and Seasonal Variations, J. Hydrometeorol., 3(6), 660–687, doi:10.1175/1525-

7541(2002)003<0660:EOFDFC>2.0.CO;2, 2002.

Davis, S. J. and Caldeira, K.: Consumption-based accounting of CO_2 emissions, Proc. Natl. Acad. Sci., 107(12), 5687–5692, doi:10.1073/pnas.0906974107, 2010.

De Kauwe, M. G., Disney, M. I., Quaife, T., Lewis, P. and Williams, M.: An assessment of the MODIS collection 5 leaf area index product for a region of mixed coniferous forest, Remote Sens. Environ., 115(2), 767–780, doi:10.1016/j.rse.2010.11.004, 2011.

Decharme, B., Delire, C., Minvielle, M., Colin, J., Vergnes, J., Alias, A., Saint-Martin, D., Séférian, R., Sénési, S. and Voldoire, A.: Recent Changes in the ISBA-CTRIP Land Surface System for Use in the CNRM-CM6 Climate Model and in Global Off-Line Hydrological Applications, J. Adv. Model. Earth Syst., 11(5), 1207–1252, doi:10.1029/2018MS001545, 2019.

Delire, C., Séférian, R., Decharme, B., Alkama, R., Carrer, D., Joetzjer, E., Morel, X. and Rocher, M.: The global land carbon cycle simulated with ISBA (in review), J. Adv. Model. Earth Syst., 2019.

Denman, K. L., Brasseur, G., Chidthaisong, A., Ciais, P., Cox, P. M., Dickinson, R. E., Hauglustaine, D., Heinze, C., Holland, E., Jacob, D., Lohmann, U., Ramachandran, S., Leite da Silva Dias, P., Wofsy, S. C. and Zhang, X.: Couplings Between Changes in the Climate System and Biogeochemistry, in Climate Change 2007: The Physical Science Basis. Contribution of Working Group I to the Fourth Assessment Report of the Intergovernmental Panel on Climate Change, edited by S. Solomon, Qin D., Manning M., Marquis M., Averyt K., Tignor M. M. B., H. L. Miller, and Chen Z. L., pp. 499–587, Cambridge University Press, Cambridge, UK and New York, USA., 2007.

Denvil-Sommer, A., Gehlen, M., Vrac, M. and Mejia, C.: LSCE-FFNN-v1: LSCE-FFNN-v1: a two-step neural network model for the reconstruction of surface ocean pCO_2 over the global ocean, Geosci. Model Dev., 12(5), 2091–2105, doi:10.5194/gmd-12-2091-2019, 2019.

DeVries, T.: The oceanic anthropogenic CO_2 sink: Storage, air-sea fluxes, and transports over the industrial era, Global Biogeochem. Cycles, 28(7), 631–647, doi:10.1002/2013gb004739, 2014.

DeVries, T., Holzer, M. and Primeau, F.: Recent increase in oceanic carbon uptake driven by weaker upper-ocean overturning, Nature, 542(7640), 215–218, doi:10.1038/nature21068, 2017.

DeVries, T., Le Quéré, C., Andrews, O., Berthet, S., Hauck, J., Ilyina, T., Landschützer, P., Lenton, A., Lima, I. D., Nowicki, M., Schwinger, J. and Séférian, R.: Decadal trends in the ocean carbon sink, Proc. Natl. Acad. Sci., doi:10.1073/pnas.1900371116, 2019.

Dlugokencky, E. and Tans, P.: Trends in atmospheric carbon dioxide, National Oceanic & Atmospheric Administration, Earth System Research Laboratory (NOAA/ESRL), available at: http://www.esrl.noaa.gov/gmd/ccgg/trends/global.html, last access: 3 November 2019., 2019.

Doney, S. C., Lima, I., Feely, R. A., Glover, D. M., Lindsay, K., Mahowald, N., Moore, J. K. and Wanninkhof, R.: Mechanisms governing interannual variability in upper-ocean inorganic carbon system and air-sea CO_2 fluxes: Physical climate and atmospheric dust, Deep. Res. Part Ii-Topical Stud. Oceanogr., 56(8–10), 640–655, doi:10.1016/j.dsr2.2008.12.006, 2009.

Duce, R. A., LaRoche, J., Altieri, K., Arrigo, K. R., Baker, A. R., Capone, D. G., Cornell, S., Dentener, F., Galloway, J., Ganeshram, R. S., Geider, R. J., Jickells, T., Kuypers, M. M., Langlois, R., Liss, P. S., Liu, S. M., Middelburg, J. J., Moore, C. M., Nickovic, S., Oschlies, A., Pedersen, T., Prospero, J., Schlitzer, R., Seitzinger, S., Sorensen, L. L., Uematsu, M., Ulloa, O., Voss, M., Ward, B. and Zamora, L.: Impacts of Atmospheric Anthropogenic Nitrogen on the Open Ocean, Science (80-.)., 320(5878), 893–897, doi:10.1126/science.1150369, 2008.

Dufour, C. O., Le Sommer, J., Gehlen, M., Orr, J. C., Molines, J. M., Simeon, J. and Barnier, B.:

Eddy compensation and controls of the enhanced sea-to-air CO_2 flux during positive
phases of the Southern Annular Mode, Global Biogeochem. Cycles, 27(3), 950–961,
doi:10.1002/gbc.20090, 2013.

Durant, A. J., Le Quéré, C., Hope, C. and Friend, A. D.: Economic value of improved
quantification in global sources and sinks of carbon dioxide, Philos Trans A Math Phys Eng
Sci, 369(1943), 1967–1979, doi:10.1098/rsta.2011.0002, 2011.

Eakins, B. W. and Sharman, G. F.: Volumes of the World's Oceans from ETOPO1; NOAA National
Geophysical Data Center, available at:
http://www.ngdc.noaa.gov/mgg/global/etopo1_ocean_volumes.html, last accessed: 27
September 2019., 2010.

EIA: U.S. Energy Information Administration, Short-Term Energy Outlook, available at:
http://www.eia.gov/forecasts/steo/outlook.cfm, last access: 27 September 2019., 2019.

ENTSO-E: The European Network of Transmission System Operators Electricity Transparency
Platform, available at: https://transparency.entsoe.eu/, last access: 3 November 2019.,
2019.

Erb, K. H., Kastner, T., Luyssaert, S., Houghton, R. A., Kuemmerle, T., Olofsson, P. and Haberl, H.:
COMMENTARY: Bias in the attribution of forest carbon sinks, Nat. Clim. Chang., 3(10), 854–
856, doi:10.1038/nclimate2004, 2013.

Etheridge, D. M., Steele, L. P., Langenfelds, R. L., Francey, R. J., Barnola, J. M. and Morgan, V. I.:
Natural and anthropogenic changes in atmospheric CO_2 over the last 1000 years from air in
Antarctic ice and firn, J. Geophys. Res., 101(D2), 4115–4128, doi:Doi 10.1029/95jd03410,
1996.

Eurostat: Supply and transformation of solid fuels - monthly data (nrg_101m), available at:
https://ec.europa.eu/eurostat/data/database, last access: 5 November 2019., 2019.

FAO: Food and Agriculture Organization of the United Nations: Global Forest Resources

Assessment 2015, available at: http://www.fao.org/forest-resources-assessment/past-

assessments/fra-2015/en/, last access: 27 September 2019, Rome, Italy., 2015.

FAOSTAT: Food and Agriculture Organization Statistics Division, available at:

http://faostat.fao.org/, last access: 27 September 2019., 2015.

Francey, R. J., Trudinger, C. M., van der Schoot, M., Law, R. M., Krummel, P. B., Langenfelds, R.

L., Steele, L. P., Allison, C. E., Stavert, A. R., Andres, R. J. and Rödenbeck, C.: Reply to

"Anthropogenic CO_2 emissions," Nat. Clim. Chang., 3(7), 604, doi:10.1038/nclimate1925,

2013.

Friedlingstein, P., Houghton, R. A., Marland, G., Hackler, J., Boden, T. A., Conway, T. J., Canadell,

J. G., Raupach, M. R., Ciais, P. and Le Quéré, C.: Update on CO_2 emissions, Nat. Geosci.,

3(12), 811–812, doi:10.1038/ngeo1022, 2010.

Friedlingstein, P., Andrew, R. M., Rogelj, J., Peters, G. P., Canadell, J. G., Knutti, R., Luderer, G.,

Raupach, M. R., Schaeffer, M., van Vuuren, D. P. and Le Quéré, C.: Persistent growth of CO_2

emissions and implications for reaching climate targets, Nat. Geosci., 7(10), 709–715,

doi:10.1038/Ngeo2248, 2014.

Friedlingstein, P., Jones, M. W., O'Sullivan, M., Andrew, R. M., Hauck, J., Peters, G. P., Peters,

W., Pongratz, J., Sitch, S., Le Quéré, C., Bakker, D. C. E., Canadell, J. G., Ciais, P., Jackson, R.,

Anthoni, P., Barbero, L., Bastos, A., Bastrikov, V., Becker, M., Bopp, L., Buitenhuis, E.,

Chandra, N., Chevallier, F., Chini, L. P., Currie, K. I., Feely, R. A., Gehlen, M., Gilfillan, D.,

Gkritzalis, T., Goll, D. S., Gruber, N., Gutekunst, S., Harris, I., Haverd, V., Houghton, R. A.,

Hurtt, G., Ilyina, T., Jain, A. K., Joetzjer, E., Kaplan, J. O., Kato, E., Goldewijk, K. K.,

Korsbakken, J. I., Landschützer, P., Lauvset, S. K., Lefèvre, N., Lenton, A., Lienert, S.,

Lombardozzi, D., Marland, G., McGuire, P. C., Melton, J. R., Metzl, N., Munro, D. R., Nabel,

J. E. M. S., Nakaoka, S.-I., Neill, C., Omar, A. M., Ono, T., Peregon, A., Pierrot, D., Poulter, B.,

Rehder, G., Resplandy, L., Robertson, E., Rödenbeck, C., Séférian, R., Schwinger, J., Smith,

N., Tans, P. P., Tian, H., Tilbrook, B., Tubiello, F. N., van der Werf, G. R., Wiltshire, A. J. and

Zaehle, S.: Supplemental data of the Global Carbon Budget 2019, available at:

https://doi.org/10.18160/gcp-2019, ICOS-ERIC Carbon Portal, last accessed: 2 October

2019, 2019.

Gasser, T., Ciais, P., Boucher, O., Quilcaille, Y., Tortora, M., Bopp, L. and Hauglustaine, D.: The

compact Earth system model OSCAR v2.2: description and first results, Geosci. Model Dev.,

10(1), 271–319, doi:10.5194/gmd-10-271-2017, 2017.

Gaubert, B., Stephens, B. B., Basu, S., Chevallier, F., Deng, F., Kort, E. A., Patra, P. K., Peters, W.,

Rödenbeck, C., Saeki, T., Schimel, D., Van der Laan-Luijkx, I., Wofsy, S. and Yin, Y.: Global

atmospheric CO₂ inverse models converging on neutral tropical

land exchange but diverging on fossil fuel and atmospheric growth rate, Biogeosciences

Discuss., 2018, 1–25, doi:10.5194/bg-2018-384, 2018.

GCP: The Global Carbon Budget 2007, available at:

http://www.globalcarbonproject.org/carbonbudget/archive.htm, last access: 7 November

2016., 2007.

General Administration of Customs of the People's Republic of China: Monthly statistics reports

(统计月报), http://www.customs.gov.cn/customs/302249/302274/302277/index.html.

Last access: 1 November 2019., 2019.

Giglio, L., Schroeder, W. and Justice, C. O.: The collection 6 MODIS active fire detection

algorithm and fire products, Remote Sens. Environ., 178, 31–41,

doi:10.1016/j.rse.2016.02.054, 2016.

Gilfillan, D., Marland, G., Boden, T. and Andres, R.: Global, Regional, and National Fossil-Fuel

CO_2 Emissions, available at: https://energy.appstate.edu/CDIAC, last access: 27 September 2019, 2019.

Gitz, V. and Ciais, P.: Amplifying effects of land-use change on future atmospheric CO 2 levels, Global Biogeochem. Cycles, 17(1), 1024, doi:10.1029/2002GB001963, 2003.

Goldewijk, K. K., Beusen, A., Doelman, J. and Stehfest, E.: Anthropogenic land use estimates for the Holocene - HYDE 3.2, Earth Syst. Sci. Data, 9(2), 927–953, doi:10.5194/essd-9-927-2017, 2017a.

Goldewijk, K. K., Dekker, S. C. and van Zanden, J. L.: Per-capita estimations of long-term historical land use and the consequences for global change research, J. Land Use Sci., 12(5), 313–337, doi:10.1080/1747423x.2017.1354938, 2017b.

Goll, D. S., Winkler, A. J., Raddatz, T., Dong, N., Colin Prentice, I., Ciais, P. and Brovkin, V.: Carbon-nitrogen interactions in idealized simulations with JSBACH (version 3.10), Geosci. Model Dev., 10(5), 2009–2030, doi:10.5194/gmd-10-2009-2017, 2017.

Goll, D. S., Joetzjer, E., Huang, M. and Ciais, P.: Low Phosphorus Availability Decreases Susceptibility of Tropical Primary Productivity to Droughts, Geophys. Res. Lett., 45(16), 8231–8240, doi:10.1029/2018GL077736, 2018.

Gray, A. R., Johnson, K. S., Bushinsky, S. M., Riser, S. C., Russell, J. L., Talley, L. D., Wanninkhof, R., Williams, N. L. and Sarmiento, J. L.: Autonomous Biogeochemical Floats Detect Significant Carbon Dioxide Outgassing in the High-Latitude Southern Ocean, Geophys. Res. Lett., 45(17), 9049–9057, doi:10.1029/2018GL078013, 2018.

Gregg, J. S., Andres, R. J. and Marland, G.: China: Emissions pattern of the world leader in CO_2 emissions from fossil fuel consumption and cement production, Geophys. Res. Lett., 35(8), L08806, doi:Artn L0880610.1029/2007gl032887, 2008.

Gruber, N., Clement, D., Carter, B. R., Feely, R. A., van Heuven, S., Hoppema, M., Ishii, M., Key,

R. M., Kozyr, A., Lauvset, S. K., Lo Monaco, C., Mathis, J. T., Murata, A., Olsen, A., Perez, F. F., Sabine, C. L., Tanhua, T. and Wanninkhof, R.: The oceanic sink for anthropogenic CO_2 from 1994 to 2007, Science (80-.)., 363(6432), 1193–1199, doi:10.1126/science.aau5153, 2019.

Hansis, E., Davis, S. J. and Pongratz, J.: Relevance of methodological choices for accounting of land use change carbon fluxes, Global Biogeochem. Cycles, 29(8), 1230–1246, doi:10.1002/2014GB004997, 2015.

Harris, I., Jones, P. D., Osborn, T. J. and Lister, D. H.: Updated high-resolution grids of monthly climatic observations - the CRU TS3.10 Dataset, Int. J. Climatol., 34(3), 623–642, doi:10.1002/joc.3711, 2014.

Haverd, V., Smith, B., Nieradzik, L., Briggs, P. R., Woodgate, W., Trudinger, C. M., Canadell, J. G. and Cuntz, M.: A new version of the CABLE land surface model (Subversion revision r4601) incorporating land use and land cover change, woody vegetation demography, and a novel optimisation-based approach to plant coordination of photosynthesis, Geosci. Model Dev., 11(7), 2995–3026, doi:10.5194/gmd-11-2995-2018, 2018.

Hertwich, E. G. and Peters, G. P.: Carbon footprint of nations: a global, trade-linked analysis, Env. Sci Technol, 43(16), 6414–6420, doi:10.1021/es803496a, 2009.

Hooijer, A., Page, S., Canadell, J. G., Silvius, M., Kwadijk, J., Wosten, H. and Jauhiainen, J.: Current and future CO_2 emissions from drained peatlands in Southeast Asia, Biogeosciences, 7(5), 1505–1514, doi:10.5194/bg-7-1505-2010, 2010.

Houghton, R. A.: Revised estimates of the annual net flux of carbon to the atmosphere from changes in land use and land management 1850-2000, Tellus Ser. B-Chemical Phys. Meteorol., 55(2), 378–390, doi:DOI 10.1034/j.1600-0889.2003.01450.x, 2003.

Houghton, R. A. and Nassikas, A. A.: Global and regional fluxes of carbon from land use and land

cover change 1850-2015, Global Biogeochem. Cycles, 31(3), 456–472, doi:10.1002/2016gb005546, 2017.

Houghton, R. A., House, J. I., Pongratz, J., Van Der Werf, G. R., Defries, R. S., Hansen, M. C., Le Quéré, C. and Ramankutty, N.: Carbon emissions from land use and land-cover change, Biogeosciences, 9(12), 5125–5142, doi:10.5194/bg-9-5125-2012, 2012.

Houweling, S., Baker, D., Basu, S., Boesch, H., Butz, A., Chevallier, F., Deng, F., Dlugokencky, E. J., Feng, L., Ganshin, A., Hasekamp, O., Jones, D., Maksyutov, S., Marshall, J., Oda, T., O'Dell, C. W., Oshchepkov, S., Palmer, P. I., Peylin, P., Poussi, Z., Reum, F., Takagi, H., Yoshida, Y. and Zhuravlev, R.: An intercomparison of inverse models for estimating sources and sinks of CO_2 using GOSAT measurements, J. Geophys. Res., 120(10), 5253–5266, doi:10.1002/2014jd022962, 2015.

Hugelius, G., Bockheim, J. G., Camill, P., Elberling, B., Grosse, G., Harden, J. W., Johnson, K., Jorgenson, T., Koven, C. D., Kuhry, P., Michaelson, G., Mishra, U., Palmtag, J., Ping, C. L., O'Donnell, J., Schirrmeister, L., Schuur, E. A. G., Sheng, Y., Smith, L. C., Strauss, J. and Yu, Z.: A new data set for estimating organic carbon storage to 3m depth in soils of the northern circumpolar permafrost region, Earth Syst. Sci. Data, 5(2), 393–402, doi:10.5194/essd-5-393-2013, 2013.

Huntzinger, D. N., Michalak, A. M., Schwalm, C., Ciais, P., King, A. W., Fang, Y., Schaefer, K., Wei, Y., Cook, R. B., Fisher, J. B., Hayes, D., Huang, M., Ito, A., Jain, A. K., Lei, H., Lu, C., Maignan, F., Mao, J., Parazoo, N., Peng, S., Poulter, B., Ricciuto, D., Shi, X., Tian, H., Wang, W., Zeng, N. and Zhao, F.: Uncertainty in the response of terrestrial carbon sink to environmental drivers undermines carbon-climate feedback predictions, Sci. Rep., 7(1), 4765, doi:10.1038/s41598-017-03818-2, 2017.

Hurtt, G., Chini, L., Sahajpal, R., Frolking, S., Calvin, K., Fujimori, S., Klein Goldewijk, K.,

Hasegawa, T., Havlik, P. and Heinemann, A.: Harmonization of global land-use change and management for the period 850–2100, in preparation, Geosci. Model Dev., 2019.

Hurtt, G. C., Chini, L. P., Frolking, S., Betts, R. A., Feddema, J., Fischer, G., Fisk, J. P., Hibbard, K., Houghton, R. A., Janetos, A., Jones, C. D., Kindermann, G., Kinoshita, T., Goldewijk, K. K., Riahi, K., Shevliakova, E., Smith, S., Stehfest, E., Thomson, A., Thornton, P., van Vuuren, D. P. and Wang, Y. P.: Harmonization of land-use scenarios for the period 1500-2100: 600 years of global gridded annual land-use transitions, wood harvest, and resulting secondary lands, Clim. Change, 109(1–2), 117–161, doi:10.1007/s10584-011-0153-2, 2011.

IEA/OECD: International Energy Agency/Organisation for Economic Cooperation and Development: CO_2 emissions from fuel combustion, available at: https://webstore.iea.org/co2-emissions-from-fuel-combustion-2018-highlights, Paris., 2018.

IEA: World Energy Statistics (2018 Edition), available at: www.iea.org, 2018.

IMD: India Meteorological Department, Ministry of Earth Sciences (IMD): 2019 Southwest Monsoon Season Rainfall and IMD's Long Range Forecasts. Available at: http://www.imd.gov.in/pages/press_release.php. Last accessed 6 November 2019., 2019.

IMF: IMF: World Economic Outlook Update, July 2019: Still Sluggish Global Growth, available at: http://www.imf.org, last access: 16 October 2019., 2019a.

IMF: World Economic Outlook: Global Manufacturing Downturn, Rising Trade Barriers. International Monetary Fund. Available at: www.imf.org. Last accessed 30 October 2019., 2019b.

IPCC: 2006 IPCC Guidelines for National Greenhouse Gas Inventories, Prepared by the National Greenhouse Gas Inventories Programme, edited by S. Eggleston, L. Buendia, K. Miwa, T. Ngara, and K. Tanabe, Intergovernmental Panel on Climate Change, Institute for Global

Environmental Strategies, Japan., 2006.

Ito, A. and Inatomi, M.: Use of a process-based model for assessing the methane budgets of global terrestrial ecosystems and evaluation of uncertainty, Biogeosciences, 9(2), 759–773, doi:10.5194/bg-9-759-2012, 2012.

Jackson, R. B., Canadell, J. G., Le Quéré, C., Andrew, R. M., Korsbakken, J. I., Peters, G. P. and Nakicenovic, N.: Reaching peak emissions, Nat. Clim. Chang., 6(1), 7–10, doi:10.1038/nclimate2892, 2016.

Jackson, R. B., Le Quéré, C., Andrew, R. M., Canadell, J. G., Korsbakken, J. I., Liu, Z., Peters, G. P. and Zheng, B.: Global energy growth is outpacing decarbonization, Environ. Res. Lett., 13(12), 120401, doi:10.1088/1748-9326/aaf303, 2018.

Jacobson, A. R., Mikaloff Fletcher, S. E., Gruber, N., Sarmiento, J. L. and Gloor, M.: A joint atmosphere-ocean inversion for surface fluxes of carbon dioxide: 2. Regional results, Global Biogeochem. Cycles, 21(1), doi:10.1029/2006GB002703, 2007.

JODI: Joint Organisations Data Initiative, available at: https://www.jodidata.org, last access: 3 November 2019., 2019.

Joetzjer, E., Delire, C., Douville, H., Ciais, P., Decharme, B., Carrer, D., Verbeeck, H., De Weirdt, M. and Bonal, D.: Improving the ISBA$_{CC}$ land surface model simulation of water and carbon fluxes and stocks over the Amazon forest, Geosci. Model Dev., 8(6), 1709–1727, doi:10.5194/gmd-8-1709-2015, 2015.

Jones, M. W., Le Quéré, C., Andrew, R., Peters, G., Chevallier, F., Ciais, P., Janssens-Maenhout, G., van der Laan-Luijkx, I., Patra, P. Peters, W. and Rödenbeck, C.: Gridded fossil CO_2 emissions and related O_2 combustion consistent with national inventories 1959-2018, in preparation, 2019.

Joos, F. and Spahni, R.: Rates of change in natural and anthropogenic radiative forcing over the

past 20,000 years, Proc. Natl. Acad. Sci., doi:10.1073/pnas.0707386105, 2008.

Jung, M., Reichstein, M., Ciais, P., Seneviratne, S. I., Sheffield, J., Goulden, M. L., Bonan, G., Cescatti, A., Chen, J., de Jeu, R., Dolman, A. J., Eugster, W., Gerten, D., Gianelle, D., Gobron, N., Heinke, J., Kimball, J., Law, B. E., Montagnani, L., Mu, Q., Mueller, B., Oleson, K., Papale, D., Richardson, A. D., Roupsard, O., Running, S., Tomelleri, E., Viovy, N., Weber, U., Williams, C., Wood, E., Zaehle, S. and Zhang, K.: Recent decline in the global land evapotranspiration trend due to limited moisture supply, Nature, 467(7318), 951–954, doi:10.1038/nature09396, 2010.

Kato, E., Kinoshita, T., Ito, A., Kawamiya, M. and Yamagata, Y.: Evaluation of spatially explicit emission scenario of land-use change and biomass burning using a process-based biogeochemical model, J. Land Use Sci., 8(1), 104–122, doi:10.1080/1747423x.2011.628705, 2013.

Keeling, C. D., Bacastow, R. B., Bainbridge, A. E., Ekdahl, C. A., Guenther, P. R., Waterman, L. S. and Chin, J. F. S.: Atmospheric Carbon-Dioxide Variations at Mauna-Loa Observatory, Hawaii, Tellus, 28(6), 538–551, doi:10.1111/j.2153-3490.1976.tb00701.x, 1976.

Keeling, R. F. and Manning, A. C.: Studies of Recent Changes in Atmospheric O2 Content, in Treatise on Geochemistry, vol. 5, edited by H. D. Holland and K. K. Turekian, pp. 385–404, Elsevier, Oxford., 2014.

Khatiwala, S., Primeau, F. and Hall, T.: Reconstruction of the history of anthropogenic CO_2 concentrations in the ocean, Nature, 462(7271), 346-U110, doi:10.1038/nature08526, 2009.

Khatiwala, S., Tanhua, T., Fletcher, S. M., Gerber, M., Doney, S. C., Graven, H. D., Gruber, N., McKinley, G. A., Murata, A., Rios, A. F. and Sabine, C. L.: Global ocean storage of anthropogenic carbon, Biogeosciences, 10(4), 2169–2191, doi:10.5194/bg-10-2169-2013,

2013.

Kirschke, S., Bousquet, P., Ciais, P., Saunois, M., Canadell, J. G., Dlugokencky, E. J., Bergamaschi, P., Bergmann, D., Blake, D. R., Bruhwiler, L., Cameron-Smith, P., Castaldi, S., Chevallier, F., Feng, L., Fraser, A., Heimann, M., Hodson, E. L., Houweling, S., Josse, B., Fraser, P. J., Krummel, P. B., Lamarque, J. F., Langenfelds, R. L., Le Quéré, C., Naik, V., O'Doherty, S., Palmer, P. I., Pison, I., Plummer, D., Poulter, B., Prinn, R. G., Rigby, M., Ringeval, B., Santini, M., Schmidt, M., Shindell, D. T., Simpson, I. J., Spahni, R., Steele, L. P., Strode, S. A., Sudo, K., Szopa, S., van der Werf, G. R., Voulgarakis, A., van Weele, M., Weiss, R. F., Williams, J. E. and Zeng, G.: Three decades of global methane sources and sinks, Nat. Geosci., 6(10), 813–823, doi:10.1038/Ngeo1955, 2013.

Kobayashi, S., Ota, Y., Harada, Y., Ebita, A., Moriya, M., Onoda, H., Onogi, K., Kamahori, H., Kobayashi, C., Endo, H., Miyaoka, K. and Takahashi, K.: The JRA-55 Reanalysis: General Specifications and Basic Characteristics, J. Meteorol. Soc. Japan, 93(1), 5–48, doi:10.2151/jmsj.2015-001, 2015.

Korsbakken, J. I., Peters, G. P. and Andrew, R. M.: Uncertainties around reductions in China's coal use and CO 2 emissions, Nat. Clim. Chang., 6(7), 687–690, doi:10.1038/nclimate2963, 2016.

Krinner, G., Viovy, N., de Noblet-Ducoudré, N., Ogée, J., Polcher, J., Friedlingstein, P., Ciais, P., Sitch, S. and Prentice, I. C.: A dynamic global vegetation model for studies of the coupled atmosphere-biosphere system, Global Biogeochem. Cycles, 19(1), 1–33, doi:10.1029/2003GB002199, 2005.

Landschützer, P., Gruber, N., Bakker, D. C. E. and Schuster, U.: Recent variability of the global ocean carbon sink, Global Biogeochem. Cycles, 28(9), 927–949, doi:10.1002/2014GB004853, 2014.

Landschützer, P., Gruber, N., Haumann, F. A., Rödenbeck, C., Bakker, D. C. E., van Heuven, S., Hoppema, M., Metzl, N., Sweeney, C., Takahashi, T., Tilbrook, B. and Wanninkhof, R.: The reinvigoration of the Southern Ocean carbon sink, Science (80-.)., 349(6253), 1221–1224, doi:10.1126/science.aab2620, 2015.

Landschützer, P., Gruber, N. and Bakker, D. C. E.: Decadal variations and trends of the global ocean carbon sink, Global Biogeochem. Cycles, 30(10), 1396–1417, doi:10.1002/2015gb005359, 2016.

Landschützer, P., Gruber, N., Bakker, D. C. E., Stemmler, I. and Six, K. D.: Strengthening seasonal marine CO_2 variations due to increasing atmospheric CO_2, Nat. Clim. Chang., 8(2), 146–150, doi:10.1038/s41558-017-0057-x, 2018.

Lasslop, G., Reichstein, M., Papale, D., Richardson, A. D., Arneth, A., Barr, A., Stoy, P. and Wohlfahrt, G.: Separation of net ecosystem exchange into assimilation and respiration using a light response curve approach: critical issues and global evaluation, Glob. Chang. Biol., 16(1), 187–208, doi:10.1111/j.1365-2486.2009.02041.x, 2010.

Lawrence, D. M., Fisher, R. A., Koven, C. D., Oleson, K. W., Swenson, S. C., Bonan, G., Collier, N., Ghimire, B., Kampenhout, L., Kennedy, D., Kluzek, E., Lawrence, P. J., Li, F., Li, H., Lombardozzi, D., Riley, W. J., Sacks, W. J., Shi, M., Vertenstein, M., Wieder, W. R., Xu, C., Ali, A. A., Badger, A. M., Bisht, G., Broeke, M., Brunke, M. A., Burns, S. P., Buzan, J., Clark, M., Craig, A., Dahlin, K., Drewniak, B., Fisher, J. B., Flanner, M., Fox, A. M., Gentine, P., Hoffman, F., Keppel-Aleks, G., Knox, R., Kumar, S., Lenaerts, J., Leung, L. R., Lipscomb, W. H., Lu, Y., Pandey, A., Pelletier, J. D., Perket, J., Randerson, J. T., Ricciuto, D. M., Sanderson, B. M., Slater, A., Subin, Z. M., Tang, J., Thomas, R. Q., Val Martin, M. and Zeng, X.: The Community Land Model version 5: Description of new features, benchmarking, and impact of forcing uncertainty, J. Adv. Model. Earth Syst., 2018MS001583,

doi:10.1029/2018MS001583, 2019.

Le Quéré, C., Raupach, M. R., Canadell, J. G., Marland, G., Bopp, L., Ciais, P., Conway, T. J.,
Doney, S. C., Feely, R. A., Foster, P., Friedlingstein, P., Gurney, K., Houghton, R. A., House, J.
I., Huntingford, C., Levy, P. E., Lomas, M. R., Majkut, J., Metzl, N., Ometto, J. P., Peters, G.
P., Prentice, I. C., Randerson, J. T., Running, S. W., Sarmiento, J. L., Schuster, U., Sitch, S.,
Takahashi, T., Viovy, N., Van Der Werf, G. R. and Woodward, F. I.: Trends in the sources
and sinks of carbon dioxide, Nat. Geosci., 2(12), 831–836, doi:10.1038/ngeo689, 2009.

Le Quéré, C., Andres, R. J., Boden, T., Conway, T., Houghton, R. A., House, J. I., Marland, G.,
Peters, G. P., van der Werf, G. R., Ahlström, A., Andrew, R. M., Bopp, L., Canadell, J. G.,
Ciais, P., Doney, S. C., Enright, C., Friedlingstein, P., Huntingford, C., Jain, A. K., Jourdain, C.,
Kato, E., Keeling, R. F., Klein Goldewijk, K., Levis, S., Levy, P., Lomas, M., Poulter, B.,
Raupach, M. R., Schwinger, J., Sitch, S., Stocker, B. D., Viovy, N., Zaehle, S. and Zeng, N.:
The global carbon budget 1959–2011, Earth Syst. Sci. Data, 5(1), 165–185,
doi:10.5194/essd-5-165-2013, 2013.

Le Quéré, C., Peters, G. P., Andres, R. J., Andrew, R. M., Boden, T. a., Ciais, P., Friedlingstein, P.,
Houghton, R. a., Marland, G., Moriarty, R., Sitch, S., Tans, P., Arneth, A., Arvanitis, A.,
Bakker, D. C. E., Bopp, L., Canadell, J. G., Chini, L. P., Doney, S. C., Harper, A., Harris, I.,
House, J. I., Jain, a. K., Jones, S. D., Kato, E., Keeling, R. F., Klein Goldewijk, K., Körtzinger,
A., Koven, C., Lefèvre, N., Maignan, F., Omar, A., Ono, T., Park, G.-H., Pfeil, B., Poulter, B.,
Raupach, M. R., Regnier, P., Rödenbeck, C., Saito, S., Schwinger, J., Segschneider, J.,
Stocker, B. D., Takahashi, T., Tilbrook, B., van Heuven, S., Viovy, N., Wanninkhof, R.,
Wiltshire, A. and Zaehle, S.: Global carbon budget 2013, Earth Syst. Sci. Data, 6(1), 235–
263, doi:10.5194/essd-6-235-2014, 2014.

Le Quéré, C., Moriarty, R., Andrew, R. M., Peters, G. P., Ciais, P., Friedlingstein, P., Jones, S. D.,

Sitch, S., Tans, P., Arneth, A., Boden, T. A., Bopp, L., Bozec, Y., Canadell, J. G., Chini, L. P.,
Chevallier, F., Cosca, C. E., Harris, I., Hoppema, M., Houghton, R. A., House, J. I., Jain, A. K.,
Johannessen, T., Kato, E., Keeling, R. F., Kitidis, V., Klein Goldewijk, K., Koven, C., Landa, C.
S., Landschützer, P., Lenton, A., Lima, I. D., Marland, G., Mathis, J. T., Metzl, N., Nojiri, Y.,
Olsen, A., Ono, T., Peng, S., Peters, W., Pfeil, B., Poulter, B., Raupach, M. R., Regnier, P.,
Rödenbeck, C., Saito, S., Salisbury, J. E., Schuster, U., Schwinger, J., Séférian, R.,
Segschneider, J., Steinhoff, T., Stocker, B. D., Sutton, A. J., Takahashi, T., Tilbrook, B., van
der Werf, G. R., Viovy, N., Wang, Y.-P., Wanninkhof, R., Wiltshire, A. and Zeng, N.: Global
carbon budget 2014, Earth Syst. Sci. Data, 7(1), 47–85, doi:10.5194/essd-7-47-2015, 2015a.

Le Quéré, C., Moriarty, R., Andrew, R. M., Canadell, J. G., Sitch, S., Korsbakken, J. I.,
Friedlingstein, P., Peters, G. P., Andres, R. J., Boden, T. A., Houghton, R. A., House, J. I.,
Keeling, R. F., Tans, P., Arneth, A., Bakker, D. C. E., Barbero, L., Bopp, L., Chang, J.,
Chevallier, F., Chini, L. P., Ciais, P., Fader, M., Feely, R. A., Gkritzalis, T., Harris, I., Hauck, J.,
Ilyina, T., Jain, A. K., Kato, E., Kitidis, V., Klein Goldewijk, K., Koven, C., Landschützer, P.,
Lauvset, S. K., Lefèvre, N., Lenton, A., Lima, I. D., Metzl, N., Millero, F., Munro, D. R.,
Murata, A., S. Nabel, J. E. M., Nakaoka, S., Nojiri, Y., O'Brien, K., Olsen, A., Ono, T., Pérez, F.
F., Pfeil, B., Pierrot, D., Poulter, B., Rehder, G., Rödenbeck, C., Saito, S., Schuster, U.,
Schwinger, J., Séférian, R., Steinhoff, T., Stocker, B. D., Sutton, A. J., Takahashi, T., Tilbrook,
B., Van Der Laan-Luijkx, I. T., Van Der Werf, G. R., Van Heuven, S., Vandemark, D., Viovy,
N., Wiltshire, A., Zaehle, S. and Zeng, N.: Global Carbon Budget 2015, Earth Syst. Sci. Data,
doi:10.5194/essd-7-349-2015, 2015b.

Le Quéré, C., Andrew, R. M., Canadell, J. G., Sitch, S., Ivar Korsbakken, J., Peters, G. P., Manning,
A. C., Boden, T. A., Tans, P. P., Houghton, R. A., Keeling, R. F., Alin, S., Andrews, O. D.,
Anthoni, P., Barbero, L., Bopp, L., Chevallier, F., Chini, L. P., Ciais, P., Currie, K., Delire, C.,

Doney, S. C., Friedlingstein, P., Gkritzalis, T., Harris, I., Hauck, J., Haverd, V., Hoppema, M., Klein Goldewijk, K., Jain, A. K., Kato, E., Körtzinger, A., Landschützer, P., Lefèvre, N., Lenton, A., Lienert, S., Lombardozzi, D., Melton, J. R., Metzl, N., Millero, F., Monteiro, P. M. S., Munro, D. R., Nabel, J. E. M. S., Nakaoka, S. I., O'Brien, K., Olsen, A., Omar, A. M., Ono, T., Pierrot, D., Poulter, B., Rödenbeck, C., Salisbury, J., Schuster, U., Schwinger, J., Séférian, R., Skjelvan, I., Stocker, B. D., Sutton, A. J., Takahashi, T., Tian, H., Tilbrook, B., Van Der Laan-Luijkx, I. T., Van Der Werf, G. R., Viovy, N., Walker, A. P., Wiltshire, A. J. and Zaehle, S.: Global Carbon Budget 2016, Earth Syst. Sci. Data, doi:10.5194/essd-8-605-2016, 2016.

Le Quéré, C., Andrew, R. M., Friedlingstein, P., Sitch, S., Pongratz, J., Manning, A. C., Korsbakken, J. I., Peters, G. P., Canadell, J. G., Jackson, R. B., Boden, T. A., Tans, P. P., Andrews, O. D., Arora, V. K., Bakker, D. C. E., Barbero, L., Becker, M., Betts, R. A., Bopp, L., Chevallier, F., Chini, L. P., Ciais, P., Cosca, C. E., Cross, J., Currie, K., Gasser, T., Harris, I., Hauck, J., Haverd, V., Houghton, R. A., Hunt, C. W., Hurtt, G., Ilyina, T., Jain, A. K., Kato, E., Kautz, M., Keeling, R. F., Klein Goldewijk, K., Körtzinger, A., Landschützer, P., Lefèvre, N., Lenton, A., Lienert, S., Lima, I., Lombardozzi, D., Metzl, N., Millero, F., Monteiro, P. M. S., Munro, D. R., Nabel, J. E. M. S., Nakaoka, S., Nojiri, Y., Padin, X. A., Peregon, A., Pfeil, B., Pierrot, D., Poulter, B., Rehder, G., Reimer, J., Rödenbeck, C., Schwinger, J., Séférian, R., Skjelvan, I., Stocker, B. D., Tian, H., Tilbrook, B., Tubiello, F. N., van der Laan-Luijkx, I. T., van der Werf, G. R., van Heuven, S., Viovy, N., Vuichard, N., Walker, A. P., Watson, A. J., Wiltshire, A. J., Zaehle, S. and Zhu, D.: Global Carbon Budget 2017, Earth Syst. Sci. Data, 10(1), 405–448, doi:10.5194/essd-10-405-2018, 2018a.

Le Quéré, C., Andrew, R. M., Friedlingstein, P., Sitch, S., Hauck, J., Pongratz, J., Pickers, P. A., Korsbakken, J. I., Peters, G. P., Canadell, J. G., Arneth, A., Arora, V. K., Barbero, L., Bastos, A., Bopp, L., Chevallier, F., Chini, L. P., Ciais, P., Doney, S. C., Gkritzalis, T., Goll, D. S., Harris,

I., Haverd, V., Hoffman, F. M., Hoppema, M., Houghton, R. A., Hurtt, G., Ilyina, T., Jain, A. K., Johannessen, T., Jones, C. D., Kato, E., Keeling, R. F., Goldewijk, K. K., Landschützer, P., Lefèvre, N., Lienert, S., Liu, Z., Lombardozzi, D., Metzl, N., Munro, D. R., Nabel, J. E. M. S., Nakaoka, S., Neill, C., Olsen, A., Ono, T., Patra, P., Peregon, A., Peters, W., Peylin, P., Pfeil, B., Pierrot, D., Poulter, B., Rehder, G., Resplandy, L., Robertson, E., Rocher, M., Rödenbeck, C., Schuster, U., Schwinger, J., Séférian, R., Skjelvan, I., Steinhoff, T., Sutton, A., Tans, P. P., Tian, H., Tilbrook, B., Tubiello, F. N., van der Laan-Luijkx, I. T., van der Werf, G. R., Viovy, N., Walker, A. P., Wiltshire, A. J., Wright, R., Zaehle, S. and Zheng, B.: Global Carbon Budget 2018, Earth Syst. Sci. Data, 10(4), 2141–2194, doi:10.5194/essd-10-2141-2018, 2018b.

Le Quéré, C., Korsbakken, J. I., Wilson, C., Tosun, J., Andrew, R., Andres, R. J., Canadell, J. G., Jordan, A., Peters, G. P. and van Vuuren, D. P.: Drivers of declining CO_2 emissions in 18 developed economies, Nat. Clim. Chang., 9(3), 213–217, doi:10.1038/s41558-019-0419-7, 2019.

Lee, T. J. and Pielke, R. A.: Estimating the Soil Surface Specific Humidity, J. Appl. Meteorol., 31(5), 480–484, doi:10.1175/1520-0450(1992)031<0480:ETSSSH>2.0.CO;2, 1992.

Li, H. and Ilyina, T.: Current and Future Decadal Trends in the Oceanic Carbon Uptake Are Dominated by Internal Variability, Geophys. Res. Lett., 45(2), 916–925, doi:10.1002/2017gl075370, 2018.

Lienert, S. and Joos, F.: A Bayesian ensemble data assimilation to constrain model parameters and land-use carbon emissions, Biogeosciences, 15(9), 2909–2930, doi:10.5194/bg-15-2909-2018, 2018.

Liu, Z., Guan, D., Wei, W., Davis, S. J., Ciais, P., Bai, J., Peng, S., Zhang, Q., Hubacek, K., Marland, G., Andres, R. J., Crawford-Brown, D., Lin, J., Zhao, H., Hong, C., Boden, T. A., Feng, K., Peters, G. P., Xi, F., Liu, J., Li, Y., Zhao, Y., Zeng, N. and He, K.: Reduced carbon emission

estimates from fossil fuel combustion and cement production in China, Nature, doi:10.1038/nature14677, 2015.

Manning, A. C. and Keeling, R. F.: Global oceanic and land biotic carbon sinks from the scripps atmospheric oxygen flask sampling network, Tellus, Ser. B Chem. Phys. Meteorol., 58(2), 95–116, doi:10.1111/j.1600-0889.2006.00175.x, 2006.

Marland, G.: Uncertainties in Accounting for CO_2 From Fossil Fuels, J. Ind. Ecol., 12(2), 136–139, doi:10.1111/j.1530-9290.2008.00014.x, 2008.

Marland, G. and Rotty, R. M.: Carbon-Dioxide Emissions from Fossil-Fuels - a Procedure for Estimation and Results for 1950-1982, Tellus Ser. B-Chemical Phys. Meteorol., 36(4), 232–261, doi:DOI 10.1111/j.1600-0889.1984.tb00245.x, 1984.

Marland, G., Hamal, K. and Jonas, M.: How Uncertain Are Estimates of CO_2 Emissions?, J. Ind. Ecol., 13(1), 4–7, doi:10.1111/j.1530-9290.2009.00108.x, 2009.

Masarie, K. A. and Tans, P. P.: Extension and Integration of Atmospheric Carbon-Dioxide Data into a Globally Consistent Measurement Record, J. Geophys. Res., 100(D6), 11593–11610, doi:Doi 10.1029/95jd00859, 1995.

Mauritsen, T., Bader, J., Becker, T., Behrens, J., Bittner, M., Brokopf, R., Brovkin, V., Claussen, M., Crueger, T., Esch, M., Fast, I., Fiedler, S., Fläschner, D., Gayler, V., Giorgetta, M., Goll, D. S., Haak, H., Hagemann, S., Hedemann, C., Hohenegger, C., Ilyina, T., Jahns, T., Jimenéz-de-la-Cuesta, D., Jungclaus, J., Kleinen, T., Kloster, S., Kracher, D., Kinne, S., Kleberg, D., Lasslop, G., Kornblueh, L., Marotzke, J., Matei, D., Meraner, K., Mikolajewicz, U., Modali, K., Möbis, B., Müller, W. A., Nabel, J. E. M. S., Nam, C. C. W., Notz, D., Nyawira, S., Paulsen, H., Peters, K., Pincus, R., Pohlmann, H., Pongratz, J., Popp, M., Raddatz, T. J., Rast, S., Redler, R., Reick, C. H., Rohrschneider, T., Schemann, V., Schmidt, H., Schnur, R., Schulzweida, U., Six, K. D., Stein, L., Stemmler, I., Stevens, B., Storch, J., Tian, F., Voigt, A.,

Vrese, P., Wieners, K., Wilkenskjeld, S., Winkler, A. and Roeckner, E.: Developments in the MPI-M Earth System Model version 1.2 (MPI-ESM1.2) and Its Response to Increasing CO_2, J. Adv. Model. Earth Syst., 11(4), 998–1038, doi:10.1029/2018MS001400, 2019.

MCI: Ministry of Commerce and Industry: Foreign Trade Data Dissemination Portal, available at: http://14.98.253.4/, last access: 3 November 2019., 2019.

McKinley, G. A., Pilcher, D. J., Fay, A. R., Lindsay, K., Long, M. C. and Lovenduski, N. S.: Timescales for detection of trends in the ocean carbon sink, Nature, 530(7591), 469–472, doi:10.1038/nature16958, 2016.

McNeil, B. I., Matear, R. J., Key, R. M., Bullister, J. L. and Sarmiento, J. L.: Anthropogenic CO_2 uptake by the ocean based on the global chlorofluorocarbon data set, Science (80-.)., 299(5604), 235–239, doi:10.1126/science.1077429, 2003.

Meiyappan, P., Jain, A. K. and House, J. I.: Increased influence of nitrogen limitation on CO_2 emissions from future land use and land use change, Global Biogeochem. Cycles, 29(9), 1524–1548, doi:10.1002/2015gb005086, 2015.

Melton, J. R. and Arora, V. K.: Competition between plant functional types in the Canadian Terrestrial Ecosystem Model (CTEM) v. 2.0, Geosci. Model Dev., 9(1), 323–361, doi:10.5194/gmd-9-323-2016, 2016.

Mercado, L. M., Bellouin, N., Sitch, S., Boucher, O., Huntingford, C., Wild, M. and Cox, P. M.: Impact of changes in diffuse radiation on the global land carbon sink, Nature, 458(7241), 1014–1017, doi:10.1038/nature07949, 2009.

Merlin, O., Al Bitar, A., Rivalland, V., Béziat, P., Ceschia, E. and Dedieu, G.: An Analytical Model of Evaporation Efficiency for Unsaturated Soil Surfaces with an Arbitrary Thickness, J. Appl. Meteorol. Climatol., 50(2), 457–471, doi:10.1175/2010JAMC2418.1, 2011.

Mikaloff Fletcher, S. E., Gruber, N., Jacobson, A. R., Doney, S. C., Dutkiewicz, S., Gerber, M.,

Follows, M., Joos, F., Lindsay, K., Menemenlis, D., Mouchet, A., Müller, S. A. and
Sarmiento, J. L.: Inverse estimates of anthropogenic CO 2 uptake, transport, and storage by
the ocean, Global Biogeochem. Cycles, 20(2), GB2002, doi:10.1029/2005GB002530, 2006.

Millar, R. J., Fuglestvedt, J. S., Friedlingstein, P., Rogelj, J., Grubb, M. J., Matthews, H. D., Skeie,
R. B., Forster, P. M., Frame, D. J. and Allen, M. R.: Emission budgets and pathways
consistent with limiting warming to 1.5 °C, Nat. Geosci., 10(10), 741–747,
doi:10.1038/ngeo3031, 2017.

Ministry of Mines: Ministry of Mines: Mineral Production, available at:
http://ibm.nic.in/index.php?c=pages&m=index&id=497, last access: 18 September 2019.,
2019.

Myhre, G., Alterskjær, K. and Lowe, D.: A fast method for updating global fossil fuel carbon
dioxide emissions, Environ. Res. Lett., 4(3), 034012, doi:10.1088/1748-9326/4/3/034012,
2009.

Myneni, R. B., Ramakrishna, R., Nemani, R. and Running, S. W.: Estimation of global leaf area
index and absorbed par using radiative transfer models, IEEE Trans. Geosci. Remote Sens.,
35(6), 1380–1393, doi:10.1109/36.649788, 1997.

Narayanan, B., Aguiar, A. and McDougall, R.: Global Trade, Assistance, and Production: The
GTAP 9 Data Base, Cent. Glob. Trade Anal. Purdue Univ., 2015(September) [online]
Available from: https://www.gtap.agecon.purdue.edu/databases/v9/default.asp, 2015.

NBS: Energy supply growth is speeding up, and the share of clean energy is continuously
increasing. The department director interprets the half-yearly report.
http://www.stats.gov.cn/tjsj/sjjd/201907/t20190717_1676924.html. Last access 23
September 2019., National Bureau of Statistics., 2019a.

NBS: National Bureau of Statistics, 2019. Statistical Communiqué of the People's Republic of

China on the 2018 National Economic and Social Development, available at: http://www.stats.gov.cn/english/PressRelease/201902/t20190228_1651335.html. Last access: 23 S., 2019b.

NBS: National Bureau of Statistics (NBS): National Data (online database). http://data.stats.gov.cn/. Last access 1 November 2019., National Bureau of Statistics., 2019c.

NOAA/ESRL: NOAA Greenhouse Gas Marine Boundary Layer Reference, available at: https://www.esrl.noaa.gov/gmd/ccgg/mbl/mbl.html, last access: 27 September 2019., 2019.

OEA: Index of Eight Core Industries, available at: http://eaindustry.nic.in/home.asp, last access: 5 November 2019., 2019.

Paulsen, H., Ilyina, T., Six, K. D. and Stemmler, I.: Incorporating a prognostic representation of marine nitrogen fixers into the global ocean biogeochemical model HAMOCC, J. Adv. Model. Earth Syst., 9(1), 438–464, doi:10.1002/2016MS000737, 2017.

Peters, G. P., Andrew, R. and Lennox, J.: Constructing an environmentally-extended multi-regional input-output table using the GTAP database, Econ. Syst. Res., 23(2), 131–152, doi:10.1080/09535314.2011.563234, 2011a.

Peters, G. P., Minx, J. C., Weber, C. L. and Edenhofer, O.: Growth in emission transfers via international trade from 1990 to 2008, Proc. Natl. Acad. Sci., 108(21), 8903–8908, doi:10.1073/pnas.1006388108, 2011b.

Peters, G. P., Davis, S. J. and Andrew, R.: A synthesis of carbon in international trade, Biogeosciences, 9(8), 3247–3276, doi:10.5194/bg-9-3247-2012, 2012a.

Peters, G. P., Marland, G., Le Quéré, C., Boden, T., Canadell, J. G. and Raupach, M. R.: Rapid growth in CO_2 emissions after the 2008–2009 global financial crisis, Nat. Clim. Chang., 2(1),

2–4, doi:10.1038/nclimate1332, 2012b.

Peters, G. P., Andrew, R. M., Boden, T., Canadell, J. G., Ciais, P., Le Quéré, C., Marland, G., Raupach, M. R. and Wilson, C.: The challenge to keep global warming below 2 °C, Nat. Clim. Chang., 3(1), 4–6, doi:10.1038/nclimate1783, 2013.

Peters, G. P., Le Quéré, C., Andrew, R. M., Canadell, J. G., Friedlingstein, P., Ilyina, T., Jackson, R. B., Joos, F., Korsbakken, J. I., McKinley, G. A., Sitch, S. and Tans, P.: Towards real-time verification of CO_2 emissions, Nat. Clim. Chang., 7(12), 848–850, doi:10.1038/s41558-017-0013-9, 2017.

Peylin, P., Law, R. M., Gurney, K. R., Chevallier, F., Jacobson, A. R., Maki, T., Niwa, Y., Patra, P. K., Peters, W., Rayner, P. J., Rödenbeck, C., van der Laan-Luijkx, I. T. and Zhang, X.: Global atmospheric carbon budget: results from an ensemble of atmospheric CO_2 inversions, Biogeosciences, 10(10), 6699–6720, doi:10.5194/bg-10-6699-2013, 2013.

Peylin, P. et al.: The new ORCHIDEE land surface model version V2.0 as used for the CMIP6 climate simulation intercomparison exercice, in preparation, 2019.

Pfeil, B., Olsen, A., Bakker, D. C. E., Hankin, S., Koyuk, H., Kozyr, A., Malczyk, J., Manke, A., Metzl, N., Sabine, C. L., Akl, J., Alin, S. R., Bates, N., Bellerby, R. G. J., Borges, A., Boutin, J., Brown, P. J., Cai, W. J., Chavez, F. P., Chen, A., Cosca, C., Fassbender, A. J., Feely, R. A., Gonzalez-Davila, M., Goyet, C., Hales, B., Hardman-Mountford, N., Heinze, C., Hood, M., Hoppema, M., Hunt, C. W., Hydes, D., Ishii, M., Johannessen, T., Jones, S. D., Key, R. M., Kortzinger, A., Landschutzer, P., Lauvset, S. K., Lefevre, N., Lenton, A., Lourantou, A., Merlivat, L., Midorikawa, T., Mintrop, L., Miyazaki, C., Murata, A., Nakadate, A., Nakano, Y., Nakaoka, S., Nojiri, Y., Omar, A. M., Padin, X. A., Park, G. H., Paterson, K., Perez, F. F., Pierrot, D., Poisson, A., Rios, A. F., Santana-Casiano, J. M., Salisbury, J., Sarma, V. V. S. S., Schlitzer, R., Schneider, B., Schuster, U., Sieger, R., Skjelvan, I., Steinhoff, T., Suzuki, T., Takahashi, T.,

Tedesco, K., Telszewski, M., Thomas, H., Tilbrook, B., Tjiputra, J., Vandemark, D., Veness, T., Wanninkhof, R., Watson, A. J., Weiss, R., Wong, C. S. and Yoshikawa-Inoue, H.: A uniform, quality controlled Surface Ocean CO_2 Atlas (SOCAT), Earth Syst. Sci. Data, 5(1), 125–143, doi:10.5194/essd-5-125-2013, 2013.

Piao, S., Huang, M., Liu, Z., Wang, X. H., Ciais, P., Canadell, J. G., Wang, K., Bastos, A., Friedlingstein, P., Houghton, R. A., Le Quéré, C., Liu, Y. W., Myneni, R. B., Peng, S. S., Pongratz, J., Sitch, S., Yan, T., Wang, Y. L., Zhu, Z. C., Wu, D. H. and Wang, T.: Lower land-use emissions responsible for increased net land carbon sink during the slow warming period, Nat. Geosci., 11(10), 739-+, doi:10.1038/s41561-018-0204-7, 2018.

Pongratz, J., Reick, C. H., Raddatz, T. and Claussen, M.: Effects of anthropogenic land cover change on the carbon cycle of the last millennium, Global Biogeochem. Cycles, doi:10.1029/2009GB003488, 2009.

Pongratz, J., Reick, C. H., Houghton, R. A. and House, J. I.: Terminology as a key uncertainty in net land use and land cover change carbon flux estimates, Earth Syst. Dyn., 5(1), 177–195, doi:10.5194/esd-5-177-2014, 2014.

Poulter, B., Frank, D. C., Hodson, E. L. and Zimmermann, N. E.: Impacts of land cover and climate data selection on understanding terrestrial carbon dynamics and the CO_2 airborne fraction, Biogeosciences, 8(8), 2027–2036, doi:10.5194/bg-8-2027-2011, 2011.

PPAC: Natural Gas. Petroleum Planning and Analysis Cell, Ministry of Petroleum and Natural Gas, available at: http://eaindustry.nic.in/home.asp, last access: 5 November 2019., 2019a.

PPAC: Petroleum. Petroleum Planning and Analysis Cell, Ministry of Petroleum and Natural Gas, available at: http://eaindustry.nic.in/home.asp, last access: 17 October 2019., 2019b.

Prentice, I. C., Farquhar, G. D., Fasham, M. J. R., Goulden, M. L., Heimann, M., Jaramillo, V. J.,

Kheshgi, H. S., Le Quéré, C., Scholes, R. J., Wallace, D. W. R. and Press, C. U.: The Carbon Cycle and Atmospheric Carbon Dioxide, in Climate Change 2001: The Scientific Basis. Contribution of Working Group I to the Third Assessment Report of the Intergovernmental Panel on Climate Change, edited by J. T. Houghton, Y. Ding, D. J. Griggs, M. Noguer, P. J. van der Linden, X. Dai, K. Maskell, and C. A. Johnson, pp. 183–237, Cambridge University Press, Cambridge, United Kingdom and New York, NY, USA., 2001.

Price, J. T. and Warren, R.: Review of the Potential of "Blue Carbon" Activities to Reduce Emissions; available at http://avoid-net-uk.cc.ic.ac.uk/wp-content/uploads/delightful-downloads/2016/03/Literature-review-of-the-potential-of-blue-carbon-activities-to-reduce-emissions-AVOID2-W., 2016.

Raupach, M. R., Marland, G., Ciais, P., Le Quéré, C., Canadell, J. G., Klepper, G. and Field, C. B.: Global and regional drivers of accelerating CO_2 emissions, Proc Natl Acad Sci U S A, 104(24), 10288–10293, doi:10.1073/pnas.0700609104, 2007.

Regnier, P., Friedlingstein, P., Ciais, P., Mackenzie, F. T., Gruber, N., Janssens, I. A., Laruelle, G. G., Lauerwald, R., Luyssaert, S., Andersson, A. J., Arndt, S., Arnosti, C., Borges, A. V., Dale, A. W., Gallego-Sala, A., Goddéris, Y., Goossens, N., Hartmann, J., Heinze, C., Ilyina, T., Joos, F., LaRowe, D. E., Leifeld, J., Meysman, F. J. R., Munhoven, G., Raymond, P. A., Spahni, R., Suntharalingam, P. and Thullner, M.: Anthropogenic perturbation of the carbon fluxes from land to ocean, Nat. Geosci., 6(8), 597–607, doi:10.1038/ngeo1830, 2013.

Remaud, M., Chevallier, F., Cozic, A., Lin, X. and Bousquet, P.: On the impact of recent developments of the LMDz atmospheric general circulation model on the simulation of CO_2 transport, Geosci. Model Dev., 11(11), 4489–4513, doi:10.5194/gmd-11-4489-2018, 2018.

Resplandy, L., Keeling, R. F., Rödenbeck, C., Stephens, B. B., Khatiwala, S., Rodgers, K. B., Long,

M. C., Bopp, L. and Tans, P. P.: Revision of global carbon fluxes based on a reassessment of oceanic and riverine carbon transport, Nat. Geosci., 11(7), 504-+, doi:10.1038/s41561-018-0151-3, 2018.

Rhein, M., Rintoul, S. R., Aoki, S., Campos, E., Chambers, D., Feely, R. A., Gulev, S., Johnson, G. C., Josey, S. A., Kostianoy, A., Mauritzen, C., Roemmich, D., Talley, L. D., Wang, F., Stocker, T., Qin, D. and Platner, G.-K.: Chapter 3: Observations: Ocean, in Climate Change 2013 The Physical Science Basis, Cambridge University Press., 2013.

Rödenbeck, C.: Estimating CO_2 sources and sinks from atmospheric mixing ratio measurements using a global inversion of atmospheric transport, Technical Report 6, available at: http://www.bgc-jena.mpg.de/CarboScope/s/tech_report6.pdf, Max Planck Institute for Biogeochemistry, Jena., 2005.

Rödenbeck, C., Houweling, S., Gloor, M. and Heimann, M.: CO_2 flux history 1982–2001 inferred from atmospheric data using a global inversion of atmospheric transport, Atmos. Chem. Phys. Discuss., 3(3), 2575–2659, doi:10.5194/acpd-3-2575-2003, 2003.

Rödenbeck, C., Keeling, R. F., Bakker, D. C. E., Metzl, N., Olsen, A., Sabine, C. and Heimann, M.: Global surface-ocean <i>p</i>^{CO₂} and sea–air CO₂ flux variability from an observation-driven ocean mixed-layer scheme, Ocean Sci., 9(2), 193–216, doi:10.5194/os-9-193-2013, 2013.

Rödenbeck, C., Bakker, D. C. E., Metzl, N., Olsen, A., Sabine, C., Cassar, N., Reum, F., Keeling, R. F. and Heimann, M.: Interannual sea–air CO₂ flux variability from an observation-driven ocean mixed-layer scheme, Biogeosciences, 11(17), 4599–4613, doi:10.5194/bg-11-4599-2014, 2014.

Rödenbeck, C., Bakker, D. C. E., Gruber, N., Iida, Y., Jacobson, A. R., Jones, S., Landschützer, P.,

Metzl, N., Nakaoka, S., Olsen, A., Park, G.-H., Peylin, P., Rodgers, K. B., Sasse, T. P., Schuster, U., Shutler, J. D., Valsala, V., Wanninkhof, R. and Zeng, J.: Data-based estimates of the ocean carbon sink variability – first results of the Surface Ocean pCO2 Mapping intercomparison (SOCOM), Biogeosciences, 12(23), 7251–7278, doi:10.5194/bg-12-7251-2015, 2015.

Rödenbeck, C., Zaehle, S., Keeling, R. and Heimann, M.: How does the terrestrial carbon exchange respond to inter-annual climatic variations? A quantification based on atmospheric CO_2 data, Biogeosciences, 15(8), 2481–2498, doi:10.5194/bg-15-2481-2018, 2018.

Rogelj, J., Schaeffer, M., Friedlingstein, P., Gillett, N. P., van Vuuren, D. P., Riahi, K., Allen, M. and Knutti, R.: Differences between carbon budget estimates unravelled, Nat. Clim. Chang., 6(3), 245–252, doi:10.1038/Nclimate2868, 2016.

Rogelj, J., Forster, P. M., Kriegler, E., Smith, C. J. and Séférian, R.: Estimating and tracking the remaining carbon budget for stringent climate targets, Nature, 571(7765), 335–342, doi:10.1038/s41586-019-1368-z, 2019.

Rypdal, K., Paciomik, N., Eggleston, S., Goodwin, J., Irving, W., Penman, J. and Woodfield, M.: Chapter 1 Introduction to the 2006 Guidelines, in 2006 IPCC Guidelines for National Greenhouse Gas Inventories, edited by S. Eggleston, L. Buendia, K. Miwa, T. Ngara, and K. Tanabe, Institute for Global Environmental Strategies (IGES), Hayama, Kanagawa, Japan., 2006.

Saatchi, S. S., Harris, N. L., Brown, S., Lefsky, M., Mitchard, E. T. A., Salas, W., Zutta, B. R., Buermann, W., Lewis, S. L., Hagen, S., Petrova, S., White, L., Silman, M. and Morel, A.: Benchmark map of forest carbon stocks in tropical regions across three continents, Proc. Natl. Acad. Sci., 108(24), 9899–9904, doi:10.1073/pnas.1019576108, 2011.

Saunois, M., Bousquet, P., Poulter, B., Peregon, A., Ciais, P., Canadell, J. G., Dlugokencky, E. J.,

    Etiope, G., Bastviken, D., Houweling, S., Janssens-Maenhout, G., Tubiello, F. N., Castaldi, S.,

    Jackson, R. B., Alexe, M., Arora, V. K., Beerling, D. J., Bergamaschi, P., Blake, D. R.,

    Brailsford, G., Brovkin, V., Bruhwiler, L., Crevoisier, C., Crill, P., Covey, K., Curry, C.,

    Frankenberg, C., Gedney, N., Höglund-Isaksson, L., Ishizawa, M., Ito, A., Joos, F., Kim, H. S.,

    Kleinen, T., Krummel, P., Lamarque, J. F., Langenfelds, R., Locatelli, R., Machida, T.,

    Maksyutov, S., McDonald, K. C., Marshall, J., Melton, J. R., Morino, I., Naik, V., O'Doherty,

    S., Parmentier, F. J. W., Patra, P. K., Peng, C., Peng, S., Peters, G. P., Pison, I., Prigent, C.,

    Prinn, R., Ramonet, M., Riley, W. J., Saito, M., Santini, M., Schroeder, R., Simpson, I. J.,

    Spahni, R., Steele, P., Takizawa, A., Thornton, B. F., Tian, H., Tohjima, Y., Viovy, N.,

    Voulgarakis, A., Van Weele, M., Van Der Werf, G. R., Weiss, R., Wiedinmyer, C., Wilton, D.

    J., Wiltshire, A., Worthy, D., Wunch, D., Xu, X., Yoshida, Y., Zhang, B., Zhang, Z. and Zhu, Q.:

    The global methane budget 2000-2012, Earth Syst. Sci. Data, 8(2), 697–751,

    doi:10.5194/essd-8-697-2016, 2016.

SCCL: Singareni Collieries Company Limited (SCCL): Provisional Production and Dispatches

    Performance. Singareni Collieries Company Limited, available at:

    https://scclmines.com/scclnew/performance_production.asp, last access: 3 September

    2019., 2019.

Schimel, D., Alves, D., Enting, I., Heimann, M., Joos, F., Raynaud, D., Wigley, T., Prater, M.,

    Derwent, R., Ehhalt, D., Fraser, P., Sanhueza, E., Zhou, X., Jonas, P., Charlson, R., Rodhe, H.,

    Sadasivan, S., Shine, K. P., Fouquart, Y., Ramaswamy, V., Solomon, S., Srinivasan, J.,

    Albritton, D., Derwent, R., Isaksen, I., Lal, M., Wuebbles, D. and Press, C. U.: Radiative

    Forcing of Climate Change, in Climate Change 1995 The Science of Climate Change.

    Contribution of Working Group I to the Second Assessment Report of the

Intergovernmental Panel on Climate Change, edited by J. T. Houghton, L. G. Meira Rilho, B. A. Callander, N. Harris, A. Kattenberg, and K. Maskell, Cambridge University Press, Cambridge, United Kingdom and New York, NY, USA., 1995.

Schimel, D., Stephens, B. B. and Fisher, J. B.: Effect of increasing CO_2 on the terrestrial carbon cycle, Proc Natl Acad Sci U S A, 112(2), 436–441, doi:10.1073/pnas.1407302112, 2015.

Schwietzke, S., Sherwood, O. A., Bruhwiler, L. M., Miller, J. B., Etiope, G., Dlugokencky, E. J., Michel, S. E., Arling, V. A., Vaughn, B. H., White, J. W. and Tans, P. P.: Upward revision of global fossil fuel methane emissions based on isotope database, Nature, 538(7623), 88–91, doi:10.1038/nature19797, 2016.

Schwinger, J., Goris, N., Tjiputra, J. F., Kriest, I., Bentsen, M., Bethke, I., Ilicak, M., Assmann, K. M. and Heinze, C.: Evaluation of NorESM-OC (versions 1 and 1.2), the ocean carbon-cycle stand-alone configuration of the Norwegian Earth System Model (NorESM1), Geosci. Model Dev., 9(8), 2589–2622, doi:10.5194/gmd-9-2589-2016, 2016.

Séférian, R., Delire, C., Decharme, B., Voldoire, A., Salas y Melia, D., Chevallier, M., Saint-Martin, D., Aumont, O., Calvet, J.-C., Carrer, D., Douville, H., Franchistéguy, L., Joetzjer, E. and Sénési, S.: Development and evaluation of CNRM Earth system model – CNRM-ESM1, Geosci. Model Dev., 9(4), 1423–1453, doi:10.5194/gmd-9-1423-2016, 2016.

Sellar, A. A., Jones, C. G., Mulcahy, J., Tang, Y., Yool, A., Wiltshire, A., O'Connor, F. M., Stringer, M., Hill, R., Palmieri, J., Woodward, S., Mora, L., Kuhlbrodt, T., Rumbold, S., Kelley, D. I., Ellis, R., Johnson, C. E., Walton, J., Abraham, N. L., Andrews, M. B., Andrews, T., Archibald, A. T., Berthou, S., Burke, E., Blockley, E., Carslaw, K., Dalvi, M., Edwards, J., Folberth, G. A., Gedney, N., Griffiths, P. T., Harper, A. B., Hendry, M. A., Hewitt, A. J., Johnson, B., Jones, A., Jones, C. D., Keeble, J., Liddicoat, S., Morgenstern, O., Parker, R. J., Predoi, V., Robertson, E., Siahaan, A., Smith, R. S., Swaminathan, R., Woodhouse, M. T., Zeng, G. and Zerroukat,

M.: UKESM1: Description and evaluation of the UK Earth System Model, J. Adv. Model. Earth Syst., 2019MS001739, doi:10.1029/2019MS001739, 2019.

Shangguan, W., Hengl, T., Mendes de Jesus, J., Yuan, H. and Dai, Y.: Mapping the global depth to bedrock for land surface modeling, J. Adv. Model. Earth Syst., 9(1), 65–88, doi:10.1002/2016MS000686, 2017.

Shevliakova, E., Pacala, S. W., Malyshev, S., Hurtt, G. C., Milly, P. C. D., Caspersen, J. P., Sentman, L. T., Fisk, J. P., Wirth, C. and Crevoisier, C.: Carbon cycling under 300 years of land use change: Importance of the secondary vegetation sink, Global Biogeochem. Cycles, 23(2), doi:10.1029/2007GB003176, 2009.

Sitch, S., Huntingford, C., Gedney, N., Levy, P. E., Lomas, M., Piao, S. L., Betts, R., Ciais, P., Cox, P., Friedlingstein, P., Jones, C. D., Prentice, I. C. and Woodward, F. I.: Evaluation of the terrestrial carbon cycle, future plant geography and climate-carbon cycle feedbacks using five Dynamic Global Vegetation Models (DGVMs), Glob. Chang. Biol., 14(9), 2015–2039, doi:10.1111/j.1365-2486.2008.01626.x, 2008.

Smith, B., Warlind, D., Arneth, A., Hickler, T., Leadley, P., Siltberg, J. and Zaehle, S.: Implications of incorporating N cycling and N limitations on primary production in an individual-based dynamic vegetation model, Biogeosciences, 11(7), 2027–2054, doi:10.5194/bg-11-2027-2014, 2014.

Stephens, B. B., Gurney, K. R., Tans, P. P., Sweeney, C., Peters, W., Bruhwiler, L., Ciais, P., Ramonet, M., Bousquet, P., Nakazawa, T., Aoki, S., Machida, T., Inoue, G., Vinnichenko, N., Lloyd, J., Jordan, A., Heimann, M., Shibistova, O., Langenfelds, R. L., Steele, L. P., Francey, R. J. and Denning, A. S.: Weak northern and strong tropical land carbon uptake from vertical profiles of atmospheric CO_2, Science (80-.)., 316(5832), 1732–1735, doi:10.1126/science.1137004, 2007.

Stocker, T., Qin, D. and Platner, G.-K.: Climate Change 2013 The Physical Science Basis, Cambridge University Press., 2013.

Swart, N. C., Fyfe, J. C., Saenko, O. A. and Eby, M.: Wind-driven changes in the ocean carbon sink, Biogeosciences, 11(21), 6107–6117, doi:10.5194/bg-11-6107-2014, 2014.

Tian, H., Xu, X., Lu, C., Liu, M., Ren, W., Chen, G., Melillo, J. and Liu, J.: Net exchanges of CO_2, CH4, and N2O between China's terrestrial ecosystems and the atmosphere and their contributions to global climate warming, J. Geophys. Res., 116(G2), doi:10.1029/2010jg001393, 2011.

Tian, H., Chen, G., Lu, C., Xu, X., Hayes, D. J., Ren, W., Pan, S., Huntzinger, D. N. and Wofsy, S. C.: North American terrestrial CO_2uptake largely offset by CH_4 and N_2O emissions: toward a full accounting of the greenhouse gas budget, Clim Chang., 129(3–4), 413–426, doi:10.1007/s10584-014-1072-9, 2015.

Todd-Brown, K. E. O., Randerson, J. T., Post, W. M., Hoffman, F. M., Tarnocai, C., Schuur, E. A. G. and Allison, S. D.: Causes of variation in soil carbon simulations from CMIP5 Earth system models and comparison with observations, Biogeosciences, 10(3), 1717–1736, doi:10.5194/bg-10-1717-2013, 2013.

UN: United Nations Statistics Division: National Accounts Main Aggregates Database, available at: http://unstats.un.org/unsd/snaama/Introduction.asp, last access: 2 January 2018., 2017.

UN: United Nations Statistics Division: Energy Statistics, available at: http://unstats.un.org/unsd/energy/, last access: 27 September 2019., 2018.

UNFCCC: National Inventory Submissions, available at: https://unfccc.int/process-and-meetings/transparency-and-reporting/reporting-and-review-under-the-convention/greenhouse-gas-inventories-annex-i-parties/national-inventory-submissions-

2019, last access: June 20., 2019.

Varadhan, S.: Coal India expects to resume a third of output at flooded Dipka mine within 10 days. Reuters. Available at: https://www.reuters.com/article/coal-india-mine-floods/refile-update-1-coal-india-expects-to-resume-a-third-of-output-at-flooded-dipka-mine-within-., 2019.

Van Der Laan-Luijkx, I. T., Van Der Velde, I. R., Van Der Veen, E., Tsuruta, A., Stanislawska, K., Babenhauserheide, A., Fang Zhang, H., Liu, Y., He, W., Chen, H., Masarie, K. A., Krol, M. C. and Peters, W.: The CarbonTracker Data Assimilation Shell (CTDAS) v1.0: Implementation and global carbon balance 2001-2015, Geosci. Model Dev., 10(7), 2785–2800, doi:10.5194/gmd-10-2785-2017, 2017.

van der Velde, I. R., Miller, J. B., Schaefer, K., van der Werf, G. R., Krol, M. C. and Peters, W.: Terrestrial cycling of CO_2; by photosynthesis, respiration, and biomass burning in SiBCASA, Biogeosciences, 11(23), 6553–6571, doi:10.5194/bg-11-6553-2014, 2014.

van der Werf, G. R., Randerson, J. T., Giglio, L., Collatz, G. J., Mu, M., Kasibhatla, P. S., Morton, D. C., DeFries, R. S., Jin, Y. and van Leeuwen, T. T.: Global fire emissions and the contribution of deforestation, savanna, forest, agricultural, and peat fires (1997–2009), Atmos. Chem. Phys., 10(23), 11707–11735, doi:10.5194/acp-10-11707-2010, 2010.

van der Werf, G. R., Randerson, J. T., Giglio, L., van Leeuwen, T. T., Chen, Y., Rogers, B. M., Mu, M., van Marle, M. J. E., Morton, D. C., Collatz, G. J., Yokelson, R. J. and Kasibhatla, P. S.: Global fire emissions estimates during 1997–2016, Earth Syst. Sci. Data, 9(2), 697–720, doi:10.5194/essd-9-697-2017, 2017.

Van Minnen, J. G., Klein Goldewijk, K., Stehfest, E., Eickhout, B., van Drecht, G. and Leemans, R.: The importance of three centuries of land-use change for the global and regional terrestrial carbon cycle, Clim. Change, 97(1–2), 123–144, doi:10.1007/s10584-009-9596-0,

2009.

Viovy, N.: CRUNCEP data set, available at:

ftp://nacp.ornl.gov/synthesis/2009/frescati/temp/land_use_change/original/readme.htm, last access: June 2016., 2016.

Walker, A. P., Quaife, T., van Bodegom, P. M., De Kauwe, M. G., Keenan, T. F., Joiner, J., Lomas, M. R., MacBean, N., Xu, C. G., Yang, X. J. and Woodward, F. I.: The impact of alternative trait-scaling hypotheses for the maximum photosynthetic carboxylation rate (V-cmax) on global gross primary production, New Phytol., 215(4), 1370–1386, doi:10.1111/nph.14623, 2017.

Wanninkhof, R., Park, G. H., Takahashi, T., Sweeney, C., Feely, R., Nojiri, Y., Gruber, N., Doney, S. C., McKinley, G. A., Lenton, A., Le Quéré, C., Heinze, C., Schwinger, J., Graven, H. and Khatiwala, S.: Global ocean carbon uptake: magnitude, variability and trends, Biogeosciences, 10(3), 1983–2000, doi:10.5194/bg-10-1983-2013, 2013.

Watson, R. T., Rodhe, H., Oeschger, H., Siegenthaler, U. and Press, C. U.: Greenhouse Gases and Aerosols, in Climate Change: The IPCC Scientific Assessment. Intergovernmental Panel on Climate Change (IPCC), edited by J. T. Houghton, G. J. Jenkins, and J. J. Ephraums, pp. 1–40, Cambridge University Press, Cambridge., 1990.

Wenzel, S., Cox, P. M., Eyring, V. and Friedlingstein, P.: Projected land photosynthesis constrained by changes in the seasonal cycle of atmospheric CO_2, Nature, 538(7626), 499–501, doi:10.1038/nature19772, 2016.

Wilkenskjeld, S., Kloster, S., Pongratz, J., Raddatz, T. and Reick, C. H.: Comparing the influence of net and gross anthropogenic land-use and land-cover changes on the carbon cycle in the MPI-ESM, Biogeosciences, 11(17), 4817–4828, doi:10.5194/bg-11-4817-2014, 2014.

Woodward, F. I. and Lomas, M. R.: Vegetation dynamics – simulating responses to climatic

change, Biol. Rev., 79(3), 643–670, doi:10.1017/S1464793103006419, 2004.

Xi, F., Davis, S. J., Ciais, P., Crawford-Brown, D., Guan, D., Pade, C., Shi, T., Syddall, M., Lv, J., Ji, L., Bing, L., Wang, J., Wei, W., Yang, K.-H., Lagerblad, B., Galan, I., Andrade, C., Zhang, Y. and Liu, Z.: Substantial global carbon uptake by cement carbonation, Nat. Geosci., 9(12), 880–883, doi:10.1038/ngeo2840, 2016.

Yin, X. W.: Responses of leaf nitrogen concentration and specific leaf area to atmospheric CO_2 enrichment: a retrospective synthesis across 62 species, Glob. Chang. Biol., 8(7), 631–642, doi:DOI 10.1046/j.1365-2486.2002.00497.x, 2002.

Zaehle, S. and Friend, A. D.: Carbon and nitrogen cycle dynamics in the O-CN land surface model: 1. Model description, site-scale evaluation, and sensitivity to parameter estimates, Global Biogeochem. Cycles, 24(1), n/a-n/a, doi:10.1029/2009GB003521, 2010.

Zaehle, S., Ciais, P., Friend, A. D. and Prieur, V.: Carbon benefits of anthropogenic reactive nitrogen offset by nitrous oxide emissions, Nat. Geosci., 4(9), 601–605, doi:10.1038/ngeo1207, 2011.

Zheng, B., Chevallier, F., Yin, Y., Ciais, P., Fortems-Cheiney, A., Deeter, M. N., Parker, R. J., Wang, Y., Worden, H. M. and Zhao, Y.: Global atmospheric carbon monoxide budget 2000–2017 inferred from multi-species atmospheric inversions, Earth Syst. Sci. Data, 11(3), 1411–1436, doi:10.5194/essd-11-1411-2019, 2019.

Zscheischler, J., Mahecha, M. D., Avitabile, V., Calle, L., Carvalhais, N., Ciais, P., Gans, F., Gruber, N., Hartmann, J., Herold, M., Ichii, K., Jung, M., Landschutzer, P., Laruelle, G. G., Lauerwald, R., Papale, D., Peylin, P., Poulter, B., Ray, D., Regnier, P., Rödenbeck, C., Roman-Cuesta, R. M., Schwalm, C., Tramontana, G., Tyukavina, A., Valentini, R., van der Werf, G., West, T. O., Wolf, J. E. and Reichstein, M.: Reviews and syntheses: An empirical spatiotemporal description of the global surface-atmosphere carbon fluxes: opportunities and data

limitations, Biogeosciences, 14(15), 3685–3703, doi:10.5194/bg-14-3685-2017, 2017.

Formatted: Font: (Default) Calibri

Tables

Table 1. Factors used to convert carbon in various units (by convention, Unit 1 = Unit 2 × conversion).

Unit 1	Unit 2	Conversion	Source
GtC (gigatonnes of carbon)	ppm (parts per million)[a]	2.124[b]	Ballantyne et al. (2012)
GtC (gigatonnes of carbon)	PgC (petagrams of carbon)	1	SI unit conversion
GtCO$_2$ (gigatonnes of carbon dioxide)	GtC (gigatonnes of carbon)	3.664	44.01/12.011 in mass equivalent
GtC (gigatonnes of carbon)	MtC (megatonnes of carbon)	1000	SI unit conversion

[a] Measurements of atmospheric CO_2 concentration have units of dry-air mole fraction. 'ppm' is an abbreviation for micromole/mol, dry air.

[b] The use of a factor of 2.124 assumes that all the atmosphere is well mixed within one year. In reality, only the troposphere is well mixed and the growth rate of CO_2 concentration in the less well-mixed stratosphere is not measured by sites from the NOAA network. Using a factor of 2.124 makes the approximation that the growth rate of CO_2 concentration in the stratosphere equals that of the troposphere on a yearly basis.

Table 2. How to cite the individual components of the global carbon budget presented here.

Component	Primary reference
Global fossil CO_2 emissions (E_{FF}), total and by fuel type	Gilfillan et al. (2019)
National territorial fossil CO_2 emissions (E_{FF})	CDIAC source: Gilfillan et al. (2019)
	UNFCCC (2019)
National consumption-based fossil CO_2 emissions (E_{FF}) by country (consumption)	Peters et al. (2011b) updated as described in this paper
Land-use change emissions (E_{LUC})	Average from Houghton and Nassikas (2017) and Hansis et al., (2015), both updated as described in this paper
Growth rate in atmospheric CO_2 concentration (G_{ATM})	Dlugokencky and Tans (2019)
Ocean and land CO_2 sinks (S_{OCEAN} and S_{LAND})	This paper for S_{OCEAN} and S_{LAND} and references in Table 4 for individual models.

Table 3. Main methodological changes in the global carbon budget since 2015. Methodological changes introduced in one year are kept for the following years unless noted. Empty cells mean there were no methodological changes introduced that year. Table A7 lists methodological changes from the first global carbon budget publication up to 2014.

Publication year	Fossil fuel emissions			LUC emissions	Reservoirs			Uncertainty & other changes
	Global	Country (territorial)	Country (consumption)		Atmosphere	Ocean	Land	
2015 Le Quéré et al. (2015a) Jackson et al. (2016)	Projection for current year based Jan-Aug data	National emissions from UNFCCC extended to 2014 also provided	Detailed estimates introduced for 2011 based on GTAP9			Based on eight models	Based on ten models with assessment of minimum realism	The decadal uncertainty for the DGVM ensemble mean now uses ±1σ of the decadal spread across models
2016 Le Quéré et al. (2016)	Two years of BP data	Added three small countries; China's (RMA) emissions from 1990 from BP data (this release only)		Preliminary E$_{LUC}$ using FRA-2015 shown for comparison; use of five DGVMs		Based on seven models	Based on fourteen models	Discussion of projection for full budget for current year
2017 Le Quéré et al. (2018a) GCB2017	Projection includes India-specific data			Average of two bookkeeping models; use of twelve DGVMs	Based on eight models that match the observed sink for the 1990s; no longer normalised		Based on fifteen models that meet observation-based criteria (see Sect. 2.5)	Land multi-model average now used in main carbon budget, with the carbon imbalance presented separately; new table of key uncertainties

2018 Le Quéré et al. (2018b) GCB2018	Revision in cement emissions; Projection includes EU-specific data	Aggregation of overseas territories into governing nations for total of 213 countries a	Use of sixteen DGVMs	Use of four atmospheric inversions	Based on seven models	Based on sixteen models; revised atmospheric forcing from CRUNCEP to CRU-JRA-55	Introduction of metrics for evaluation of individual models using observations
2019 (this study)	Global emissions calculated as sum of all countries plus bunkers, rather than taken directly from CDIAC.		Use of fifteen DGVMs (a)	Use of three atmospheric inversions	Based on nine models	Based on sixteen models	

(a) E_{LUC} is still estimated based on bookkeeping models, as in 2018 (Le Quéré et al., 2018b), but the number of DGVMs used to characterise the uncertainty has changed.

Table 4. References for the process models, pCO$_2$-based ocean flux products, and atmospheric inversions included in Figs. 6-8. All models and products are updated with new data to end of year 2018, and the atmospheric forcing for the DGVMs has been updated as described in Section 2.2.2.

Model/data name	Reference	Change from Global Carbon Budget 2018 (Le Quéré et al., 2018b)
Bookkeeping models for land-use change emissions		
BLUE	Hansis et al. (2015)	No change.
H&N2017	Houghton and Nassikas (2017)	No change.
Dynamic global vegetation models		
CABLE-POP	Haverd et al. (2018)	Thermal acclimation of photosynthesis; Residual stomatal conductance (g0) now non-zero; stomatal conductance set to maximum of g0 and vapour-pressure-deficit-dependent term
CLASS-CTEM	Melton and Arora (2016)	20 soil layers used. Soil depth is prescribed following Shangguan et al. (2017). - The bare soil evaporation efficiency was previously that of Lee and Pielke (1992). This has been replaced by that of Merlin et al. (2011). - Plant roots can no longer grow into soil layers that are perennially frozen (permafrost). - The Vcmax value of C3 grass changes from 75 umol CO$_2$/m2/s to 55 umol CO$_2$/m2/s which is more in line with observations (Alton 2017) - Land use change product pools are now tracked separately (rather than thrown into litter and soil C pools). They behave the same as previously but now it is easier to distinguish the C in those pools from other soil/litter C.
CLM5.0	Lawrence et al. (2019)	Added representation of shifting cultivation, fixed a bug in the fire model, used updated & higher resolution lightening strike dataset
DLEM	Tian et al. (2015) (a)	No Change.
ISAM	Meiyappan et al. (2015)	No Change.
ISBA-CTRIP	Decharme et al. (2019) (b)	Updated spinup protocol + model name updated (SURFEXv8 in GCB2017)
JSBACH	Mauritsen et al. (2019)	No Change.
JULES-ES	Sellar et al., (2019) (c)	Major update. Model configuration is now JULES-ES v1.0, the land surface and vegetation component of the UK Earth System Model (UKESM1). Includes interactive Nitrogen scheme, extended number of plant functional types represented, trait based physiology and crop harvest.
LPJ-GUESS	Smith et al. (2014) (d)	Using daily climate forcing instead of monthly forcing. Using nitrogen inputs from NMIP. Adjustment in the spinup procedure. Growth suppression mortality parameter of PFT IBS changed to 0.12.
LPJ	Poulter et al. (2011) (e)	No Change.
LPX-Bern	Lienert and Joos (2018)	Using Nitrogen input from NMIP.

OCN	Zaehle and Friend (2010) (f)	No change (uses r294).
ORCHIDEE-CNP	Goll et al. (2017) (g)	Refinement of parameterization (r6176); change in N forcing (different N deposition, no (N &P) manure)
ORCHIDEE-Trunk	Krinner et al. (2005), Peylin et al. (in prep) (h)	No major changes, except some small bug corrections linked to the implementation of land cover changes
SDGVM	Walker et al. (2017) (i)	1) Changed the multiplicative scale parameters of these diagnostic output variables from: evapotranspft, evapo, transpft 2.257e6->2.257e6/(30*24*3600) swepft NA->0.001 2) The autotrophic respiration diagnostic output variable is now properly initialized to zero for bare ground. 3) A very minor change that prevents the soil water limitation scalar (often called beta) being applied to g0 in the stomatal conductance (gs) equation. Previously it was applied to both g0 and g1 in the gs equation. Now beta is applied only to g1 in the gs equation. 4) The climate driving data and land cover data are in 0.5degree resolution.
VISIT	Kato et al. (2013) (j)	No change.
Global ocean biogeochemistry models		
NEMO-PlankTOM5	Buitenhuis et al. (2013)	No change
MICOM-HAMOCC (NorESM-OC)	Schwinger et al. (2016)	Flux calculation improved to take into account correct land-sea mask after interpolation
MPIOM-HAMOCC6	Paulsen et al. (2017)	No change
NEMO3.6-PISCESv2-gas (CNRM)	Berthet et al. (2019)	No change
CSIRO	Law et al (2017)	No change
MITgcm-REcoM2	Hauck et al. (2018)	No change
MOM6-COBALT (Princeton)	Adcroft et al. (2019)	New this year
CESM-ETHZ	Doney et al. (2009)	New this year
NEMO-PISCES (IPSL)	Aumont et al. (2015)	updated spin-up procedure
pCO2-based flux ocean products		
Landschützer (MPI-SOMFFN)	Landschützer et al. (2016)	update to SOCATv2019 measurements
Rödenbeck (Jena-MLS)	Rödenbeck et al. (2014)	update to SOCATv2019 measurements. Interannual NEE variability estimated through a regression to air temperature anomalies. Using 89 atmospheric stations. Fossil fuel emissions taken from Jones et al (in prep) consistent with country totals of this study.

CMEMS	Denvil-Sommer et al. (2019)	New this year

Atmospheric inversions

CAMS	Chevallier et al. (2005) (k)	Updated version of atmospheric transport model LMDz
CarbonTracker Europe (CTE)	van der Laan-Luijkx et al. (2017)	No change.
Jena CarboScope	Rödenbeck et al. (2003, 2018)	Temperature-NEE relations additionally estimated

a See also Tian et al. (2011)

b See also Joetzjer et al., (2015), Séférian et al. (2016) and Delire et al. (in review)

c JULES-ES is the Earth System configuration of the Joint UK Land Environment Simulator. See also Best et al. (2011) and Clarke et al. (2011).

d To account for the differences between the derivation of shortwave radiation from CRU cloudiness and DSWRF from CRUJRA, the photosynthesis scaling parameter αa was modified (-15%) to yield similar results.

e Compared to published version, decreased LPJ wood harvest efficiency so that 50 % of biomass was removed off-site compared to 85 % used in the 2012 budget. Residue management of managed grasslands increased so that 100 % of harvested grass enters the litter pool.

f See also Zaehle et al. (2011).

g see also Goll et al (2018).

h Compared to published version: revised parameters values for photosynthetic capacity for boreal forests (following assimilation of FLUXNET data), updated parameter values for stem allocation, maintenance respiration and biomass export for tropical forests (based on literature), and CO_2 down-regulation process added to photosynthesis. Hydrology model updated to a multi-layer scheme (11 layers). See also Peylin et al. (in prep)

i See also Woodward and Lomas (2004)

j See also Ito and Inatomi (2012).

k see also Remaud et al. (2018)

Table 5. Comparison of results from the bookkeeping method and budget residuals with results from the DGVMs and inverse estimates for different periods, the last decade, and the last year available. All values are in GtCyr^{-1}. The DGVM uncertainties represent ±1σ of the decadal or annual (for 2018 only) estimates from the individual DGVMs: for the inverse models the range of available results is given. All values are rounded to the nearest 0.1 GtC and therefore columns do not necessarily add to zero.

	Mean (GtC yr^{-1})						
	1960-1969	1970-1979	1980-1989	1990-1999	2000-2009	2009-2018	2018
Land-use change emissions (E_{LUC})							
Bookkeeping methods (1a)	1.4 ± 0.7	1.2 ± 0.7	1.2 ± 0.7	1.3 ± 0.7	1.4 ± 0.7	1.5 ± 0.7	1.5 ± 0.7
DGVMs (1b)	1.3 ± 0.5	1.3 ± 0.5	1.4 ± 0.5	1.2 ± 0.4	1.5 ± 0.4	2.0 ± 0.5	2.3 ± 0.6
Terrestrial sink (S_{LAND})							
Residual sink from global budget ($E_{FF}+E_{LUC}-G_{ATM}-S_{OCEAN}$) (2a)	1.7 ± 0.9	1.8 ± 0.9	1.6 ± 0.9	2.6 ± 0.9	3.0 ± 0.9	3.6 ± 1.0	3.7 ± 1.0
DGVMs (2b)	1.3 ± 0.4	2.0 ± 0.3	1.8 ± 0.5	2.4 ± 0.4	2.7 ± 0.6	3.2 ± 0.6	3.5 ± 0.7
Total land fluxes ($S_{LAND} - E_{LUC}$)							
GCB2019 Budget (2b - 1a)	-0.2 ± 0.8	0.9 ± 0.8	0.6 ± 0.9	1.0 ± 0.8	1.3 ± 0.9	1.7 ± 0.9	2.0 ± 1.0
Budget constraint (2a - 1a)	0.3 ± 0.5	0.6 ± 0.5	0.4 ± 0.6	1.3 ± 0.6	1.6 ± 0.6	2.1 ± 0.7	2.2 ± 0.7
DGVMs (2b - 1b)	-0.1 ± 0.5	0.7 ± 0.6	0.4 ± 0.6	1.2 ± 0.6	1.1 ± 0.6	1.0 ± 0.8	1.0 ± 0.8
Inversions*	—	—	-0.1–0.1	0.5–1.1	0.7–1.5	1.1–2.2	0.9–2.7

*Estimates are adjusted for the pre-industrial influence of river fluxes and adjusted to common E_{FF} (Sect. 2.7.2). The ranges given include 2 inversions from 1980-1999 and 3 inversions from 2001 onwards (Table A3).

Table 6. Decadal mean in the five components of the anthropogenic CO_2 budget for different periods, and last year available. All values are in GtC yr^{-1}, and uncertainties are reported as ±1σ. The table also shows the budget imbalance (B_{IM}), which provides a measure of the discrepancies among the nearly independent estimates and has an uncertainty exceeding ± 1 GtC yr^{-1}. A positive imbalance means the emissions are overestimated and/or the sinks are too small. All values are rounded to the nearest 0.1 GtC and therefore columns do not necessarily add to zero.

	Mean (GtC yr^{-1})						
	1960-1969	1970-1979	1980-1989	1990-1999	2000-2009	2009-2018	2018
Total emissions ($E_{FF}+E_{LUC}$)							
Fossil CO_2 emissions (E_{FF})	3.0 ± 0.2	4.7 ± 0.2	5.5 ± 0.3	6.4 ± 0.3	7.8 ± 0.4	9.5 ± 0.5	10.0 ± 0.5
Land-use change emissions (E_{LUC})	1.4 ± 0.7	1.2 ± 0.7	1.2 ± 0.7	1.3 ± 0.7	1.4 ± 0.7	1.5 ± 0.7	1.5 ± 0.7
Total emissions	4.5 ± 0.7	5.8 ± 0.7	6.7 ± 0.8	7.7 ± 0.8	9.2 ± 0.8	11.0 ± 0.8	11.5 ± 0.9
Partitioning							
Growth rate in atmospheric CO_2 concentration (G_{ATM})	1.8 ± 0.07	2.8 ± 0.07	3.4 ± 0.02	3.1 ± 0.02	4.0 ± 0.02	4.9 ± 0.02	5.1 ± 0.2
Ocean sink (S_{OCEAN})	1.0 ± 0.6	1.3 ± 0.6	1.7 ± 0.6	2.0 ± 0.6	2.2 ± 0.6	2.5 ± 0.6	2.6 ± 0.6
Terrestrial sink (S_{LAND})	1.3 ± 0.4	2.0 ± 0.3	1.8 ± 0.5	2.4 ± 0.4	2.7 ± 0.6	3.2 ± 0.6	3.5 ± 0.7
Budget imbalance							
$B_{IM} = E_{FF}+E_{LUC} - (G_{ATM}+S_{OCEAN}+S_{LAND})$	0.5	−0.2	−0.2	0.3	0.3	0.4	0.3

Formatted: Font color: Auto
Formatted: Font color: Auto
Formatted: Font color: Auto
Formatted: Font color: Auto
Formatted: Font color: Auto
Formatted: Font color: Auto
Formatted: Font color: Auto
Formatted: Font color: Auto
Formatted: Font color: Auto
Formatted: Font color: Auto
Formatted: Font color: Auto
Deleted: 2
Formatted: Font color: Auto
Formatted: Font color: Auto
Deleted: 7
Formatted: Font color: Auto
Formatted: Font color: Auto
Deleted: 7
Formatted: Font color: Auto
Formatted: Font color: Auto
Formatted: Font color: Auto
Deleted: 3
Formatted: Font color: Auto
Deleted: 1
Formatted: Font color: Auto
Formatted: Font color: Auto

Table 7. Comparison of the projection with realised fossil CO_2 emissions (E_{FF}). The 'Actual' values are first estimate available using actual data, and the 'Projected' values refers to estimate made before the end of the year for each publication. Projections based on a different method from that described here during 2008-2014 are available in Le Quéré et al., (2016). All values are adjusted for leap years.

	World Projected	World Actual	China Projected	China Actual	USA Projected	USA Actual	EU28 Projected	EU28 Actual	India Projected	India Actual	Rest of World Projected	Rest of World Actual
2015 (a)	−0.6% (−1.6 to 0.5)	0.06%	−3.9% (−4.6 to −1.1)	−0.7%	−1.5% (−5.5 to 0.3)	−2.5%	−	−	−	−	1.2% (−0.2 to 2.6)	1.20%
2016 (b)	−0.2% (−1.0 to +1.8)	0.20%	−0.5% (−3.8 to +1.3)	−0.3%	−1.7% (−4.0 to +0.6)	−2.1%	−	−	−	−	1.0% (−0.4 to +2.5)	1.30%
2017 (c)	2.0% (+0.8 to +3.0)	1.60%	3.5% (+0.7 to +5.4)	1.50%	−0.4% (−2.7 to +1.0)	−0.5%	−	−	2.00% (+0.2 to +3.8)	3.90%	1.6% (0.0 to +3.2)	1.90%
2018 (d)	2.7% (+1.8 to +3.7)	2.13%	4.7% (+2.0 to +7.4)	2.30%	2.5% (+0.5 to +4.5)	2.76%	-0.7% (-2.6 to +1.3)	-2.08%	6.3% (+4.3 to +8.3)	8.02%	1.8% (+0.5 to +3.0)	1.69%
2019 (e)	0.5% (-0.3 to +1.4)	−	2.6% (+0.7 to +4.4)	−	-2.4% (-4.7 to -0.1)	−	-1.7% (-5.1% to +1.8%)	−	1.8% (-0.7 to +3.7)	−	0.5% (-0.8 to +1.8)	−

(a) Jackson et al. (2016) and Le Quéré et al. (2015a). (b) Le Quéré et al. (2016). (c) Le Quéré et al. (2018a). (d) Le Quéré et al. (2018b). (e) This study.

Table 8. Cumulative CO_2 for different time periods in gigatonnes of carbon (GtC). All uncertainties are reported as ±1σ. The budget imbalance provides a measure of the discrepancies among the nearly independent estimates. Its uncertainty exceeds ±60 GtC. The method used here does not capture the loss of additional sink capacity from reduced forest cover, which is about 20 GtC for the years 1850-2018 and would exacerbate the budget imbalance (see Sect. 2.8.4). All values are rounded to the nearest 5 GtC and therefore columns do not necessarily add to zero.

Units of GtC	1750-2018	1850-2014	1959-2018	1850-2018	1850-2019 (a)
Emissions					
Fossil CO_2 emissions (E_{FF})	440 ± 20	400 ± 20	365 ± 20	440 ± 20	450 ± 20
Land-use change CO_2 emissions (E_{LUC})	235 ± 75 (b)	195 ± 60 (c)	80 ± 40 (d)	205 ± 60 (c)	205 ± 60
Total emissions	675 ± 80	600 ± 65	445 ± 30	645 ± 65	655 ± 65
Partitioning					
Growth rate in atmospheric CO_2 concentration (G_{ATM})	275 ± 5	235 ± 5	200 ± 5	255 ± 5	260 ± 5
Ocean sink (S_{OCEAN}) (e)	170 ± 20	150 ± 20	105 ± 20	160 ± 20	160 ± 20
Terrestrial sink (S_{LAND})	220 ± 50	185 ± 40	130 ± 25	195 ± 40	200 ± 40
Budget imbalance					
$B_{IM} = E_{FF}+E_{LUC} - (G_{ATM}+S_{OCEAN}+S_{LAND})$	10	30	10	30	30

(a) Using projections for year 2019 (Sect. 3.4). Uncertainties are the same as 1850-2018 period
(b) Cumulative E_{LUC} 1750-1849 of 30 GtC based on multi-model mean of Pongratz et al. (2009), Shevliakova et al. (2009), Zaehle et al. (2011), Van Minnen et al. (2009). 1850-2018 from mean of H&N (Houghton and Nassikas, 2017) and BLUE (Hansis et al., 2015). 1750-2018 uncertainty is estimated from standard deviation of DGVMs over 1850-2018 scaled by 1750-2018 emissions.
(c) Cumulative E_{LUC} based on H&N and BLUE. Uncertainty is estimated from the standard deviation of DGVM estimates
(d) Cumulative E_{LUC} based on H&N and BLUE. Uncertainty is formed from the uncertainty in annual E_{LUC} over 1959-2018, which is 0.7 GtC/yr multiplied by length of the time series
e Ocean sink uncertainty from IPCC (Denman et al., 2007)

Table 9. Major known sources of uncertainties in each component of the Global Carbon Budget, defined as input data or processes that have a demonstrated effect of at least ±0.3 GtC yr^{-1}.

Source of uncertainty	Time scale (years)	Location	Status	Evidence
Fossil CO$_2$ emissions (E$_{FF}$; Section 2.1)				
energy statistics	annual to decadal	Global, but mainly China & major developing countries	see Sect. 2.1	(Korsbakken et al., 2016)
carbon content of coal	annual to decadal	Global, but mainly China & major developing countries	see Sect. 2.1	(Liu et al., 2015)
System boundary	annual to decadal	All countries	see Sect. 2.1	
Emissions from land-use change (E$_{LUC}$; section 2.2)				
land-cover and land-use change statistics	continuous	global; in particular tropics	see Sect. 2.2	(Houghton et al., 2012)
sub-grid-scale transitions	annual to decadal	global	see Table A1	(Wilkenskjeld et al., 2014)
vegetation biomass	annual to decadal	global; in particular tropics	see Table A1	(Houghton et al., 2012)
wood and crop harvest	annual to decadal	global; SE Asia	see Table A1	(Arneth et al., 2017)
peat burning (a)	multi-decadal trend	global	see Table A1	(van der Werf et al., 2010)
loss of additional sink capacity	multi-decadal trend	global	not included; Section 2.7.4	(Gitz and Ciais, 2003)
Atmospheric growth rate (G$_{ATM}$) no demonstrated uncertainties larger than ±0.3 GtC yr^{-1} (b)				
Ocean sink (S$_{OCEAN}$)				
variability in oceanic circulation (c)	semi-decadal to decadal	global	see Sect. 2.4	(DeVries et al., 2017, 2019)
Internal variability	annual to decadal	high latitudes; Equatorial Pacific	no ensembles/ coarse resolution	(McKinley et al., 2016)
anthropogenic changes in nutrient supply	multi-decadal trend	global	not included	(Duce et al., 2008)
Land sink (S$_{LAND}$)				
strength of CO$_2$ fertilisation	multi-decadal trend	global	see Sect. 2.5	(Wenzel et al., 2016)

response to variability in temperature and rainfall	annual to decadal	global; in particular tropics	see Sect. 2.5	(Cox et al., 2013)
nutrient limitation and supply	multi-decadal trend	global	see Sect. 2.5	(Zaehle et al., 2011)
response to diffuse radiation	annual	global	see Sect. 2.5	(Mercado et al., 2009)

a As result of interactions between land-use and climate

b The uncertainties in G_{ATM} have been estimated as ±0.2 GtC yr^{-1}, although the conversion of the growth rate into a global annual flux assuming instantaneous mixing throughout the atmosphere introduces additional errors that have not yet been quantified.

c Could in part be due to uncertainties in atmospheric forcing (Swart et al., 2014)

Appendix A. Supplementary tables.

Table A1. Comparison of the processes included in the bookkeeping method and DGVMs in their estimates of E_{LUC} and S_{LAND}. See Table 4 for model references. All models include deforestation and forest regrowth after abandonment of agriculture (or from afforestation activities on agricultural land). Processes relevant for E_{LUC} are only described for the DGVMs used with land-cover change in this study (Fig. 6 top panel).

| | Bookkeeping Models | | DGVMs | | | | | | | | | | | | | | |
	H&N	BLUE	CABLE-POP	CLASS-CTEM	CLM5.0	DLEM	ISAM	ISBA-CTRIP (h)	JSBACH	JULES-ES	LPJ-GUESS	LPJ	LPX-Bern	OCN	ORCHIDEE-CNP	ORCHIDEE-Trunk	SDGVM
Processes relevant for E_{LUC}																	
Wood harvest and forest degradation (a)	yes	yes	yes	no	yes	yes	yes	no	yes	no	yes	yes	no (d)	yes	no	yes	no
Shifting cultivation / Subgrid scale transitions	no (b)	yes	yes	no	yes	no	no	no	yes	no	yes	yes	no (d)	no	no	no	no
Cropland harvest (removed, r, or added to litter, l)	yes (r)(l)	yes (r)(l)	yes (r)	yes (added to litter)	yes (r)	yes	yes	no	yes (r+l)	no	yes (r)	yes (l)	yes (r)	yes (r+l)	yes (r)	yes	yes (r)
Peat fires	yes	yes	no	no	yes	no	no	no	no	no	no	no	no	no	no	no	no
fire as a management tool	yes (i)	yes (i)	no	no	no	no	no	no	no	no	no	no	no	no	no	no	no
N fertilization	yes (i)	yes (i)	no	no	yes	yes	yes	no	no	no	yes	no	yes	yes	yes	no	no
tillage	yes (i)	yes (i)	yes	yes (g)	no	no	no	no	no	no	yes	no	no	no	no	yes	no
irrigation	yes (i)	yes (i)	no	no	yes	yes	yes	no	no	no	yes	no	yes	yes	no	no	no
wetland drainage	yes (i)	yes (i)	no	no	no	no	no	no	no	no	no	no	no	no	no	no	no
erosion	yes (i)	yes (i)	no	no	no	no	no	no	no	no	no	no	no	no	no	no	no
South East Asia peat drainage	yes	yes	no	no	no	no	no	no	no	no	no	no	no	no	no	no	no
Grazing and mowing Harvest (removed, r, or added to litter, l)	yes (r)(l)	yes (r)(l)	yes (r)	no	no	no	yes (l)	no	yes (l)	no	yes (r)	yes (l)	no	yes (r+l)	no	no	no

Formatted … [71]
Formatted … [72]
Formatted Table … [73]
Formatted Table … [74]
Deleted: z
Deleted: z
Deleted: no
Deleted: z
Deleted: z
Deleted: z
Deleted: z
Deleted: no
Deleted: yes
Deleted: no
Deleted: yes
Deleted: no
Deleted: z
Deleted: z
Deleted: yes
Deleted: no
Deleted: yes
Deleted: no
Deleted: z
Deleted: z
Deleted: no
Deleted: yes
Deleted: no
Deleted: yes
Deleted: no
Deleted: z
Deleted: z
Deleted: z
Deleted: z
Deleted: z
Deleted: z
Deleted: z

Processes also relevant for S_{LAND}

Fire simulation and/or suppression	for US only	no	no	yes	yes	yes	no	yes	yes	no	yes	yes	yes	no	no	no	yes
Climate and variability	no	no	yes	yes	yes	yes	yes	yes	yes	yes	yes	yes	yes	yes	yes	yes	yes
CO_2 fertilisation	no (i)	no (i)	yes	yes	yes	yes	yes	yes	yes	yes	yes	yes	yes	yes	yes		yes
Carbon-nitrogen interactions, including N deposition	no (j)	no (j)	yes	no (f)	yes	yes	yes	no (e)	yes	no	yes	no	yes	yes	yes	no	yes (c)

(a) Refers to the routine harvest of established managed forests rather than pools of harvested products.

(b) No back- and forth-transitions between vegetation types at the country-level, but if forest loss based on FRA exceeded agricultural expansion based on FAO, then this amount of area was cleared for cropland and the same amount of area of old croplands abandoned.

(c) Limited. Nitrogen uptake is simulated as a function of soil C, and Vcmax is an empirical function of canopy N. Does not consider N deposition.

(d) Available but not active.

(e) Simple parameterization of nitrogen limitation based on Yin (2002; assessed on FACE experiments)

(f) Although C-N cycle interactions are not represented, the model includes a parameterization of down-regulation of photosynthesis as CO_2 increases to emulate nutrient constraints (Arora et al., 2009)

(g) Tillage is represented over croplands by increased soil carbon decomposition rate and reduced humification of litter to soil carbon.

(h) ISBA-CTRIP corresponds to SURFEXv8 in GCB2018

(i) Bookkeeping models include effect of CO_2-fertilization as captured by observed carbon densities, but not as an effect transient in time.

(j) Process captured implicitly by use of observed carbon densities.

Formatted Table

s

Formatted Table

Formatted: Font: (Default) Times New Roman, 12 pt

Formatted Table

Formatted: French

Deleted: preivous

Table A2. Comparison of the processes and model set up for the Global Ocean Biogeochemistry Models for their estimates of S_{OCEAN}. See Table 4 for model references.

	NEMO-PlankTOM5	MICOM-HAMOCC (NorESM-OC)	MPIOM-HAMOCC6	NEMO3.6-PISCESv2-gas (CNRM)	CSIRO	MITgcm-REcoM2	MOM6-COBALT (Princeton)	CESM-ETHZ	NEMO-PISCES (IPSL)
Atmospheric forcing for simulation A	NCEP	CORE-I (spin-up) / NCEP-R1 with CORE-II corrections	NCEP / NCEP+ERA-20C (spin-up)	NCEP with CORE-II corrections	JRA55	JRA-55, https://doi.org/10.5065/D6HH6H41	JRA-55 version 1.4	JRA-55 version 1.3	JRA-55
Atmospheric forcing for simulation B (constant climate and CO_2)	NCEP 1980	CORE-I	spin-up initial restart file (278) with cyclic 1957 NCEP; run 1957-2017 with 278	NCEP with CORE-II corrections cycling over 1948-1957	JRA55 1958	JRA climatology	JRA-55 version 1.4 year 1959	normal year forcing created from JRA-55 version 1.3, NYF = climatology with anomalies from the year 2001	interannual forcing JRA-55
Initialisation of carbon chemistry	GLODAPv1 corrected for anthropogenic carbon from Sabine et al (2004) to 1920	GLODAP v1 preindustrial + spin-up 1000 years	initialization from previous model simulations	GLODAPv2	GLODAPv1 preindustrial	GLODAPv1 preindustrial	GLODAPv2, DIC is corrected to 1959 level for the historical simulation and to pre-industrial level for the control simulation using Khatiwala et al 2009, 2013.	GLODAPv2 preindustrial	GLODAPv2 preindu...
Spin-up procedure	Spin-up 39 years: 28 years (1920-1947) NCEP1980, followed by interannual forcing (in simulations A and D) from 1948	Initialisation from WOA/GLODAPv1 and 1000 years spin-up simulation using CORE-I (normal-year) forcing	spin-up with ERA20C	300 years online cycling over 1948-1957	Spin-up 300+ years BGC and 800 years for physics, historical carbon 1850-1957 (constant climate)	Spin-up 116 years (2 cycles JRA55), either with constant (278 ppm, RunB) or increasing (RunA) atm CO_2	Spin-up 81 years using JRA-55 year 1959	Spin-up from initial conditions for 180 years, using CORE forcing and preindustrial atm. CO_2 and N cycle, switch to JRA forcing, additional 14 years spin-up with JRA forcing. Production run: starting from preindustrial spin-up, 3x cycling through JRA with historical forcing (simulation A) including time-varying N inputs, or normal year forcing, constant atm. CO_2 (simulation B).	Spin-up starting in 1836 with 3 loops of JRA forcing.
Physical ocean model	NEMOv2.3-ORCA2	MICOM (NorESM-OCv1.2)	MPIOM	NEMOv3.6-GELATOv6-eORCA1L75	MOM5	MITgcm (checkpoint 66k)	MOM6-SIS2	CESMv1.4 (ocean model based on POP2)	NEMO-v3.6
Biogeochemistry model	PlankTOM5.3	HAMOCC (NorESM-OCv1.2)	HAMOCC6	PISCESv2-gas	WOMBAT	REcoM-2	COBALTv2	BEC (modified & extended)	PISCESv2
Horizontal resolution	2o lon, 0.3 to 1.5o lat	1° lon, 0.17 to 0.25 lat	1.5°	1° lon, 0.3 to 1° lat	1° x1° with enhanced	2° lon, 0.38-2° lat,	0.5° lon, 0.25 to 0.5° lat	Lon: 1.125°, Lat varying from 0.53° in the	2° long, 0.3 to 1.5° lat

					resolution at the tropics and in the high lat Southern Ocean			extratropics to 0.27° near the equator	
Vertical resolution	31 levels	51 isopycnic layers + 2 layers representing a bulk mixed layer	40 levels, layer thickness increase with depth	75 levels, 1m at surface	50 levels, 20 in the upper 200m	30 levels (9 in the upper 200 m)	75 levels hybrid coordinates, 2 m at surface	60 levels (z-coordinates)	31 levels
Total ocean area on native grid (km2)	357200000	360060000	365980000	362700000	357640000	352050000	362000000	359260000	362700

Formatted: Left

Table A3. Comparison of the inversion set up and input fields for the atmospheric inversions. Atmospheric inversions see the full CO_2 fluxes, including the anthropogenic and pre-industrial fluxes. Hence they need to be adjusted for the pre-industrial flux of CO_2 from the land to the ocean that is part of the natural carbon cycle before they can be compared with S_{OCEAN} and S_{LAND} from process models. See Table 4 for references.

	CarbonTracker Europe (CTE)	Jena CarboScope	CAMS
Version number	CTE2019-FT	sEXTocNEET_v4.3	v18r2
Observations			
Atmospheric observations	Hourly resolution (well-mixed conditions) obspack GLOBALVIEWplus v4.2 and NRT_v4.4 (a)	Flasks and hourly (outliers removed by 2-sigma criterion)	Daily averages of well-mixed conditions - OBSPACK GLOBALVIEWplus v4.2a& NRT v4.4, WDCGG, RAMCES and ICOS ATC
Prior fluxes			
Biosphere and fires	SiBCASA-GFED4s (b)	No prior	ORCHIDEE (climatological), GFEDv4.1 & GFAS
Ocean	Ocean inversion by Jacobson et al. (2007)	oc_v1.7 updates: from 1993, interannual variability from PlankTOM5 (Buitenhuis et al) GOBM; before 1985, linear transition over the years in between (update of Rödenbeck et al., 2014)	Landschützer et al. (2018)
Fossil fuels	EDGAR+IER, scaled to GCP2018 and GCP2019	Jones et al. (in prep.) - EDGAR scaled nationally and by fuel type to GCP2019	EDGAR scaled to GCP2019
Transport and optimization			
Transport model	TM5	TM3	LMDZ v6A
Weather forcing	ECMWF	NCEP	ECMWF
Resolution (degrees)	Global: 3° x 2°, Europe: 1° x 1°, North America: 1° x 1°	Global: 4° x 5°	Global: 3.75° x 1.875°
Optimization	Ensemble Kalman filter	Conjugate gradient (re-ortho-normalization) (c)	Variational

a (GLOBALVIEW, 2018;Carbontracker Team, 2017)

b (van der Velde et al., 2014)

c ocean prior not optimised

Table A4. Attribution of fCO$_2$ measurements for the year 2018 included in SOCATv2019 (Bakker et al., 2016) to inform ocean pCO$_2$-based flux products.

Platform	Regions	No. of samples	Principal Investigators	No. of data sets	Platform Type
AkzoNobel	North Atlantic; Southern Ocean	553	Tanhua, T.; Gutekunst, S.	1	Ship
Allure of the Seas	Tropical Atlantic	118652	Wanninkhof, R.; Pierrot, D.	50	Ship
Aurora Australis	Southern Ocean	59586	Tilbrook, B.	3	Ship
Bjarni Saemundsson	North Atlantic	7938	Benoit-Cattin-Breton, A.; Ólafsdóttir, S.R.	1	Ship
Cap Blanche	Southern Ocean; Tropical Pacific	28554	Cosca, C.; Alin, S.; Feely, R.; Herndon, J.; Collins A.	5	Ship
Cap San Lorenzo	Tropical Atlantic	16071	Lefèvre, N.	4	Ship
Colibri	North Atlantic; Tropical Atlantic	6541	Lefèvre, N.	1	Ship
Equinox	Tropical Atlantic	119384	Wanninkhof, R.; Pierrot, D.	48	Ship
F.G. Walton Smith	North Atlantic	2830	Millero, F.; Wanninkhof, R.	2	Ship
Finnmaid	North Atlantic	135597	Rehder, G.; Glockzin, M.	9	Ship
G.O. Sars	North Atlantic	105172	Skjelvan, I.	11	Ship
Gordon Gunter	North Atlantic	73634	Wanninkhof, R.; Pierrot, D.	12	Ship
Henry B. Bigelow	North Atlantic	64935	Wanninkhof, R.; Pierrot, D.	14	Ship
Heron Island	Tropical Pacific	3631	Tilbrook, B.	2	Mooring
Investigator	Southern Ocean	88217	Tilbrook, B.	6	Ship
Isabu	North Pacific	2350	Park, G.-H.	1	Ship
Kangaroo Island	Southern Ocean	4016	Tilbrook, B.	2	Mooring
Laurence M. Gould	Southern Ocean	28666	Sweeney, C.; Takahashi, T.; Newberger, T.; Sutherland, S.C.; Munro, D.R.	5	Ship
Maria Island	Southern Ocean	4015	Tilbrook, B.	2	Mooring
Marion Dufresne	Southern Ocean; Indian	6796	Lo Monaco, C.; Metzl, N.	1	Ship
New Century 2	North Pacific; Tropical Pacific; North Atlantic	33316	Nakaoka, S.-I.	14	Ship
Nuka Arctica	North Atlantic	143430	Becker, M.; Olsen, A.	23	Ship
Ronald H. Brown	North Atlantic; Tropical Pacific	28239	Wanninkhof, R.; Pierrot, D.	5	Ship
Simon Stevin	North Atlantic	33760	Gkritzalis, T.	8	Ship
Soyo Maru	North Pacific	91491	Ono, T.	5	Ship
Station M	North Atlantic	1313	Skjelvan, I.; Lauvset, S. K.	1	Mooring
Tangaroa	Southern Ocean	136893	Currie, K.I.	8	Ship
Trans Carrier	North Atlantic	12966	Omar, A. M.; Johannessen, T.	1	Ship
Trans Future 5	North Pacific; Tropical Pacific; Southern Ocean	27856	Nakaoka, S.-I.; Nojiri, Y.	19	Ship
Turn the Tide on Plastic	North Atlantic; Tropical Atlantic; Southern Ocean; Tropical Pacific	13043	Gutekunst, S.	1	Ship
Wakmatha	Tropical Pacific	25457	Tilbrook, B.	8	Ship

Table A5. Funding supporting the production of the various components of the global carbon budget in addition to the authors' supporting institutions (see also acknowledgements).

Funder and grant number (where relevant)	Author Initials
Australia, Integrated Marine Observing System (IMOS)	BT, CN
Australian Government as part of the Antarctic Science Collaboration Initiative program	AL
Australian Government National Environment Science Program (NESP)	JGC, VH
Belgium Research Foundation – Flanders (FWO) (grant number UA C130206-18)	TG
BNP Paribas Foundation through Climate & Biodiversity initiative, philanthropic grant for developments of the Global Carbon Atlas	PC, AP
BONUS INTEGRAL	GR
EC Copernicus Atmosphere Monitoring Service implemented by ECMWF	FC
EC Copernicus Marine Environment Monitoring Service implemented by Mercator Ocean	MG
EC H2020 (AtlantOS: grant no 633211)	SV, MG
EC H2020 (CCiCC; grant no 821003)	PF, RMA, SS, GPP, MOS, JIK, SL, NG, PL
EC H2020 (CHE; grant no 776186)	MWJ
EC H2020 (CRESCENDO: grant no. 641816)	RS, EJ
EC H2020 European Research Council (ERC) Synergy grant (IMBALANCE-P; grant no. ERC-2013-SyG-610028)	DSG
EC H2020 ERC (QUINCY; grant no. 647204)	SZ
EC H2020 (RINGO: grant no. 730944)	DB
EC H2020 project (VERIFY: grant no. 776810)	CLQ, GPP, JIK, RMA, MWJ, PC
European Space Agency Climate Change Initiative ESA-CCI RECCAP2 project 655 (ESRIN/4000123002/18/I-NB)	PF, PC, SS, MOS
French Institut National des Sciences de l'Univers (INSU) and Institut Pau-Emile Victor (IPEV), Sorbonne Universités (OSU Ecce-Terra)	NM
French Institut de Recherche pour le Développement (IRD)	NL
French Integrated Carbon Observation System (ICOS) France Océan;	NL
German Integrated Carbon Observation System (ICOS), Federal Ministry for Education and Research (BMBF);	GR
German Future Ocean (grant number CP1756)	SG
German Helmholtz Association in its ATMO programme	PA
German Helmholtz Association Innovation and Network Fund (VH-NG-1301)	JH
German Research Foundation's Emmy Noether Programme (grant no. PO1751/1-1)	JP
Japan Ministry of the Environment (grant number E1432)	TO
Japan Global Environmental Research Coordination System, Ministry of the Environment (grant number E1751)	SN
Netherlands Organization for Scientific Research (NWO; Ruisdael Infrastructure)	NS
Norwegian Research Council (grant no. 270061)	JS
Norwegian ICOS Norway and OTC Research Infrastructure Project, Research Council of Norway (grant number 245927)	SV, MB, AO
New Zealand, NIWA SSIF Funding	KC
Swiss National Science Foundation (grant no. 200020_172476)	SL
UK Natural Environment Research Council (SONATA: grant no. NE/P021417/1)	ETB
UK Newton Fund, Met Office Climate Science for Service Partnership Brazil (CSSP Brazil)	AW, ER
UK Royal Society (grant no RP\R1\191063)	CLQ
USA Department of Agriculture, National Institute of Food and Agriculture (grants no. 2015-67003-23489 and 2015-67003-23485)	DLL

USA Department of Commerce, NOAA/OAR's Global Observations and Monitoring of the Oceans Program	RF
USA Department of Commerce, NOAA/OAR's Ocean Observations and Monitoring Division (grant number 100007298);	LB, DP
USA Department of Commerce, NOAA/OAR's Ocean Acidification Program	DP, LB
USA Department of Energy, Office of Science and BER prg. (grant no. DE-SC000 0016323)	ATJ
USA Department of Energy, SciDac award number is DESC0012972; IDS grant award number is 80NSSC17K0348	LC, GH
USA CIMAS, a Cooperative Institute of the University of Miami and the National Oceanic and Atmospheric Administration (cooperative agreement NA10OAR4320143)	DP, LB
USA NASA Interdisciplinary Research in Earth Science Program.	BP
US National Science Foundation (grant number 1461590)	JOK
US National Science Foundation (grant number 1903722)	HT
US National Science Foundation (grant number PLR-1543457)	DM
USA Princeton University Environmental Institute and the NASA OCO2 science team, grant number 80NSSC18K0893.	LR
Computing resources	
Norway UNINETT Sigma2, National Infrastructure for High Performance Computing and Data Storage in Norway (NN2980K/NS2980K)	JS
Japan National Institute for Environmental Studies computational resources	EK
TGCC under allocation 2018-A0050102201" made by GENCI	FC
UK Centre for Environmental Data Analysis (CEDA) JASMIN Super-data-cluster	PCM
Supercomputing time was provided by the Météo-France/DSI supercomputing center.	RS, EJ
CarbonTracker Europe was supported by the Netherlands Organization for Scientific Research (NWO; grant no. SH-312, 17616)	WP, NS
Deutsches Klimarechenzentrum (allocation bm0891)	JEMSN, JP
PRACE for awarding access to JOLIOT CURIE at GENCI@CEA, France	LB
Support for aircraft measurements in Obspack	
L. V. Gatti, M. Gloor, J.B. Miller: AMAZONICA consortium project was funded by NERC (NE/F005806/1), FAPESP (08/58120-3), GEOCARBON project (283080)	
The CESM project is supported primarily by the National Science Foundation (NSF). This material is based upon work supported by the National Center for Atmospheric Research, which is a major facility sponsored by the NSF under Cooperative Agreement No. 1852977. Computing and data storage resources, including the Cheyenne supercomputer (doi:10.5065/D6RX99HX), were provided by the Computational and Information Systems Laboratory (CISL) at NCAR. We thank all the scientists, software engineers, and administrators who contributed to the development of CESM2.	DLL

Table A6. Aircraft measurement programs archived by Cooperative Global Atmospheric Data Integration Project (CGADIP, 2019) that contribute to the evaluation of the atmospheric inversions (Figure B3).

Measurement program name in Obspack	Specific doi	Data providers
Alta Floresta		Gatti, L.V.; Gloor, E.; Miller, J.B.;
Aircraft Observation of Atmospheric trace gases by JMA		ghg_obs@met.kishou.go.jp
Beaver Crossing, Nebraska		Sweeney, C.; Dlugokencky, E.J.
Bradgate, Iowa		Sweeney, C.; Dlugokencky, E.J.
Briggsdale, Colorado		Sweeney, C.; Dlugokencky, E.J.
Cape May, New Jersey		Sweeney, C.; Dlugokencky, E.J.
CONTRAIL (Comprehensive Observation Network for TRace gases by AIrLiner)	http://dx.doi.org/10.17595/20180208.001	Machida, T.; Matsueda, H.; Sawa, Y. Niwa, Y.
Carbon in Arctic Reservoirs Vulnerability Experiment (CARVE)		Sweeney, C.; Karion, A.; Miller, J.B.; Miller, C.E.; Dlugokencky, E.J.
Dahlen, North Dakota		Sweeney, C.; Dlugokencky, E.J.
Estevan Point, British Columbia		Sweeney, C.; Dlugokencky, E.J.
East Trout Lake, Saskatchewan		Sweeney, C.; Dlugokencky, E.J.
Fairchild, Wisconsin		Sweeney, C.; Dlugokencky, E.J.
Molokai Island, Hawaii		Sweeney, C.; Dlugokencky, E.J.
Homer, Illinois		Sweeney, C.; Dlugokencky, E.J.
HIPPO (HIAPER Pole-to-Pole Observations)	https://doi.org/10.3334/CDIAC/HIPPO_010	Wofsy, S.C.; Stephens, B.B.; Elkins, J.W.; Hintsa, E.J.; Moore, F.
INFLUX (Indianapolis Flux Experiment)		Sweeney, C.; Dlugokencky, E.J.; Shepson, P.B.; Turnbull, J.
NASA Goddard Space Flight Center Aircraft Campaign		Kawa, S.R.; Abshire, J.B.; Riris, H.
Park Falls, Wisconsin		Sweeney, C.; Dlugokencky, E.J.
Offshore Corpus Christi, Texas		Sweeney, C.; Dlugokencky, E.J.
Offshore Portsmouth, New Hampshire (Isles of Shoals)		Sweeney, C.; Dlugokencky, E.J.
Oglesby, Illinois		Sweeney, C.; Dlugokencky, E.J.
Poker Flat, Alaska		Sweeney, C.; Dlugokencky, E.J.
Rio Branco		Gatti, L.V.; Gloor, E.; Miller, J.B.
Rarotonga		Sweeney, C.; Dlugokencky, E.J.
Santarem		Sweeney, C.; Dlugokencky, E.J.
Charleston, South Carolina		Sweeney, C.; Dlugokencky, E.J.
Southern Great Plains, Oklahoma		Sweeney, C.; Dlugokencky, E.J.; Biraud, S.
Harvard University Aircraft Campaign		Wofsy, S.C.
Tabatinga		Gatti, L.V.; Gloor, E.; Miller, J.B.
Trinidad Head, California		Sweeney, C.; Dlugokencky, E.J.
West Branch, Iowa		Sweeney, C.; Dlugokencky, E.J.

Table A7. Main methodological changes in the global carbon budget from first publication until 2014. Post-2014 methodological changes are presented in Table 3. Methodological [Deleted: since] changes introduced in one year are kept for the following years unless noted. Empty cells mean there were no methodological changes introduced that year.

Publication year	Global	Fossil fuel emissions		LUC emissions	Reservoirs			Uncertainty & other changes
		Country (territorial)	Country (consumption)		Atmosphere	Ocean	Land	
2006 (a)		Split in regions						
2007 (b)				E_{LUC} based on FAO-FRA 2005; constant E_{LUC} for 2006	1959-1979 data from Mauna Loa; data after 1980 from global average	Based on one ocean model tuned to reproduced observed 1990s sink		±1σ provided for all components
2008 (c)				Constant E_{LUC} for 2007				
2009 (d)		Split between Annex B and non-Annex B	Results from an independent study discussed	Fire-based emission anomalies used for 2006-2008		Based on four ocean models normalised to observations with constant delta	First use of five DGVMs to compare with budget residual	
2010 (e)	Projection for current year based on GDP	Emissions for top emitters		E_{LUC} updated with FAO-FRA 2010				
2011 (f)			Split between Annex B and non-Annex B					
2012 (g)		129 countries from 1959	129 countries and regions from 1990-2010 based on GTAP8.0	E_{LUC} for 1997-2011 includes interannual anomalies from fire-based emissions	All years from global average	Based on 5 ocean models normalised to observations with ratio	Ten DGVMs available for S_{LAND}; First use of four models to compare with E_{LUC}	
2013 (h)		250 countries	134 countries and regions 1990-2011 based on GTAP8.1, with detailed estimates for years 1997, 2001, 2004, and 2007	E_{LUC} for 2012 estimated from 2001-2010 average		Based on six models compared with two data-products to year 2011	Coordinated DGVM experiments for S_{LAND} and E_{LUC}	Confidence levels; cumulative emissions; budget from 1750
2014 (i)	Three years of BP data	Three years of BP data	Extended to 2012 with updated GDP data	E_{LUC} for 1997-2013 includes		Based on seven models	Based on ten models	Inclusion of breakdown of

	interannual anomalies from fire-based emissions	the sinks in three latitude bands and comparison with three atmospheric inversions

a Raupach et al. (2007)

b Canadell et al. (2007)

c Online

d Le Quéré et al. (2009)

e Friedlingstein et al. (2010)

f Peters et al. (2012b)

g Le Quéré et al. (2013), Peters et al. (2013)

h Le Quéré et al. (2014)

I Le Quéré et al. (2015b)

Figure Captions

Formatted: Font color: Auto
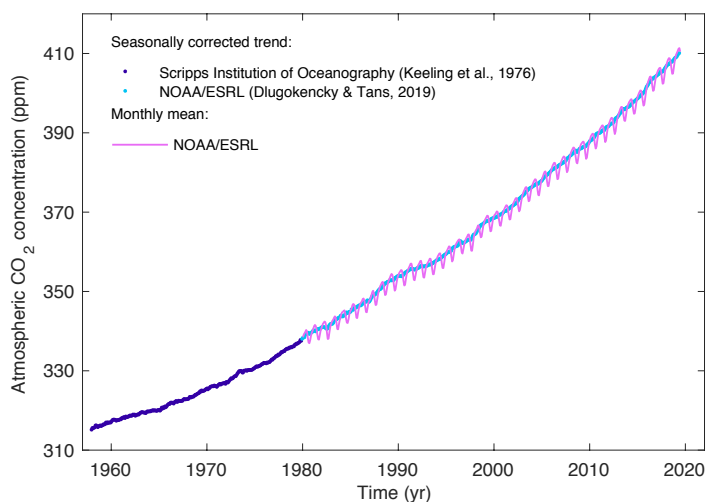
Figure 1. Surface average atmospheric CO_2 concentration (ppm). The 1980-2018 monthly data are from NOAA/ESRL (Dlugokencky and Tans, 2019) and are based on an average of direct atmospheric CO_2 measurements from multiple stations in the marine boundary layer (Masarie and Tans, 1995). The 1958-1979 monthly data are from the Scripps Institution of Oceanography, based on an average of direct atmospheric CO_2 measurements from the Mauna Loa and South Pole stations (Keeling et al., 1976). To take into account the difference of mean CO_2 and seasonality between the NOAA/ESRL and the Scripps station networks used here, the Scripps surface average (from two stations) was deseasonalised and harmonised to match the NOAA/ESRL surface average (from multiple stations) by adding the mean difference of 0.542 ppm, calculated here from overlapping data during 1980-2012.
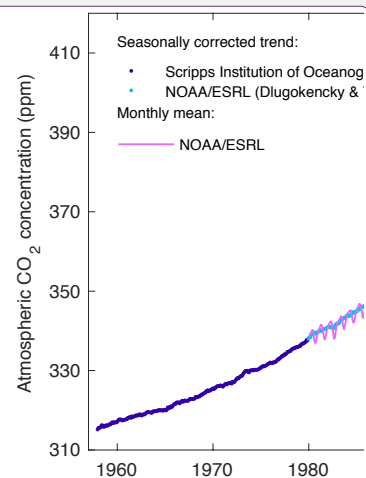
Deleted:

Formatted: Font color: Auto

Formatted: Font color: Auto
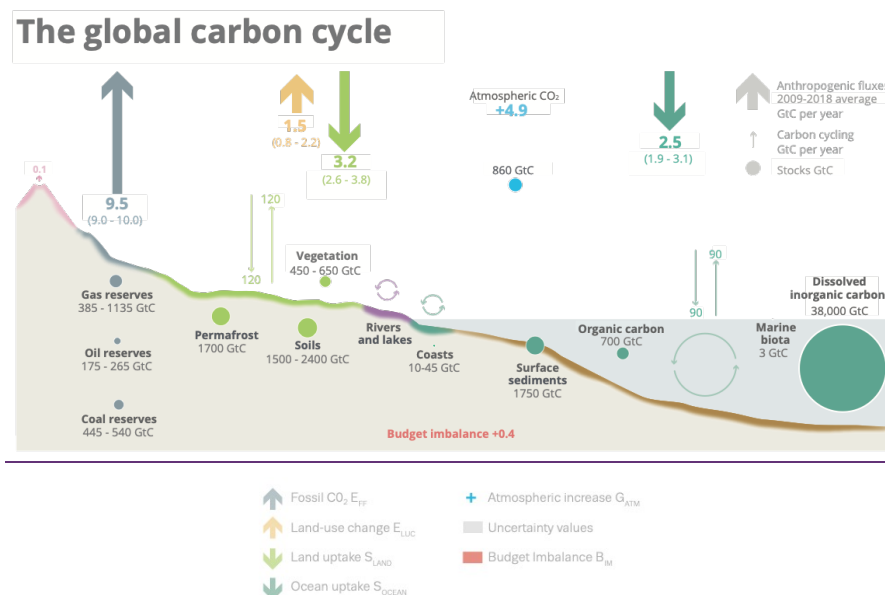
Figure 2. Schematic representation of the overall perturbation of the global carbon cycle caused by anthropogenic activities, averaged globally for the decade 2009-2018. See legends for the corresponding arrows and units. The uncertainty in the atmospheric CO_2 growth rate is very small (±0.02 Gt C yr^{-1}) and is neglected for the figure. The anthropogenic perturbation occurs on top of an active carbon cycle, with fluxes and stocks represented in the background and taken from Ciais et al. (2013) for all numbers, with the ocean gross fluxes updated to 90 GtC yr^{-1} to account for the increase in atmospheric CO_2 since publication, and except for the carbon stocks in coasts which is from a literature review of coastal marine sediments (Price and Warren, 2016).
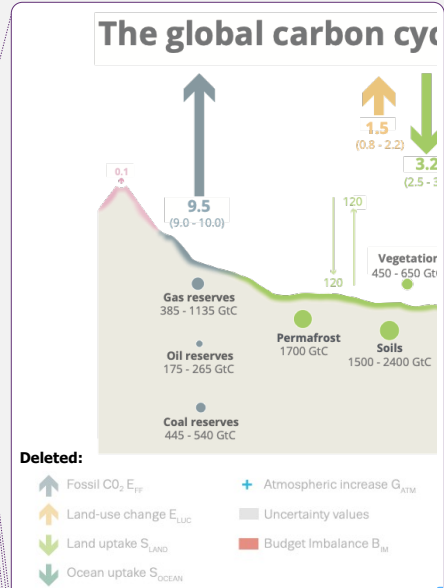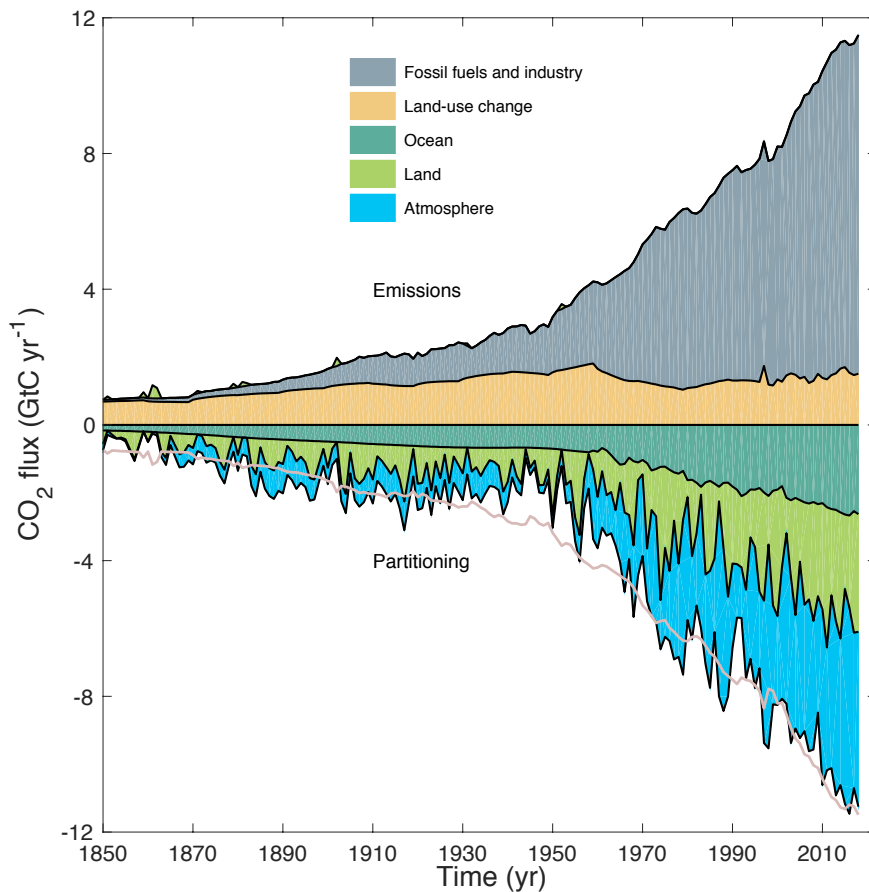
Figure 3. Combined components of the global carbon budget illustrated in Fig. 2 as a function of time, for fossil CO_2 emissions (E_{FF}; grey) and emissions from land-use change (E_{LUC}; brown), as well as their partitioning among the atmosphere (G_{ATM}; blue), ocean (S_{OCEAN}; turquoise), and land (S_{LAND}; green). The partitioning is based on nearly independent estimates from observations (for G_{ATM}) and from process model ensembles constrained by data (for S_{OCEAN} and S_{LAND}), and does not exactly add up to the sum of the emissions, resulting in a budget imbalance which is represented by the difference between the bottom pink line (reflecting total emissions) and the sum of the ocean, land and atmosphere. All time series are in GtC yr^{-1}. G_{ATM} and S_{OCEAN} prior to 1959 are based on different methods. E_{FF} are primarily from (Gilfillan et al.
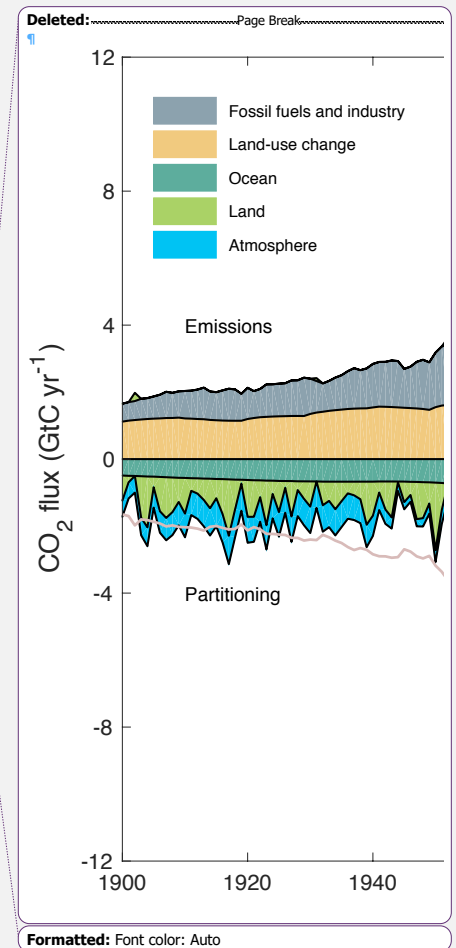
2019), with uncertainty of about ±5% (±1σ); E_{LUC} are from two bookkeeping models (Table 2) with uncertainties of about ±50%; G_{ATM} prior to 1959 is from Joos and Spahni (2008) with uncertainties equivalent to about ±0.1-0.15 GtC yr^{-1}, and from Dlugokencky and Tans (2019) from 1959 with uncertainties of about ±0.2 GtC yr^{-1}; S_{OCEAN} prior to 1959 is averaged from Khatiwala et al. (2013) and DeVries (2014) with uncertainty of about ±30%, and from a multi-model mean (Table 4) from 1959 with uncertainties of about ±0.5 GtC yr^{-1}; S_{LAND} is a multi-model mean (Table 4) with uncertainties of about ±0.9 GtC yr^{-1}. See the text for more details of each component and their uncertainties.
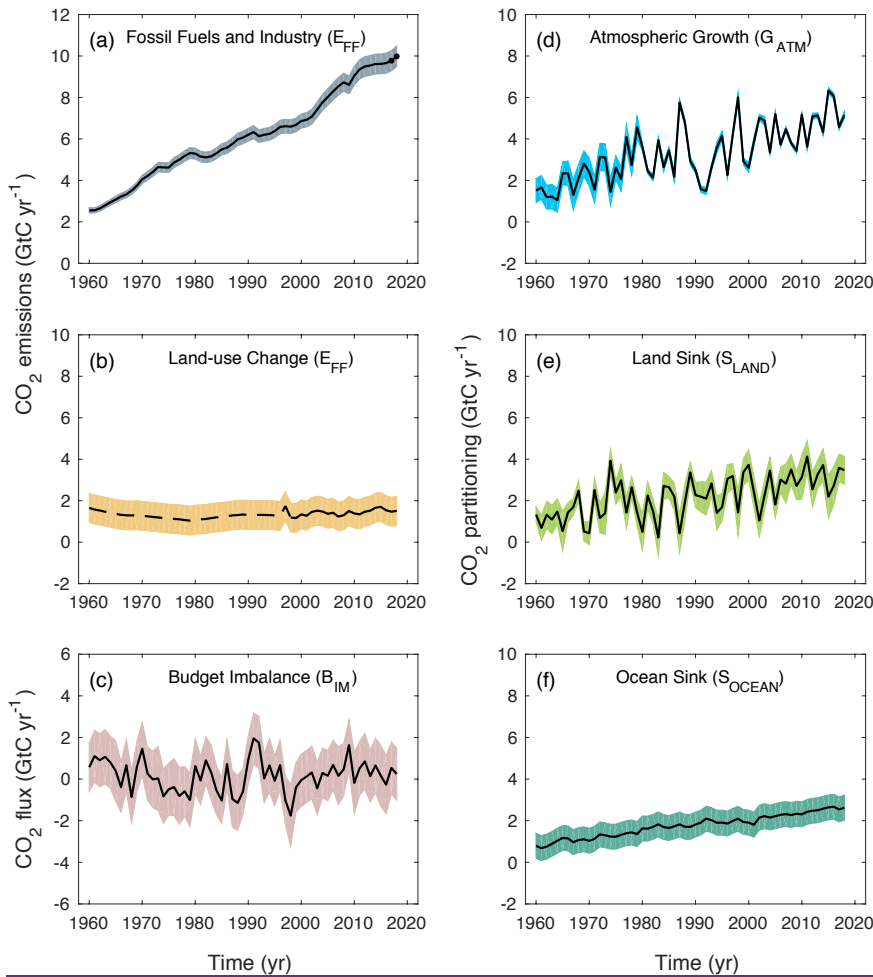
Figure 4. Components of the global carbon budget and their uncertainties as a function of time, presented individually for **(a)** fossil CO_2 emissions (E_{FF}), **(b)** emissions from land-use change (E_{LUC}), **(c)** the budget imbalance that is not accounted for by the other terms, **(d)** growth rate in atmospheric CO_2 concentration (G_{ATM}), and **(e)** the land CO_2 sink (S_{LAND}, positive indicates a flux from the atmosphere to the land), **(f)** the ocean CO_2 sink (S_{OCEAN}, positive indicates a flux from the atmosphere to the ocean). All time series are in GtC yr^{-1} with the uncertainty bounds representing ±1σ in shaded colour. Data sources are as in Fig. 3. The black dots in **(a)** show

Deleted: ¶
¶

Formatted: Font color: Auto
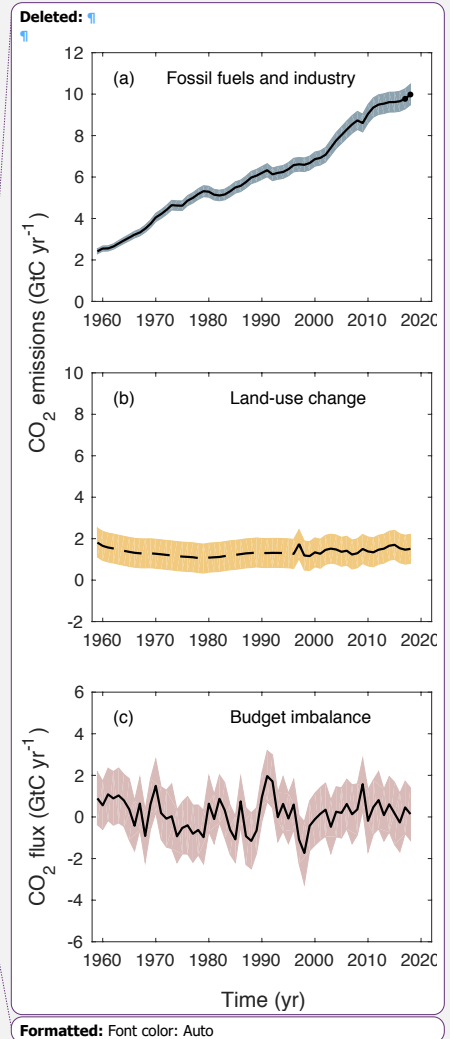
values for 2017-2018 that originate from a different data set to the remainder of the data (see text). The dashed line in **(b)** identifies the pre-satellite period before the inclusion of emissions from peatland burning.
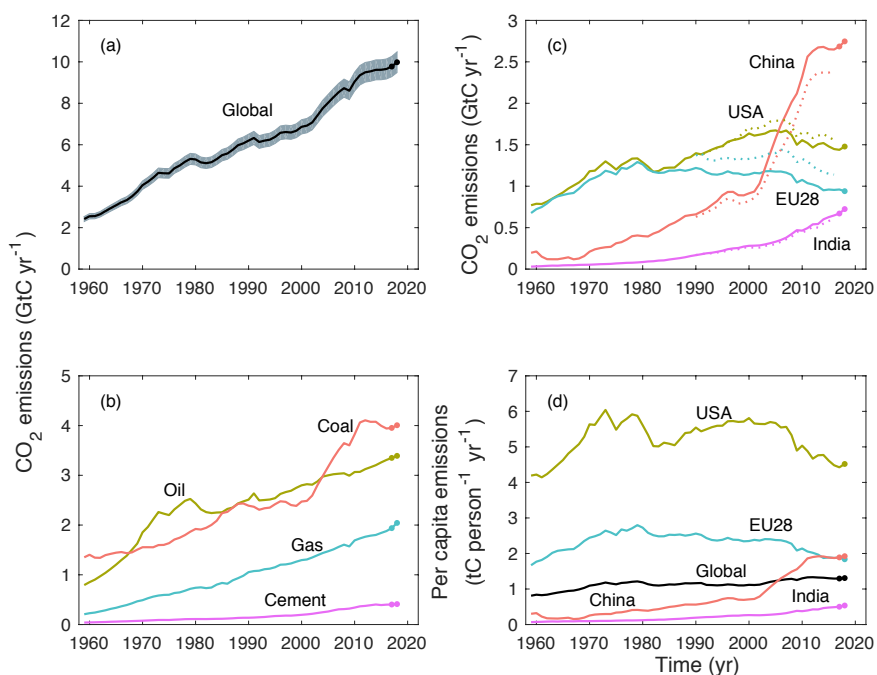
Figure 5. Fossil CO_2 emissions for **(a)** the globe, including an uncertainty of ± 5% (grey shading), and the emissions extrapolated using BP energy statistics (black dots), **(b)** global emissions by fuel type, including coal (salmon), oil (olive), gas (turquoise), and cement (purple), and excluding gas flaring which is small (0.6% in 2013), **(c)** territorial (solid lines) and consumption (dashed lines) emissions for the top three country emitters (USA - olive; China - salmon; India - purple) and for the European Union (EU; turquoise for the 28 member states of the EU as of 2012), and **(d)** per-capita emissions for the top three country emitters and the EU (all colours as in panel **(c)**) and the world (black). In **(b-c)**, the dots show the data that were extrapolated from BP energy statistics for 2017-2018. All time series are in GtC yr⁻¹ except the per-capita emissions **(d)**, which are in tonnes of carbon per person per year (tC person⁻¹ yr⁻¹). Territorial emissions are primarily from Gilfillan et al. (2019) except national data for the USA and EU28 (the 28 member states of the EU) for 1990-2017, which are reported by the countries to the UNFCCC as detailed in the text; consumption-based emissions are updated from Peters et al. (2011a). See Section 2.1.1 for details of the calculations and data sources.
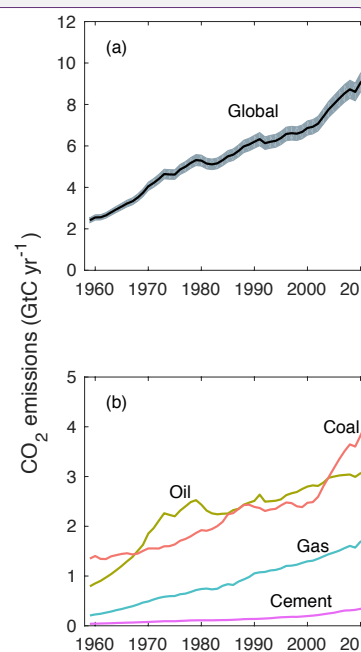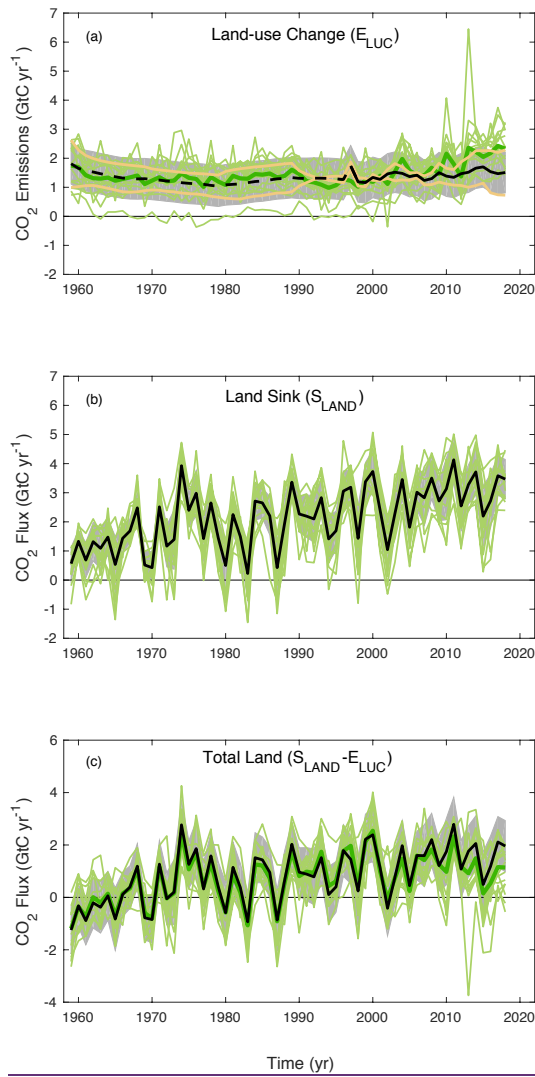
Figure 6. CO_2 exchanges between the atmosphere and the terrestrial biosphere as used in the global carbon budget (black with ±1σ uncertainty in grey shading), for **(a)** CO_2 emissions from land-use change (E_{LUC}), showing also individually the two bookkeeping models (two brown lines) and the DGVM model results (green) and their multi-model mean (dark green). The dashed line identifies the pre-satellite period before the inclusion of peatland burning; **(b)** Land
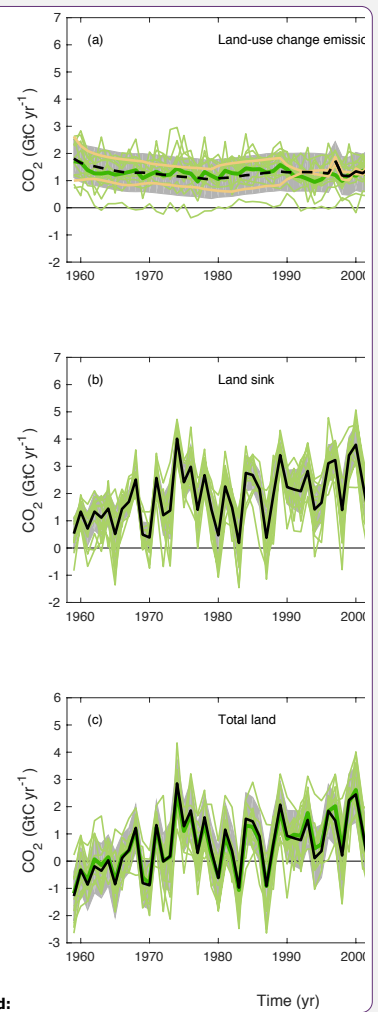
CO$_2$ sink (S$_{LAND}$) with individual DGVMs (green); **(c)** Total land CO$_2$ fluxes (**b minus a**) with individual DGVMs (green) and their multi-model mean (dark green).
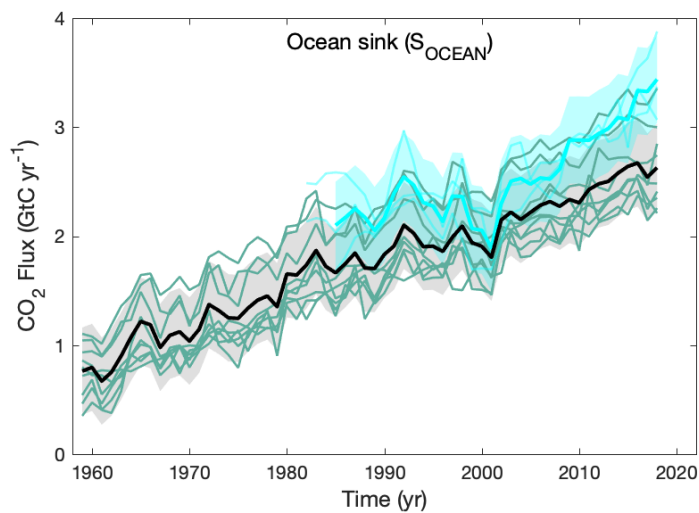
Figure 7. Comparison of the anthropogenic atmosphere-ocean CO_2 flux showing the budget values of S_{OCEAN} (black; with ±1σ uncertainty in grey shading), individual ocean models (teal), and the three ocean pCO_2-based flux products (light blue; with ±1σ uncertainty in light blue shading see Table 4). The pCO_2-based flux products were adjusted for the pre-industrial ocean source of CO_2 from river input to the ocean, which is not present in the ocean models, by adding a sink of 0.78 GtC yr^{-1} (Resplandy et al., 2018), to make them comparable to S_{OCEAN}. This adjustment does not take into account the anthropogenic contribution to river fluxes (see Section 2.7.3)
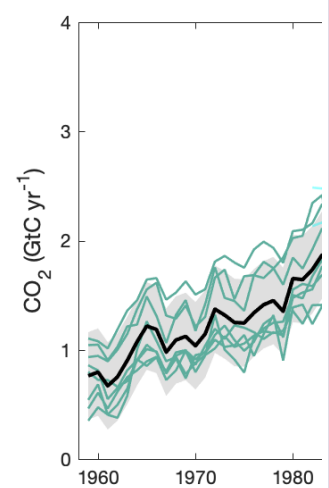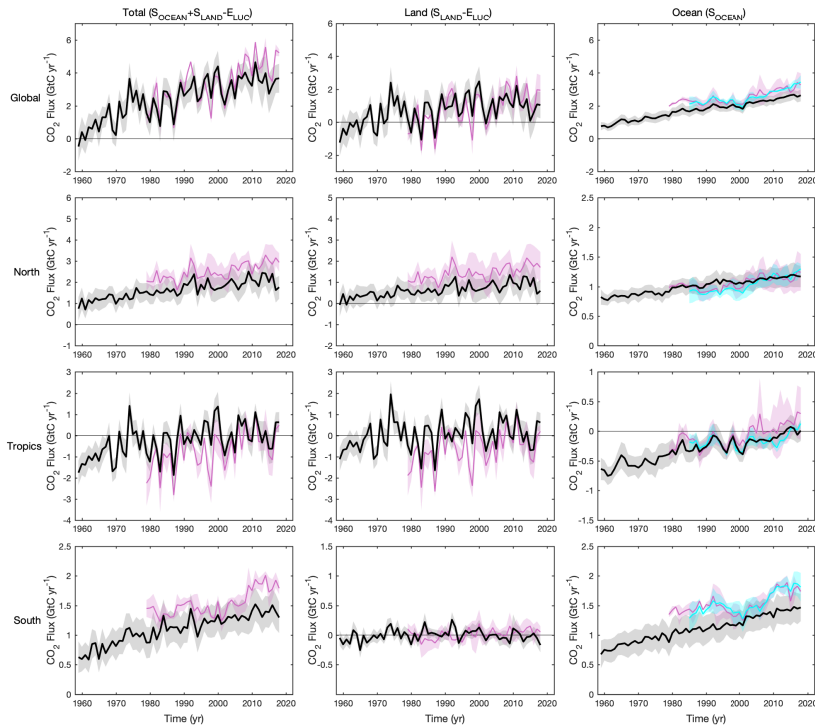
Figure 8. CO_2 fluxes between the atmosphere and the surface, S_{OCEAN} and $(S_{LAND} - E_{LUC})$ by latitude bands for the (top) globe, (2nd row) north (north of 30°N), (3rd row) tropics (30°S-30°N), and (bottom) south (south of 30°S), and over (left) total ($S_{OCEAN} + S_{LAND} - E_{LUC}$), (middle) land only ($S_{LAND} - E_{LUC}$) and (right) ocean only (S_{OCEAN}). Positive values indicate a flux from the atmosphere to the land and/or ocean. Mean estimates from the combination of the process models for the land and oceans are shown (black line) with ±1σ of the model ensemble (grey shading). For total uncertainty, the land and ocean uncertainties are summed in quadrature. Mean estimates from the atmospheric inversions are shown (pink lines) with their ±1σ spread (pink shading). Mean estimates from the pCO_2-based flux products are shown for the ocean domain (cyan lines) with their ±1σ spread (cyan shading). The global S_{OCEAN} (upper right) and the
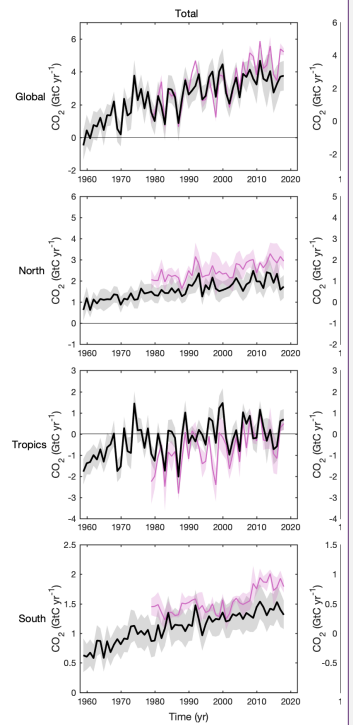
sum of S_{OCEAN} in all three regions represents the anthropogenic atmosphere-to-ocean flux based on the assumption that the preindustrial ocean sink was 0 GtC yr^{-1} when riverine fluxes are not considered. This assumption does not hold on the regional level, where preindustrial fluxes can be significantly different from zero. Hence, the regional panels for S_{OCEAN} represent a combination of natural and anthropogenic fluxes. Bias-correction and area-weighting were only applied to global S_{OCEAN}, hence the sum of the regions is slightly different from the global estimate (<0.05 GtC yr^{-1}).
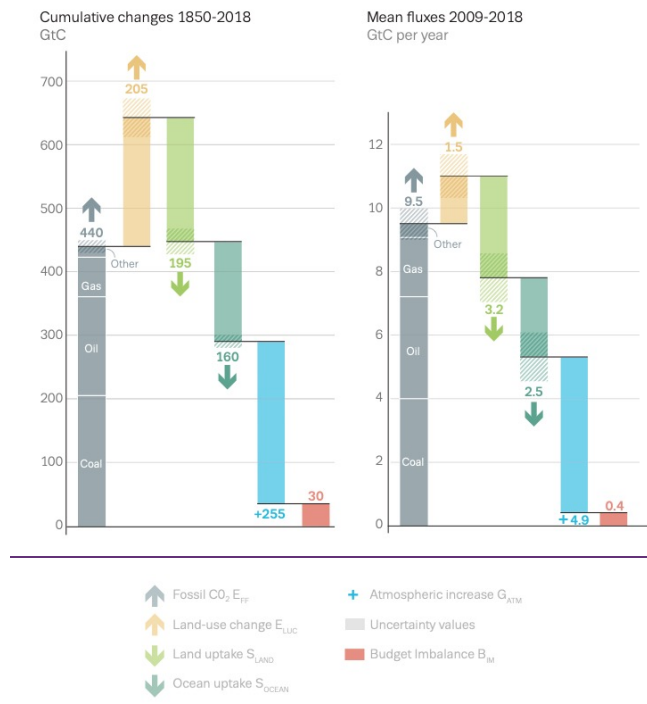
Figure 9. Cumulative changes during 1850-2018 and mean fluxes during 2009-2018 for the anthropogenic perturbation as defined in the legend.
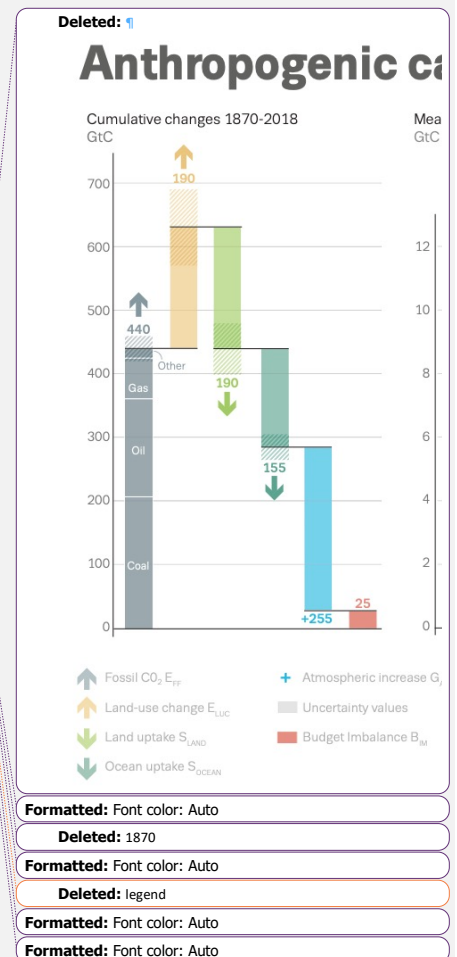
Appendix B. Supplementary figures.
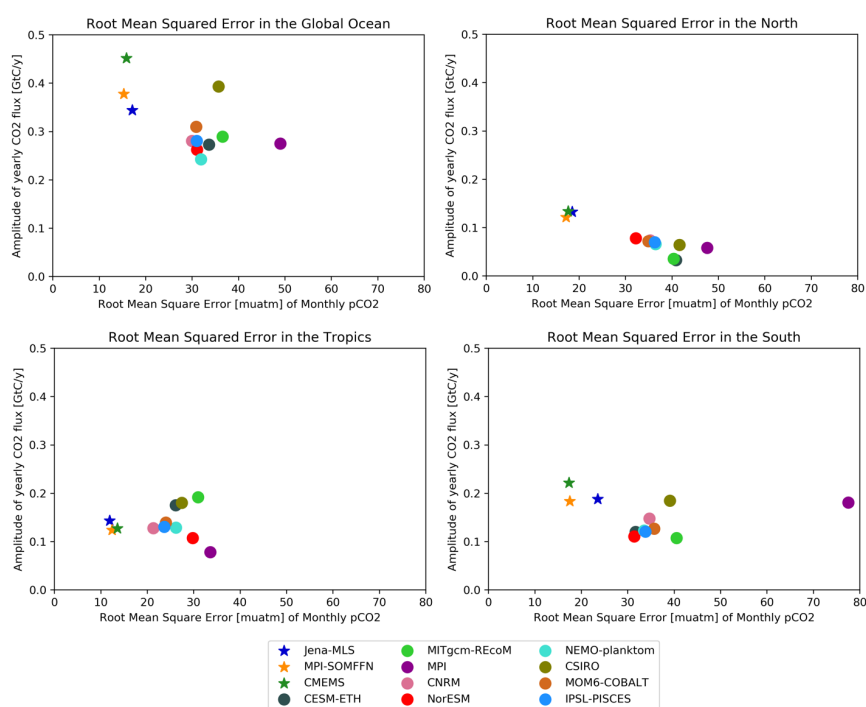
Figure B1. Evaluation of the GOBMs and flux products using the root mean squared error (RMSE) for the period 1985 to 2018, between the individual surface ocean pCO₂ estimates and the SOCAT v2019 database. The y-axis shows the amplitude of the interannual variability (A-IAV, taken as the standard deviation of a 12-months running mean over the monthly flux time-series, Rödenbeck et al., 2015). Results are presented for the globe, north (>30°N), tropics (30°S-30°N), and south (<30°S) for the GOBMs (circles) and for the pCO₂-based flux products (star symbols). The three pCO₂-based flux products use the SOCAT database and therefore are not fully independent from the data (see section 2.4.1).
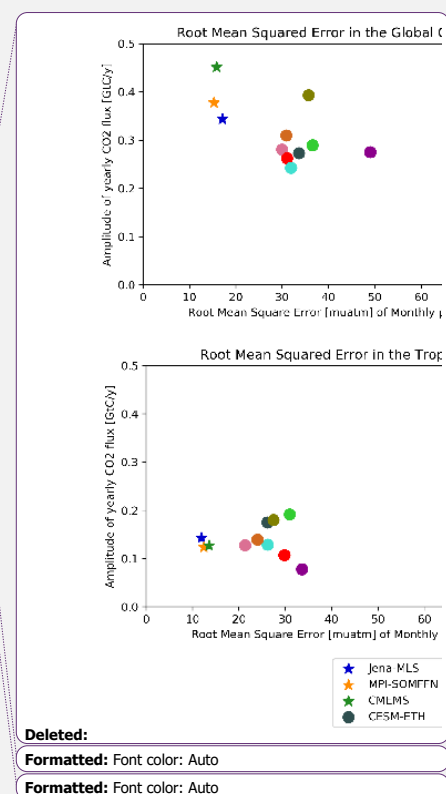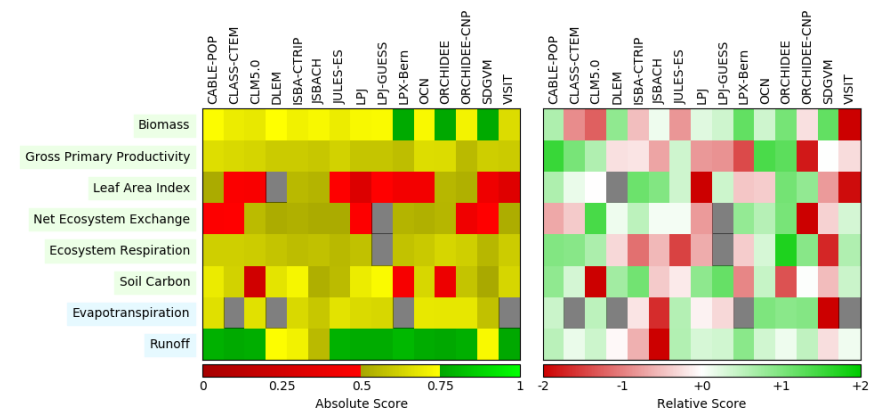
Figure B2. Evaluation of the DGVM using the International Land Model Benchmarking system (ILAMB; Collier et al., 2018) (left) absolute skill scores and (right) skill scores relative to other models. The benchmarking is done with observations for vegetation biomass (Saatchi et al., 2011; and GlobalCarbon unpublished data; Avitabile et al., 2016), GPP (Jung et al., 2010;Lasslop et al., 2010), leaf area index (De Kauwe et al., 2011;Myneni et al., 1997), net ecosystem exchange (Jung et al., 2010;Lasslop et al., 2010), ecosystem respiration (Jung et al., 2010;Lasslop et al., 2010), soil carbon (Hugelius et al., 2013;Todd-Brown et al., 2013), evapotranspiration (De Kauwe et al., 2011), and runoff (Dai and Trenberth, 2002). For each model-observation comparison a series of error metrics are calculated, scores are then calculated as an exponential function of each error metric, finally for each variable the multiple scores from different metrics and observational data sets are combined to give the overall variable scores shown in the left panel. Overall variable scores increase from 0 to 1 with improvements in model performance. The set of error metrics vary with data set and can include metrics based on the period mean, bias, root mean squared error, spatial distribution, interannual variability and seasonal cycle. The relative skill score shown in the right panel is a Z-score, which indicates in units of standard deviation the model scores relative to the multi-model mean score for a given variable. Grey boxes represent missing model data.

Deleted:

Formatted: Font color: Auto

Formatted: Font color: Auto

Formatted: Font color: Auto
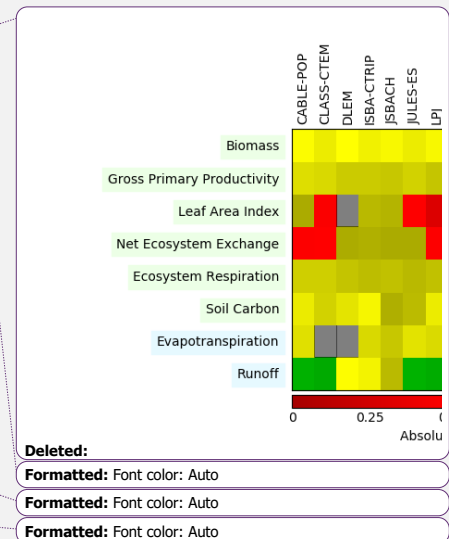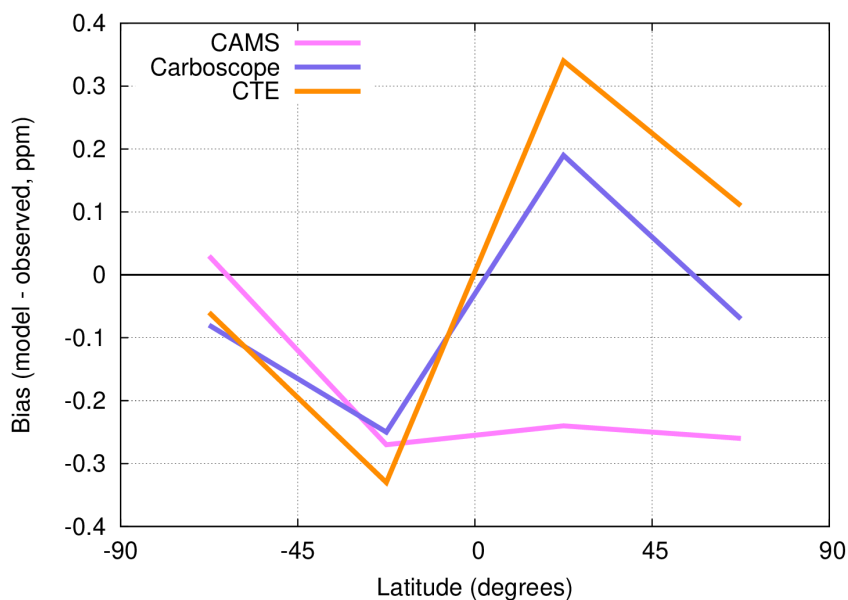
Figure B3. Evaluation of the atmospheric inversion products. The mean of the model minus observations is shown for four latitude bands. The four models are compared to independent CO_2 measurements made onboard aircraft over many places of the world between 2 and 7 km above sea level. Aircraft measurements archived in the Cooperative Global Atmospheric Data Integration Project (CGADIP, 2019) from sites, campaigns or programs that cover at least 9 months between 2001 and 2017 and that have not been assimilated, have been used to compute the biases of the differences in four 45∘ latitude bins. Land and ocean data are used without distinction. The number of data for each latitude band is 5000 (90–45∘S), 124000 (45∘S–0), 1042000 (0–45∘N), and 139000 (45–90∘N), rounded off to the nearest thousand.

Deleted: ·················Page Break··················
¶

Formatted: Font color: Auto
Formatted: Font color: Auto
Formatted: Font color: Auto
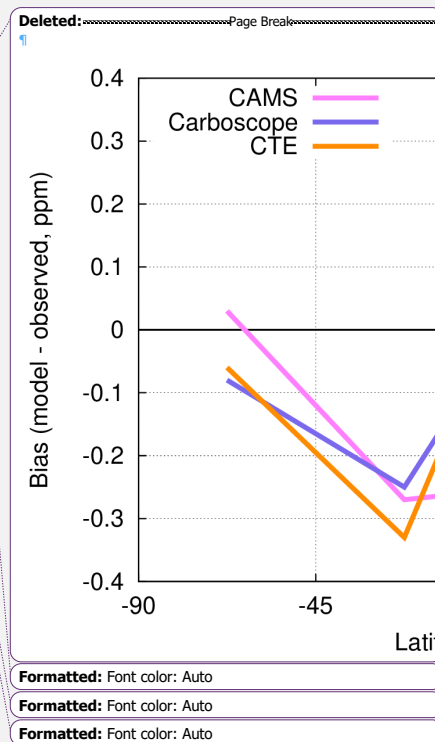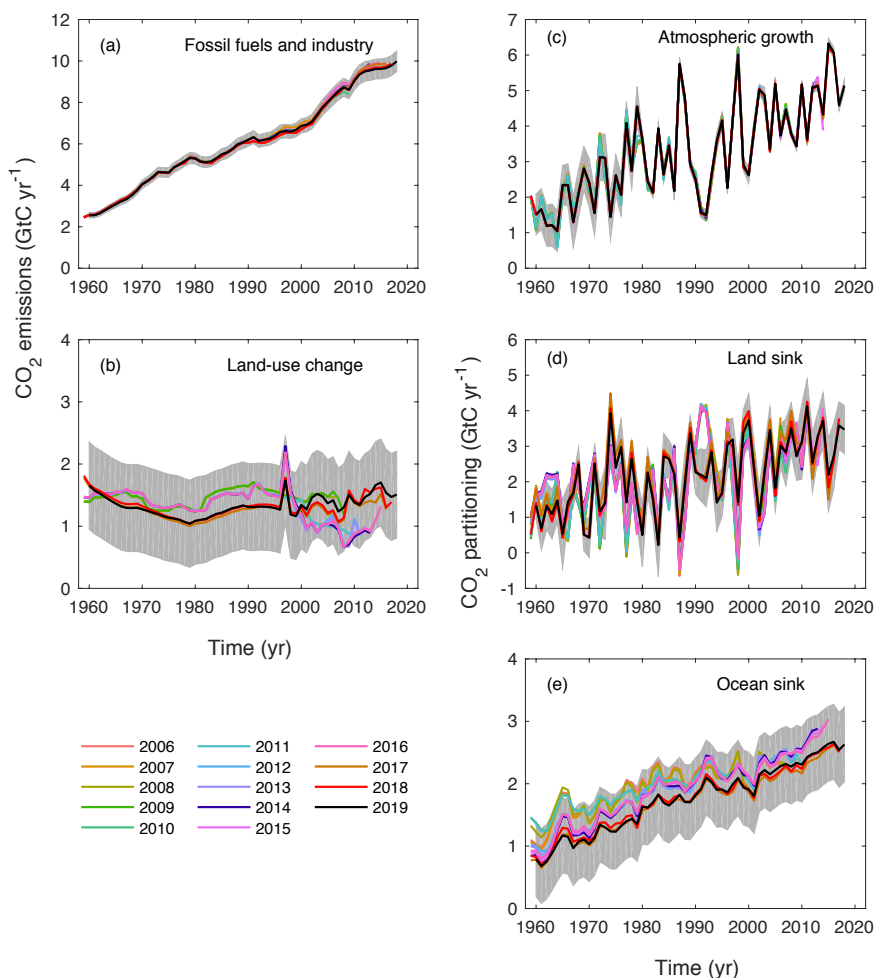
Figure B4. Comparison of global carbon budget components released annually by GCP since 2006. CO_2 emissions from **(a)** fossil CO_2 emissions (E_{FF}), and **(b)** land-use change (E_{LUC}), as well as their partitioning among **(c)** the atmosphere (G_{ATM}), **(d)** the land (S_{LAND}), and **(e)** the ocean (S_{OCEAN}). See legend for the corresponding years, and Tables 3 and A7 for references. The budget year corresponds to the year when the budget was first released. All values are in GtC yr^{-1}. Grey shading shows the uncertainty bounds representing ±1σ of the current global carbon budget.
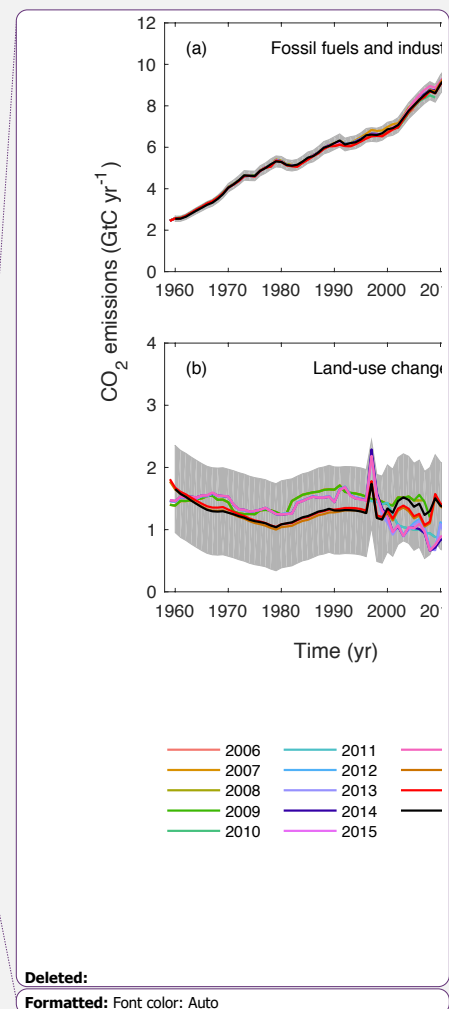
Page 25: [1] Formatted	New submission	11/8/19 12:12:00 PM

Font color: Auto, English (US)

Page 25: [2] Formatted	New submission	11/8/19 12:12:00 PM

Font color: Auto, English (US)

Page 25: [3] Formatted	New submission	11/8/19 12:12:00 PM

Font color: Auto, English (US)

Page 25: [4] Formatted	New submission	11/8/19 12:12:00 PM

Font color: Auto, English (US)

Page 25: [5] Formatted	New submission	11/8/19 12:12:00 PM

Font color: Auto, English (US)

Page 25: [6] Formatted	New submission	11/8/19 12:12:00 PM

Font color: Auto, English (US)

Page 25: [7] Formatted	New submission	11/8/19 12:12:00 PM

Font color: Auto, English (US)

Page 25: [8] Formatted	New submission	11/8/19 12:12:00 PM

Font color: Auto, English (US)

Page 25: [9] Formatted	New submission	11/8/19 12:12:00 PM

Font color: Auto, English (US)

Page 25: [10] Deleted	New submission	11/8/19 12:12:00 PM

▼

Page 25: [11] Formatted	New submission	11/8/19 12:12:00 PM

Font color: Auto, English (US)

Page 25: [12] Formatted	New submission	11/8/19 12:12:00 PM

Font color: Auto, English (US)

Page 25: [13] Deleted	New submission	11/8/19 12:12:00 PM

▼

Page 25: [14] Formatted	New submission	11/8/19 12:12:00 PM

Font color: Auto, English (US)

Page 25: [15] Formatted	New submission	11/8/19 12:12:00 PM

Font color: Auto, English (US)

Page 25: [16] Formatted	New submission	11/8/19 12:12:00 PM

Font color: Auto, English (US)

Page 25: [17] Formatted	New submission	11/8/19 12:12:00 PM

Font color: Auto, English (US)

Page 25: [18] Formatted	New submission	11/8/19 12:12:00 PM

Font color: Auto, English (US)

Page 25: [19] Formatted	New submission	11/8/19 12:12:00 PM

Font color: Auto, English (US)

Page 25: [20] Formatted	New submission	11/8/19 12:12:00 PM

Font color: Auto, English (US)

Page 25: [21] Formatted	New submission	11/8/19 12:12:00 PM

Font color: Auto, English (US)

Page 25: [22] Deleted	New submission	11/8/19 12:12:00 PM

▼

Page 25: [23] Formatted	New submission	11/8/19 12:12:00 PM

English (US)

Page 25: [24] Formatted	New submission	11/8/19 12:12:00 PM

English (US)

Page 25: [25] Formatted	New submission	11/8/19 12:12:00 PM

English (US)

Page 25: [26] Deleted	New submission	11/8/19 12:12:00 PM

▼

Page 25: [27] Formatted	New submission	11/8/19 12:12:00 PM

Not Strikethrough

Page 55: [28] Formatted	New submission	11/8/19 12:12:00 PM

Font color: Black

Page 55: [29] Formatted	New submission	11/8/19 12:12:00 PM

Font color: Black

Page 55: [30] Formatted	New submission	11/8/19 12:12:00 PM

Font color: Black

Page 55: [30] Formatted	New submission	11/8/19 12:12:00 PM

Font color: Black

Page 55: [31] Formatted	New submission	11/8/19 12:12:00 PM

Font color: Black

Page 55: [32] Formatted	New submission	11/8/19 12:12:00 PM

Font color: Black

Page 55: [33] Formatted	New submission	11/8/19 12:12:00 PM

Font color: Black

Page 55: [34] Formatted	New submission	11/8/19 12:12:00 PM

Font color: Black

Page 55: [34] Formatted	New submission	11/8/19 12:12:00 PM

Font color: Black

Page 55: [34] Formatted	New submission	11/8/19 12:12:00 PM

Font color: Black

Page 55: [35] Formatted	New submission	11/8/19 12:12:00 PM

Font color: Black

Page 55: [35] Formatted	New submission	11/8/19 12:12:00 PM

Font color: Black

Page 55: [36] Formatted	New submission	11/8/19 12:12:00 PM

Font color: Black

Page 55: [37] Formatted	New submission	11/8/19 12:12:00 PM

Font color: Black

Page 55: [38] Formatted	New submission	11/8/19 12:12:00 PM

Font color: Black

Page 55: [39] Formatted	New submission	11/8/19 12:12:00 PM

Font color: Black

Page 55: [39] Formatted	New submission	11/8/19 12:12:00 PM

Font color: Black

Page 55: [40] Formatted	New submission	11/8/19 12:12:00 PM

Font color: Black

Page 55: [40] Formatted	New submission	11/8/19 12:12:00 PM

Font color: Black

Page 55: [41] Deleted	New submission	11/8/19 12:12:00 PM

Page 55: [41] Deleted	New submission	11/8/19 12:12:00 PM

Page 55: [41] Deleted	New submission	11/8/19 12:12:00 PM

Page 55: [42] Formatted	New submission	11/8/19 12:12:00 PM

Font color: Black

Page 55: [42] Formatted	New submission	11/8/19 12:12:00 PM

Font color: Black

Page 55: [43] Formatted	New submission	11/8/19 12:12:00 PM

Font color: Black

Page 55: [44] Formatted	New submission	11/8/19 12:12:00 PM

Font color: Black

Page 55: [45] Formatted	New submission	11/8/19 12:12:00 PM

Font color: Black

Page 55: [45] Formatted	New submission	11/8/19 12:12:00 PM

Font color: Black

Page 55: [45] Formatted	New submission	11/8/19 12:12:00 PM

Font color: Black

Page 55: [45] Formatted	New submission	11/8/19 12:12:00 PM

Font color: Black

Page 55: [45] Formatted	New submission	11/8/19 12:12:00 PM

Font color: Black

Page 55: [46] Formatted	New submission	11/8/19 12:12:00 PM

Font color: Black

Page 55: [47] Deleted	New submission	11/8/19 12:12:00 PM

Page 55: [47] Deleted	New submission	11/8/19 12:12:00 PM

Page 55: [48] Formatted	New submission	11/8/19 12:12:00 PM

Font color: Black

Page 55: [49] Formatted	New submission	11/8/19 12:12:00 PM

Font color: Black

Page 55: [49] Formatted	New submission	11/8/19 12:12:00 PM

Font color: Black

Page 55: [49] Formatted	New submission	11/8/19 12:12:00 PM

Font color: Black

Page 55: [49] Formatted	New submission	11/8/19 12:12:00 PM

Font color: Black

Page 55: [50] Formatted	New submission	11/8/19 12:12:00 PM

Font color: Black

Page 55: [51] Formatted	New submission	11/8/19 12:12:00 PM

Font color: Black

Page 55: [51] Formatted	New submission	11/8/19 12:12:00 PM

Font color: Black

Page 55: [52] Formatted	New submission	11/8/19 12:12:00 PM

Font color: Black

Page 55: [53] Formatted	New submission	11/8/19 12:12:00 PM

Font color: Black

Page 55: [53] Formatted	New submission	11/8/19 12:12:00 PM

Font color: Black

Page 55: [54] Formatted	New submission	11/8/19 12:12:00 PM

Font color: Black

Page 55: [55] Formatted	New submission	11/8/19 12:12:00 PM

Font color: Black

Page 55: [56] Formatted	New submission	11/8/19 12:12:00 PM

Font color: Black

Page 55: [57] Formatted	New submission	11/8/19 12:12:00 PM

Font color: Black

Page 56: [58] Deleted	New submission	11/8/19 12:12:00 PM

▼

Page 56: [58] Deleted	New submission	11/8/19 12:12:00 PM

▼

Page 56: [58] Deleted	New submission	11/8/19 12:12:00 PM

▼

Page 56: [58] Deleted	New submission	11/8/19 12:12:00 PM

▼

Page 56: [58] Deleted	New submission	11/8/19 12:12:00 PM

▼

Page 56: [58] Deleted	New submission	11/8/19 12:12:00 PM

▼

Page 56: [58] Deleted	New submission	11/8/19 12:12:00 PM

▼

Page 56: [58] Deleted	New submission	11/8/19 12:12:00 PM

▼

Page 56: [58] Deleted	New submission	11/8/19 12:12:00 PM

▼

| Page 56: [58] Deleted | New submission | 11/8/19 12:12:00 PM |

| Page 56: [58] Deleted | New submission | 11/8/19 12:12:00 PM |

| Page 56: [59] Deleted | New submission | 11/8/19 12:12:00 PM |

| Page 56: [59] Deleted | New submission | 11/8/19 12:12:00 PM |

| Page 56: [59] Deleted | New submission | 11/8/19 12:12:00 PM |

| Page 56: [59] Deleted | New submission | 11/8/19 12:12:00 PM |

| Page 56: [59] Deleted | New submission | 11/8/19 12:12:00 PM |

| Page 56: [59] Deleted | New submission | 11/8/19 12:12:00 PM |

| Page 56: [59] Deleted | New submission | 11/8/19 12:12:00 PM |

| Page 56: [59] Deleted | New submission | 11/8/19 12:12:00 PM |

| Page 56: [59] Deleted | New submission | 11/8/19 12:12:00 PM |

| Page 56: [59] Deleted | New submission | 11/8/19 12:12:00 PM |

| Page 56: [59] Deleted | New submission | 11/8/19 12:12:00 PM |

| Page 56: [59] Deleted | New submission | 11/8/19 12:12:00 PM |

| Page 56: [59] Deleted | New submission | 11/8/19 12:12:00 PM |

| Page 56: [59] Deleted | New submission | 11/8/19 12:12:00 PM |

| Page 56: [60] Deleted | New submission | 11/8/19 12:12:00 PM |

| Page 56: [60] Deleted | New submission | 11/8/19 12:12:00 PM |

| Page 56: [60] Deleted | New submission | 11/8/19 12:12:00 PM |

| Page 56: [60] Deleted | New submission | 11/8/19 12:12:00 PM |

| Page 56: [60] Deleted | New submission | 11/8/19 12:12:00 PM |

| Page 56: [60] Deleted | New submission | 11/8/19 12:12:00 PM |

| Page 56: [60] Deleted | New submission | 11/8/19 12:12:00 PM |

| Page 56: [60] Deleted | New submission | 11/8/19 12:12:00 PM |

| Page 56: [61] Formatted | New submission | 11/8/19 12:12:00 PM |

Font color: Black

| Page 56: [61] Formatted | New submission | 11/8/19 12:12:00 PM |

Font color: Black

| Page 152: [62] Formatted | New submission | 11/8/19 12:12:00 PM |

Font color: Auto

| Page 152: [62] Formatted | New submission | 11/8/19 12:12:00 PM |

Font color: Auto

Page 152: [63] Formatted	New submission	11/8/19 12:12:00 PM

Font color: Auto

Page 152: [63] Formatted	New submission	11/8/19 12:12:00 PM

Font color: Auto

Page 152: [64] Formatted	New submission	11/8/19 12:12:00 PM

Font color: Auto

Page 152: [64] Formatted	New submission	11/8/19 12:12:00 PM

Font color: Auto

Page 152: [65] Formatted	New submission	11/8/19 12:12:00 PM

Font color: Auto

Page 152: [65] Formatted	New submission	11/8/19 12:12:00 PM

Font color: Auto

Page 152: [66] Formatted	New submission	11/8/19 12:12:00 PM

Font color: Auto

Page 152: [66] Formatted	New submission	11/8/19 12:12:00 PM

Font color: Auto

Page 152: [67] Formatted	New submission	11/8/19 12:12:00 PM

Font color: Auto

Page 152: [67] Formatted	New submission	11/8/19 12:12:00 PM

Font color: Auto

Page 152: [68] Formatted	New submission	11/8/19 12:12:00 PM

Font color: Auto

Page 152: [68] Formatted	New submission	11/8/19 12:12:00 PM

Font color: Auto

Page 152: [69] Formatted	New submission	11/8/19 12:12:00 PM

Font color: Auto

Page 152: [69] Formatted	New submission	11/8/19 12:12:00 PM

Font color: Auto

Page 152: [70] Formatted	New submission	11/8/19 12:12:00 PM

Font color: Auto

Page 152: [70] Formatted	New submission	11/8/19 12:12:00 PM

Font color: Auto

Page 155: [71] Formatted	New submission	11/8/19 12:12:00 PM

Font color: Auto

Page 155: [72] Formatted	New submission	11/8/19 12:12:00 PM

Font: 9 pt

Page 155: [73] Formatted Table	New submission	11/8/19 12:12:00 PM

Formatted Table

Page 155: [74] Formatted Table	New submission	11/8/19 12:12:00 PM

Formatted Table

Page 156: [75] Deleted	New submission	11/8/19 12:12:00 PM